

RE-ENTRY AND SPACE SYSTEMS PROGRAMS

FINAL REPORT

---

RESEARCH, DEVELOPMENT, AND PRELIMINARY DESIGN  
FOR THE LUNAR PENETROMETER SYSTEM  
APPLICABLE TO THE APOLLO PROGRAM

For  
Contract Change Notice 2A  
To  
Contract No. NAS1-4923

Prepared for: National Aeronautics and Space Administration  
Langley Research Center  
Hampton, Virginia

Approved by:

  
R. S. Kraemer  
Program Engineer

  
V. Skoro  
Program Supervisor

  
W. Hostetler  
Manager  
Space Programs

3 June 1966

## CONTENTS

SECTION		PAGE
1	INTRODUCTION . . . . .	1-1
2	SUMMARY. . . . .	2-1
3	SOUNDING DEVICE APPLICATION STUDY	
3.1	System Description	
3.1.1	Purpose. . . . .	3-1
3.1.2	Constraints. . . . .	3-5
3.1.3	Operation. . . . .	3-6
3.1.4	Further Study. . . . .	3-10
3.2	Analyses	
3.2.1	Data Model . . . . .	3-17
3.2.2	Deployment . . . . .	3-22
3.2.3	Communications . . . . .	3-59
3.2.4	Data Processing. . . . .	3-68
3.2.5	Display. . . . .	3-83
3.3	Functional Specifications	
3.3.1	LEM Interface. . . . .	3-93
3.3.2	LEM Sounding Probe . . . . .	3-98
3.3.3	Penetrometer . . . . .	3-110
3.3.4	Deployment Launcher. . . . .	3-111
3.3.5	Communications . . . . .	3-115
3.3.6	Data Processor . . . . .	3-119
3.3.7	Display. . . . .	3-123

CONTENTS (Continued)

SECTION		PAGE
4	LEM PAD IMPACT TESTING AND DATA ANALYSIS	
	4.1 LEM Pad Impact Testing	
	4.1.1 Test Objectives and Description . . . . .	4-1
	4.1.2 Dynamic Test Results. . . . .	4-2
	4.2 Data Correlation and Analytical Models	
	4.2.1 LEM Pad Test Data . . . . .	4-11
	4.2.2 Continued Detailed Study of Penetrometer Data . . . . .	4-11
	4.2.3 Soil Mechanics Studies. . . . .	4-15
5	EVALUATION AND IMPROVEMENT OF PROTOTYPE PENETROMETERS	
	5.1 Testing of Prototpye Penetrometers	
	5.1.1 Impact Tests. . . . .	5-1
	5.1.2 Captive Hyge Shock Test . . . . .	5-10
	5.1.3 Disassembly and Diagnostic Testing. . . . .	5-13
	5.1.4 Summary of Calibration and Performance Anomalies . . . . .	5-13
	5.1.5 Signal Electronics - Accelerometer Compatibility Tests . . . . .	5-16
	5.1.6 AM Demodulator Waveform Sensitivity Tests . . . . .	5-20
	5.1.7 40 KHz Multivibrator Frequency Stability Tests . . . . .	5-23
	5.1.8 Internal vs. External Power Performance Tests . . . . .	5-23
	5.1.9 Residual 40 KHz Offset in Prototype Number 3. . . . .	5-26
	5.1.10 Acceleration Trace Hang-up. . . . .	5-26
	5.2 Penetrometer Module Evaluation	
	5.2.1 Crystal-Controlled Oscillator Module. . . . .	5-28
	5.2.2 Calibration Signal Injection. . . . .	5-30
	5.2.3 Shock Qualification of Epoxy- Encapsulated Diodes . . . . .	5-31
	5.2.4 Shock Investigation of Metal-Film Resistors . . . . .	5-33

CONTENTS (Continued)

SECTION		PAGE
5.2.5	Substitution of MOS FET'S with Junction FET'S . . . . .	5-33
5.2.6	High-Megohm Metal Film Resistor Search. . . . .	5-34
5.2.7	Establishment of American Battery Source. . . . .	5-34
5.3	Critical Long-Lead-Time Parts Procurement . .	5-39

## SECTION 1

### INTRODUCTION

This report presents the results of additional work on the Lunar Penetrometer System (LPS) conducted by Aeronutronic for the Langley Research Center, National Aeronautics and Space Administration, under Contract No. NAS1-4923. This reported effort covered the period from 15 March to 13 May 1966. The effort was accomplished in accordance with a work statement specifying four technical tasks which were extensions of the work performed during the prior year under the initial LPS program.

The first task was a preliminary study of the application of the developed penetrometers as sounding devices for a landing Apollo LEM. Two tasks were concerned with a continuation of LEM pad impact testing and data analysis. The other task involved further development and evaluation of the prototype penetrometers built in the initial program. This report presents the analytical and conceptual design study results, preliminary functional specifications, test results, test result evaluations, and redesign evaluations obtained in these activities.

Many of the subjects discussed in this report are best understood by reference to the two final report volumes of the initial contractual work, i.e., Aeronutronic Publication No. U-3556, "Final Report - Research, Development, and Preliminary Design for the Lunar Penetrometer System Applicable to the Apollo Program," and Publication No. U-3557, "Flight Hardware Development and Delivery for the Lunar Penetrometer System Applicable to the Apollo Program," both dated 27 April 1966.

## SECTION 2

### SUMMARY

In a brief but intensive study, the previously developed Lunar Penetrometers were studied as potential Sounding Probes for a manned Apollo LEM landing. The effort was divided into three main portions:

- (1) A preliminary system concept was formulated for using Penetrometers as Sounding Probes for the LEM descent.
- (2) Trade-off studies were performed of how the penetrometers could be deployed, the data handled, and the results interpreted.
- (3) Preliminary functional specifications were prepared describing the major assemblies of the system and their interfaces with the LEM vehicle.

Among the important results of the study were the findings that the Sounding Probe application appears feasible with a relatively simple system, there is a limited range of possible launch times during the LEM descent trajectory, and penetrometer impact angles and velocities are relatively fixed for all favorable launch conditions. Emphasis in the study was placed on showing trade-offs available and system limitations rather than concluding with a fixed system design.

Throughout the Sounding Probe Study, it was definitely assumed that the probe system was an add-on device to the LEM requiring minimum interfaces and that the data results from the impacting penetrometer spheres would only assist the astronauts in their landing decision - not make the abort or landing decision.

LEM Pad impact testing was continued by performing an additional 12 simulated Lunar drop tests at 3 and 7 ft/sec into several types of Nevada sand. These tests were conducted with the test equipment described in previous reports. All of the tabulated data are contained in this report. Curves are presented showing LEM Pad penetration as functions of bearing strength, soil material and time.

The data analysis and analytical work in support of the LEM Pad testing were continued. Again, it was found that the dynamic penetration depths measured exceeded those predicted by analytical models based on measured static characteristics. The so-called "jack-hammer" effect of crushing honeycomb was absolved of causing the added penetration. Possible theories for the dynamic effects were reviewed, but it was concluded that additional fundamental soil mechanics research work is needed.

During this contractual period, additional effort was placed on testing and evaluating the two prototype penetrometers fabricated during the initial LPS program. Some of the operational anomalies under extreme impact conditions were explained by the discovery of such things as damaged integrated circuits, low battery voltages, and zero drift in the test calibrations. A number of possible module circuit improvements were investigated and are recommended for inclusion in future penetrometer models. Among the recommended changes are:

- (1) A new method of calibration signal injection.
- (2) Replacement of glass diodes with epoxy-pac diodes.
- (3) Use of metal-film resistors in place of carbon composition resistors.
- (4) Possible replacement of the integrated circuit amplifiers with an improved model.
- (5) Elimination of one MOS-FET.

Encouraging shock test results were achieved with a crystal-controlled oscillator. There would be many benefits in replacing the present LC oscillator with a crystal-controlled model, but more test experience is required first.

An extensive search was made to find an American source for the required penetrometer battery. The results were not too encouraging but all negotiations could not be completed in time for this report. However, an alternative plan using fewer but larger battery cells with a DC to DC converter was suggested and should be independently pursued.

## SECTION 3

### SOUNDING DEVICE APPLICATION STUDY

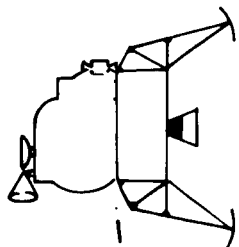
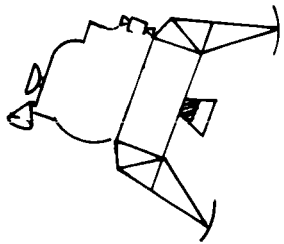
The original use contemplated for the Penetrometers was as surface measuring instruments to be deployed from a Lunar Survey Probe vehicle which descended to near the lunar surface from an orbiting Apollo spacecraft. The penetrometers would obtain scientific data on surface characteristics as well as certify a prospective landing site for a later Apollo LEM landing. However, it became obvious during the original LPS contract period, that the developed penetrometers could also serve a valuable function on an actual landing Apollo LEM as a sounding device to assist in making an on-the-spot decision whether a safe landing could be made. Therefore, a brief but intensive system study was undertaken to evaluate the penetrometer for this application. This study included analysis, trade-offs, conceptual design, and preparation of preliminary functional specifications.

It should be noted that a study of this short duration could only begin to define and solve the problems in integrating the Sounding Device into an Apollo LEM mission. A system concept is functionally described, but it is expected to be considerably modified as the system definition progresses. Study areas requiring early attention are outlined in this section.

#### 3.1 SYSTEM DESCRIPTION

##### 3.1.1 PURPOSE

The LEM Sounding Probe will be used by the LEM crew to test the condition of the lunar surface prior to landing. Its sensors are Penetrometer spheres that are launched either singly or in salvo from the vicinity of Low Gate in the descent trajectory as shown in Figure 3-1. They are automatically aimed to land within the nominal LEM landing zone and during their moment of contact with the surface will most likely be seen by the crew. Each

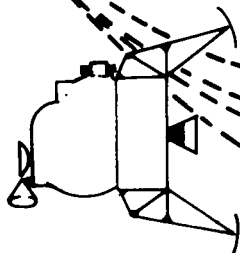


ORIENT AND FIRE PENETROMETERS

$\Delta V = 40/100$  FPS

ALTITUDE = 500/1000 FT

RANGE = 1200/3200 FT



LUNAR SURFACE

PENETROMETER  
IMPACT PATTERN

FO4346 U

FIGURE 3-1. SOUNDING PROBE OPERATIONAL PROFILE

Penetrometer transmits an acceleration-time profile during impact. From the profile are deduced characteristics of surface hardness. On board the LEM is a separate receiver, data processor, and display console that digests the data and indicates the advisability of landing. The final decision to land, however, rests with the crew. Other than drawing power and monitoring LEM navigational data, the Sounding Probe operates autonomously and is categorized as an add-on device. In Table 3.1 is a summary of its salient characteristics.

Minimal crew activity is required to operate the unit. Turn-on of the equipment and pressing the launch button are all that are necessary. No sighting or aiming through a reticle is necessary since the launcher attitude is varied and continuously updated during flight to control launch angle. Within a certain range, even the LEM altitude is not critical. This permits the crew to select any convenient launch time near Low Gate. Neither the nominal LEM attitude nor trajectory are affected since launch angle data are continuously corrected throughout the descent phase. The Sounding Probe has its own computer so there is no interference nor changes in the LEM electronics to accommodate this device.

The purpose of a recent phase of the program for which this report is submitted was to perform trade-off studies and submit functional specifications for the Sounding Probe. Areas of chief concern to each of the subsystems were investigated and tentative design considerations listed. These are:

- (1) Data Model. Interpretation of Penetrometer data insofar as it is understood at this time is discussed in Paragraph 3.2.1. Preferred parameters to measure and their confidence are designated.
- (2) Deployment. Both LEM and Penetrometer trajectory data are graphically displayed. There is only a limited range of parameters within which a choice of launch time is permitted. These data are presented in Paragraph 3.2.2.
- (3) Communications. The ability to launch more than one Penetrometer in a salvo requires a multichannel diversity receiver. Its characteristics are discussed in Paragraph 3.2.3.
- (4) Data Processing. The logic circuitry for measuring parameters and rendering a decision are studied in Paragraph 3.2.4.

TABLE 3.1

MAJOR FEATURES OF SOUNDING PROBE

Operating Mode	Automatic with selective launch time
Launch Altitude	1000 feet
Number of Penetrometers	4 (nominal)
Weight	30 pounds
Operating Time	2 minutes
Data Display	Digital Lights: go/no-go Analog Meter: Vernier assessment
Power Consumption	50 watts
Aiming and Sighting	None required by Crew
Landing or Abort Decision	Up to Crew
Changes to LEM Equipment	Minor
Changes to LEM Trajectory	None
Installation	Add-on

- (5) Display. Alternate concepts for presenting the data and automatically tracking Penetrometer impact locations relative to the LEM are discussed in Paragraph 3.2.5.
- (6) Specifications. An interface specification with the LEM as well as preliminary functional specifications for the complete Sounding Probe and its five major subsystems are given in Paragraph 3.3.

### 3.1.2 CONSTRAINTS

Specific constraints that have been observed during this study are:

- (1) The nominal LEM trajectory during the descent phase is shown in Figure 3-9. If these data change, then the flight mechanics of the Penetrometer as shown in Figures 3-8, 3-10 and 3-11 will also change.
- (2) Penetrometer data are to be acquired, processed, displayed, and assimilated by the crew by the time the LEM reaches an altitude of 200 feet from the lunar surface.
- (3) It is desirable but not mandatory to restrain the impact velocity of the Penetrometer to a low value where parameters describing soft uncertain surfaces are more readily discernable.
- (4) The decision to land or abort must be left to the LEM crew.
- (5) Only five pounds of controls and display are allowed in the ascent stage. The remainder of the equipment is in the descent stage. No attachments are to be made to the exterior skin of the LEM. The launch pod may not be attached to a primary or secondary strut or to a foot pad.
- (6) The system is to perform site verification (certification) with site selection as a secondary objective.
- (7) Penetrometers are to be manually fired by the LEM crew.
- (8) Penetrometer data are to be simultaneously relayed to Earth.

Although not constraints, further ground rules have been observed during this study and are referred to as assumptions.

- (1) LEM altitude, horizontal range to touchdown, horizontal and vertical velocity components and pitchback angle are available from the LEM navigational computer. A continuous flow of this information to the Sounding Probe during the last five minutes of flight is desired.
- (2) Power is available from the LEM at an average level of 50 watts for ten minutes during descent. Surge power for handling up to 8 squibs simultaneously is also available.
- (3) The launch velocity of the Penetrometers is fixed but the launch angle is varied by a control mechanism so that impact will occur within the nominal LEM landing footprint. Further study may well eliminate the variable launch angle requirement.
- (4) There is no display for recording the location in space of impacted Penetrometer.
- (5) The LEM does not yaw appreciably during descent. Otherwise, yaw angle must be used to correct the launch angle of the Penetrometers, or else a yaw limitation must be imposed at the moment of launch.
- (6) In the crew cabin, panel 8 is available for arming and launching switches and panel 10 is available for the remainder of displays and controls.
- (7) Penetrometer transmitters do not turn on until launch and automatically turn-off shortly after impact.
- (8) Within any 28-foot diameter circle the lunar surface is relatively homogeneous.
- (9) Thermal control for components mounted on the LEM descent stage is provided by the Sounding Probe.

### 3.1.3 OPERATION

Three modes of operating are worthy of mention and are identified by the manner in which the Penetrometers are launched. Assume for this discussion

that four Penetrometers are stowed in the launch pod. Based upon Penetrometer data alone, the probability of a safe landing is 0.9 if four independent penetrometers are launched toward a surface whose area is only 30 percent acceptable. By launching all four in one salvo there is minimum distraction of the crew, but a 4-channel diversity receiver is required. The number of channels required in the receiver matches the number of Penetrometers that are simultaneously in flight.

To allow the crew as much time as possible to make a decision after the data are displayed, all Penetrometers should be launched at an altitude of about 1000 feet. The control system orients the launch pod so that if the Penetrometers are ejected at a velocity of 50 ft/sec, the pod is canted at an angle of 60 degrees above a horizontal reference plane. There will be 18 seconds left from the time they impact the surface until the LEM reaches an altitude of 200 feet. To process the data, up to 2 seconds are required for each Penetrometer. Data from one are displayed within the first 2 seconds, the second within the first 4 seconds, the third within the first 6 seconds, and the fourth within the first 8 seconds leaving 10 seconds of additional time for the crew to make a decision prior to reaching an altitude of 200 feet.

Another mode is to launch the four Penetrometers sequentially. As can easily be seen, if the first is launched at the same altitude as before and more than 2 seconds elapses between launchings, then there will be less time than before to make a decision. This mode requires more attention from the crew for launching but only demands a single channel receiver.

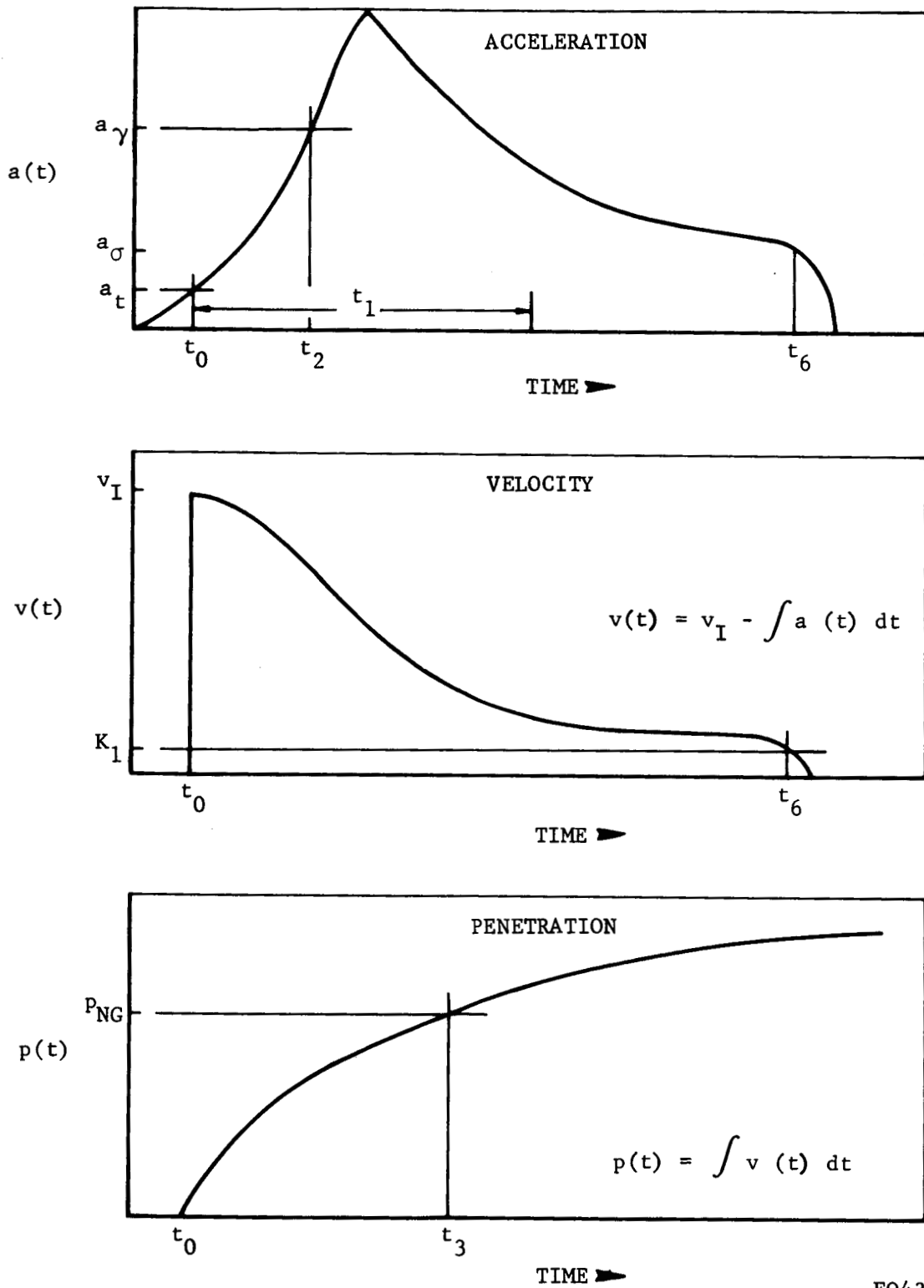
As a compromise, a salvo of only two may be launched at the same altitude as before. Again there are 18 seconds from the time they impact until the LEM reaches an altitude of 200 feet. Deducting 4 seconds for processing leaves 14 seconds. Using 2 of these for crew interpretation still leaves 12 seconds, which is just sufficient time to make another salvo launch of the two remaining Penetrometers into a selected zone and still have 2 seconds after processing to make a decision before reaching the 200-foot altitude. The advantages and disadvantages of each mode are summarized in Table 3.2. It would appear that a system designed to launch multiple salvos (maybe not more than 2 are needed) represents a preferred compromise.

The Data Processor automatically analyzes the acceleration data from each Penetrometer. For illustrative purposes three parameters shown in Figure 3-2 have been selected and are subjected to examination. The parameter operations occur in parallel in that any or all may be deleted and substituted with other measurements. The results of these measurements are independent output signals and are used to formulate and transfer a single decision to the display. If a peak in the acceleration signal exceeds a preset threshold there is good indication that the density of the surface may be satisfactory for a LEM landing. This must be attained prior to

TABLE 3.2

SALVO VERSUS SELECTIVE LAUNCHING  
(4 Penetrometers)

	<u>4 Launches of 1 each</u>	<u>2 Salvo of 2 each</u>	<u>1 Salvo of 4</u>
Receiver	Smallest		Largest
Required Crew Attention	Most	Somewhere Between	Least
Time Available for Crew Decision	Least	the to Extremes	Most
Impact Zone Selection	Most		Least



FO4347 U

FIGURE 3-2. HYPOTHETICAL TIME PROFILES OF ACCELERATION, VELOCITY AND PENETRATION

a precalculated time that is analogous to a depth beyond which the LEM and ascent stage cannot be recovered. Another measurement is the total depth of penetration as calculated from the second successive integral of acceleration. It also may not exceed a preset value. Lastly, the small plateau that appears at the tail of most acceleration profiles is a good measure of the surface bearing strength. If its value exceeds a specified threshold, then again there is a good reason to believe the surface is safe for landing. A composite result of these measurements for each Penetrometer is provided as both a digital go/no-go display and also as a pointer on a continuous scale to give the degree of goodness. Either or both may be accepted or rejected by the crew.

Major assemblies of the Sounding Probe are listed in Table 3.3. Figures 3-3 and 3-4 show the functions and locations of the subsystems. Table 3.4 is a summary of the salient features of the subsystems.

#### 3.1.4 FURTHER STUDY

For the next phase of system definition and conceptual design of the Sounding Probe, it appears appropriate to cite specific areas that deserve more rigorous attention and analysis. Major trade-offs still remaining include:

- Number of Penetrometers versus system weight.
- Penetrometer impact velocity versus time left for crew to make decision.
- Launch mode versus multichannel receiver weight.
- Crew decision time versus multichannel Data Processor weight.

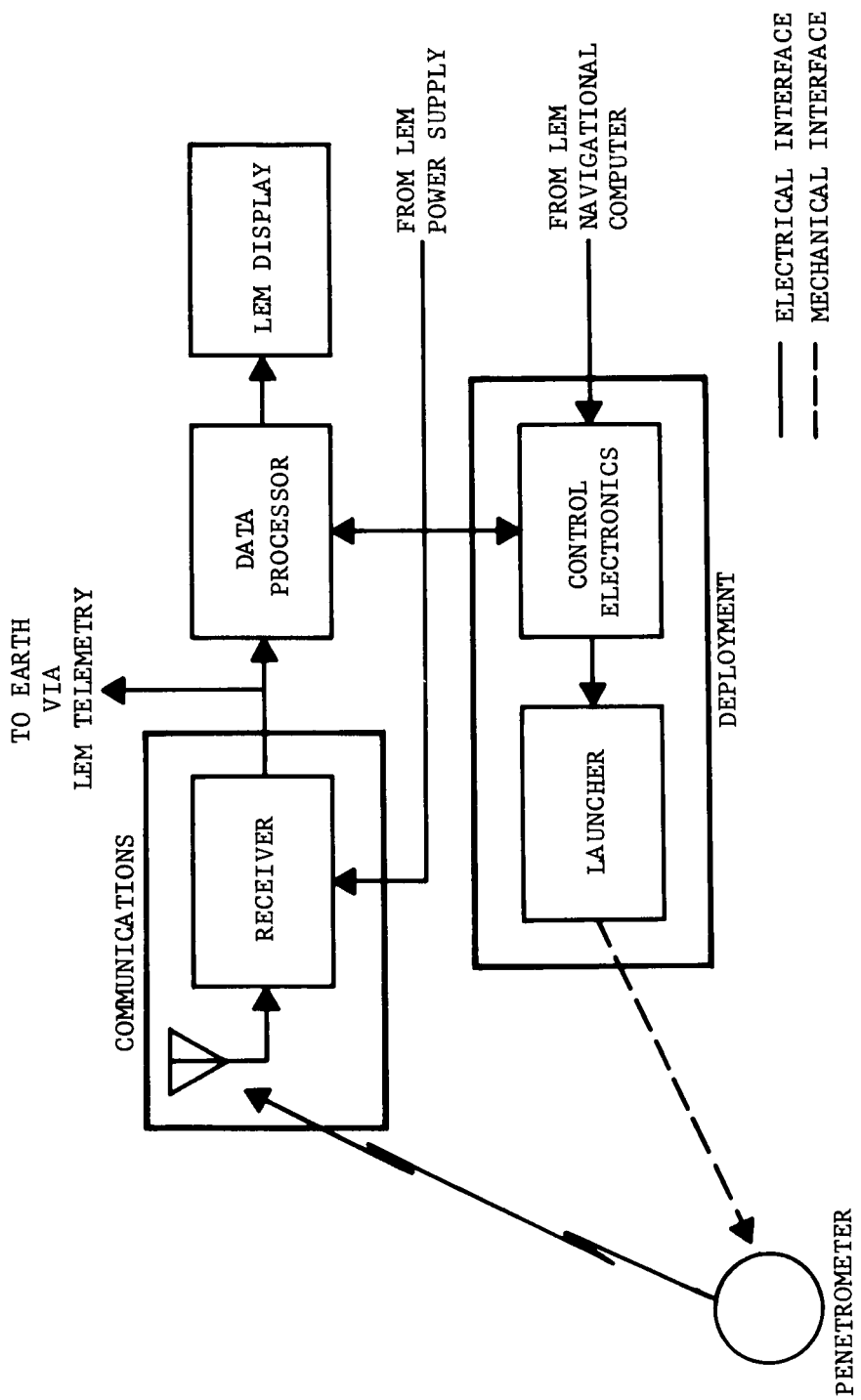
To solve these trade-offs there is obviously a necessity to formulate conclusions in the following study areas:

- (1) Determine if any other parameter(s) should be measured aside from the three that have been considered during this study. Possible contenders derivable from acceleration data are:
  - Time to second peak
  - Onset rate
  - Rise time
  - Pulse duration
  - Ratio of peak-to-tail

TABLE 3.3

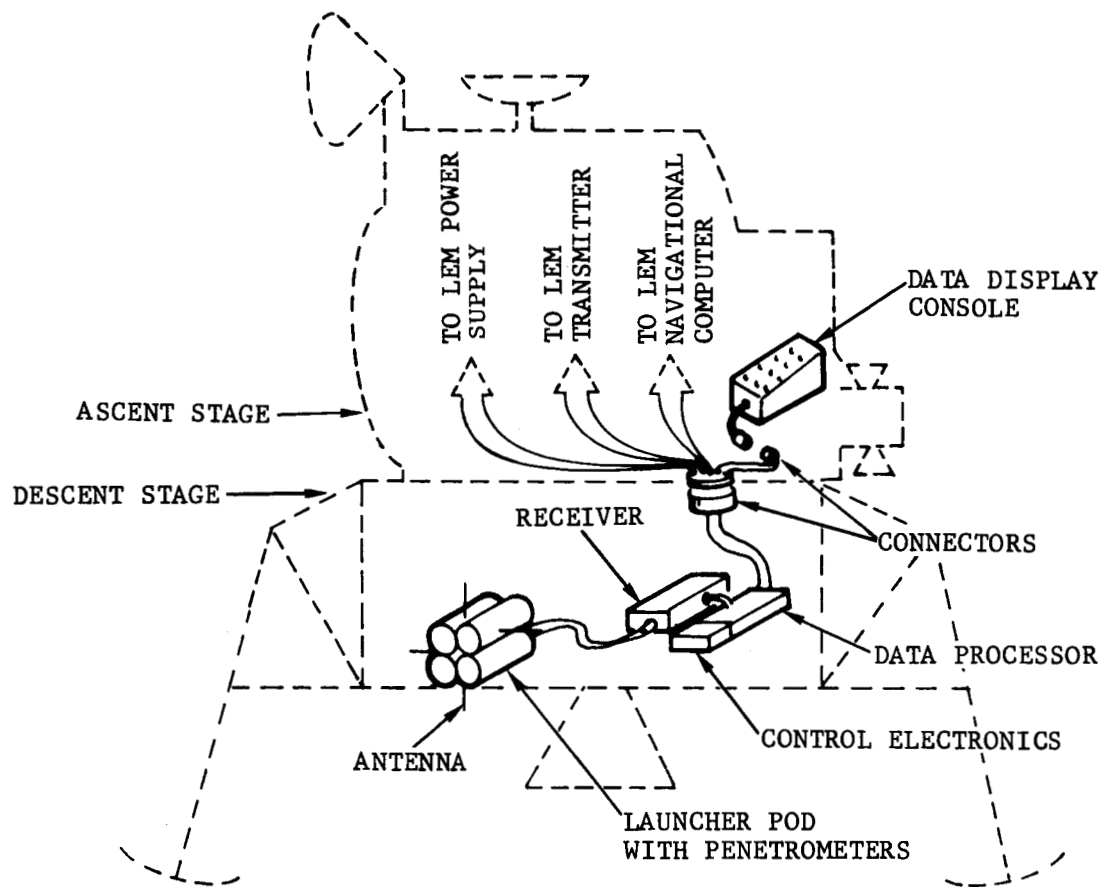
## SOUNDING PROBE WEIGHT BUDGET

	<u>Estimated Weight Pounds</u>
Penetrometers (4)	14.0
Data Processing	3.0
Display	1.5
Launch Pod	3.0
Receiver (single channel)	2.5
Antenna	0.8
Thermal Control	1.1
Cabling	1.1
Mounting Bracketry	1.2
Growth Allowance	<u>2.0</u>
TOTAL	30.0



FO4348 U

FIGURE 3-3. SOUNDING PROBE FUNCTIONAL DIAGRAM



FO4349 U

FIGURE 3-4. SOUNDING PROBE SUBSYSTEM DISTRIBUTION

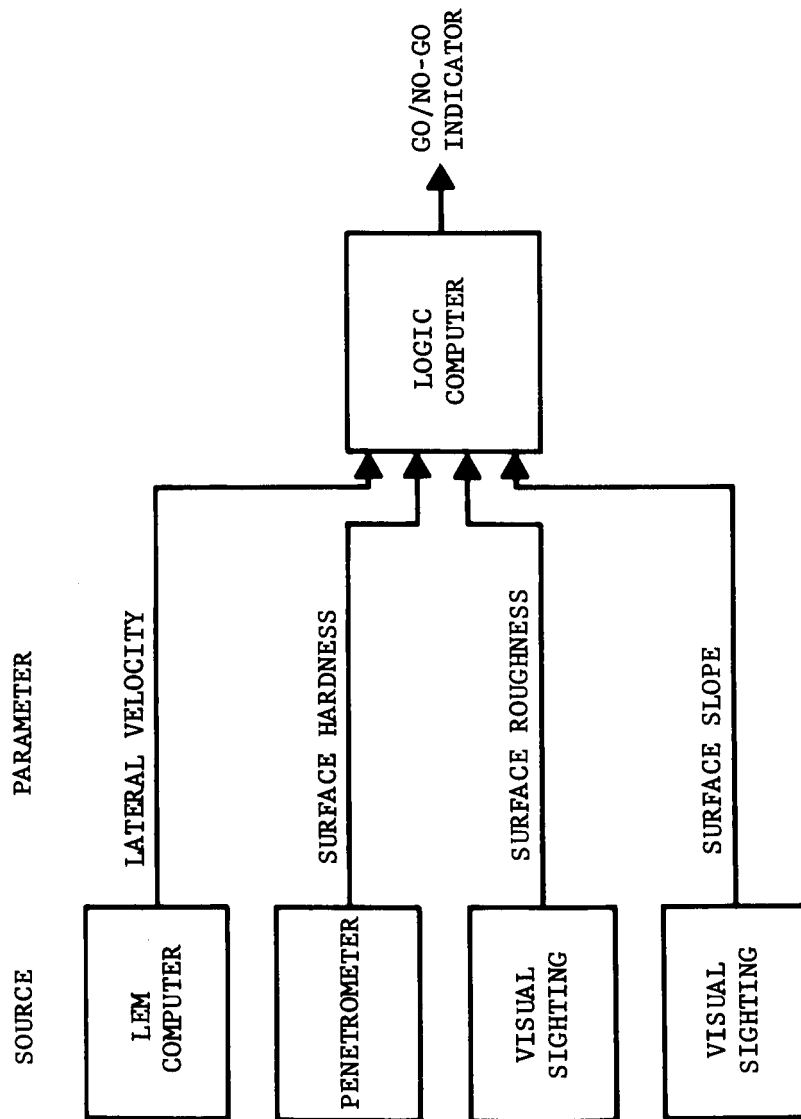
TABLE 3.4

SUBSYSTEM CHARACTERISTICS

PENETROMETER	Omni-directional within $\pm$ 10 percent, 50 g to 7000 g
COMMUNICATIONS	Diversity reception (multi- channel optional)
DATA PROCESSOR	Multichannel simultaneous input, sequential output, 2 seconds computation per channel.
DISPLAY	Digital lights: 3 level go/no-go.  Analog Meter: continuous vernier assessment.
DEPLOYMENT	Fixed launch velocity vari- able launch angle.

Also, determine relative weights to assign to each measurement. Then, either by hand or computer, test the theoretical data processor for all possible inputs.

- (2) Define thermal control for not only the launch pod assembly but also the electronics in the descent stage.
- (3) Program Penetrometer flight trajectory and error analysis on a computer so that sensitivity of the design to changes in the nominal LEM trajectory can be evaluated.
- (4) More detailed study of the servo control of the launch pod is required.
- (5) Penetrometer data could be just one of the many inputs toward formulating a landing decision. Figure 3-5 illustrates four inputs to a mechanization. The question that needs answering is, "Can the crew make all of these decisions in their heads?"
- (6) Conduct a trade-off study of the Data Processor to determine the weight versus processing time for analog versus digital circuitry. This decision is dependent not only on weight of equipment but also on accuracy, speed and flexibility of operation.
- (7) Visibility of the landing site as well as effects of the rocket plume and the solar lighting angle deserve consideration.
- (8) The desirability and configuration of a landing site selection device to augment the Penetrometers should be studied further.
- (9) Devise a truly analog output to a meter display.
- (10) Determine the launch pattern, the method of propulsion and analyze the launch impulse and its effect upon the LEM.
- (11) Features to visually track the Penetrometers and identify the point of impact such as flares, streamers, tracers, dye markers, etc., must be defined.



F04350 U

FIGURE 3-5. MULTIPLE INPUT LANDING DECISION

## 3.2 ANALYSES

### 3.2.1 DATA MODEL

a. Critical Parameters. The minimum bearing strength of an engineering model of a structurally weak layer has been defined by NASA as a material for which a:

- (1) Static load of 1 psi will penetrate no more than 3.9 inches (10 cm).
- (2) Dynamic load of 12 psi will penetrate no more than 23.6 inches (60 cm).

Coupling this definition to an assessment of lunar geology provides a basis for determining the critical lunar surface types to be measured. The significant lunar surface models appear to be:

- (1) Low bearing strength materials, including:
  - o Suspended dust (low density and low bearing strength).
  - o "Fairy castle" structure (high density and low bearing strength).
  - o Structurally weak rock froths (low density and low bearing strength).
- (2) Thin, penetrable crusts overlying and concealing:
  - o Voids
  - o Low bearing strength materials.
- (3) Thin, structurally weak layers overlying and concealing:
  - o Voids
  - o Rugged, blocky subsurfaces.

The dynamic reaction of the penetrometer to these critical materials and surfaces must be correlated with the dynamic reaction of a LEM landing pad to similar materials and surfaces in order to predict a safe landing mode for the LEM vehicle. This correlation will have to be accomplished in terms of soil properties including all of the soil mechanics parameters that define bearing strength and density terms.

b. Acceleration Signature. The pulse resulting from the impact of a penetrometer at velocities ranging from 20 to 250 fps can be directly related to the properties of the target materials. A gross analysis of the pulse signature can be obtained by relating certain characteristics of the pulse curve to the gross density and the static bearing strength of the target material. The gross density term represents:

- (1) The gross density of the solid particles and water films or coatings.
- (2) The gross porosity of the material

The static bearing strength term for particulate materials is related to the following soil property expressions:

- (1) The Coulomb Theory effect which relates the shearing resistance of a particulate material to its cohesion and coefficient of internal friction.
- (2) The Terzaghi effective stress concept which modifies the normal stress on the shearing plane due to grain shapes and pore air pressure build-up effects (which occur as the grain size and/or permeability are decreased).
- (3) Particle contact distribution theories that are related to the degree of sorting and compaction of particulate target materials.

For materials that react to impact like a low bearing strength solid, e.g., a foam, the density and static bearing strength terms define the character of the pulse and the resulting depth of penetration very well. For particulate materials, the reaction and resulting pulse and displacement value must be modified to include a volume of target materials directly displaced by the penetrometer and moving with it in obedience to the effects discussed above.

The descriptive characteristics of the acceleration signature (a-t) pulse include the onset rate or the initial slope of the peak g curve, the peak g value, the time to peak g value, the g level of the tail-off plateau, and the total pulse duration. If layered materials are involved, the time to the second peak g point and its peak g value should be added to the list. In the layered material case, the tail-off plateau will be descriptive of the last material penetrated. These descriptive characteristics of an a-t pulse can be related to the soil parameters previously discussed. This relation and the degree of accuracy expressed by the relation is illustrated on the matrix presented as Table 3-5. This matrix was employed to select



measurement parameters evaluated for processing in the Data Processor. The soil models designated in Table 3-5 were defined as follows:

CLASS I - HOMOGENEOUS MATERIAL MODELS:

Model 1. NASA minimum bearing strength model:

Material: Loosely packed, crushed olivine basalt silt (325 mesh) prepared by bubbling nitrogen or compressed air through a diffuser and up through the material.

Properties: The bearing strength properties of this material are very close to the NASA minimum criteria:

- Static bearing strength - 1 psi at 3 inches penetration.
- Dynamic bearing strength - 20 psi at 23 inches penetration.

Model 2. Intermediate "fairy castle" structure, bonded, cohesive granular model consisting of three submodels:

Material: Submodel A: Scott reticuled foam (high permeability lattice) filled with bonded (slow hardening epoxy), high density, Ba SO<sub>4</sub> (barite) sand (60-120 mesh).

Submodel B: Sublimed or leached dispersion of bonded (hard asphalt) Ba SO<sub>4</sub> sand particles in a volatile or soluble matrix (e.g., very coarse salt grains, 1/4 to 1/2 inch).

Submodel C: Bonded (quick drying polyester) Ba SO<sub>4</sub> sand sprayed from a Flint-kote Sealzit spray gun into a container elevated at 45° to 90° to form a "fairy castle" network of particle chains.

Properties: Low bearing strength, high density and very high permeability and void ratio models. Submodel A can be prepared to investigate 40-60 lb/ft<sup>3</sup> materials; submodel B, 30-40 lb/ft<sup>3</sup>; and submodel C, 10-30 lb/ft<sup>3</sup> materials.

Model 3. Absolute minimum bearing strength flocculent, suspended dust model;

Material: Compacted Cabosil prepared by initially bubbling nitrogen or compressed air through a diffuser and then through the material and finally compacting the loose Cabosil with a vibrating hose.

Properties: The bearing strength characteristics of this minimum model are:

- Static bearing strength = 1 psi at 15 inches penetration.
- Dynamic bearing strength = 13 psi at 54 inches penetration.

CLASS II - MODELS OF MIXTURES FOR STATISTICAL SERIES OF TESTS:

Model 1. Poorly graded, non-cohesive agglomerate:

Material: Prepared by mixing equal volumes of crushed olivine basalt cobbles, pebbles, sand and silt and Cabosil.

Note: This model will support a LEM landing; it is included to test statistical variations in the a-t signatures.

Model 2. Isolated cobbles in a structurally weak material:

Material: Evenly dispersed cobbles of olivine basalt in a poured Cabosil matrix ( $\approx$  9:1 ratio of matrix to cobbles).

Note: This model is included to statistically test the a-t signatures that result from isolated hard particles in a low bearing strength material.

CLASS III - MODELS OF LAYERED MATERIALS AND CRUSTS:

Model 1. Vacuum bonded crust model:

Material: A preformed layer of 1-2 feet of "Fairy castle" structure material (Model IIA or IIB) overlying compacted Cabosil.

Model 2. Thin lava crust model:

Material: A 6-inch thick sawed pumice block overlying compacted Cabosil.

Model 3. Meteorite slag crust model:

Material: A sheet of window glass or a layer of preformed slag (metal and silicate slag) overlying compacted Cabosil.

Note: Any or all of the above models could also be suspended over a void and test the case of hard to cohesive crusts overlying voids.

Model 4. Minimum bearing strength, structurally weak material overlying a rigid surface:

Material: Compacted Cabosil overlying a rigid steel plate.

### 3.2.2 DEPLOYMENT

a. Penetrometer Trajectory. An analysis was made to determine launch, flight and impact parameters of penetrometers launched from the LEM Vehicle during final approach. Launch velocity can vary between 30 and 130 ft/sec; launch angle between  $60^{\circ}$  above to  $20^{\circ}$  below the local horizontal requiring launch angle control to achieve precise range control; impact velocities are limited to a maximum of 200 ft/sec and may be as low as 120 ft/sec; at these velocities impact angles vary between  $54^{\circ}$  and  $62^{\circ}$  from the vertical; for the trajectory used, the earliest a penetrometer can be launched is at a range of 3400 feet and an altitude of 1075 feet; time available to the crew for analysis of penetrometer data can be as long as 16 seconds.

The following presents the development of penetrometer trajectory equations and a discussion of the results.

(1) Equation Derivation. The equations describing penetrometer ballistic flight and impact on the lunar surface are derived in this section. Basic equations are developed to describe penetrometer flight time, range, impact velocity, and impact angle in terms of LEM altitude and velocity, and penetrometer launch angle and velocity.

For ease in handling equations, the vehicle and penetrometer velocities are defined in terms of horizontal and vertical components as shown in

Figure 3-6. The linear vertical distance covered by the launched penetrometer is defined in terms of the vertical velocity as:

$$H = \bar{v}_{yo} t + 1/2 at^2 \quad (1)$$

where

H = vehicle altitude at penetrometer deployment, ft.

$\bar{v}_{yo}$  = Initial vertical component of Penetrometer velocity, ft/sec =  $(v_{yi} + V_y)$

$V_y$  = Vehicle vertical velocity at launch, ft/sec

$v_{yi}$  = Vertical velocity imparted by launcher, ft/sec

a = lunar gravity -  $5.315 \text{ ft/sec}^2$ .

Substituting for  $\bar{v}_{yo}$ , Equation (1) becomes:

$$H = (v_{yi} + V_y) t + 1/2 at^2 \quad (2)$$

from which penetrometer time of flight, t, is found to be:

$$t = - \frac{v_{yi} + V_y}{a} + \sqrt{\left(\frac{v_{yi} + V_y}{a}\right)^2 + \frac{2H}{a}} \quad (3)$$

Range of penetrometer flight is simply:

$$R = (v_{xi} + V_x) t, \quad (4)$$

Where:

$(v_{xi} + V_x)$  = Horizontal component of penetrometer velocity, ft/sec.

$V_x$  = Vehicle horizontal velocity at launch, ft/sec

$v_{xi}$  = Horizontal velocity imparted by launcher, ft/sec.

The velocity,  $v_i$ , imparted to the penetrometer, and the launch angle,  $\delta$ , relative to the local horizontal are defined in terms of  $v_{yi}$  and  $v_{xi}$  as:

$$v_i \cos \delta = v_{xi} \quad (5)$$

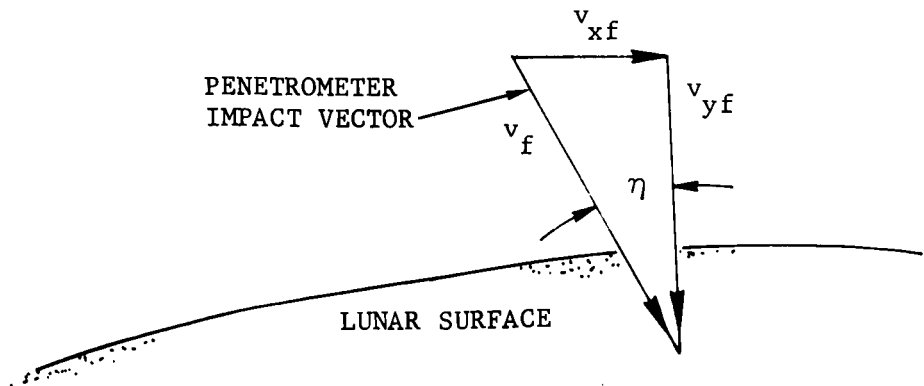
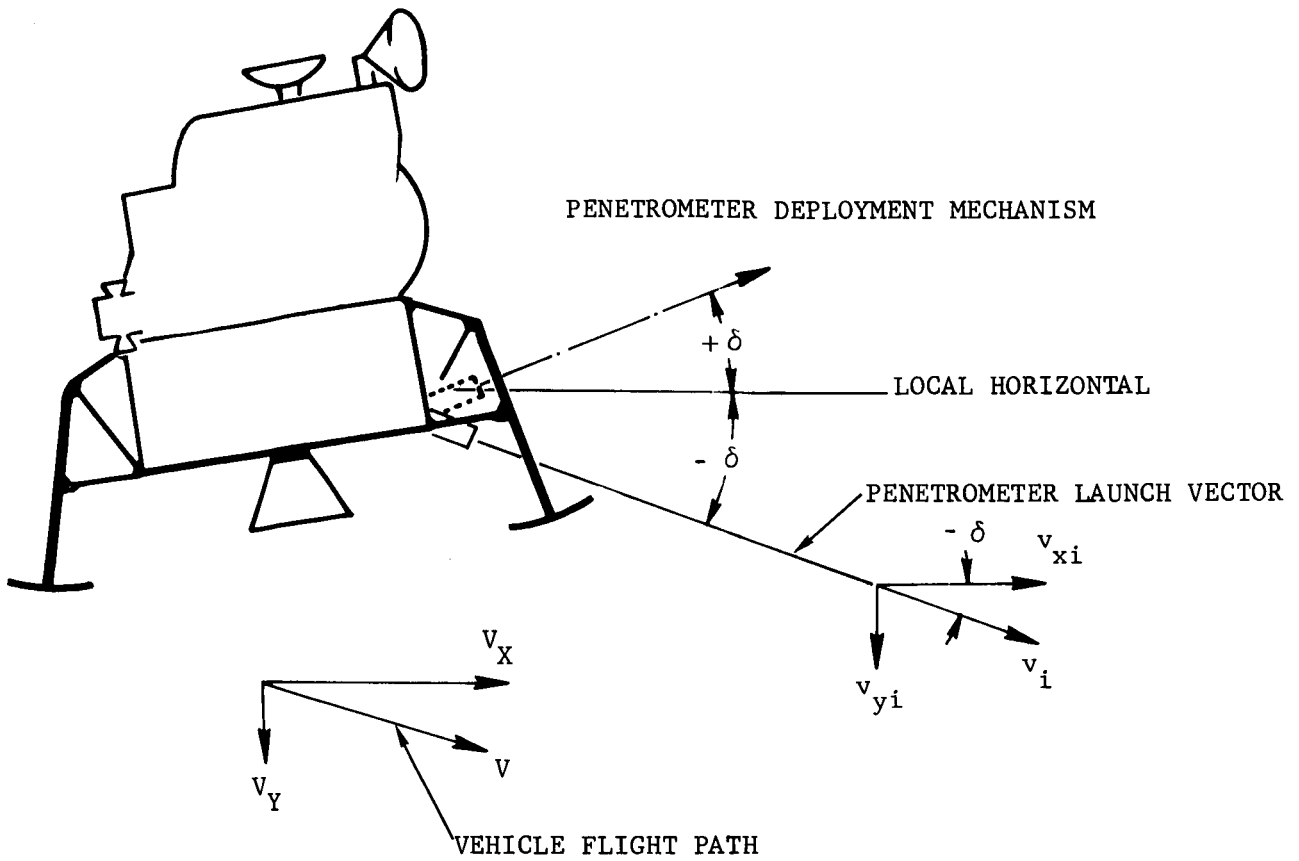


FIGURE 3-6. PENETROMETER DEPLOYMENT PARAMETERS

$$v_i \sin \delta = v_{yi} \quad (6)$$

where  $\delta$  is positive above the local horizontal and negative below. Vertical velocity components are defined as positive in the downward direction so that a  $+\delta$  goes with a  $-v_{yi}$ . Horizontal velocity components are positive in the direction of flight.

Examination of the components of velocity of the penetrometer at impact (Figure 3-6), reveals that the horizontal and vertical velocity components are:

$$v_{xf} = v_{xi} + V_x \quad (7)$$

$$v_{yf} = v_{yi} + V_y + at \quad (8)$$

from which impact velocity,  $v_f$  is found to be:

$$v_f = \sqrt{(v_{xi} + V_x)^2 + (v_{yi} + V_y + at)^2} \quad (9)$$

impact angle,  $\eta$ , is defined in terms of impact velocity,  $v_f$ , and the horizontal impact velocity component as:

$$\sin \eta = \frac{v_{xi} + V_x}{v_f} \quad (10)$$

Equations (3) through (6), and (9) and (10) completely defines a penetrometer launch for any single point in the LEM trajectory (Figure 3-7). A typical display of these six equations, presents flight time, impact angle, impact velocity, and range of flight as functions of launch angle,  $\delta$ , and launch velocity,  $v_i$ . This is for a single point in time in the LEM trajectory (an obsolete trajectory was used to compute these data). Since it is desirable to investigate penetrometer launch requirements as functions of LEM approach position (effectively time), the six equations are redefined to produce a set of curves that collectively define launch requirements for any position in the LEM approach trajectory.

Examination of the six basic equations in light of the nominal LEM trajectory shows that the practical limits of impact angle,  $\eta$ , are  $40^\circ$  to  $70^\circ$ . This, in addition to the knowledge that acceptable impact velocities are limited to a maximum of approximately 200 ft/sec aids in selecting  $\eta$  and  $v_f$  as independent parameters. Equations (3) and (6) are retained in their original form, and the following four equations are derived by combining Equations (3) through (6) and (9) and (10).

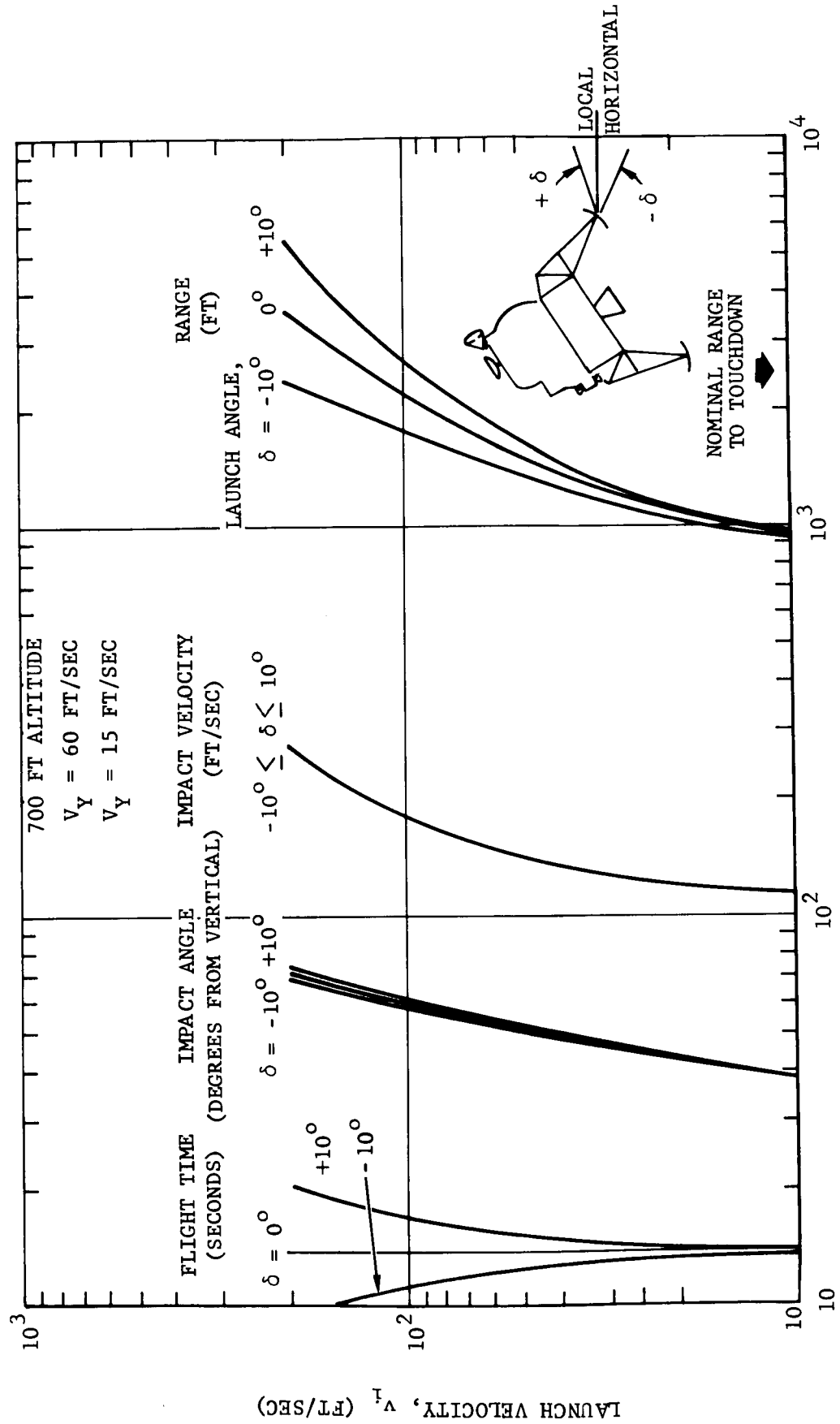


FIGURE 3-7. DEPLOYMENT TRADE-OFF

F04352 U

$$R = (v_f \sin \eta) \left[ \sqrt{v_f^2 - \frac{(v_f \sin \eta)^2}{a}} - \sqrt{\left\{ \frac{v_f^2 - (v_f \sin \eta)^2}{a} \right\}^2 - \frac{2H}{a}} \right] \quad (11)$$

$$R = t v_f \sin \eta \quad (12)$$

$$v_{xi} = v_f \sin \eta - V_x \quad (13)$$

$$v_{xi} = v_{yi} \cot \delta \quad (14)$$

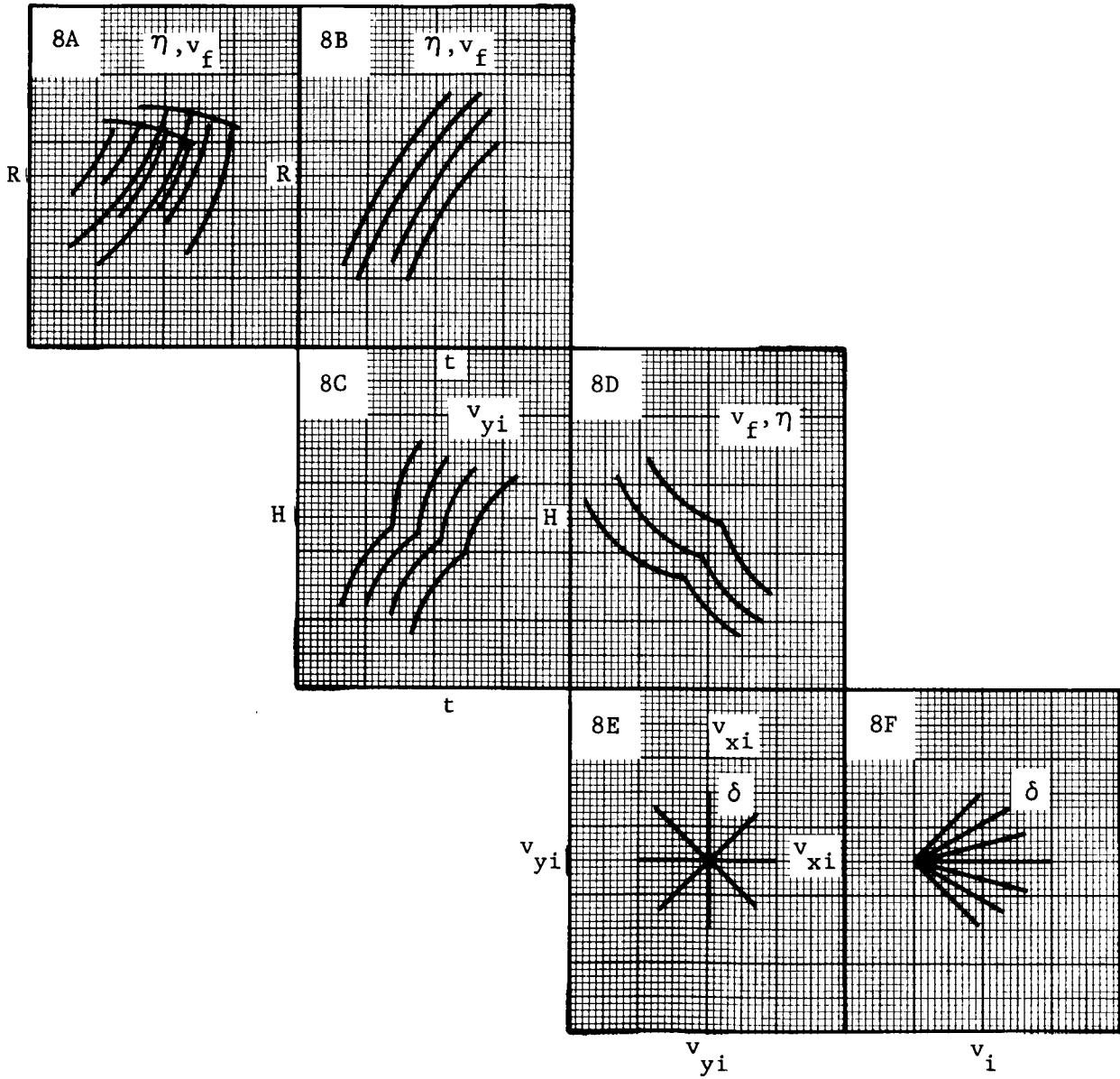
(2) Trade-Off Curves. The above six equations are shown in a master curve matrix of Figure 3-8. Arranging the curves in this manner aids in a quick determination of launch velocity and launch angle as functions of LEM position in the approach trajectory and desired penetrometer impact velocity. To preserve resolution of the curves, however, they are presented independently as Figures 3-8A through 3-8F. Figure 3-8 does show their interrelationships and sharing of ordinates and abscissas. The nominal LEM trajectory parameters of Figure 3-9 are implicit in Figure 3-8 by means of Figures 3-8C and 3-8D. However, the other four curves constituting Figure 3-8 are independent of approach trajectory.

Examination of Figure 3-8A reveals that for the nominal trajectory shown, an impact velocity,  $v_f$ , as low as 200 ft/sec cannot be achieved prior to the 1075 ft altitude point. Further, a  $v_f$  of 150 ft/sec is not possible until an altitude of about 740 ft is reached. A 100 ft/sec impact cannot be attained until after the LEM has gone through the Low Gate Point (500 ft altitude, 1200 ft range).

Looking at Figure 3-8B of the matrix, the time of flight for the earliest possible 100 ft/sec impact launch ( $H = 400$  ft,  $R = 900$  ft from Figure 3-8A) is about 12 seconds. The time to the 200 ft altitude at this point in the trajectory is about 18 seconds, leaving only 6 seconds for data processing and analysis before a decision has to be made.

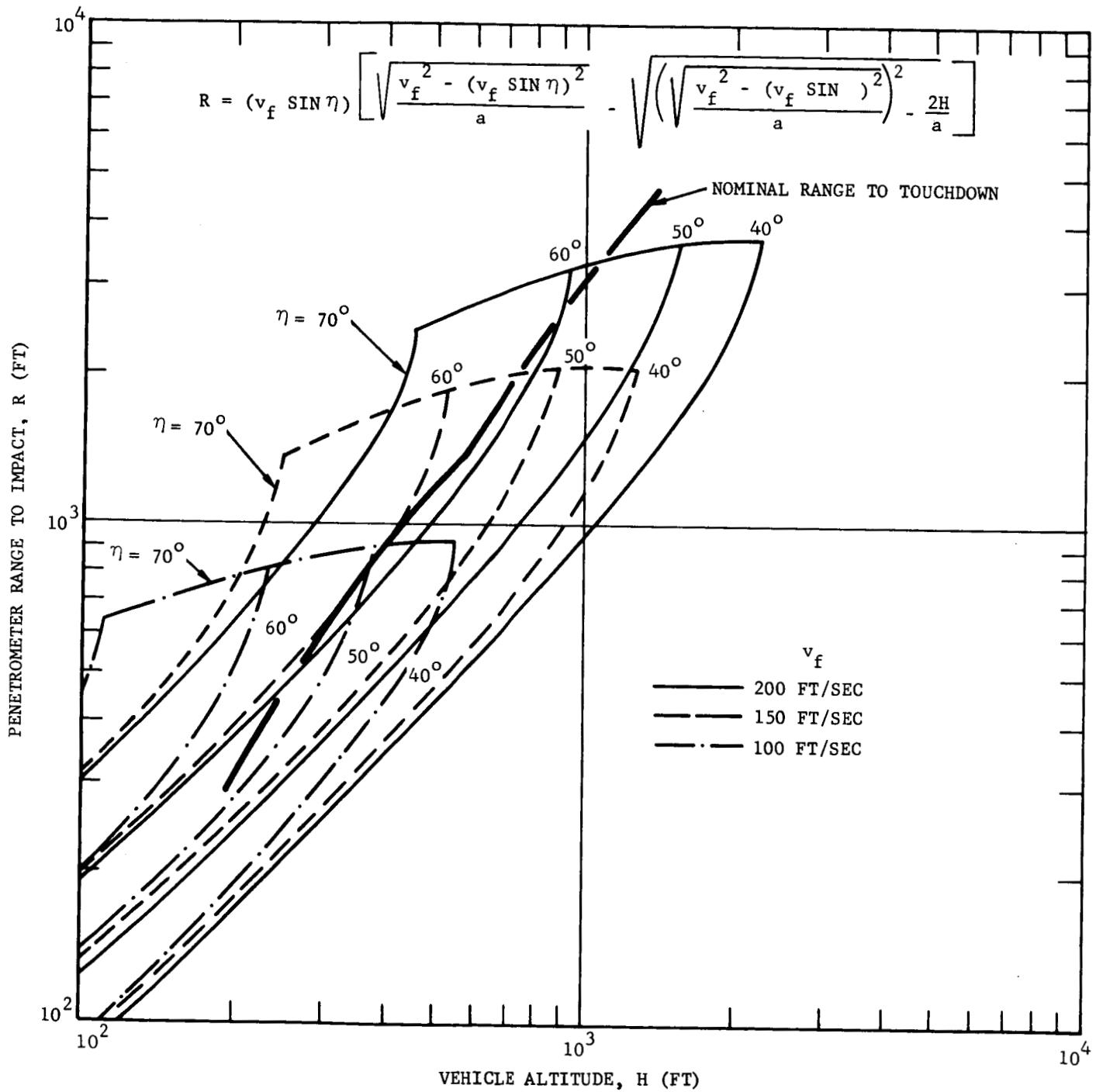
As will be shown later in this discussion, the lower velocity impacts do not appear feasible because of the short time available for interpretation.

Further examination of Figure 3-8A shows that impact angles,  $\eta$ , are generally between 50 and 60 degrees. The larger angles are associated with the larger impact velocities.



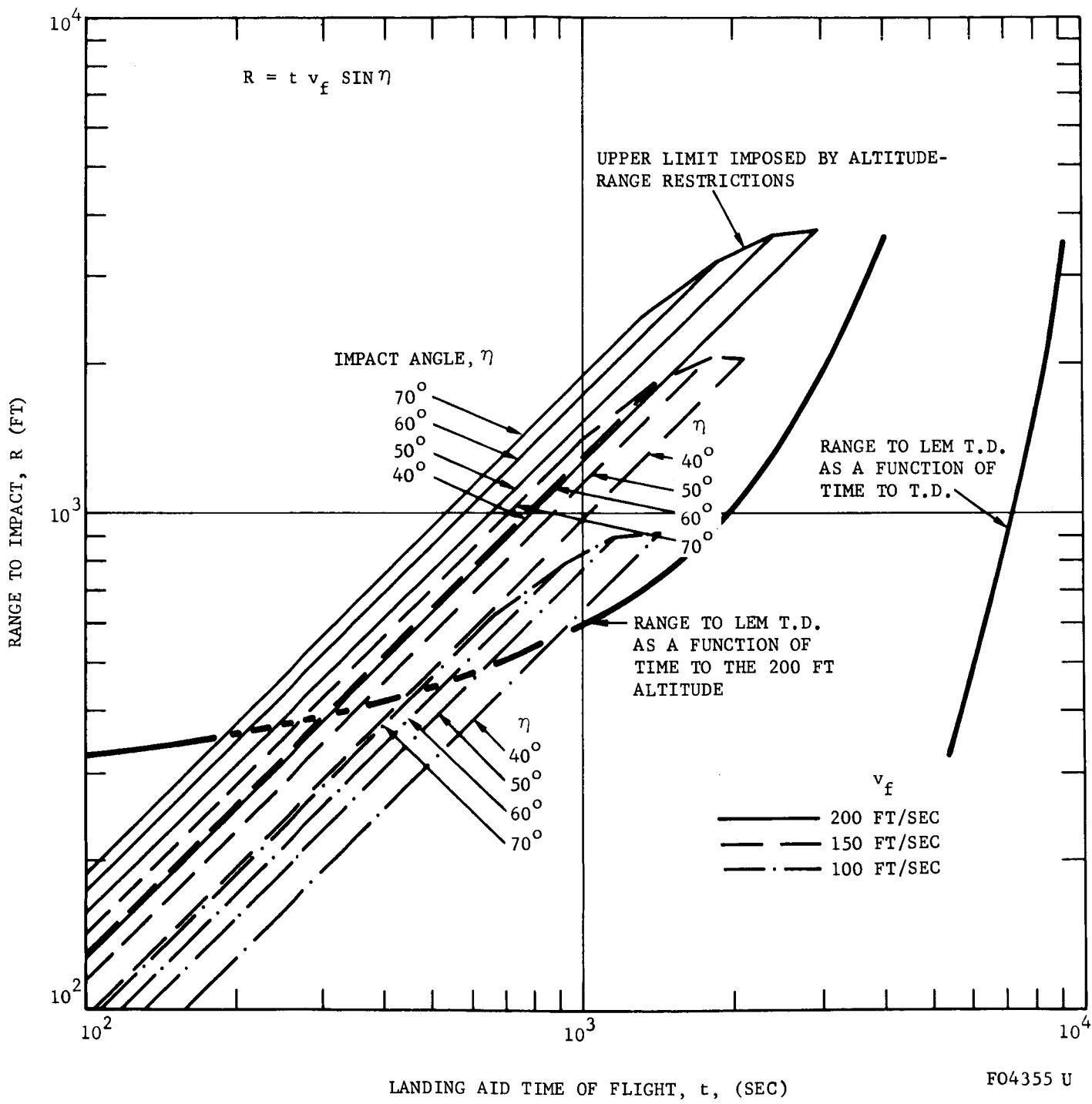
FO4353 U

FIGURE 3-8. PENETROMETER DEPLOYMENT DESIGN ANALYSIS CURVE MATRIX



FO4354 U

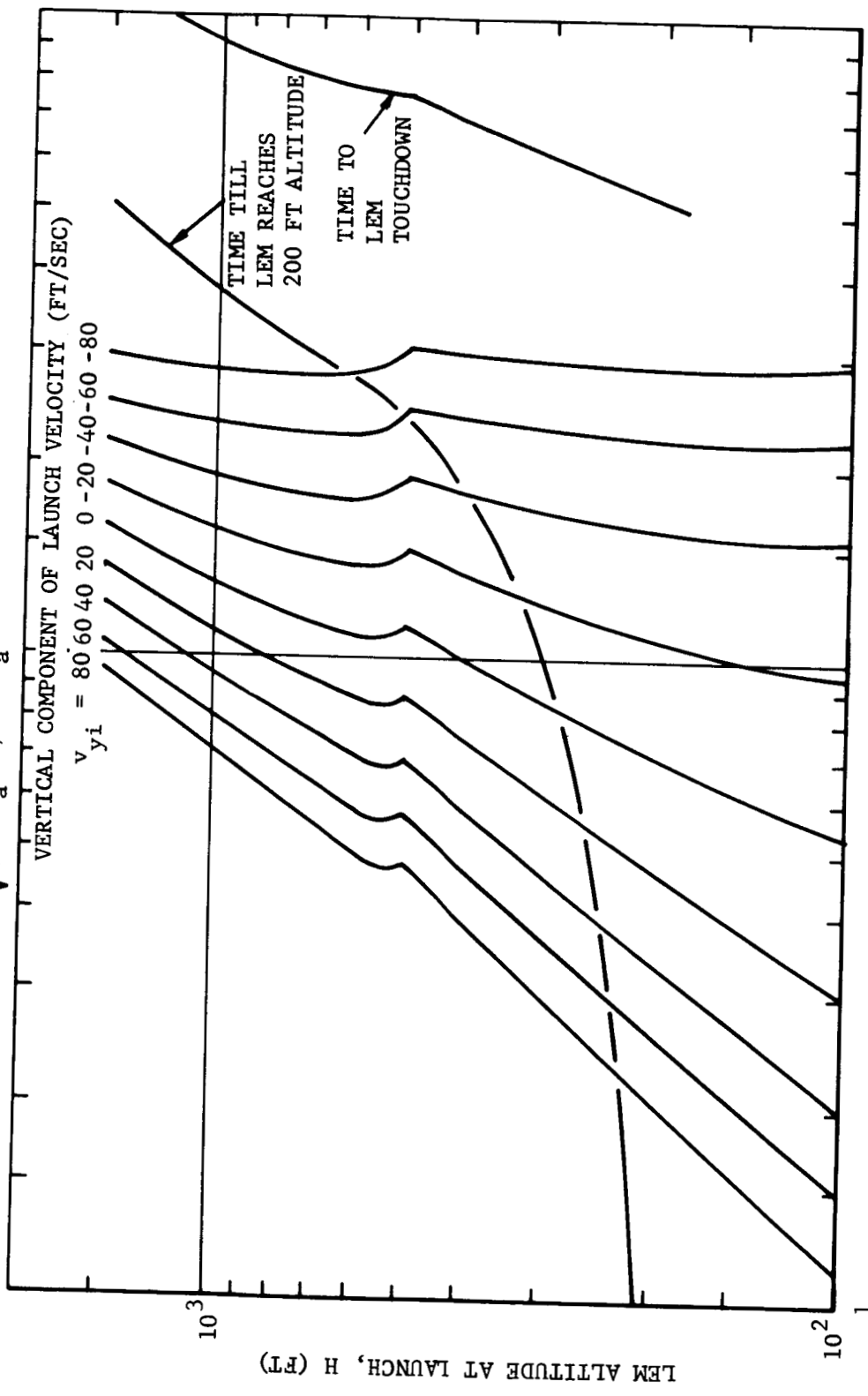
FIGURE 3-8A.



FO4355 U

FIGURE 3-8B.

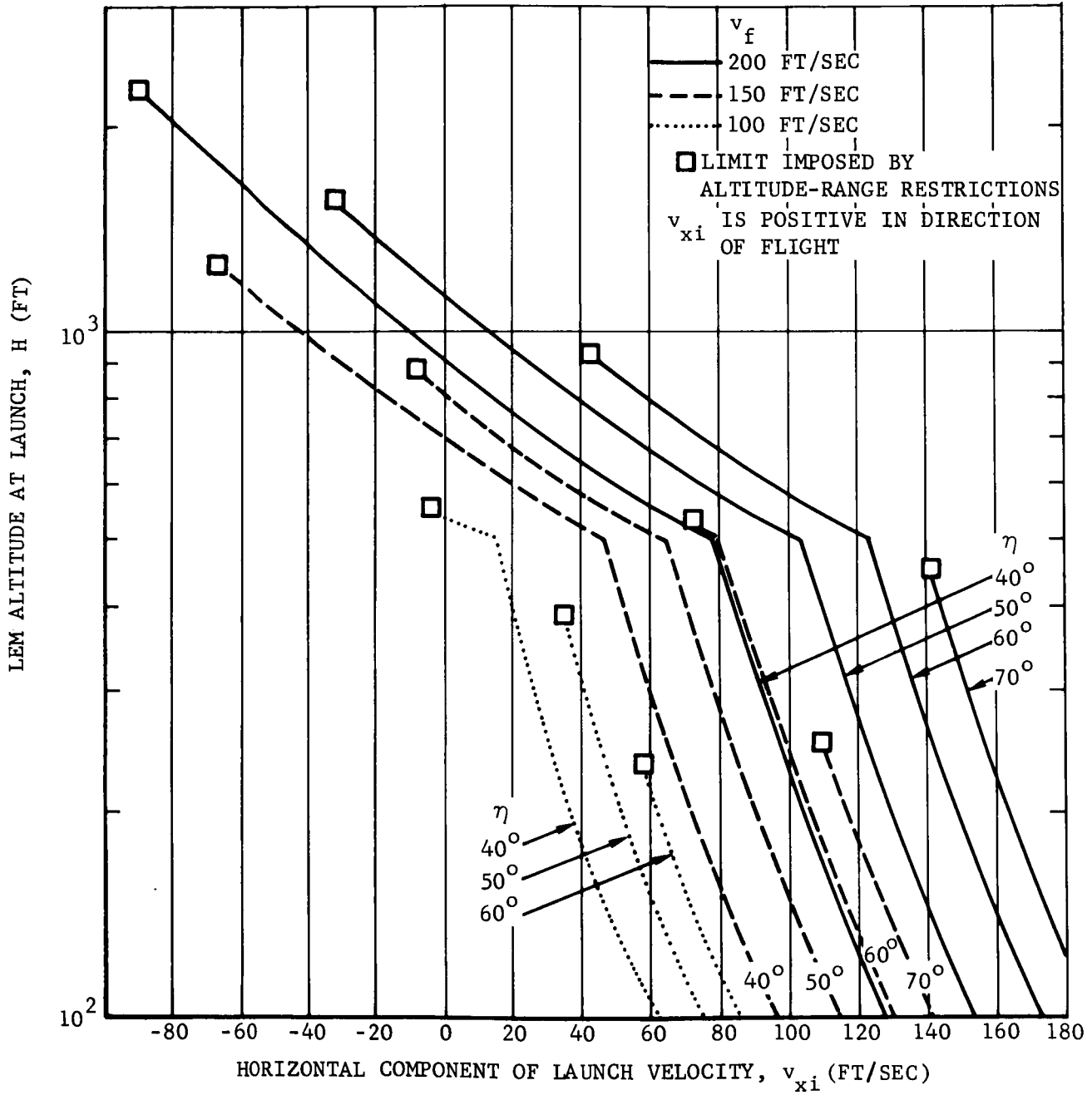
$$t = -\frac{v_i + v}{a} y + \sqrt{\left(\frac{v_i + v}{a} y\right)^2 + \frac{2H}{a}}$$



F04356 U

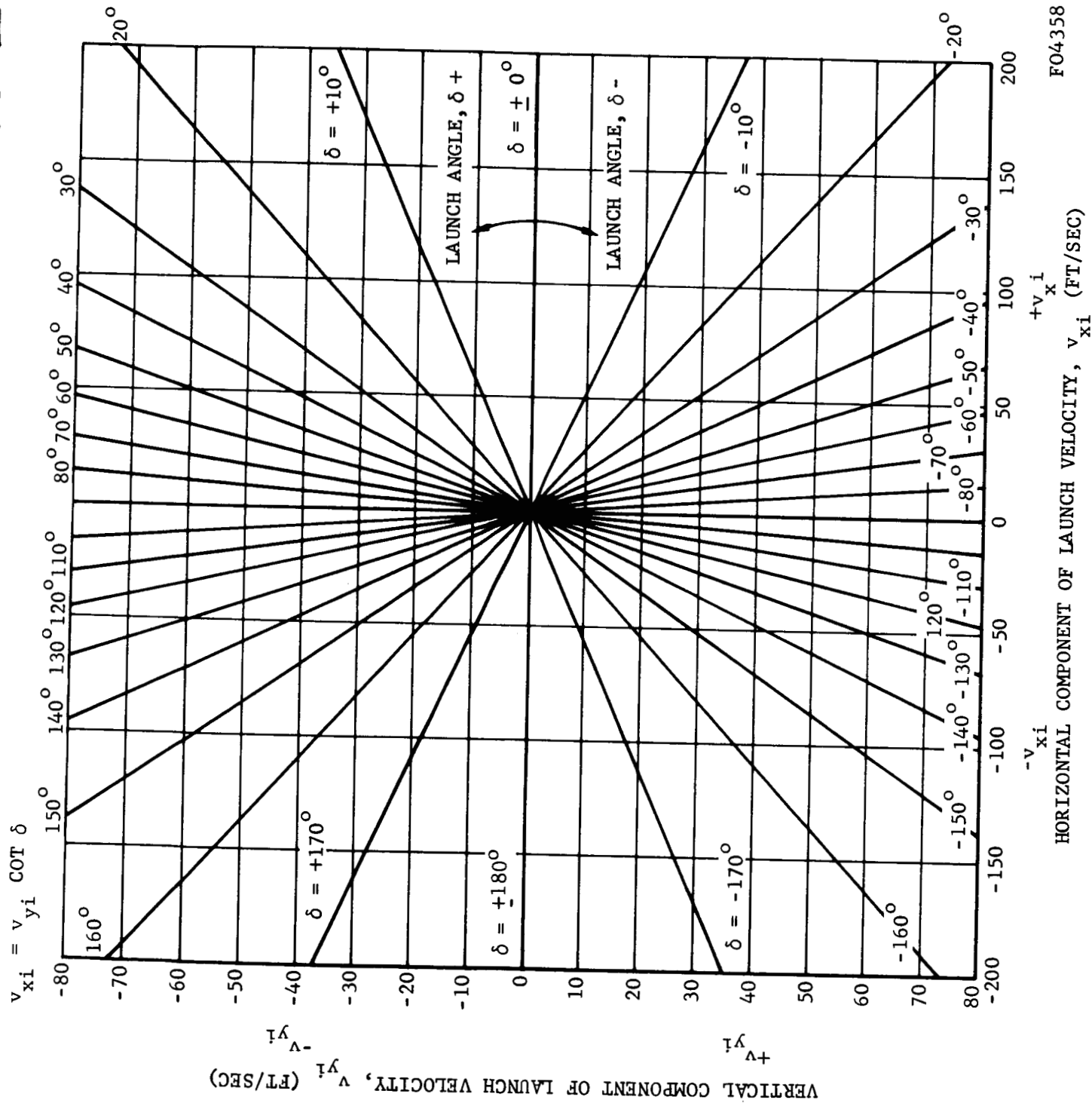
FIGURE 3-8C

$$v_{xi} = v_f \sin \eta - v_x$$



F04357 U

FIGURE 3-8D.



FO4358 U

FIGURE 3-8E.

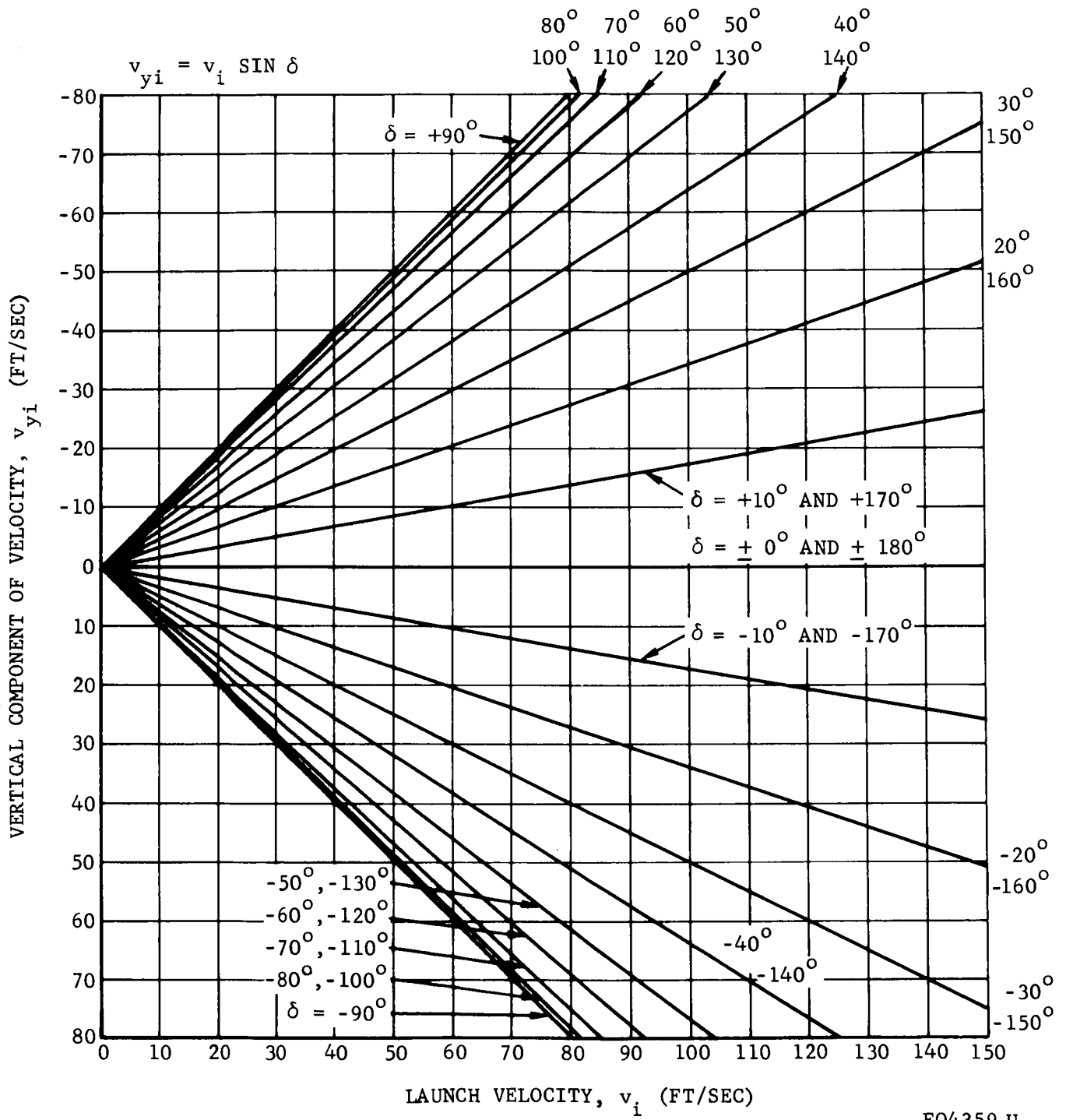
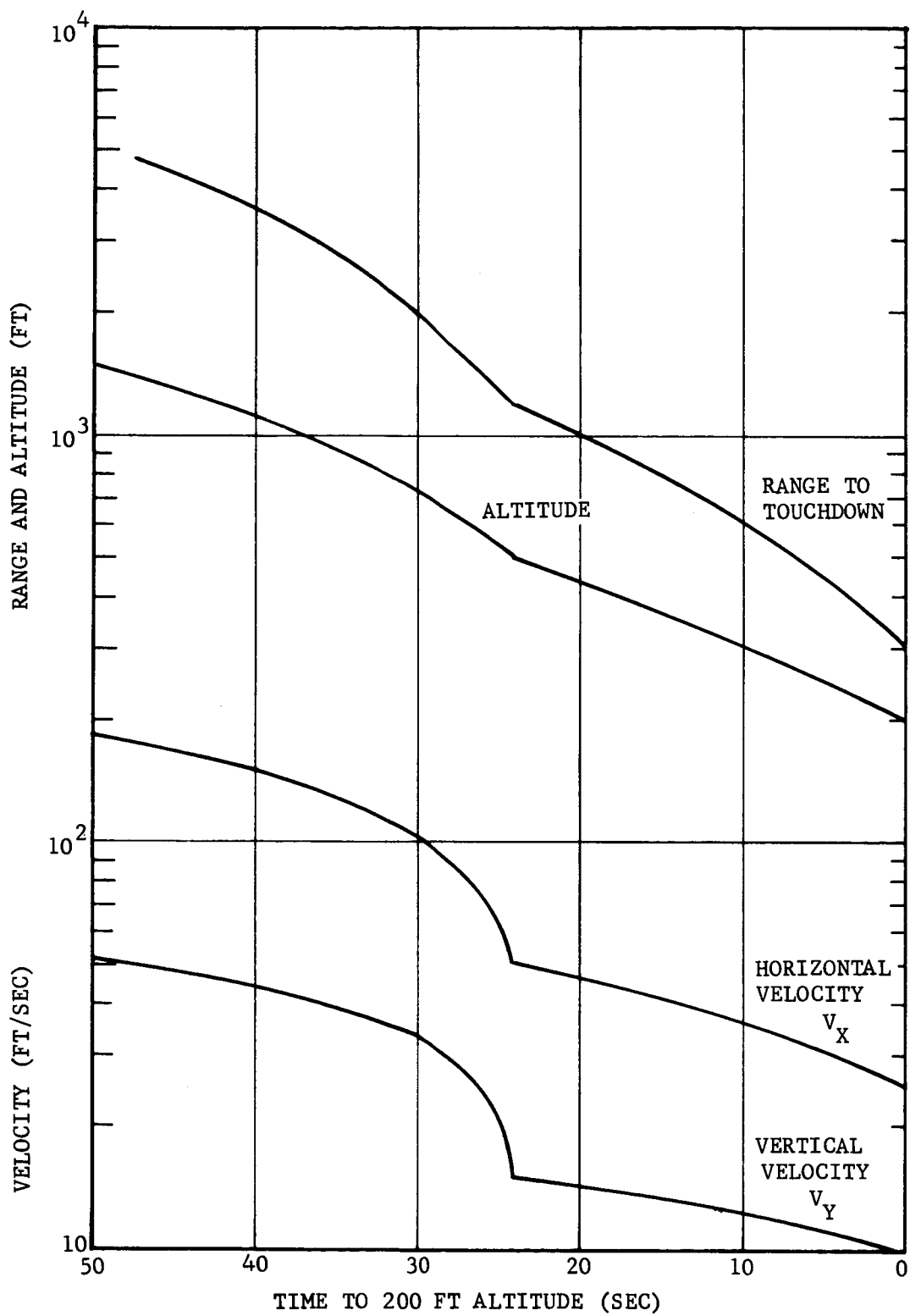


FIGURE 3-8F.



FO4360 U

FIGURE 3-9. LEM APPROACH TRAJECTORY

The matrix is used to define the required penetrometer launch velocity,  $v_i$ , and launch angle,  $\delta$ , for deployment from any position in the LEM approach trajectory below an altitude of approximately 1000 ft. Fixing three of the significant parameters H, R, t,  $\eta$  and  $v_f$  determines all other parameters. For example, selecting H = 500 ft, R = 1200 ft, and  $v_f = 200$  ft/sec on Figure 3-8A fixes  $\eta = 62^\circ$  on Curve A and  $t = 6.8$  sec,  $\delta = -17^\circ$ , and  $v_i = 134$  ft/sec on subsequent curves.

The nominal range to touchdown point for the approach trajectory in Figure 3-9 is shown as a function of LEM altitude on Figure 3-8A of the matrix. This trajectory curve and the  $v_f$ ,  $\eta$  curves are independent of one another. The trajectory curve is plotted to give a reference range. The above selected point, 500 ft altitude at 1200 ft range, is the Low Gate Point in the nominal trajectory used in this analysis. At H = 500, R = 1200, and  $v_f = 200$  ft/sec,  $\eta$  is  $62^\circ$ . Going to Figure 3-8B with the angle  $\eta = 62^\circ$  at R = 1200 and  $v_f = 200$ , time of flight is found to be 6.8 seconds. For reference, the time to the 200 ft altitude and the time to touchdown are shown as functions of range to touchdown on Figure 3-8B. Again, these trajectory curves and the  $\eta$ ,  $v_f$  curves are independent.

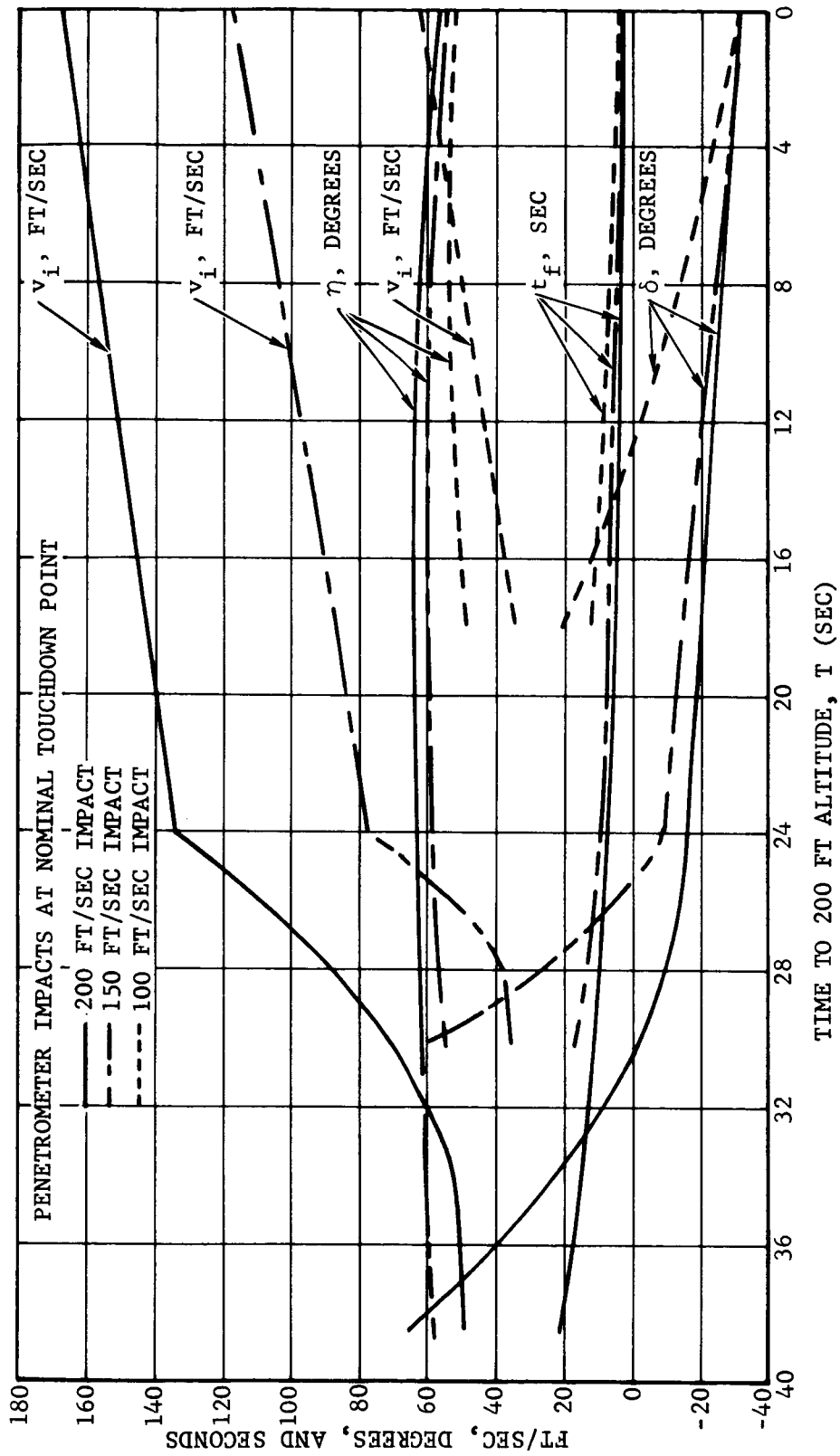
Using the time of flight from Figure 3-8B and the selected 500 ft altitude, the vertical component of velocity,  $v_{yi}$ , is found to be 40 ft/sec on Figure 3-8C. Reference times are shown in Curve C as functions of altitude. Figure 3-8C is dependent on the LEM approach trajectory used in the analysis.

From Figure 3-8D, the horizontal component of velocity,  $v_{xi}$ , is 128 ft/sec at H = 500 ft and  $\eta = 62^\circ$ . Figure 3-8D is also dependent on the selected approach trajectory.

Using the values of  $v_{yi}$  and  $v_{xi}$  found from Figures 3-8C and 3-8D, the launch angle,  $\delta$ , is derived from Figure 3-8E. In this case  $\delta = -17^\circ$ . Using  $v_{yi}$  and  $\delta$ , the launch velocity,  $v_i$ , is found to be 134 ft/sec on Figure 3-8F. Both Figures 8-E and F are independent of the LEM approach trajectory.

(3) Data Interpretation. Data from the curve matrix can be more readily understood by referring to Figure 3-10 which presents the launch velocities and launch angles required to achieve 100, 150 and 200 ft/sec impacts at the nominal touchdown point. These parameters, along with impact angle and time of flight are presented as functions of time to the 200 ft altitude and are constrained to the trajectory shown in Figure 3-9.

A significant point made by this figure is that the time available for analysis of a 100 ft/sec impact is probably not adequate for a decision to be made by the time the 200 ft altitude is reached. For example, if a penetrometer is launched at 18 seconds at a velocity of  $v_i = 34.5$  ft/sec, flight time,  $t_f = 12.5$  seconds. The penetrometer will impact at 5.5 seconds before the 200 ft altitude is reached. Allowing 1/2 second (500 milliseconds) to record an impact and 2 seconds to process the signal, only 3



F04361 U

FIGURE 3-10. PENETROMETER LAUNCH AND IMPACT PARAMETERS

seconds is left to the astronaut to make a decision based on the data from one penetrometer. Data from a second penetrometer would be available two seconds later or one second before the 200 ft altitude is reached. This is shown in Table 3.6 and compared with 150 and 200 ft/sec impact launches. Also shown in Table 3.6 are vehicle altitudes and ranges at launch and impact. These latter data are from Figure 3-9. Table 3.6 is for a single launch of 4 penetrometers.

It is interesting to consider a two salvo mode where two penetrometers are fired, the data displayed, and then two more are fired. Referring to Figure 3-10 and using the 200 ft/sec impact curves, the data in Table 3.7 can be developed. Again, the ground rules for data handling are: 500 millisecond allowance for recording impact data and 2 seconds for processing data from each penetrometer.

If the second salvo, Table 3.7, were delayed until 8 seconds before the 200 ft altitude point, the times available for data analysis would read: Pen. #1, 7.5 sec; Pen. #2, 5.5 sec; Pen. #3, 2 sec; Pen. #4, 0 sec.

Figure 3-11 is a cross plot of Figure 3-10 showing launch and impact parameter variations with time for a constant launch velocity,  $v_i = 50$  ft/sec. This curve is based on 4 points for each parameter and is shown only to indicate data trends. Impact velocity, launch angle, and flight time decrease steadily as launch time is delayed. Table 3.8 summarizes data for launches at the extremes.

#### (4) Summary

- (a) Impact velocities that are compatible with the 200 ft altitude decision point vary between approximately 150 and 200 ft/sec.
- (b) For the LEM trajectory used in this study, the penetrometers cannot be launched before the 1075 ft altitude point is reached without exceeding 200 ft/sec at impact.
- (c) Very low impact velocities (100 ft/sec or less) do not appear to be attainable within the constraints of this study.
- (d) Impact angle at the attainable impact velocities is limited to between  $54^\circ$  and  $62^\circ$  from the vertical.
- (e) No significant gain in data analysis time is realized by launching penetrometers prior to Low Gate.

TABLE 3.6

COMPARISON OF PENETRATOR LAUNCH TIMES AND VELOCITIES  
SALVO LAUNCH OF 4 PENETRATORS

* Time at Launch (Sec)	LEM Altitude At Launch (Ft)	** Range At Launch (Ft)	Launch Velocity (Ft/Sec)	Impact Velocity (Ft/Sec)	* Time At Impact (Sec)	LEM Altitude At Impact (Ft)	** Range At Impact (Ft)	* Time Available to Crew For Data Analysis (Sec)			
								#1	#2	#3	#4
18.0	408	925	34.5	100	5.5	253	470	3.0	1.0	-1.0	-3.0
14.2	354	770	40.0	100	5.2	250	455	2.7	0.7	-1.3	-3.3
30.0	740	1950	35.5	150	14.0	352	765	11.5	9.5	7.5	5.5
26.3	590	1440	50.0	150	14.3	355	770	11.8	9.8	7.8	5.8
24.0	500	1200	77.5	150	14.5	358	780	12.0	10.0	8.0	6.0
38.5	1030	3400	50.0	200	18.0	408	925	15.5	13.5	11.5	9.5
29.0	700	1800	78.0	200	18.5	415	940	16.0	14.0	12.0	10.0
24.0	500	1200	134.0	200	17.5	400	700	15.0	13.0	11.0	9.0

\* Time is time remaining until 200 ft. altitude point is reached.

\*\* Range is range to touchdown point (also range to impact point).

These figures are based in part on a 500 millisecond data readout at impact and a 2 second data processing time.

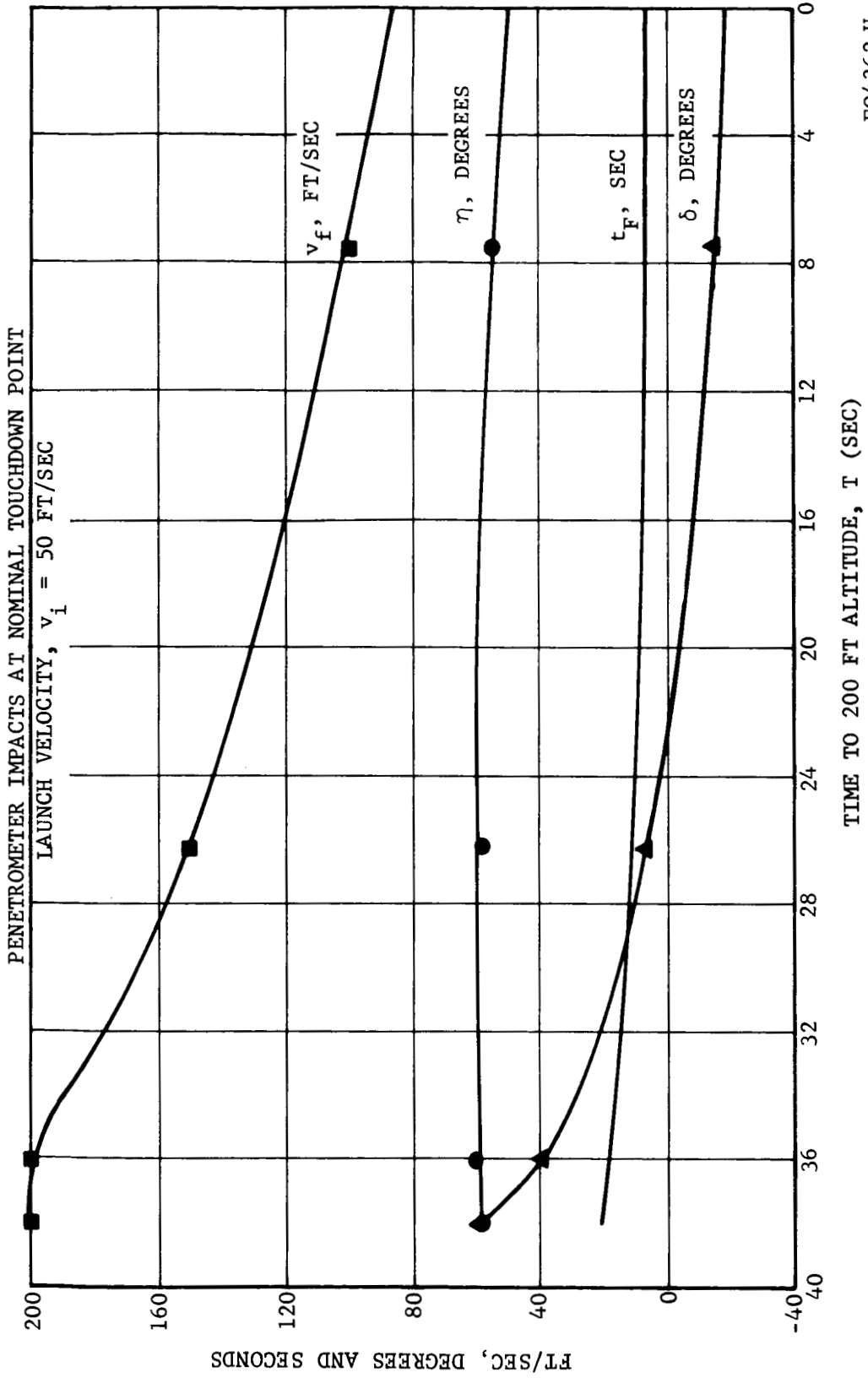
TABLE 3.7

TWO SALVO LAUNCH

Salvo	*Time at Launch (Sec)	*Time at Impact (Sec)	** Time Available to Crew for Data Analysis (Sec)			
			<u>Pen. #1</u>	<u>Pen. #2</u>	<u>Pen. #3</u>	<u>Pen. #4</u>
1	38.5	18	4.5	2.5	--	--
2	11.0	7	--	--	4.5	2.5

\*Time is time remaining before 200 ft. altitude point is reached.

\*\*Time available for analysis of the first two penetrometers was arbitrarily chosen to allow a similar time for analysis of the 3rd & 4th Penetrometers.



FO4362 U

FIGURE 3-11. PENETROMETER TRAJECTORY PARAMETERS FOR CONSTANT LAUNCH VELOCITY

TABLE 3.8  
 COMPARISON OF CONSTANT LAUNCH VELOCITY  
 TRAJECTORY PARAMETERS

$v_i = 50 \text{ ft/sec}$

<u>*Launch Time (Sec)</u>	<u>Launch Angle (Degrees)</u>	<u>Impact Velocity (Ft/Sec)</u>	<u>Impact Angle (Degrees)</u>	<u>*Time Available to Crew for Data Analysis (Sec)</u>			
				<u>Pen #1</u>	<u>Pen #2</u>	<u>Pen #3</u>	<u>Pen #4</u>
38	60	200	58	15.5	13.5	11.5	9.5
16	-8	118	58	6.0	4.0	2.0	0

\*Time is time remaining before 200 ft. altitude point is reached.

- (f) The small gain in analysis time that results from launch prior to Low Gate is accompanied by an increase in impact velocity.
- (g) Launch angles range approximately between 60° above and 20° below the local horizontal.
- (h) The launcher will require launch angle control by computer logic to achieve precise range control, unless the exact altitude range, horizontal velocity, vertical velocity, and vehicle altitude at the launch point are fixed quantities.
- (i) Launcher "muzzle velocity" ranges approximately between 30 and 130 ft/sec depending on launch point and desired impact velocity.
- (j) A single simultaneous launch of all penetrometers requires that all impact at nearly the same velocity and impact angle.
- (k) Two launches, of half the penetrometers at each launch, results in an impact velocity difference between the two flights of up to 80 ft/sec.
- (l) Time available to the crew for data analysis, prior to reaching the 200 ft altitude, can be as long as 16 sec.

b. Control Electronics. It appears practical to design the launchers to provide a fixed impulse to the Penetrometers regardless of when they are launched. But since the penetrometers must impact within a given landing area (LEM footprint) the angle of launch must be varied to account for changing launch altitude and range. If the launch angle is held fixed relative to the LEM, there is only one time in the trajectory when the Penetrometers can be launched. This would require a completely automatic system with no option for launching by the crew. This does not appear desirable. Therefore, a variable signal will be generated to control a servo that regulates the launch angle of the pod. (Adjusting the LEM pitchback angle in order to launch Penetrometers is not permitted). This allows a variable time of launch within the constraints of the trajectory.

The equations of the Penetrometer trajectory have been derived in the previous section and are repeated below with, in some cases, new symbols.

$$R = (v_H + V_H) \tau \quad (15)$$

$$\tau^2 + 2 \frac{v_v + V_v}{a} \tau - \frac{2A}{a} = 0 \quad (16)$$

$$v_I = \left[ (v_H + V_H)^2 + (v_v + V_v + a \tau)^2 \right]^{\frac{1}{2}} \quad (17)$$

$$\eta = \text{Sin}^{-1} \left( \frac{v_H + V_H}{v_I} \right) \quad (18)$$

$$v_M^2 = v_v^2 + v_H^2 \quad (19)$$

$$v_H = v_M \cos \delta \quad (20)$$

Where

A: LEM altitude

$V_H$ : LEM horizontal component of velocity

$V_v$ : LEM vertical component of velocity

$\alpha$ : LEM pitchback angle relative to horizontal reference

T: LEM time to go to touchdown

R: LEM horizontal range to touchdown

$v_H$ : Penetrometer horizontal component of launch velocity relative to LEM

$v_v$ : Penetrometer vertical component launch velocity relative to LEM

$v_M$ : Penetrometer total muzzle velocity relative to LEM

$\delta$ : Penetrometer launch angle relative to horizontal reference

$\tau$ : Penetrometer time of flight to impact

$v$ : Penetrometer impact velocity

$\eta$ : Penetrometer impact angle relative to local vertical

a: Gravitational field

Those that must be used to derive the launch angle are Equations (15), (16), (19) and (20) as shown in Figure 3-12. Since some of the same inputs are also required to solve for the theoretical impact velocity and impact angle, they are solved here. These data are continuously revised as the LEM flies along the track. The latter two parameters are necessary initial conditions to the Data Processor subsystem. If the time of flight of the Penetrometer is calculated to be greater than that of the LEM, the launch circuit is inhibited.

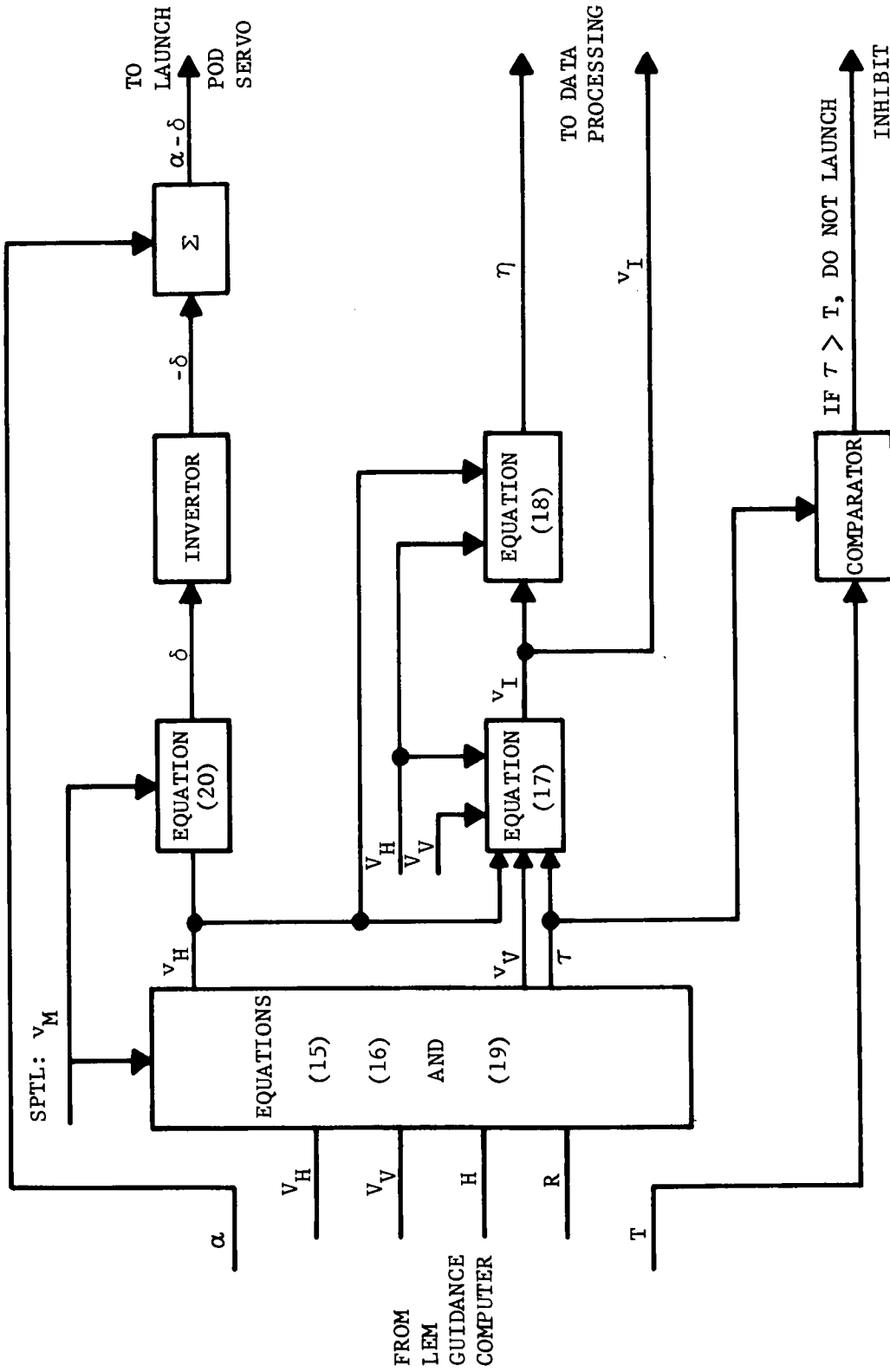
In a typical arrangement, the control electronics would have an input to the Display Subsystem to indicate when a Penetrometer has been launched, as shown in Figure 3-13. As soon as the launch occurs, but before the Penetrometer transmitter is turned on, the launch lamp is lighted. However, as soon as an r-f signal is received and its rms value exceeds a predetermined threshold for more than 1 second a one-shot multi-vibrator inhibits the launch lamp and lights the signal lamp. As soon as there is a data signal from the impacting penetrometer, there is a signal at  $X_I$  which inhibits the signal lamp. The quality of surface is displayed within two seconds on another lamp bank.

The control circuit sequences an electronic commutator through the proper channels as soon as Penetrometers are launched. If more than one are launched simultaneously, then the Data Processor is alternately connected to each channel for 2 seconds. During the 2-second interval that a single channel is interrogated, all of the outputs from the decision circuit in the Data Processor are monitored through an OR gate so that as soon as data activates the display console, there is a pulse from the OR gate back to the commutator sequencer. This deactivates that switch position so the channel is not needlessly monitored again.

The commutator sequencer is continuously updated as to which Penetrometers have been launched. The switch cycles through only those channels that are about to receive data or those that have received data but have not as yet had it processed.

As soon as the switch interrogates a channel it must reset all of the data processor circuits to the proper initial conditions for that channel. As soon as a launch occurs, theoretical values of impact velocity  $v_I$  and angle  $\eta$  for that Penetrometer must be temporarily stored for use by the Data Processor. Figure 3-14 shows the general manner by which this is accomplished. A holding circuit retains these values indefinitely. The circuit may be interrogated many times before the data is actually used. Since the exact form of both  $v_I$  and  $\eta$  are undefined at this time, the type of nondestruct holding circuit is not specified.

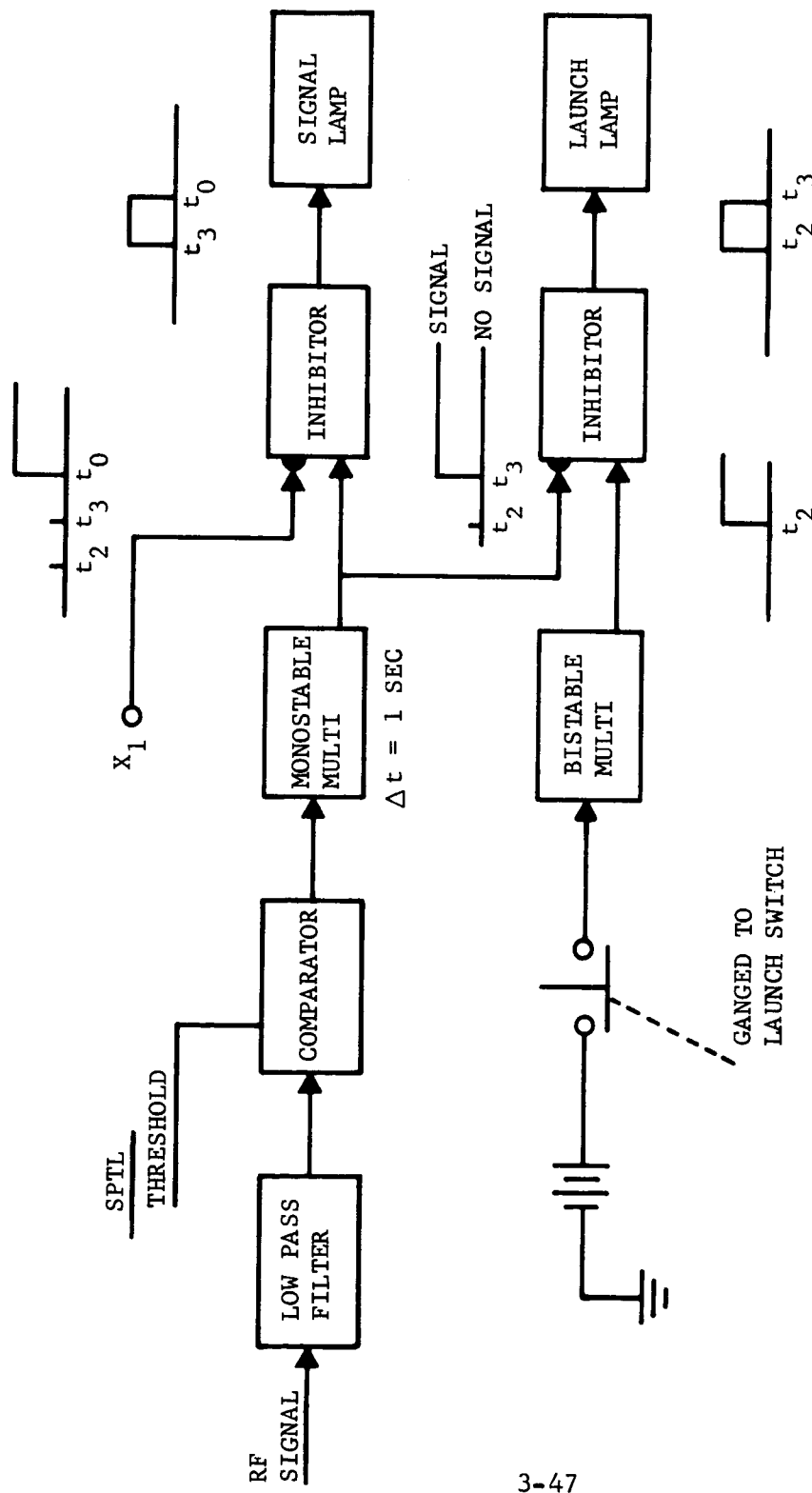
c. Launcher Tip-Off. A brief analysis was made to investigate the effect of penetrometer deployment on LEM attitude rates. Pitch, yaw, and roll rates introduced by a 4-penetrometer salvo were determined for each of



NOTATION SPTL: SET PRIOR TO LAUNCH

FO4363 U

FIGURE 3-12. PENETROMETER LAUNCH ANGLE CONTROL



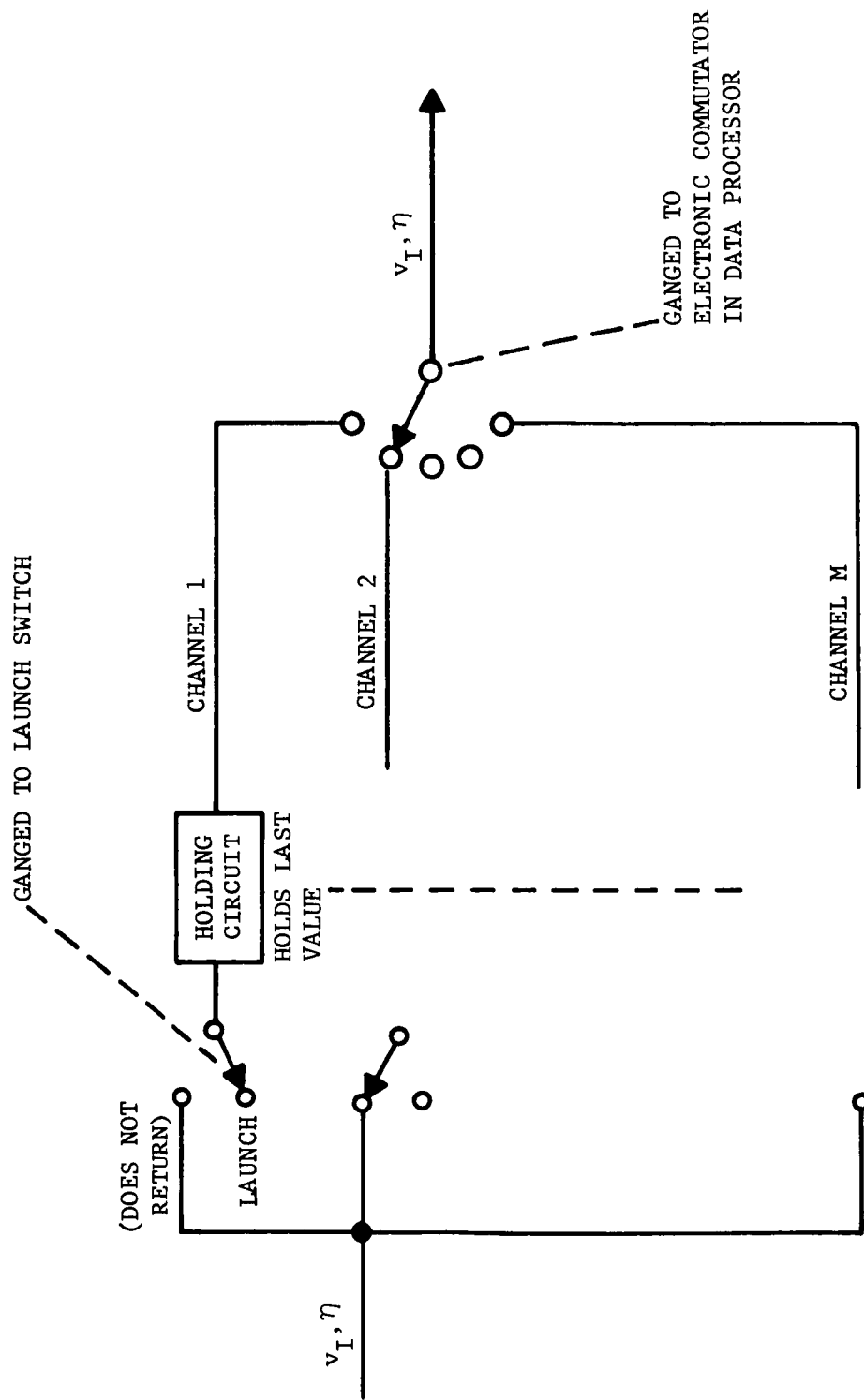
$t_2$  : TIME OF LAUNCH

$t_3$  : TIME AT WHICH CARRIER IS RECEIVED

NOTATION

SPTL: SET PRIOR TO LAUNCH

FIGURE 3-13. LAUNCH AND SIGNAL STRENGTH DISPLAY



FO4364 U

FIGURE 3-14. STORAGE NETWORK FOR PENETROMETER IMPACT VELOCITY AND ANGLE

two locations of the launcher shown in Figure 3-15. The two locations are (1) above the fixed forward leg braces, and (2) above a fixed side leg brace. Pitch rates only are introduced at the forward locations while both yaw and roll rates are introduced at the side location. The sense of the yaw and roll rates shown in Table 3.9 are not indicated, because it is assumed the launcher can be located at either side thereby causing yaw and roll in either direction.

The values in Table 3.9 are, hopefully, worst cases. The launches used in this analysis achieve an impact velocity of 200 ft/sec which requires the highest expected launch velocity, and therefore introduce the highest attitude rates.

The forward strut may not be a good location because of launcher interference with the astronaut's exit from the vehicle after touchdown. If the yaw and roll rates introduced by the side located launcher are not acceptable, an alternate approach would be to deploy 2 penetrometers simultaneously from each side location. This approach would result in a heavier system but would introduce no attitude rates during launch.

(1) Derivation. Change in rotation rate of a free body is given by:

$$\omega - \omega_0 = \frac{I_a}{J_m} \quad (21)$$

Where:

$\omega_0$  = Initial rotation rate, radians/sec

$I_a$  = Angular impulse, lb-ft-sec

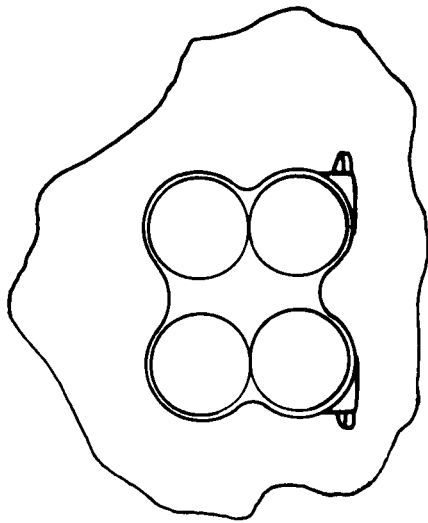
$J_m$  = Mass moment of inertia, slug-ft<sup>2</sup>

Angular impulse,  $I_a$ , is the product of torque and the time the torque acts. In the case of penetrometer launch, the (force x time) portion of angular impulse is a function of the mass of the penetrometer and the velocity imparted to the penetrometer:

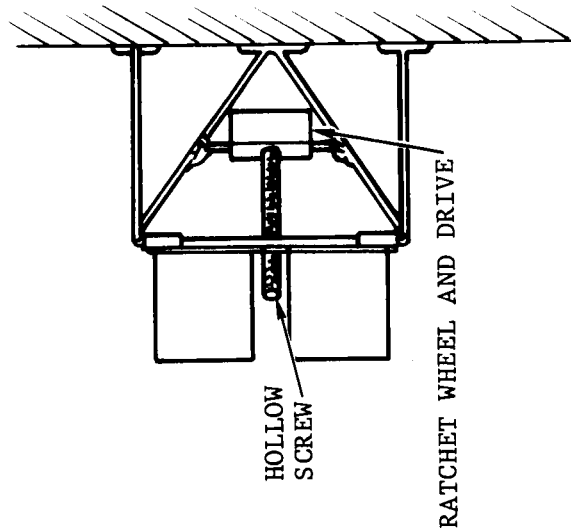
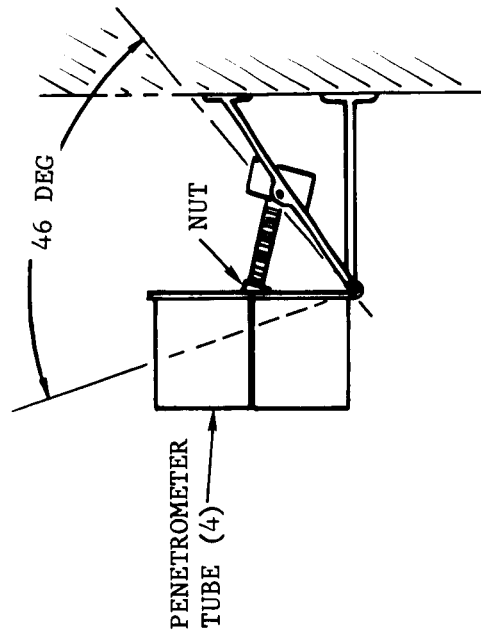
$$F = ma = m \frac{dv}{dt}$$

$$F \int_0^t dt = m \int_0^{v_i} dv \quad (22)$$

$$Ft = mv_i$$



VIEW FROM FRONT  
SHOWING PLASTIC  
OVER BARRELS



FO4366 U

FIGURE 3-15. PENETROMETER LAUNCHER CONCEPT

TABLE 3.9  
 ATTITUDE RATES INDUCED BY PENETROMETER LAUNCH  
 (4 PENETROMETER SALVO)

<u>Launcher Location</u>	<u>*Launch Time (Sec)</u>	<u>Pitchup (Deg/Sec)</u>	<u>Pitchdown (Deg/Sec)</u>	<u>Yaw (Deg/Sec)</u>	<u>Roll (Deg/Sec)</u>
Front Brace	T-38	--	0.2	--	--
Front Brace	T-24	0.9	--	--	--
Side Brace	T-38	--	--	1.0	0.2
Side Brace	T-24	--	--	2.5	0.9

\* Launch time is relative to the time the 200 ft altitude is reached. T-38 sec. is the earliest time a 200 ft/sec impact can be obtained. T-24 is Low Gate position.

Where:

F = force applied to each penetrometer, lb

t = time force is applied, seconds

m = mass of penetrometer, slugs

$v_i$  = muzzle velocity of penetrometer, ft/sec

Allowing L to equal the moment arm of the force acting to impart an attitude rate to the LEM, the angular impulse imparted by each penetrometer is:

$$I_a = F \times t \times L = (mv_i)_\delta L, \quad (23)$$

where the term  $(mv_i)_\delta$  is the component of impulse that acts on moment arm L.  $(mv_i)_\delta$  is a function of launcher location vehicle attitude, and launch angle,  $\delta$ .

(2) Launcher Locations. Two launcher locations are examined, one on top of the forward fixed landing gear brace, and the other above the side brace. The moment arm L is estimated to be 9.5 ft for both locations.

The launcher imparted lateral and vertical forces relative to the vehicle coordinate system are functions of launch time. Two launch times are selected, one prior to Low Gate where the vehicle pitchback angle is assumed to be  $44^\circ$  and one at Low Gate where the pitchback angle is  $11^\circ$ .

For the forward launcher location, the lateral component of force (relative to the vehicle) is assumed to pass through the center of gravity and not impart an attitude rate. The vertical force is found to be:

$$F_v = F \sin 27^\circ = \frac{(mv_i)_\delta}{t} \sin 27^\circ \quad (24)$$

at Low Gate (-24 seconds relative to the 200 ft altitude point,) and:

$$F_v = F \sin 16^\circ = \frac{(mv_i)_\delta}{t} \sin 16^\circ \quad (25)$$

at -38 seconds. Substituting Equations (4) and (5) into (3) for four 3.5 lb penetrometers at 134 ft/sec at -24 seconds, and at 50 ft/sec at -38 sec, the angular impulses for the forward strut location is found to be:

$I_a = 252$  lb-ft sec at -24 seconds (pitch up)

$I_a = 57.1$  lb-ft-sec at -38 seconds (pitch down)

For the side launch location, the lateral force produces a yawing motion, while the vertical force produces a rolling motion. The same angles ( $27^\circ$  and  $16^\circ$ ) also apply to this location. The angular impulses for salvo launch of 4 penetrometers at  $v_i = 134$  ft/sec (-24 sec) and  $v_i = 50$  ft/sec (-38 sec) are found to be:

$$I_a = 252 \text{ lb-ft-sec at } -24 \text{ seconds (roll)}$$

$$I_a = 495 \text{ lb-ft-sec at } -24 \text{ seconds (yaw)}$$

$$I_a = 57.1 \text{ lb-ft-sec at } -38 \text{ seconds (roll)}$$

$$I_a = 199 \text{ lb-ft-sec at } -38 \text{ seconds (yaw).}$$

(3) LEM Moments of Inertia. Pitch, yaw, and roll moments of inertia for the LEM are determined assuming the vehicle to be approximated by a solid cylinder 13 ft in diameter, 15 ft long, and weighing 17,000 lbs. Pitch and roll moments are given by

$$J_m \text{ (pitch or roll)} = \frac{1}{12} \frac{W}{g} (3r^2 + h^2) = 16,000 \text{ slug-ft}^2$$

The yaw moment is found by:

$$J_m \text{ (yaw)} = \frac{1}{2} \frac{W}{g} r^2 = 11,200 \text{ slug ft}^2$$

(4) Induced Attitude Rates. Substituting the moments of inertia and the proper values of angular impulse into Equation (21), and assuming the initial rotation rate  $\omega_0$  to be zero, the pitch, yaw and roll rates summarized in Table 3.9 are computed.

d. Launcher Thermal Control. A brief analysis was made to specify thermal control to maintain penetrometer battery temperature at a nominal  $+50^\circ\text{F}$  during Cislunar transit. The system consists of a super insulation blanket that completely surrounds the launcher and the penetrometers plus a 0.2 watt resistance heater and a 6.4 oz, 1.56 volt wet-cell battery.

The super insulation blanket, NRC-2 or equivalent, is approximately 0.35 in. thick and weighs approximately 0.37 lb. The heater operates intermittently throughout the Earth-Moon orbit phase. A bimetal switch provides the required control to maintain the temperature within specified limits.

The heater and insulation are conservatively sized considering complete exposure to space with no heat input from either the sun or LEM vehicle. The launcher temperature is found with the package exposed to the Sun to

determine if a cooling requirement exists; no cooling requirement exists. The required heat input will vary, however, as the package is alternately exposed to Sun and dark space, hence the bimetal switch.

(1) Insulation -- Heater Trade-offs. The launcher insulation package is assumed to be a rectangular box 10 in. x 10 in. x 5 in. with the heater centrally located. The launcher, penetrometers and inner surface of the insulation are assumed to be isothermal. With no external heat input, and with a view factor to outer space of one, the equilibrium heat balance is:

$$q = \frac{KA}{X} (T_i - T_o) = \epsilon A \sigma T_o^4 \quad (26)$$

Where:

- q = Heater output, BTU/hr
- K = Insulation thermal conductivity, BTU/hr-°r-ft<sup>2</sup>/in
- X = Insulation thickness, in
- T<sub>i</sub> = Inner package temperature = 50°F = 510°R
- T<sub>o</sub> = Outer insulation surface temperature, °R
- ε = Infrared emissivity of outer surface = 0.05
- A = surface area of package (outer and inner surface areas assumed to be equal)
- σ = Stefan-Boltzman Constant

The equation is shown in Figure 3-16 for three values of thermal conductivity. Experience has shown that a conductivity of about 3 x 10<sup>-4</sup> is attainable and the tentative design point is shown at that value. A more detailed study could show an overall system weight decrease by increasing insulation thickness slightly.

(2) Temperature of Launcher in Direct Sunlight. The selected design is analyzed with direct solar heat input to determine if equilibrium temperature in this case is too high. Assuming the Sun 'sees' one 10 in. x 10 in. side and all other sides see dark space (again neglecting heat exchange between LEM and Launcher), package equilibrium temperatures are given by:

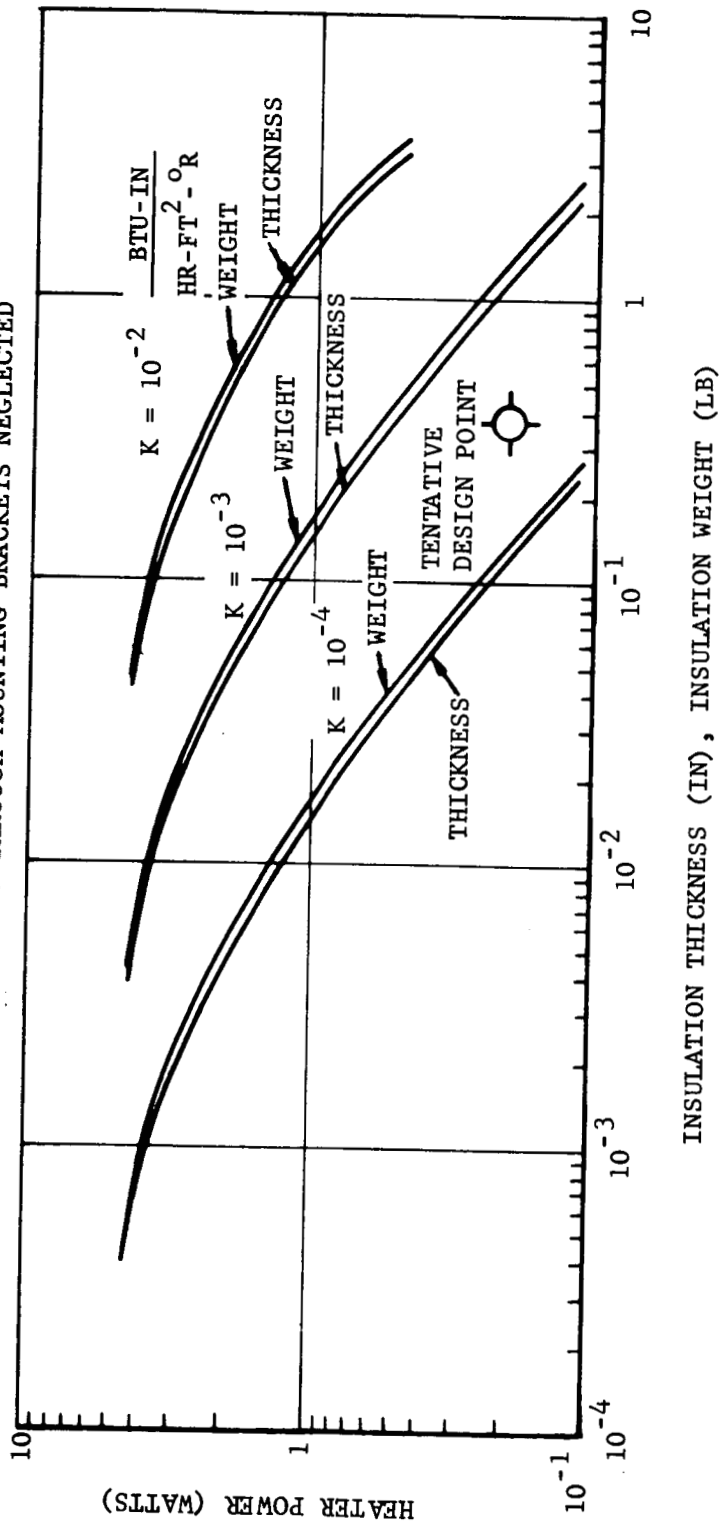
$$\epsilon A_2 \sigma T_2^4 = \frac{KA_2}{X} (T_i - T_2) = \frac{KA_1}{X} (T_1 - T_i) = \alpha A_i S - \epsilon A_1 \sigma T_1^4 \quad (27)$$

ASSUMPTIONS:

NO SOLAR HEAT INPUT

LAUNCHER SURROUNDED BY SUPER INSULATION

HEAT LOSS THROUGH MOUNTING BRACKETS NEGLECTED



FO4367 U

FIGURE 3-16. THERMAL CONTROL TRADE-OFF PARAMETERS

Where:

$A_2$  = Area of package exposed to dark space

$T_2$  = Temperature of all external surfaces not looking at Sun

$T_i$  = Temperature of launcher and inner surface of insulation

$A_1$  = 10 x 10 in. area of package exposed to Sun

$T_1$  = Temperature of side facing Sun

$\alpha$  = Solar absorptivity of outer surface = 0.12

and all other parameters are as previously discussed. The above three simultaneous equations are solved to find:

$T_1$  = 210°F

$T_2$  = -258°F

$T_i$  = -91°F

The fact that the internal temperature is lower than desired, shows that heat input is required whether the package is in sun or shadow.

e. Number of Penetrometers. Expressions for the probability of success of a landing on the moon are given for differing mission definitions and reliability considerations. From these expressions, the number of penetrometers required for a predetermined probability of success can be evaluated as a function of the a priori probability that a point on the Moon's surface will sustain a landing.

The following definitions facilitate the ensuing analysis:

$n$  - The number of penetrometers employed

$P_g$  - The a priori probability that a point on the Moon's surface will sustain a landing.

$P_r$  - The probability (reliability) that a penetrometer will report correctly the state (i.e., will or will not sustain a landing) of a point on the Moon's surface.

$P_s$  - The probability of the landing mission success.

Case 1. Penetrometer reliability ignored, success being defined as at least one penetrometer indicating a point which will sustain a landing.

$$P_S = 1 - (1 - P_g)^n \quad (28)$$

Case 2. Penetrometer reliability ignored with success being defined as at least one acceptable landing spot being found. This may be accomplished by 'n' penetrometers, or failing this, the astronauts may - in effect - elect to make the LEM the '+1' item, thus indicating the probability that one additional sample will indicate a success.

$$P_S = 1 - (1 - P_g)^{n+1} \quad (29)$$

Case 3. Success defined as at least one penetrometer indicating, although not necessarily correctly, that a point on the Moon's surface will sustain a landing. Furthermore, for the landing point selected, the penetrometer correctly reports the landing capability.

$$P_S = P_r [1 - (1 - P_G)^n] \quad (30)$$

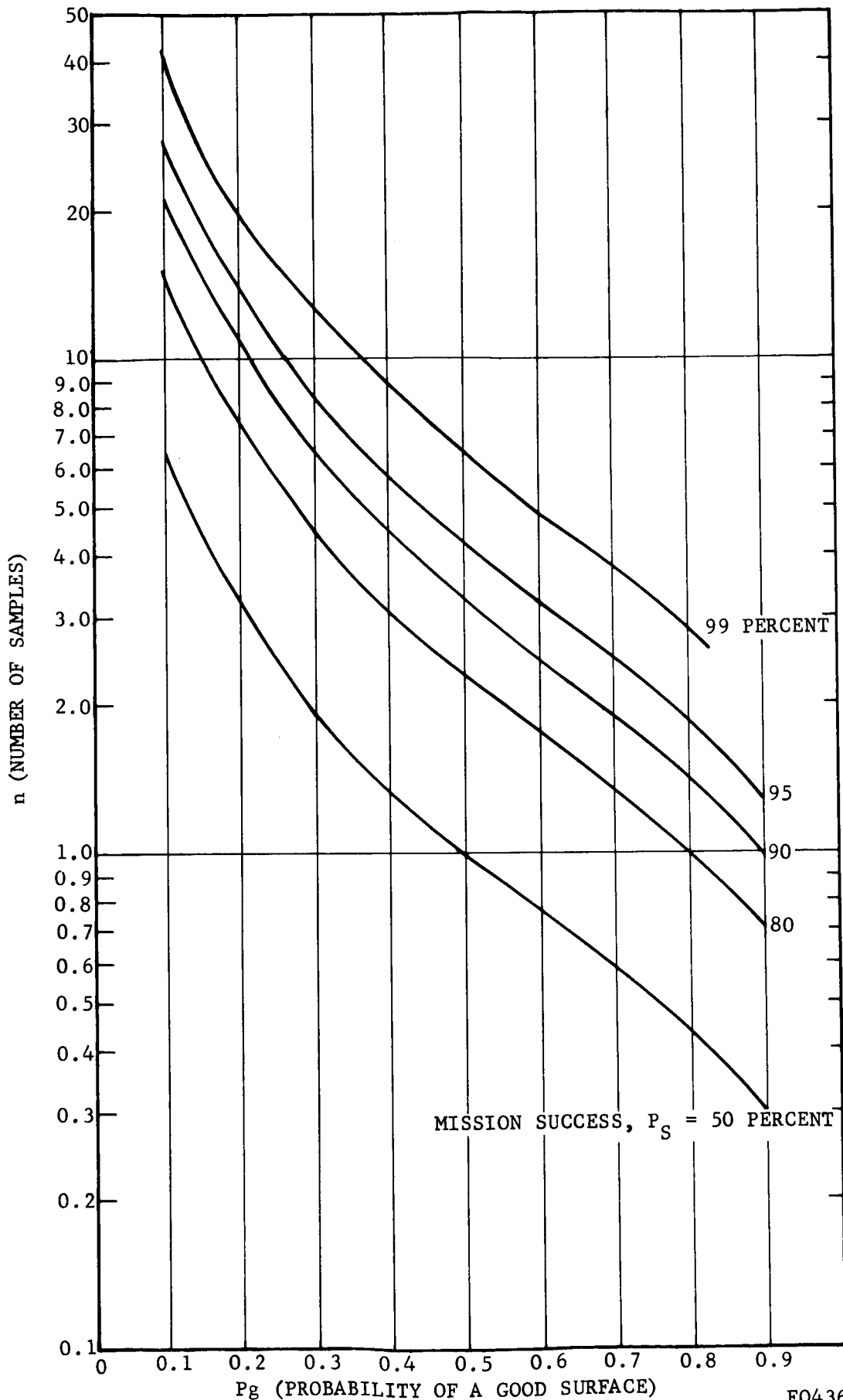
where  $P_G$ , the probability that a penetrometer will indicate, correctly or not, that a point will sustain a landing, is determined from

$$P_G = P_g P_r + (1 - P_g) (1 - P_r) \quad (31)$$

Case 4. Success defined as either that which is defined in Case 3, or, if no penetrometers indicate a suitable landing point, an arbitrary chosen additional point -- as in Case 2 -- will sustain the landing.

$$P_S = P_r - (P_r - P_g) (1 - P_G)^n$$

Case I, Equation (28), is shown in Figure 3-17. (Because of the similarity between Equations (28) and (29), Case II is implicitly shown in Figure 3-17). Notice that mission success is never certain with unit probability. The number of penetrometers required to satisfy an increase in this requirement, grows very rapidly. On a surface that is 70 percent good, only two penetrometers are necessary for 90 percent success. A success of 99 percent demands twice the number of measurements, or 4 samples. On a 50-50 surface, 4 penetrometers will yield a mission success of about 0.94. For lack of definitive data about the surface, there appears to be a reasonable selection criterion for the number of penetrometers to be launched.



F04368 U

FIGURE 3-17. PROBABILITY OF MISSION SUCCESS

### 3.2.3 COMMUNICATIONS

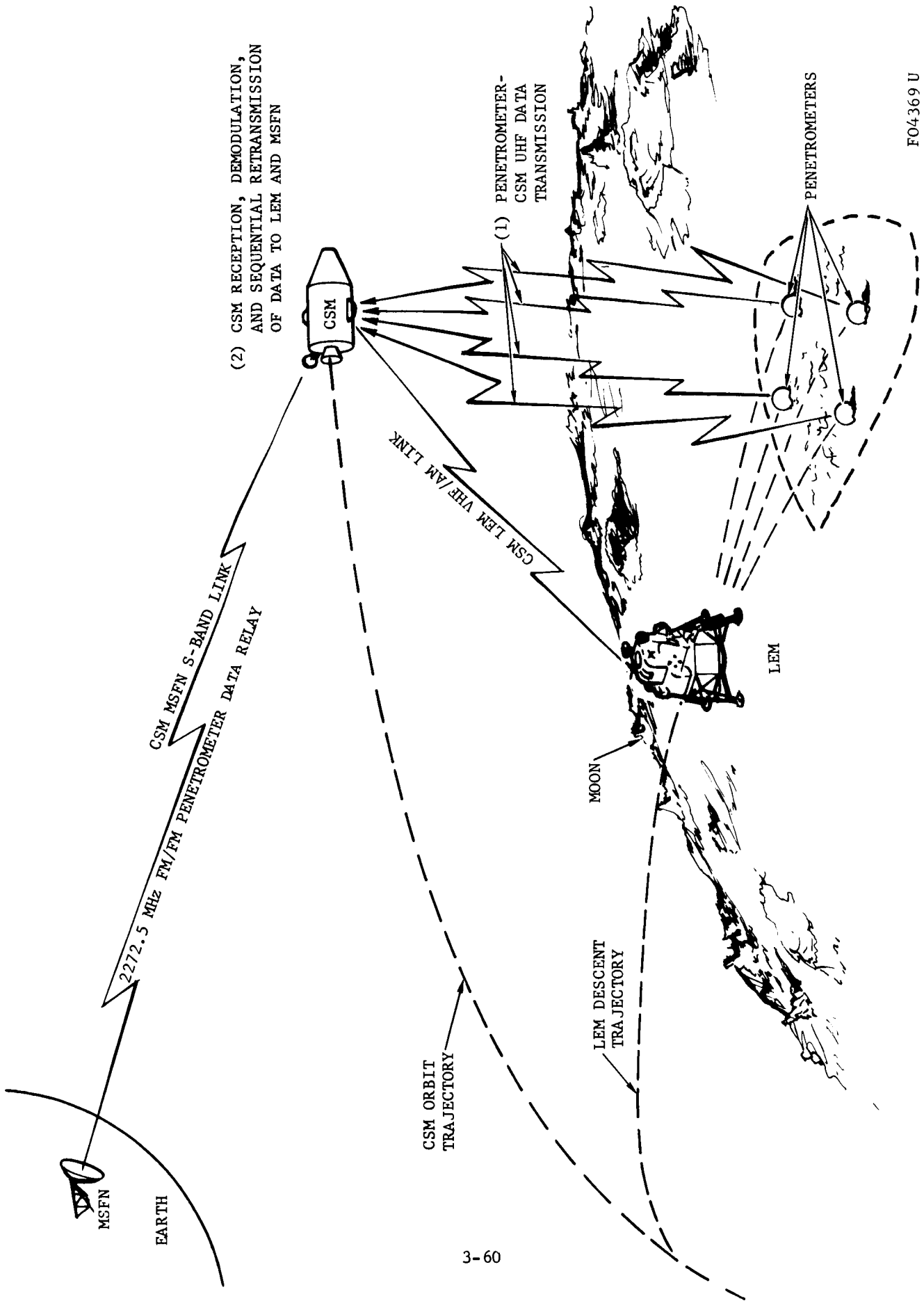
a. Introduction. Several alternate approaches have been considered for both reception of Penetrometer data and retransmission of these data to Earth. Both a direct Penetrometer-LEM communications link and an indirect link utilizing the orbiting CSM as a relay have been investigated. The impact upon system weight and complexity versus the operational simplifications resulting from a salvo firing in lieu of a sequential launch has been considered. A preliminary look has been taken at the possibility of eliminating diversity reception techniques with the attendant reductions in system weight and complexity. For retransmission of the acceleration signatures to Earth, both direct LEM-MSFN transmission and indirect LEM to CSM transmission for subsequent CSM relay to the MSFN have been investigated. The trade-offs made and conclusions reached in each of these areas are presented below.

b. Penetrometer Data Reception Trade-offs.

(1) Direct Link Versus CSM Relay. An early look was taken at the possibility of utilizing the orbiting CSM for reception and retransmission to the LEM of the Penetrometer-derived acceleration versus time signatures. Such an indirect link would enable the removal of the weight of the sounding probe communication subsystem from the LEM and placing it upon the CSM, where weight is somewhat less critical. (Figure 3-18 illustrates the potential indirect Penetrometer/CSM/LEM communications link.) This relay technique would also enable the CSM to re-transmit the Penetrometer data directly to the MSFN, thus eliminating an interface with the LEM S-band communications system.

Unfortunately, an investigation of the transmission range capability of the Penetrometers reveals that their RF output power falls considerably short of meeting the requirements for transmission over the 100 nautical mile slant range to the orbiting CSM. Table 3-10 summarizes the circuit margin calculations for both Penetrometer-to-LEM and Penetrometer-to-CSM transmission links. The former link assumes a nominal 1200 foot slant range from the Penetrometer to the LEM at Penetrometer impact. The circuit margin calculations for this link, which assume diversity reception on-board the LEM will exceed the minimum requirement by a nominal 28.2 db. However, the circuit margins for the Penetrometer-CSM communications link are inadequate by more than 28 db. This degree of inadequacy completely precludes the use of this relay communications mode, even if better CSM antenna gain and higher output Penetrometer transmitter power are considered.

(2) Salvo Versus Sequential Launch Considerations. Salvo launching of  $m$  Penetrometers as opposed to sequential firing has distinct operational advantages. Simultaneous launching of all the Penetrometers early in the terminal LEM landing maneuvers yields a maximum time period to which to



FO4369 U

FIGURE 3-18. POTENTIAL INDIRECT PENETROMETER-CSM-LEM DATA RELAY LINK

TABLE 3.10  
 PENETROMETER DATA TRANSMISSION  
 SIGNAL MARGIN CALCULATIONS

Parameter	Nominal Value (db)	
	A. Direct Penetro- meter-to-LEM Link	B. Indirect Penetro- meter to CSM Link
1. Penetrometer RF Output	- 3.0 dbw	- 3.0 dbw
2. Transmitting Circuit Loss	- 1.0	- 1.0
3. Transmitting Antenna Gain	- 3.0	- 3.0
4. Polarization Loss	- 3.0	- 3.0
5. Space Loss (at 450 MHz)	-77.8 (1/5 N. mile)	-130.9
6. Receiving Antenna Gain	+ 4.5	0.0
7. Receiving Circuit Loss	- 1.0	3.5
8. Received Signal Power	-84.3 dbw	-144.4 dbw
9. Receiver Noise Bandwidth (700 kHz)	58.5 db·Hz	58.5 db·Hz
10. Subsystem Noise Figure	15.0	6.0
11. Noise Spectral Density	<u>-204.0 dbw/Hz</u>	<u>-204.0 dbw/Hz</u>
12. Received Noise Power	-130.5 dbw	-139.5 dbw
13. Required Threshold SNR	<u>+ 23.5 db</u>	<u>+ 23.5 db</u>
14. Required Signal Power	-107.0 dbw	-116.0 dbw
15. SNR <sub>if</sub> (8 minus 12)	+ 46.2 db	- 4.9
16. SNR <sub>out</sub> (at 7000 g) (at 50 g)	77.7 db 51.7 db	
17. Margin (at 50 g)	28.2 db	
18. Margin (carrier) (8 minus 14)	22.7 db	

analyze the resulting impact data. A single, salvo firing significantly reduces the operational tasks imposed upon the LEM crew over the tasks required for sequential launching. However, a requirement for salvo launching imposes considerable weight, volume, and complexity penalties upon the Sounding Probe System.

For a launch of  $m$  Penetrometers simultaneously, a separate receiver, scanning diversity selection circuit, multiplexer port, and subcarrier demodulator are required for each Penetrometer. A time delay device is also required to enable sequential processing of the several impact data traces received simultaneously. The time delay device, or recorder, also enables sequential retransmission of the acceleration data to the MSFN.

Reliability and communication link signal quality may also be affected by a salvo launch design. If a simple power divider type multiplexer is used (as is contemplated for its weight advantages) each additional multiplexer channel reduces the amount of signal available to each receiver. The time delay device in series with the other communications functions has an adverse reliability effect.

The operational advantages in salvo Penetrometer launching may prove to outweigh the disadvantages listed above. However, a quantitative trade-off study is required before the final choice of salvo versus sequential launching is made

(3) Diversity Switching. The preliminary conceptual design for the Sounding Probe communications subsystem utilizes scanning diversity reception of data from each Penetrometer. This antenna selection technique requires additional equipment, however, and further investigation of the necessity for diversity reception should be made prior to final selection of system design.

A diversity reception system is desirable due to the random orientation a Penetrometer may have at impact. Depending upon the "look angle" to the Penetrometer, the polarization state exhibited by its transmitted RF carrier can be right circular, linear (any direction), left circular, or any intermediate degree of elliptical polarization. Hence, there exists a finite probability that the polarization losses exhibited between a Penetrometer and a single receiving antenna onboard the LEM, regardless of the latter's polarization sense, will be too high to enable adequate reception.

To minimize this probability, the conceptual design for the Sounding Probe uses two orthogonally polarized antennas. A receiver may be connected to either of the two antennas through its scanning diversity selection circuit. This circuit is essentially a threshold selection device, i.e., it senses the input signal strength to its associated receiver. When this signal

level drops below a fixed, predetermined level, the diversity selection circuit automatically switches the receiver over to operate on the other antenna. A simplified block diagram of a typical scanning diversity antenna selection circuit is given in Figure 3-19.

A diversity system such as the one described above has considerable impact upon equipment complexity with the attendant weight, volume, and reliability penalties. An extra antenna, feed system, and multiplexer is required. In addition, a separate RF switch, switch driver circuit, and receiver signal level sensing circuit is required for each receiver channel. Hence, if the necessity for diversity switching could be eliminated, considerable weight savings and system simplification could be achieved.

The fundamental question to be answered before considering the deletion of diversity reception is: what is the probability of a Penetrometer impact with such an adverse orientation that adequate signal margins no longer exist? i.e., over what portion of the "look angle" sphere would the antenna nulls as seen by a single, linearly polarized receiving antenna be so deep as to drop the received signal strength below the minimum required threshold level? The answer to this question is a function of both Penetrometer antenna pattern and the system circuit margins relative to an ideal, 0 db gain Penetrometer transmitting antenna gain. In Table 3.10 it was shown that a nominal positive circuit margin of 28.2 db exists with a -3 db transmitting antenna gain and a -3 db polarization loss. Hence, antenna pattern nulls of almost +35 db relative to isotropic must occur before the received signal drops below the acceptable level. Moreover, this margin is based upon a receiving system not utilizing a low noise preamplifier. With such a preamp, antenna nulls below 40 db would have to occur before the signal becomes unacceptable. Such extreme nulls are highly improbable, and it is recommended that quantitative measurements be made of the Penetrometer antenna patterns to determine the proportion of the sphere containing these nulls. If this proportion is sufficiently small, consideration should be given, based upon overall system reliability predictions, to simplifying the receiving system by removing the diversity reception feature.

c. LEM Communication Capabilities for Transmitting Sounding Probe Data To Earth. For transmission to Earth, analog Penetrometer data is acquired from the downstream side of the electronic commutator in the Data Processor. Data will not be received on Earth until it is simultaneously being processed; it may be held in the queuing circuit for many seconds. However, its purpose on Earth is merely to monitor and record for later detailed analysis. All data will be acquired prior to the LEM reaching the 200-foot altitude. If it proves desirable to transmit the computed values of impact velocity and impact angle along with the impact data, all must be tagged to identify the Penetrometer channel. As engineering data, it is probably desirable to transmit the inputs that go to the control electronics that are obtained from the LEM navigational computer. Launch angle, data

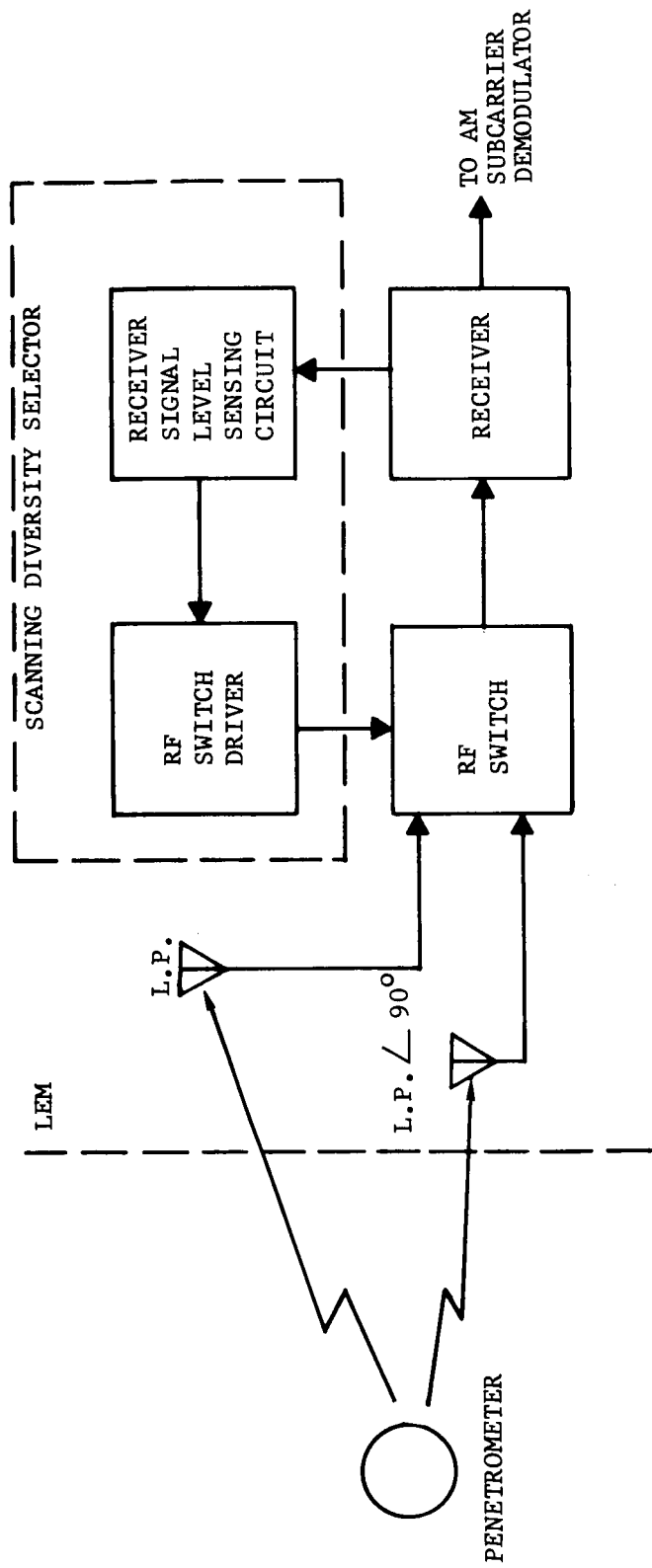


FIGURE 3-19. SCANNING DIVERSITY SELECTOR SIMPLIFIED BLOCK DIAGRAM

generated by the initial condition generator in the Data Processor, and inputs to the Display, and various check prints in the Data Processor may also be of interest on Earth. Several of these data may already be programmed for transmission via the LEM 51.2 KBPS PCM telemetry. For those data which cannot be handled by the LEM PCMTE (Pulse Code Modulation and Timing Equipment), signal processing must be provided within the Data Processor to enable time sharing the transmission of the data with the acceleration traces.

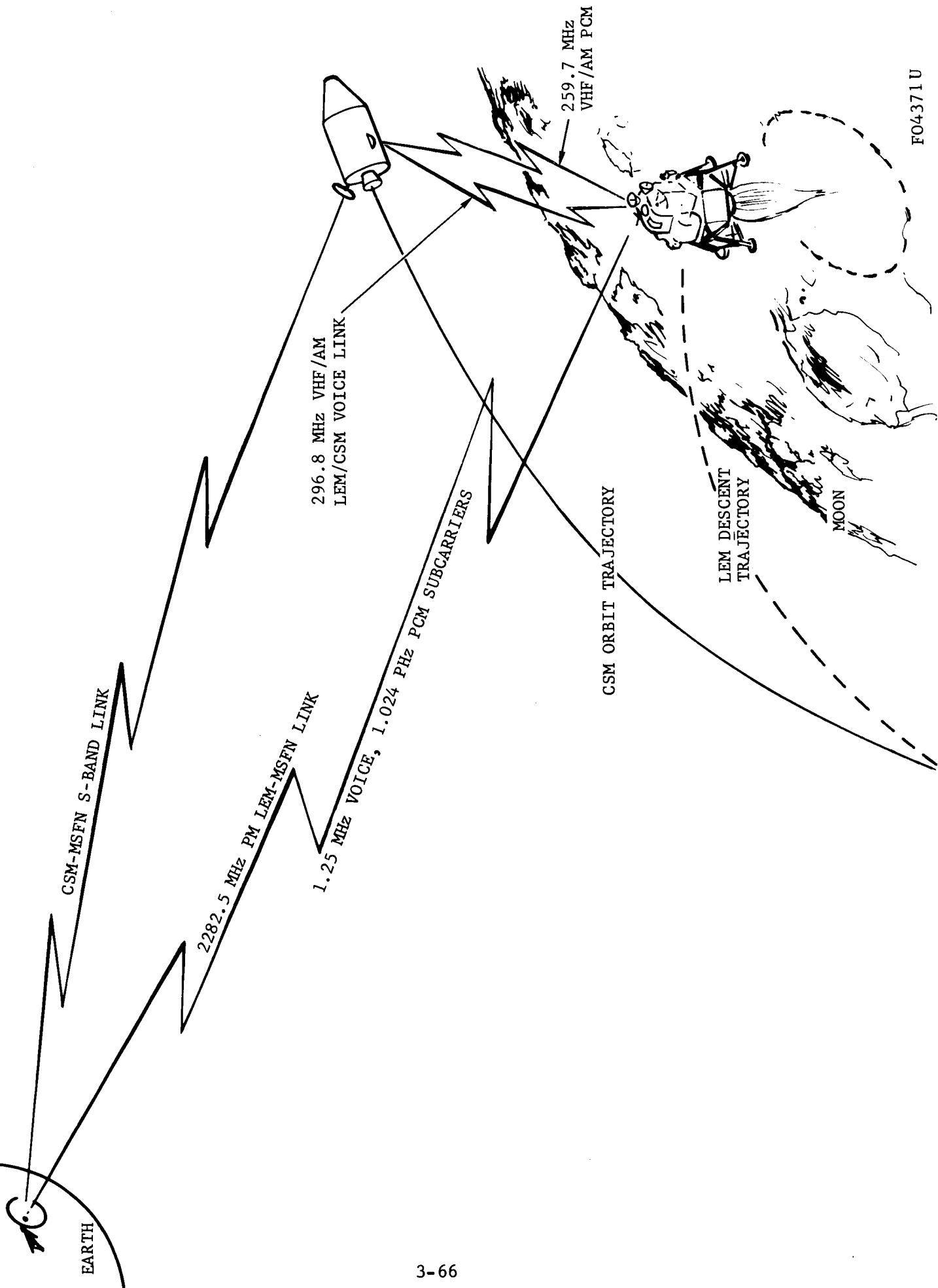
A preliminary investigation was made of the LEM communication capabilities available for use during landing to transmit Sounding Probe data to Earth.

The LEM has two communications methods available for maintaining contact with the Manned Space Flight Network (MSFN) during landing. The primary method utilizes a direct S-band transmission link with the MSFN. The back-up mode utilizes the orbiting CSM as a relay. These RF links are illustrated in Figure 3-20.

(1) Direct Link. The direct link S-band carrier is phase modulated by 1.25 MHz voice and 1.024 MHz telemetry subcarriers. The design of the communication equipment is somewhat inflexible, making it difficult to add another subcarrier directly on the carrier to carry the penetrometer data. The 1.25 MHz voice subcarrier capability is normally used during lunar stay activities to relay suit and biomed data from the extra-vehicular crewmen. It is available during landing for transmitting penetrometer data. The acceleration trace from a penetrometer can be modulated onto a 12.5 KHz (Channel 1C) constant bandwidth SCO. This SCO, in turn, can be summed with the crew's voice and the composite used to modulate the 1.25 MHz voice subcarrier. This method of transmitting penetrometer data can be easily implemented with little impact upon the present LEM communication system design.

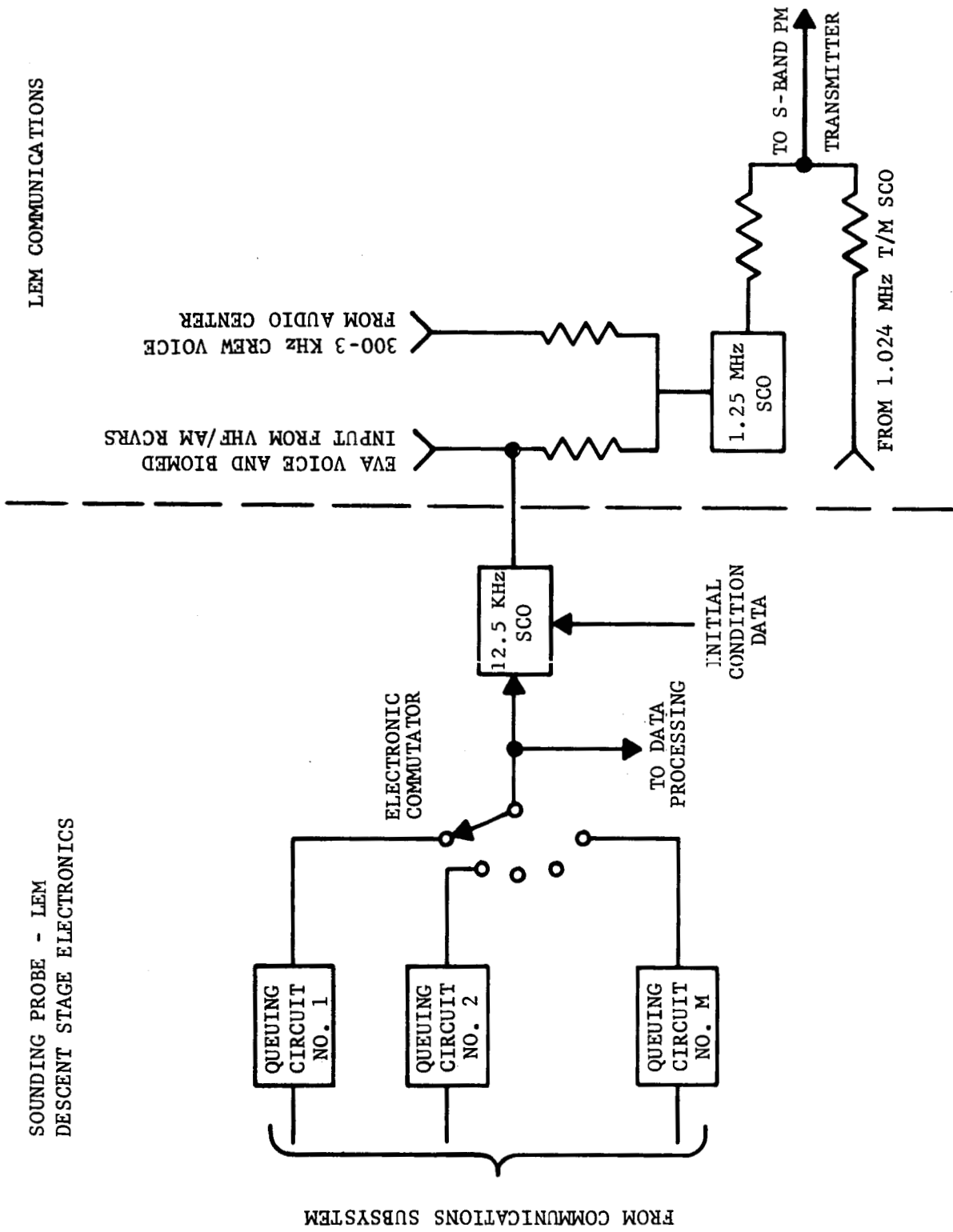
Use of this technique is contingent upon the capability to transmit the data from the several penetrometers sequentially, instead of in parallel. If the penetrometers are launched sequentially, this presents no problem. If salvo firing is used, however, this technique of transmitting the data to Earth necessitates a more complex data recording and sequential playback. Figure 3-21 illustrates in block diagram form the Sounding Probe LEM communications interface, using the EVA channel, for a salvo launch. An alternate transmission technique should salvo be used would be to add a third subcarrier on the S-band carrier. This subcarrier in turn, would be modulated with the number of SCO's required to transmit in real-time the data received simultaneously from the penetrometers. However, considerable modification to the existing LEM communication equipment would be required.

(2) CSM Relay. Figure 3-20 illustrates the two RF links available between the LEM and the orbiting CSM. These consist of a 2-way 296.8 MHz VHF/FM simplex voice link and a 250.7MHz VHF/AM PCM transmission link. The latter link is utilized when the LEM is unable to transmit directly to the



FO4371U

FIGURE 3-20. LEM LUNAR LANDING COMMUNICATION MODELS



FO4372 U

FIGURE 3-21. SOUNDING PROBE-LEM COMMUNICATIONS INTERFACE

the MSFN. Use of either of these links appears less feasible than the direct transmission to the MSFN, when the latter link is available. When it is not available (e.g., when the LEM landing takes place on the back side of the moon), both VHF channels are required for voice and telemetry data and hence are not available for use in transmitting penetrometer data.

#### 3.2.4 DATA PROCESSING

Signal data from the sensors are returned to the LEM in real time and are rapidly processed. The extracted information is then presented to the LEM crew in a manner that requires minimum interpretation to assimilate. Presenting the raw data itself, the acceleration-time history, is inappropriate since it detracts from their duties to analyze the trace. Rather, the analysis is mechanized and presented on a simple display console.

There are distinct advantages to both analog and digital readout. A discrete go/no-go display demands least interpretation time but transfers little information. This is unsatisfactory if there is time and a desire by the crew to have additional knowledge. What is needed is an indication of how bad is bad and how good is good. This can be partially obtained by having a go/maybe/no-go readout display or even up to five levels. Beyond this there may be much confusion. Alternately, an analog readout giving a continuous readout range allows for further interpretation, but its data is not assimilated as quickly as the simple 2- or 3-state digital display. The design that allows for both of these readouts sacrifices neither of the merits of the other. This is similar to that used on a vacuum tube tester; a continuous readout from a pointer attached to an analog meter and backed up with lights, the color and location of which are indicative of the amount of meter deflection.

Transforming an acceleration profile to satisfy the display is the functional requirement of the Data Processor subsystem. With inputs from the receiver, the LEM navigational computer and the control electronics providing the initial conditions, an output is provided that is indicative of surface landability. This may be done with the data as it occurs naturally in analog fashion, or it may be put through an analog-to-digital converter to be sampled, quantized, and encoded so that digital operations can be performed. The latter would most likely not occur in real time since all of the data would have to be digitized and stored prior to performing operations on it. The delay may only be seconds but could be sufficiently long to offset any savings in weight that it would offer through the use of micro-electronics. The results of this trade-off will have to await a complete analysis of the weights and volumes of each.

The study presented here is more one of logic than mechanization. It functionally describes the operations required on the data and demonstrates the general way this is accomplished in analog circuitry. With digital circuits

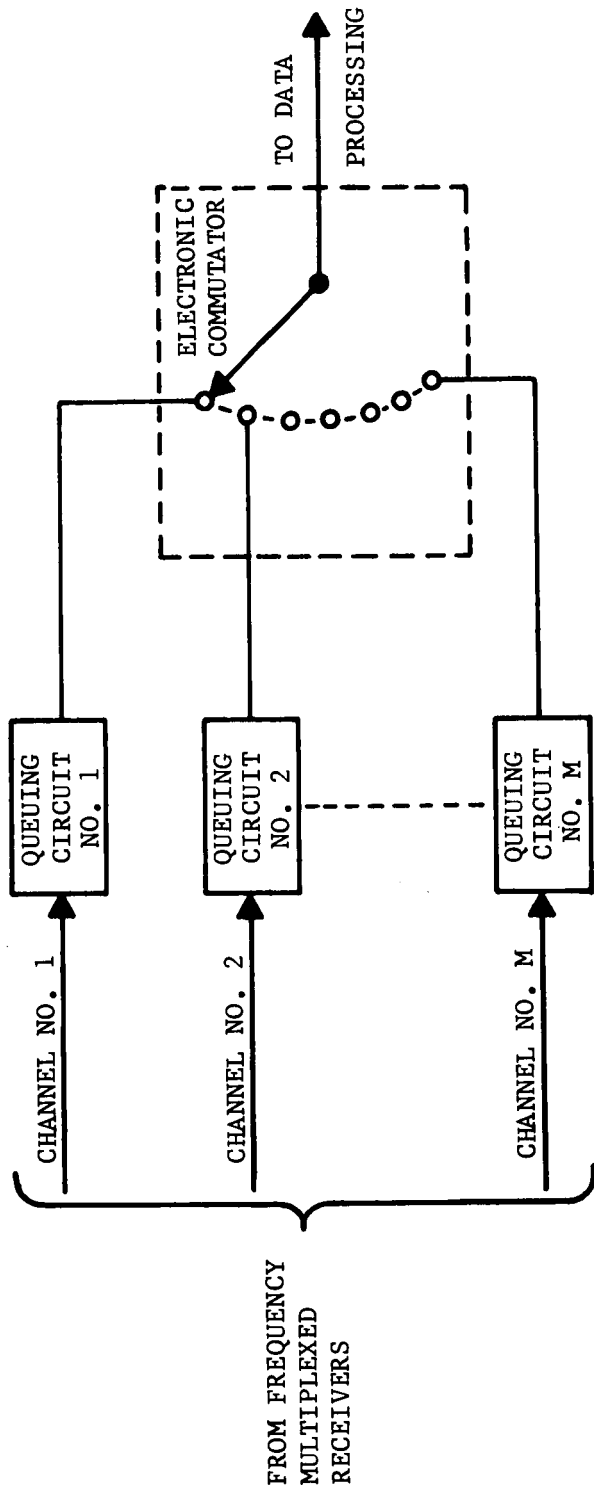
the steps are the same but represent operations that are stored in a digital computer as a preprogrammed subroutine. In contrast, what is described here is an analog computer with switching gates.

The Data Processor described in the following section is designed assuming that all Penetrometers are returning data simultaneously. This places the largest load requirements on its operation. Either a multi-channel processor can be used or temporary storage with a single processing channel must be provided. For illustrative purposes the latter is shown. Furthermore, of the many measurements that may be made on the data, only three have been chosen for discussion here. They are performed concurrently so that in the event that one or more should later be found to be inappropriate, they may easily be deleted. The three parameter equations appear at this time to be the most likely candidates.

a. Queuing. The analog signal into the receiver may represent the simultaneous reception of acceleration data from a multiplicity of Penetrometers. This places the most severe operating requirements on the electronics and normally is from the salvo launching. Even ripple firing is no better since the one launched first may have longer flight time than the one launched last due to either the LEM attitude or surface contours or both. The receiver separates these into discrete channels. In order to conserve weight and volume, only one computer is provided so that there must be some means for storing data as suggested in Figure 3-22.

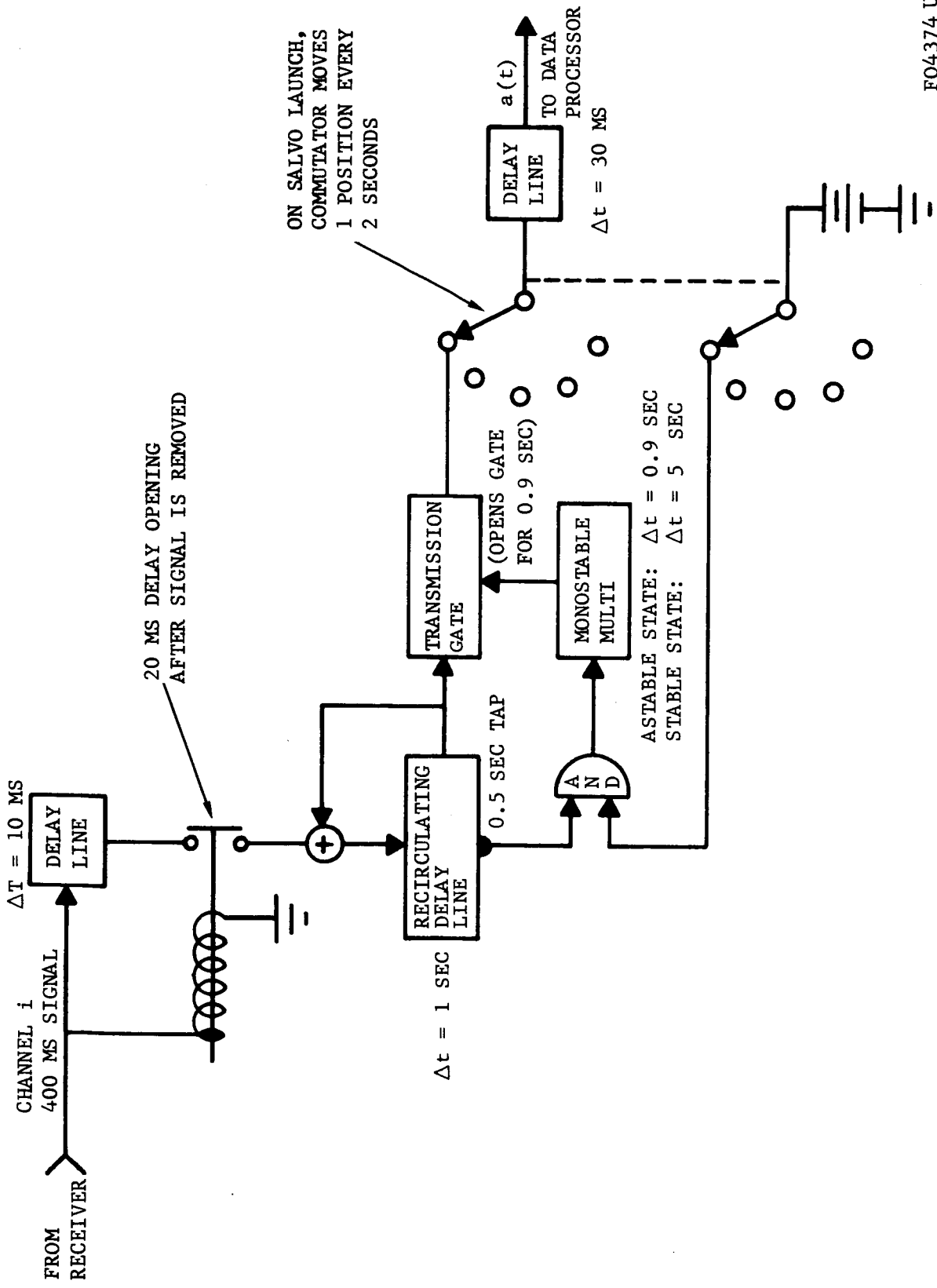
In analog systems a convenient means of short term storage is an equivalent delay line (magnetic tape, rotating disk, etc.) that continuously cycles the data. If the data is not recycled too many times and there is little signal attenuation, then no rejuvenation is required. Otherwise, signal enhancement with low noise figure may be introduced in the feedback loop. Figure 3-23 illustrates a queuing circuit to accommodate a signal in the  $i$ th channel that consumes no more than 400 milliseconds. There is one of these circuits for each of  $m$  channels. To place the signal in the "loop" a switch is closed 10 msec prior to the signal and opened 20 msec after the signal. The cycle time is one second which allows for at least 470 msec of dead time in the loop. If there were no other control between the delay line and the automatic commutator, then the latter would have to be accurately timed so that it would not switch into a channel and break into the acceleration profile, thus missing part of the beginning. Since the signals in the  $m$  channels are random in length and have random starting times with respect to each other, it would be too complex to program the automatic commutator to switch into a channel during a dead time of the loop. The control that is shown allows a queuing circuit to be connected to the data processor and the entire signal transferred without interruption.

Since the ganged commutator also places a continuous step on the AND gate it only requires that the signal trip the gate that switches state of a one-shot multivibrator. This has a time constant that allows the transmission



FO4373 U

FIGURE 3-22. TIME DELAY PROVISION FOR PENETROMETER DATA FROM SALVO LAUNCH



FO4374 U

FIGURE 3-23. QUEUING CIRCUIT

gate to open for 0.9 second even if the signal is removed from the AND gate. Assuming no time delay nor phase change from the 1/2-second tap on the delay line to opening of the transmission gate, means that the 400 msec signal does not get to the data processor until 500 msec later. At most, a 400-msec signal passes through before the gate closes. The commutator is programmed to spend two seconds on each channel, even though the maximum duration signal is only 400 msec. This allows about one second for the data processor to operate on the data, activate the display console, and reset circuits to be receptive for the next channel of data. Therefore, the circulating delay line and loop must be completely drained of the signal during the first time the gate is opened or else the AND gate will reopen 100 msec later and will effectively be an interference in the data processor for a subsequent channel. However, as a precautionary measure and in case there are some transients in the loop that may inadvertently open the AND gate, the flip-flop has a delay of 5 seconds in its stable state before being triggered again, so that it should only open the transmission gate once for the commutator.

The 30 msec delay line allows time for resetting circuits before  $a(t)$  arrives for processing.

b. Initial Conditions. An acceleration-time profile must be analyzed, parameters measured and decisions made as to whether these values indicate the surface is or is not acceptable for LEM landing. Fundamentally, the data processor is as shown in Figure 3-24. Successive integration of the acceleration  $a(t)$  provides the velocity  $v(t)$  and penetration  $p(t)$  of the Penetrometer into the Moon as indicated in Figure 3-25. Operations on these data must yield discrete parameter values which in turn are weighted, compared and correlated to yield one of a set of decisions to a display. The parameter measurements must be inclusive and the complete operation must provide for a correct decision on every conceivable surface whether it be homogeneous, a mixture, or layered. To do this the processor has been designed to expose the data to tests that search for the following three pieces of information:

- (1) Determine the existence of a layer with density  $\gamma$  acceptable for the LEM.
- (2) Determine the existence of a layer with bearing strength  $\sigma$  acceptable for the LEM.
- (3) Determine if an acceptable layer is at an acceptable depth for the LEM.

To do this, three parameters of the time profiles are compared with those that have been determined to be acceptable for the LEM. Figure 3-25 illustrates the standard values  $a_\gamma$ ,  $a_\sigma$ , and  $p_{ng}$ . Figure 3-26 indicates that they are each dependent upon the impact velocity  $v_I$  and impact angle  $\eta$  of the

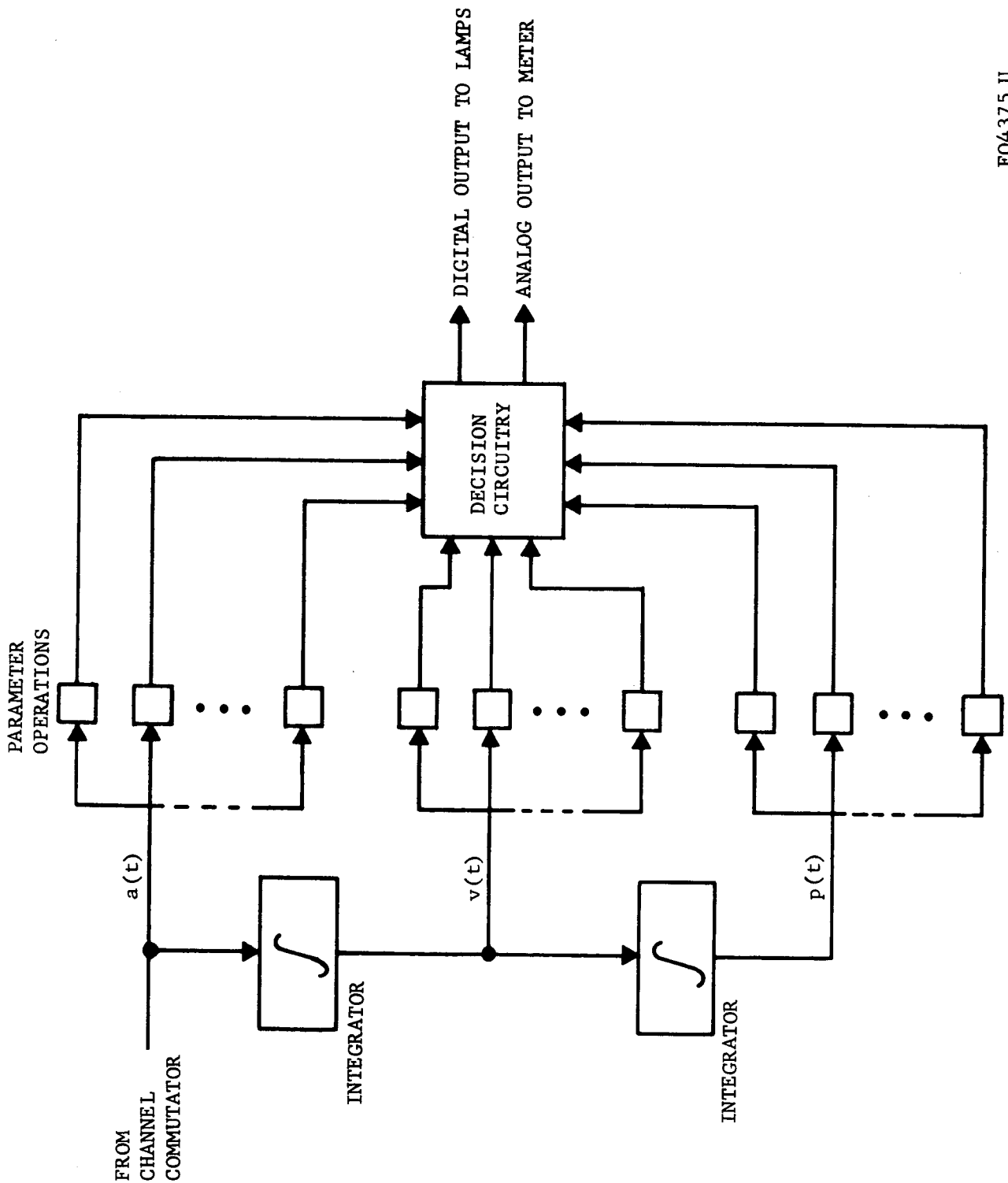
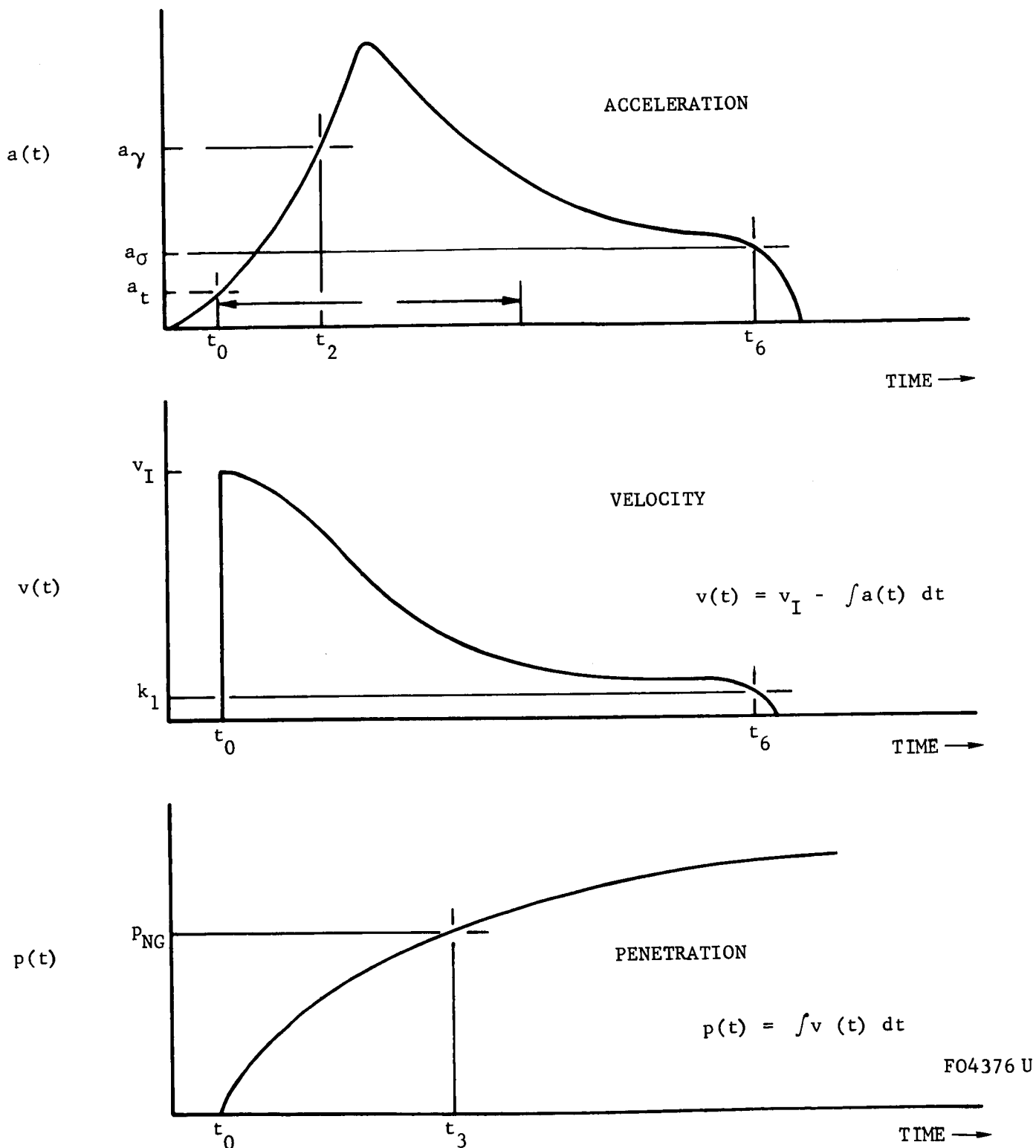


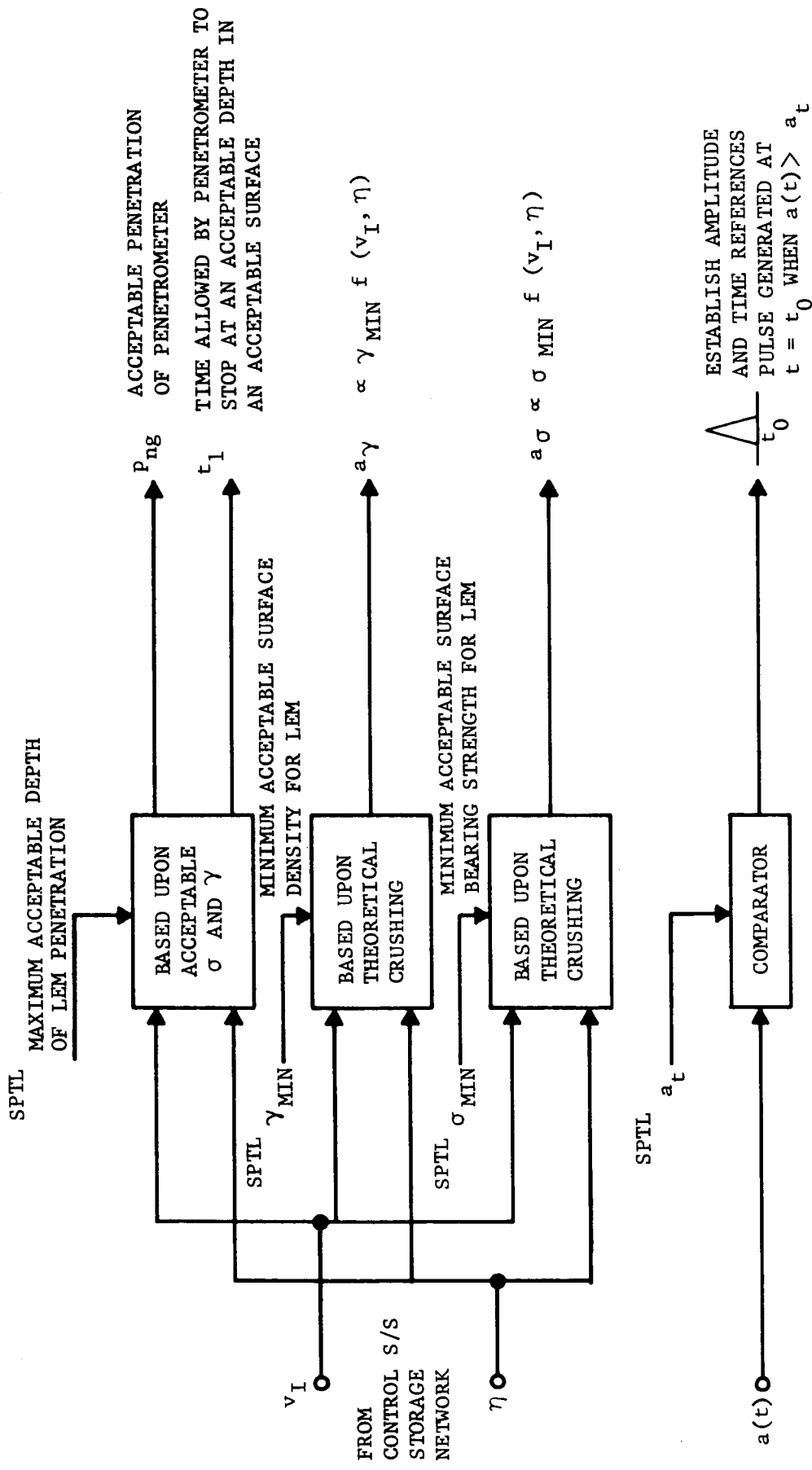
FIGURE 3-24. DATA PROCESSOR

FO4375 U



FO4376 U

FIGURE 3-25. HYPOTHETICAL TIME PROFILES OF ACCELERATION, VELOCITY AND PENETRATION



SPTL: SET PRIOR TO LAUNCH

FIGURE 3-26. INITIAL CONDITION GENERATOR

FO4377 U

Penetrometer on the Moon. Theoretical inputs are provided by the control computer. The three threshold values are continuously updated in flight, but require that a theoretical transformation characteristic be known prior to launch. Minimum acceptable values of density  $\gamma_{\min}$  and hardness  $\sigma_{\min}$  and maximum depth  $p_{ng}$  must be uniquely related to  $v_I$  and  $\eta$ .

To establish time and amplitude bases, the pulse occurring at  $t_0$  is generated when  $a(t)$  exceeds a low preset value  $a_t$ . This plus  $v_I$  and  $a(t)$  are used to generate  $v(t)$  and  $p(t)$  as shown in Figure 3-27. Note that  $a(t)$  is delayed an additional 30 msec to allow the initial condition generator to set the proper threshold values. The purpose of the feedback loop around the first integrator is not only for convenience to stop integration, but also to determine the specific time when  $v(t)$  has diminished to a small fraction of  $v_I$ . This time is used later to locate the tail-off in  $a(t)$ .

c. Criteria. For a given  $v_I$  and  $\eta$ , the time allowable for  $a(t)$  to reach  $a_Y$  is designated  $t_1$ . In Figure 3-28, a pulse from  $t_0$  to  $t_0 + t_1$  is generated and is designated  $X_1$ .

In Figure 3-29, a pulse is generated if  $a(t)$  exceeds  $a_Y$ . If  $t_2$  occurs before  $t_0 + t_1$ , the duration of the output  $X_2$  must extend beyond  $t_0 + t_1$ ; after that it may be stopped anywhere. Arbitrarily, it is stopped 400 msec after starting since it is not anticipated that  $t_1$  will ever exceed 400 msec.

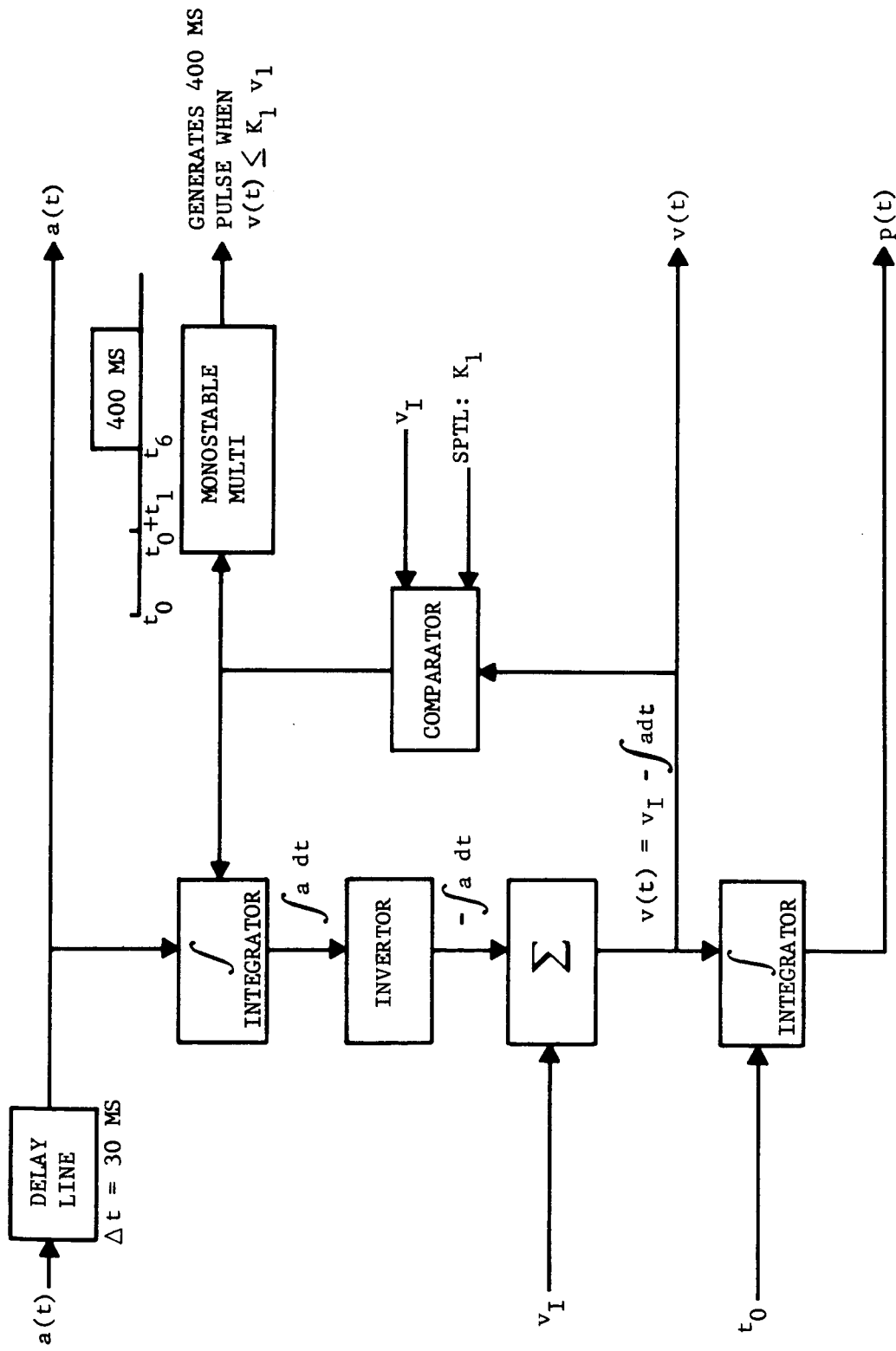
Similarly, if a depth greater than the no-go depth  $P_{ng}$  is exceeded, a pulse is generated at the time this occurs,  $t_3$ . Figure 3-30 shows the output  $X_3$  lasting for 400 msec for the same reasons as above.

Each of  $X_2$  and  $X_3$  are compared with  $X_1$  in Figure 3-31. If a layer with density greater than  $\gamma_{\min}$  and at an acceptable depth is detected, a pulse of duration  $(t_0 + t_1) - t_2$  is generated. If no such layer is detected ( $X_2 = 0$ ) or it occurs at an unacceptable depth ( $t_0 + t_1 < t_2$ ) no pulse is generated at  $X_4$ . If the Penetrometer does not go very deep ( $X_3 = 0$ ), or if it does and it takes a long time to get there ( $t_0 + t_1 < t_3$ ), then no pulse is generated at  $X_5$ .

The amplitude of the tail of the acceleration profile before it drops to zero is a measure of bearing strength. In Figure 3-32, as soon as a pulse appears at time  $t_6$ ,  $a(t)$  is compared to  $a_\sigma$ . If it is greater, then a pulse is produced at  $X_6$  for 400 msec.

From the previous discussion the three separate criteria may be expressed as follows:

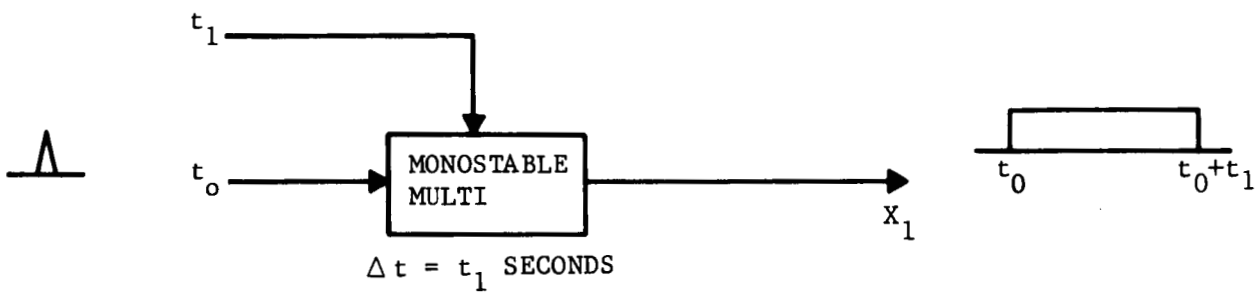
- (1) If  $a(t) > a_Y$  when  $t \leq t_0 + t_1$  then a layer with density greater than  $\gamma_{\min}$  is within an acceptable depth for LEM.



SPTL : SET PRIOR TO LAUNCH

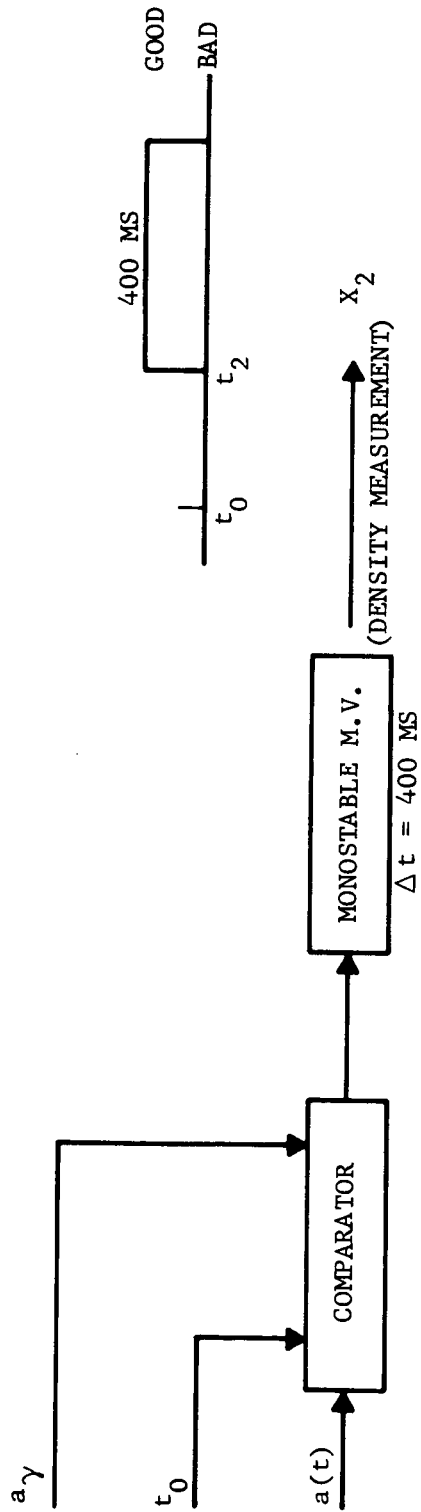
F04378 U

FIGURE 3-27. VELOCITY AND PENETRATION CALCULATOR



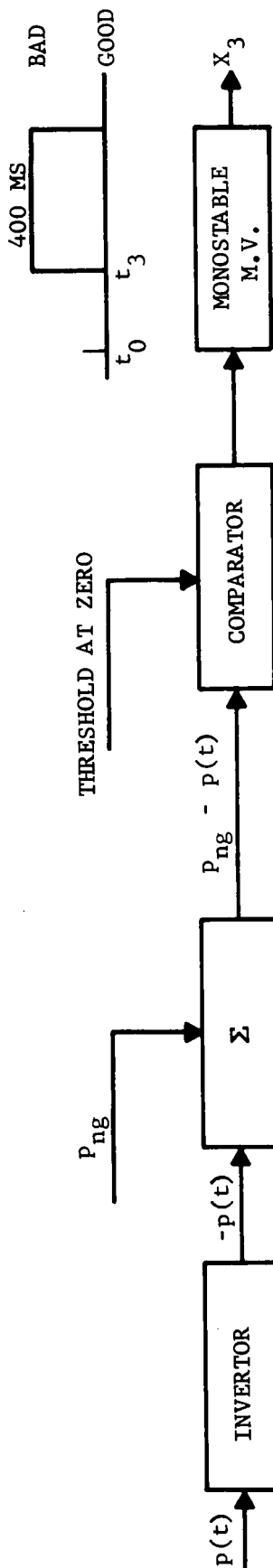
FO4379 U

FIGURE 3-28. ALLOWABLE TIME FOR  $a(t)$  TO REACH  $a_v$



IF  $a(t) > a_\gamma$ , OUTPUT IS PULSE.  
 PRESENCE OF PULSE MEANS THAT  
 DENSITY IS GREATER THAN  $\gamma_{\text{MIN}}$

FIGURE 3-29. CRITERION - PEAK ACCELERATION



IF  $p(t) > P_{ng}$ ,  
 OUTPUT IS PULSE  
 PRESENCE OF PULSE  
 MEANS THAT THERE  
 IS A SOFT LAYER

FO4381 U

FIGURE 3-30. CRITERION - DEPTH OF PENETRATION

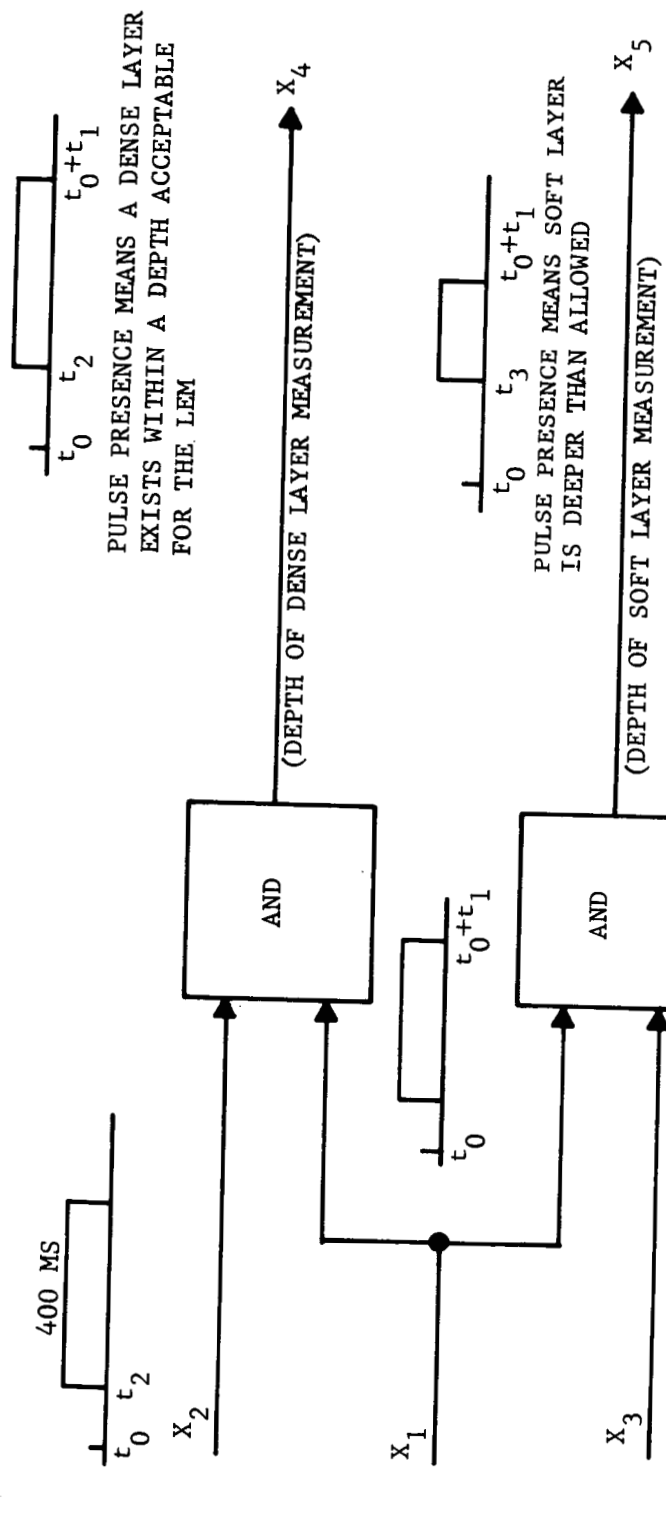
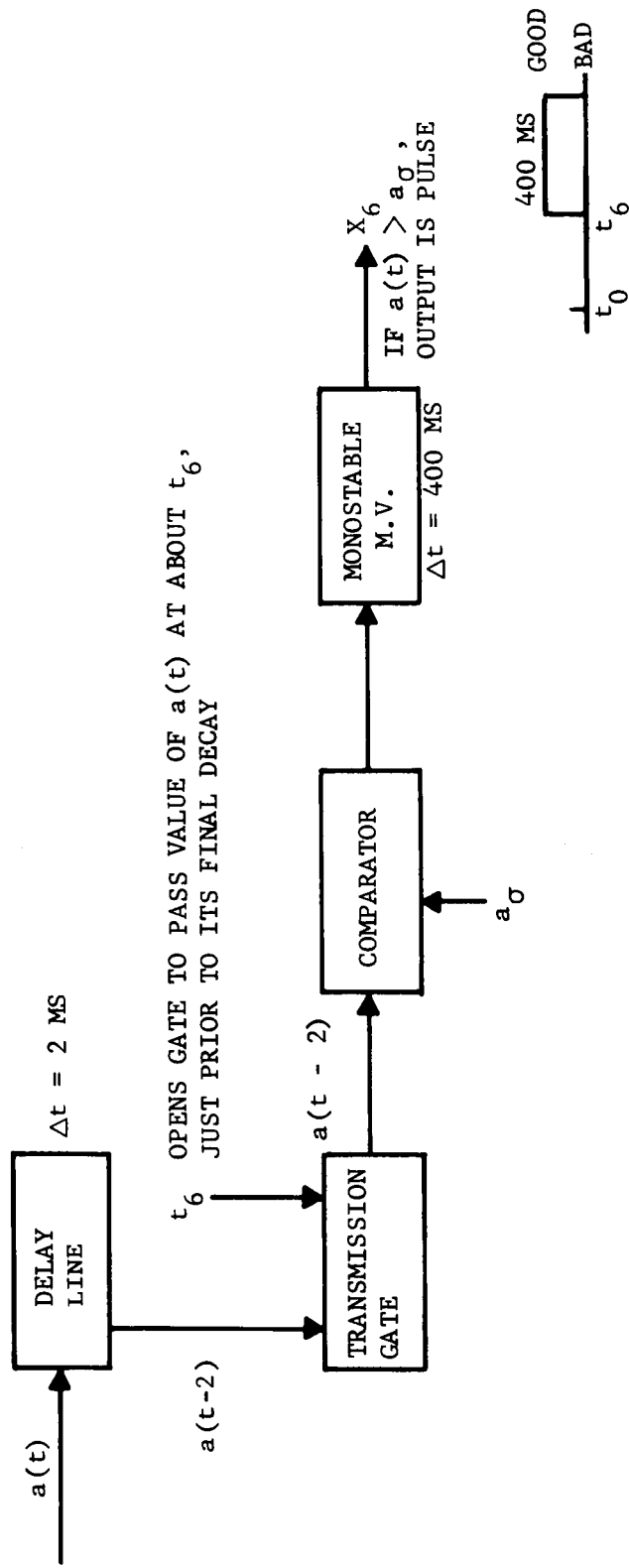


FIGURE 3-31. COMPARISON CIRCUITRY



PRESENCE OF PULSE MEANS THAT SURFACE IS HARDER THAN  $\sigma_{min}$

FO4383 U

FIGURE 3-32. CRITERION - TAIL-OFF ACCELERATION

- (2) If  $a(t) > a_{\sigma}$  when  $v(t) \leq k_1 v_I$  then a layer with bearing strength greater than  $\sigma_{\min}$  is present.
- (3) If  $p(t) > P_{ng}$  when  $t \leq t_0 + t_1$ , then a soft layer is deeper than the LEM limits.

d. Decision. A surface is either acceptable or it is not. Therefore, if all Penetrometer readings agree, the LEM will either sink into an unacceptable depth or it will not. And when the landing is finished it will either be successful or it will not. The crew either gets back to Earth alive or it does not. On the other hand, predicting such an event is not as clear. Uncertainties arise not only from the instrument but also in the theoretical models being used. Therefore, on the display there is an acceptable zone (HARD) an unacceptable zone (SOFT) and an uncertainty zone (MEDIUM), the latter region being necessary because of uncertainty in the measurement.

Three discrete results are the outputs  $X_4$ ,  $X_5$ , and  $X_6$ . At  $X_4$  if a pulse is present, the indication is good, while at  $X_5$  a pulse is bad news. These pulses occur prior to  $t_0 + t_1$ . At  $X_6$  if a pulse is present the surface is acceptable but the pulse may likely occur after  $t_0 + t_1$ . To correlate their presence, or absence,  $X_4$  and  $X_5$  are stretched by flip-flops.

Each of the three outputs should be weighted relative to each other since there are varying degrees of confidence in the measurements. With weights  $K_4$ ,  $K_5$  and  $K_6$  for unit pulses  $X_4$ ,  $X_5$  and  $X_6$ , respectively, the deflection of a display meter is:

$$\text{meter deflection} = \text{bias} + K_4 X_4 + K_5 X_5 + K_6 X_6.$$

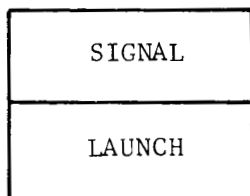
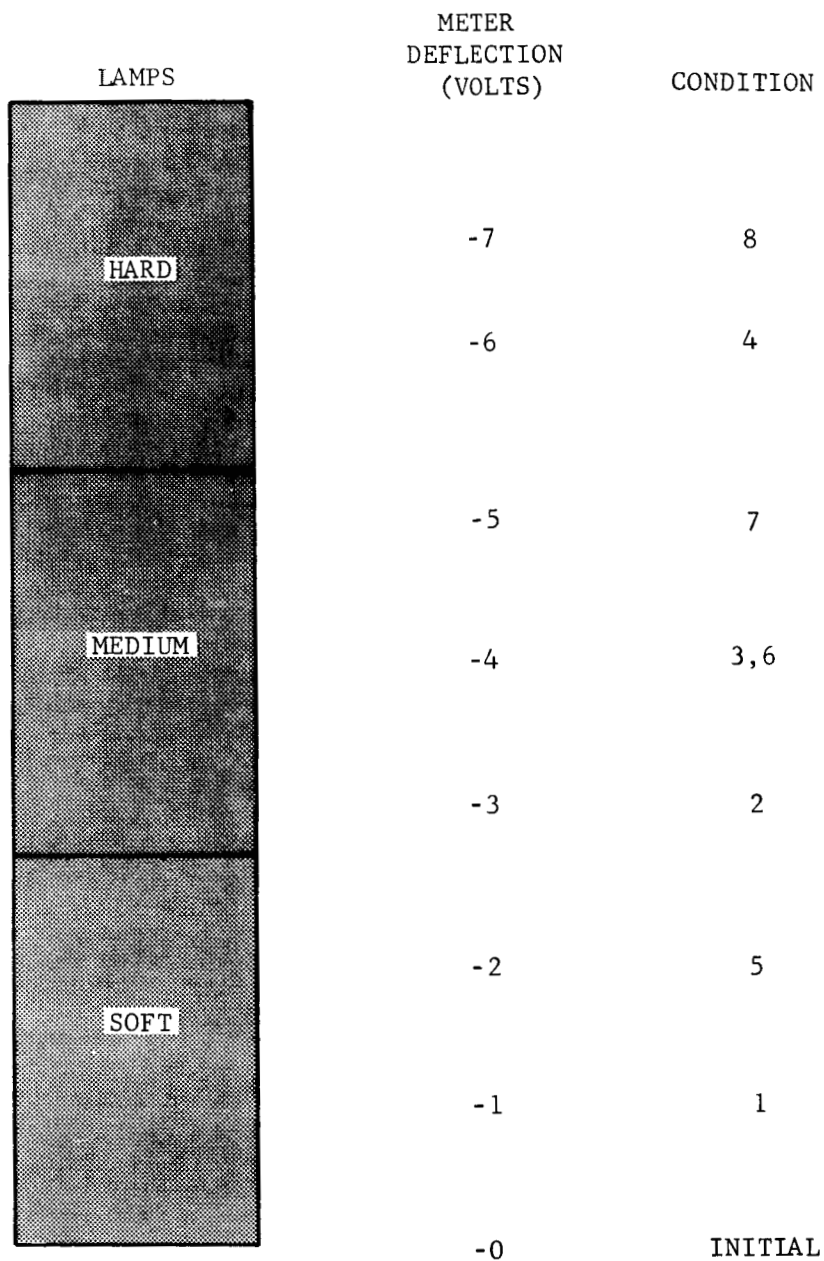
For example, if the depth indicator  $X_5$  is 1-1/2 times more reliable than the hardness measurement  $X_6$ , and if the latter is twice as reliable as the density measurement  $X_4$ , then the weights might be  $K_4 = 1$ ,  $K_5 = 3$ ,  $K_6 = 2$ . With a 1 volt bias the decision logic appears as in Table 3.11 on a display as in Figure 3-33. The excitation for the lamps and meter are mechanized according to Figure 3-34. Or deflection may be assigned by some other criterion based upon data validity.

### 3.2.5 DISPLAY

The primary function of the display is to indicate the landability of surface at the point impacted by each Penetrometer. It would add further value to the display if it were also able to indicate the relative location of each Penetrometer-sampled area. This secondary function will be discussed first.

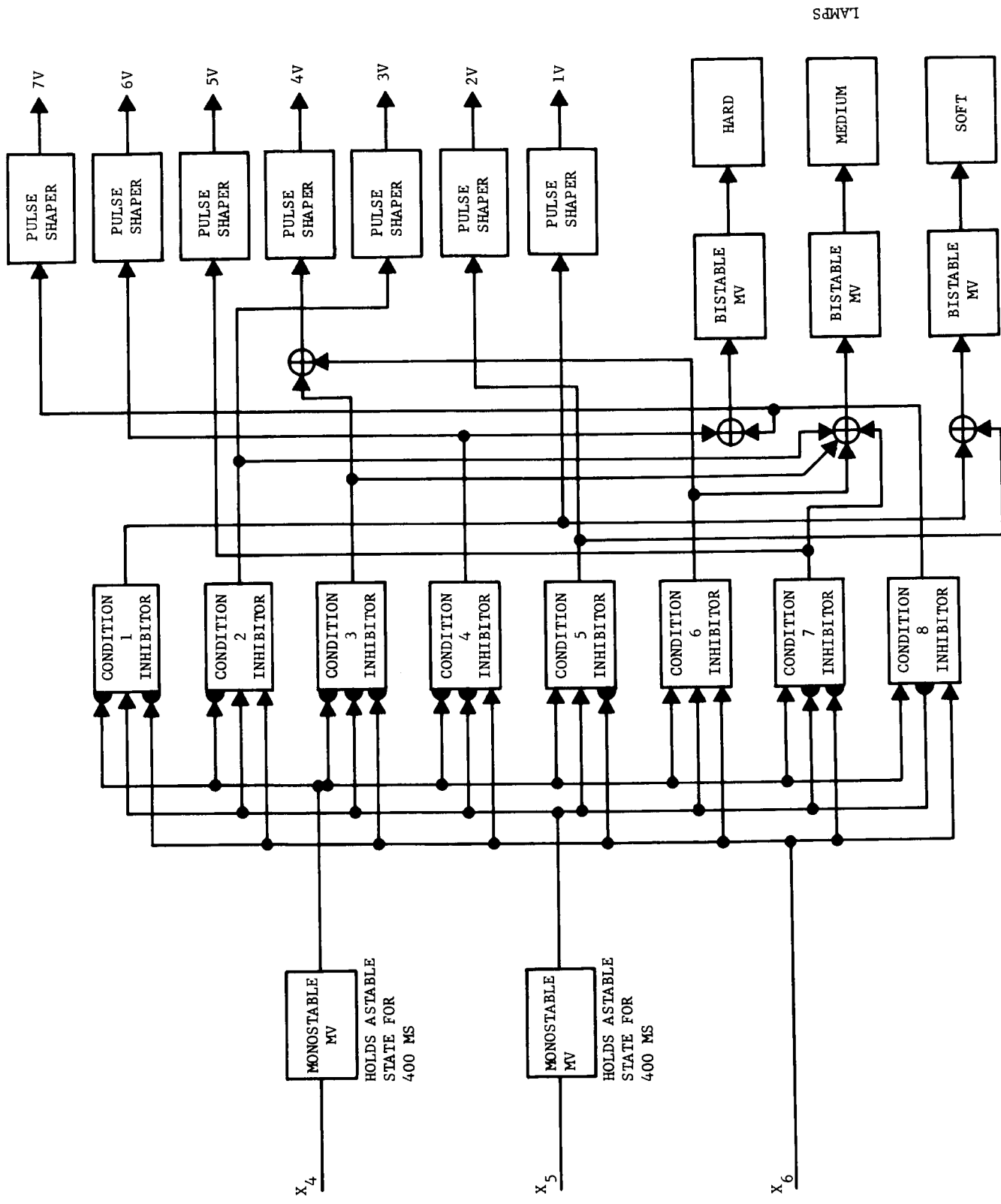
TABLE 3.11  
DECISION LOGIC

Condition	Density $X_4$	Depth $X_5$	Hardness $X_6$	Meter Deflection (Volts)
				(1 Volt Bias)
1	No Good (No Pulse)	No Good (Pulse)	No Good (No Pulse)	$1 + 0 = 1$
2	No Good (No Pulse)	No Good (Pulse)	Good (Pulse)	$1 + 2 = 3$
3	No Good (No Pulse)	Good (No Pulse)	No Good (No Pulse)	$1 + 3 = 4$
4	No Good (No Pulse)	Good (No Pulse)	Good (Pulse)	$1 + 5 = 6$
5	Good (Pulse)	No Good (Pulse)	No Good (No Pulse)	$1 + 1 = 2$
6	Good (Pulse)	No Good (Pulse)	Good (Pulse)	$1 + 3 = 4$
7	Good (Pulse)	Good (No Pulse)	No Good (No Pulse)	$1 + 4 = 5$
8	Good (Pulse)	Good (No Pulse)	Good (Pulse)	$1 + 6 = 7$



FO4384 U

FIGURE 3-33. DIAGRAM OF DISPLAY FOR ONE CHANNEL



FO4385 U

FIGURE 3-34. DECISION CIRCUIT AND DISPLAY

a. Tracking. Ideally, the display should be a visual representation of each deployed Penetrometer indicated on a topographical model or facsimile of the pre-landing footprint with instantaneous updating for spacecraft attitude, pitch, yaw, and other time dependent functions. This representation instantly indicates, both to the astronauts and to the MSC, the LEM position with respect to range, azimuth, and remaining time for each Penetrometer with a "go" reading, as well as whether or not that Penetrometer is still within range of the LEM, based on remaining on-board fuel. This type of display requires an imaging device, fiber optics, the full use of the LEM computer, and a complete set of unique subroutines. It also requires a data rate substantially greater than the present capability.

A less sophisticated system uses an updated footprint facsimile (three steps -- 10,000, 2,000 and 100 foot altitudes) which would require the astronaut to mark the location of each impacting Penetrometer by its number, and indicate the go or no-go reading. The updating would indicate the footprint for each altitude, and mental extrapolation would serve to indicate whether a particular penetrometer was still reachable from the LEM's present position.

This system still requires an imaging device (though a Polaroid camera would be very easy to use) plus a crayon or similar marking tool, in addition to the indicator or Landing Aids panel for go/no-go readings on the individual Penetrometers.

An even less sophisticated scheme involves a sketch pad in conjunction with the Sounding Probe panel. The astronaut hurriedly sketches the impact locations of the Penetrometers as well as pertinent landscape markers. In this fashion the updating is continuous, and commencing with a given envelope at a particular altitude, the size of the footprint can be indicated in a manner similar to polar graph paper techniques.

The obvious disadvantage to this type of locating system is that it requires both visual tracking of each Penetrometer from launch to impact, and a sustaining effort on the part of one of the pilots to keep the landing sites in view, plus updating his maneuver capability so that he can determine whether he can reach a particular Penetrometer at any given point along the touchdown approach.

Earth-bound tests (in atmosphere) under less than optimum viewing conditions show that with normal eyesight (corrected to 20-20), a four-inch iridescent sphere can be readily seen by an observer at ranges up to 0.4 statute miles. Sun angle is the major variable in viewing, with maximum capability when the sun is at the viewer's back and minimum acuity when viewing into the sun. The LEM mission plan calls for the solar subpoint to be at the east and at an angle of from 15 to 45 degrees, assuring

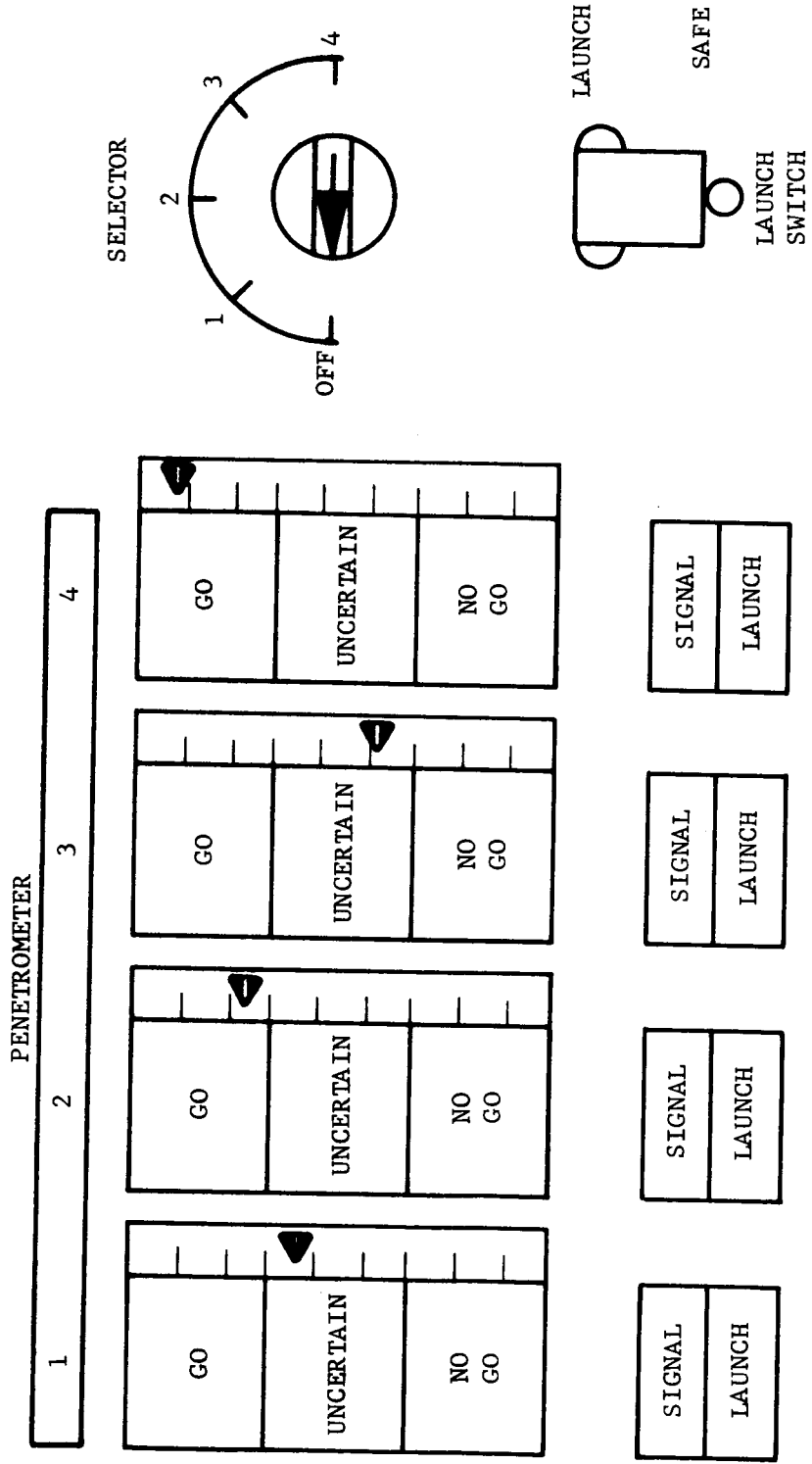
lighting conditions for maximum viewing. Iridescent colors are superior for terrestrial differential viewing, and it is assumed that a similar condition will exist on the Moon. The absence of light scattering atmosphere will naturally make the landscape stronger in contrast, though probably less variegated in coloring or hue than Earth terrain. It is believed that bright (iridescent) colors will show up at least as well on the Moon as on Earth so long as they are in direct sunlight. The use of the color differentiating capability is intended for real time tracking from Penetrometer launch until impact. An additional piece of decision-making information becomes available to the astronaut in this mode of tracking; namely, if he tracks a sphere down to impact and then sees that it bounces off the lunarscape, a very important piece of information has been gained. The combined use of this visual cue and the Display panel indicator should provide maximum data.

The number of Penetrometers to be deployed is assumed to be four. This does not appear to be too many for which to recall position and condition. The problem arises when the conditions are mixes of go and no-go. In the event that each penetrometer reports a "go" condition, and the astronaut can visually assess the area as being apparently homogeneous, his concern over finding the exact impact point with one of the LEM footpads will be small compared to that which he will have on variegated landscape.

Therefore, since automatic tracking techniques appear to be complex, requiring much equipment, and manual tracking and record keeping do not appear feasible, the single expedient of launching 2 salvos of not more than 2 different colored Penetrometers each is an acceptable mode of operation.

b. Go/No-Go. A display in the LEM cabin is required to provide the astronaut with an electronic assessment of the go/no-go condition for each Penetrometer. One type would reproduce the entire curve of g-loading versus time for each penetrometer to allow the astronaut to evaluate each curve independently. The amount of training as well as the time during the descent phase required for the astronauts to properly evaluate each curve, plus the equipment necessary for the display within the LEM cockpit would be excessive for this mission. An alternate method is required in which there is a decision to go or not to go, based on the independent reaction of each Penetrometer.

The arrangement of the Display panel is shown in Figure 3-35 as it might appear prior to the launching of any penetrometers. Each vertical scale contains a three-color indicator (each color being a segment), plus a linear pointer that holds its deflection. In addition, a portion of the firing control panel is shown. Two modes of Penetrometer deployment are available with this system. The first entails moving the selector to the desired Penetrometer number (1-4), and the Launch Switch to "Launch." This will fire only the Penetrometer selected. An alternate to this single shot



FO4386 U

FIGURE 3-35. DISPLAY PANEL

technique is to put the switch on "launch" and then rotate the Selector from "Off" through 1, 2, 3 and 4, thereby salvoing the entire load of Penetrometers. The mode of deployment selected is dependent on the anticipated pattern of impact based on time and communication restraints.

An analysis of the bearing strength, density and time profile is made by the data processing subsystem and electrical signals sent to the display. These signals are of two distinct types; namely, (1) a dc go/no-go signal for each of the colored lamps in each indicator, and (2) an analog output for driving the linear pointer.

The threshold for these two types of signals is coordinated such that the indicator lamp goes on coincident with the movement of the linear pointer. The reason for this is that the lighted indicator gives an immediate visual stimulus to denote that a threshold value has been reached, whereas the pointer operates on a continuous scale and thus shows by how far a particular threshold has been exceeded. The two independent readout mechanisms also provide a check and balance for each other, thus increasing the astronaut's confidence at a very small investment in circuitry and weight.

c. Installation. Responsibility for the operation of the Sounding Probe should be assigned to the astronaut who is least occupied during the time span involved. The display (that is, the vertical light bars with the linear pointer assemblies) can be designed into a case no larger than 3 inches high, 4 inches long, and 2 inches deep that can be readily discerned. Location of the display is not critical for color identification, but a reading distance of approximately 18 inches is required to ascertain the linear pointer position, even with back illumination.

The natural action for both astronauts, duties permitting, will be the visual surveillance of the lunar terrain for the maximum amount of time to glean as much data as possible during this unique experience. It has been established in prior studies that cyclomotor reflexes are easily controlled, even under involuntary conditions; thus it is felt that the ideal display would be a much smaller wrist mounted unit for each of the astronauts (the launch control would still be the responsibility of one astronaut), say 1 x 2 x 3 inches. This location would assure ease of observation, since the arm could be moved, rotated, or raised to permit maximum viewing angles with a minimum of head turn. Each astronaut should have a display for correlating purposes as well as functional back-up. Should the pilot be assigned the Sounding Probe operation and the Command Pilot not be aware of the landing position of the Penetrometers, difficulties could arise in one astronaut's trying to instruct the other to a particular ground location, if the general appearance is homogeneous. If each astronaut has a display and if they share tracking of the penetrometers or track alternate launches, the ability to recall two locations is much less than trying to recall four, plus the tying together of a location and a go or no-go

condition is simplified. It appears to be a situation which can be adequately handled by one man of astronaut caliber, but can be more easily handled by two, to their mutual satisfaction.

If the wrist portion of the astronauts' arms are occupied by other counterments and actions during this time, alternate display locations are acceptable. The available areas within the cabin where the display can be located are on either side, in the rear of the cabin or overhead. The most desirable location for a single display is where both astronauts can see it with a minimum of head turn. The control does not have to be near the display. It is more critical that safety be the prime consideration for locating the control, whereas visibility is the prime prerequisite for the display.

Table 3.12 summarizes the prime attributes and characteristics of the various mounting locations for the display. The hand held and window displays are listed along with side and rear consoles. The side console requires a maximum size capability, since it must be capable of being read from across the cabin. The rear display can be centrally located as previously stated, and since the main indicator is a color coded response, no difficulty in astronaut interpretation is anticipated.

One of the desirable attributes of the display is that it be capable of being removed from the ascent stage in the event it is decided to fly without it on subsequent missions, and particularly for off-loading on the lunar surface, thus reducing the ascent weight. It is thus intended that a single mating interface connector carry the complete display circuitry. In this manner a panel-mounted display could be readily dismantled and left after unmating the electrical connector. The hand-held system would merely require disconnecting the electrical circuit.

From the matrix two mounting sites are feasible. That preferred for visibility, mobility, weight and convenience is the wrist model, one for each astronaut. The alternate location is at the rear, with a mirror positioned such that each astronaut has ample visibility to the display.

TABLE 3-12  
 DISPLAY CONSOLE MOUNTING MATRIX

LOCATION	HAND HELD	SIDE CONSOLE	IN WINDOW	REAR
Size Limit	2" x 3" x 4"	8" x 24"	Limited to window for display	No limit*
Weight Limit	0.2-0.3 pounds each (two required)	No limit*	No limit*	No limit*
Connection	Connect to console	Integrate or add-on	Integrated in window	Integrated or add-on
Viewing Ease and Correlation	Good - maneuverable (undesirable if both astronauts must see a single unit or if it must be relinquished)	Not good. Requires from 80 to 150° turn and refocusing in short time span.	Excellent - superimposed on window, requires only refocusing	Not bad-use mirrors (has advantage of being mounted between astronauts and thus is readily viewable by either or both.)
Physical Interference	Could be very bad	Minimum - out of way	Could be bad	Minimum - out of way
Mech. Interface	Minimum	Moderate to min.	Moderate to max.	Moderate to min.
Development Risk	Minimum	Minimum	Maximum	Minimum
Ease of Replaceability	Excellent	Good	Poor	Good
Off-Loading Capability	Excellent - Little residual ≈ .1 pound	Fair - residual = 2 pounds	Poor - residual = 10 pounds	Fair - residual = 2.2 pounds
Estimated Total Descent Weight	0.5-0.6 pound	4 pounds	14 pounds (exclusive of window)	4.2 pounds

### 3.3 FUNCTIONAL SPECIFICATIONS

The following functional specifications are preliminary and subject to change as the system becomes better defined.

#### 3.3.1 LEM INTERFACE

a. Purpose. This specification describes the LEM interface characteristics relevant to the conceptual design of the LEM Sounding Probe System.

b. Description. The Sounding Probe mission has been described in Paragraph 3.1. The Lunar Excursion Module is a manned vehicle used to deliver two of the three-man Apollo crew from an 80 miles circular orbit to the lunar surface. The LEM and its companion vehicle, the Command and Service Module (CSM) are launched by a Saturn V Booster from Cape Kennedy, Florida. The LEM is stowed in a protective housing (the Spacecraft LEM Adapter) until the LEM and CSM are fired out of Earth orbit into a translunar trajectory by the S-IVB stage of the Saturn V configuration. The CSM then detaches from the SLA, "yaws" 180 degrees, and docks nose-to-nose with the LEM vehicle. At this point the SLA and the spent S-IVB booster stage are jettisoned, and the CSM and LEM continue their nominally 65 hour trip to the moon. During this launch and translunar portion of the Apollo mission the LEM systems are essentially inactive. Passive thermal control is supplied during the translunar flight by slowly rotating the CSM-LEM configuration about its longitudinal axis in a plane normal to the solar vector. The amount of incident solar radiation intercepted by the Sounding Probe subsystems and subsequent thermal control required will be determined to a large degree by their location upon the LEM.

After the LEM and CSM have been placed into an 80-mile circular orbit around the moon by the Service Module propulsion system, two of the three-man crew enter the LEM and prepare for their descent to the lunar surface. After completion of these preparations, the LEM separates a short distance from the CSM and fires the descent engine for a short time to place the LEM into an elliptical Hohmann descent transfer orbit with a 50,000 feet pericyynthian. The LEM then coasts along this descent trajectory until the pericynthian, approximately 225 miles shy of the selected landing site, is reached. At this point the LEM descent engine is reignited and a powered descent maneuver brings the LEM to the High Gate condition several thousand feet above the lunar surface. At this point the LEM is re-oriented to give the crew continuous visibility of the selected landing site for the remainder of the mission.

The LEM continues descending from High Gate with this revised attitude until it reaches the Low Gate condition, several hundred feet above the lunar surface and approximately 2500 feet short of the selected landing site. The mission profile from this point until touchdown is discussed in

Paragraphs 3.1 and 3.2. It is during this LEM mission phase that the Sounding Probe is utilized to determine the suitability of the landing site.

c. Physical Configuration. The external LEM configuration is illustrated in Figure 3-36. The LEM descent stage houses the descent engine and propellents, landing gear, and all operational and scientific equipment not required during the subsequent ascent for rendezvous with the CSM. The ascent stage houses the two-man crew, the ascent engine, reaction control system (RCS), LEM Guidance Computer (LGC), and other subsystems required for the lunar ascent mission phase.

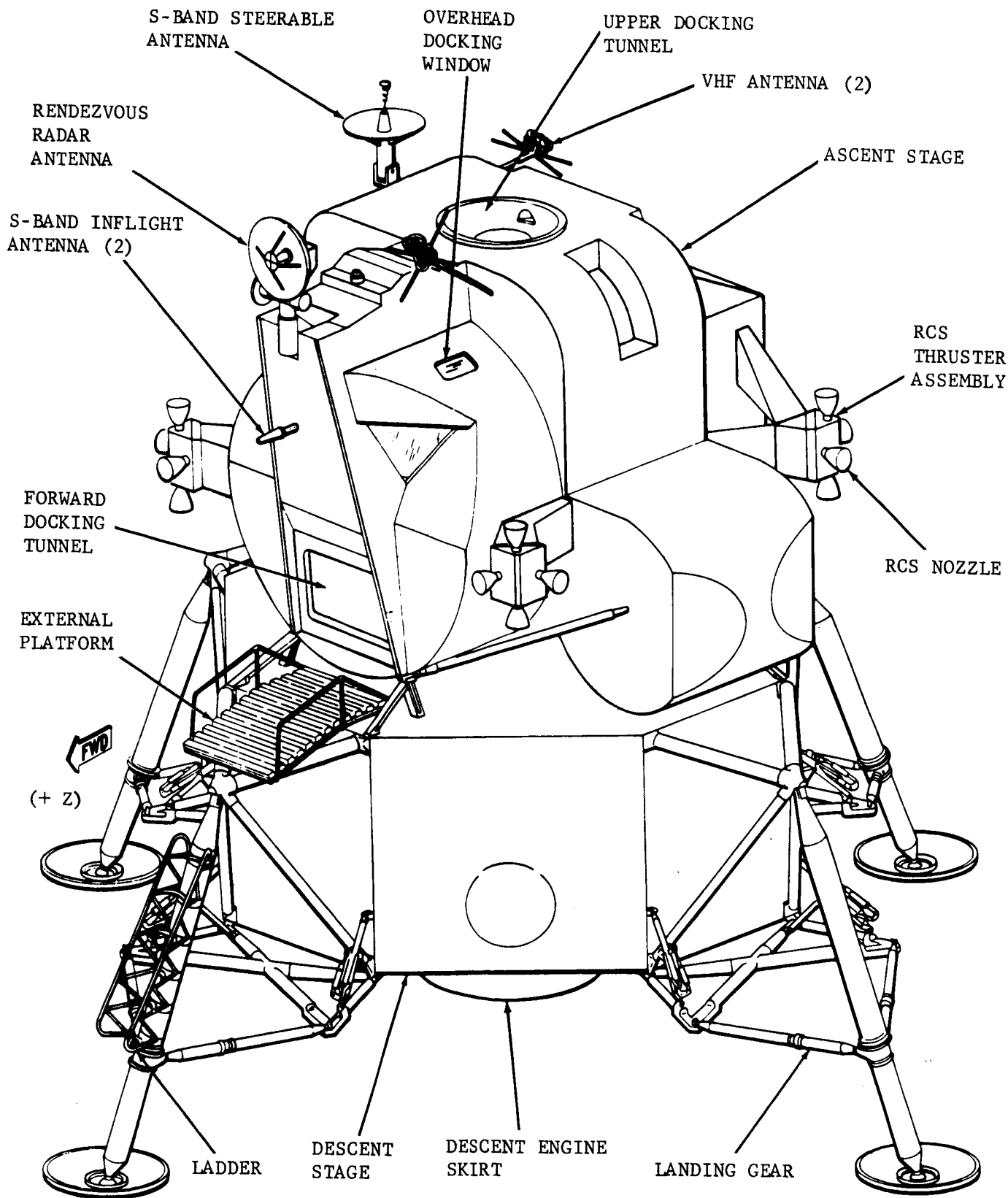
(1) Descent Stage. Since the Sounding Probe is required only during the descent phase, all system equipment that it is possible to do so will be located upon the descent stage. This stage is constructed of aluminum alloy. The inner structural skin is surrounded by a thin layer of insulating material. This insulation is not allowed to be penetrated by any mounting techniques used to attach the Sounding Probe equipments to the LEM. It may be more feasible to attach the equipment to the front landing gear leg in lieu of directly mounting it upon the descent stage.

As illustrated in Figure 3-36, the landing gear is of the cantilever type. The landing gear is stowed in a retracted position until the crew enters the LEM during lunar orbit. Hence, the envelope dimensions of any equipment mounted to the legs are constrained not to interfere with this stowed position. Another constraint upon any equipment located upon the front landing gear leg is that it not protrude to block the crew's visibility of the selected landing site.

Additional constraints upon equipments located upon the descent stage are:

- (a) The equipment must not interfere with other LEM system, such as the Landing Radar.
- (b) The locations must be out of the descent engine plume.
- (c) The equipment cannot extend to within 3 feet of the bottom of the LEM foot pad in order to prevent contact with the lunar surface during LEM touchdown.

(2) Ascent Stage. The primary physical interfaces with the ascent stage will be in the areas of display and control and electrical wiring. No more than 5 pounds of displays and control equipments are permitted on the ascent stage. Sufficient space is required for the displays and controls to permit system activation, arming and deployment of the penetrometers, and display of the data processor decision concerning landing site suitability.



FO4387 U

FIGURE 3-36 LEM STRUCTURE  
3-95

d. Flight Trajectory. The flight path of the LEM during lunar descent is as shown in Figure 3-37.

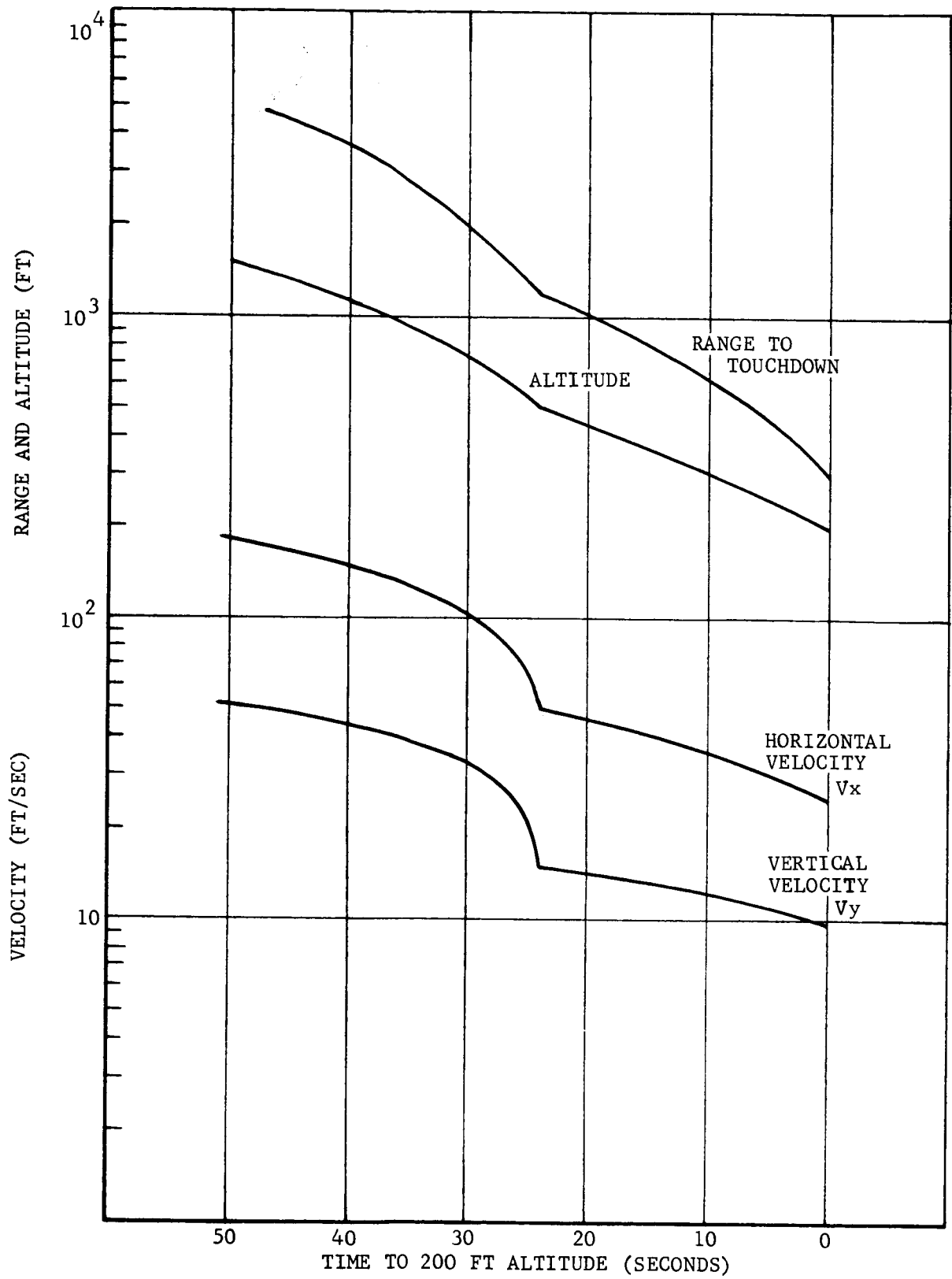
e. Guidance and Navigation. The LEM guidance and navigation data is primarily derived during the landing phase from the Landing Radar. The landing radar subsystem derives altitude range and three-dimensional range rate from a 25,000 foot altitude until touchdown. Altitude range data is presented in binary form to the LEM Guidance Computer (LGC). The LEM velocity components ( $V_x$ ,  $V_y$ , and  $V_z$ ) are presented as prf outputs to controls and displays. The Sounding Probe will require inputs of LEM altitude, horizontal range,  $V_x$  and  $V_z$  velocity, and pitchback angle at the moment the penetrometers are launched in order to predict the penetrometer impact velocity and impact angle. An LGC callup of horizontal range at penetrometer deployment, if this information is not read out continuously, may be necessitated. If the LEM flight trajectory is rather well defined prior to the Apollo launch, it is possible that this callup will not be required, but that the landing radar altitude and velocity outputs will suffice. An electrical interface between the Data Processor and the landing radar outputs to displays and controls may be required.

If the LEM attitude at the instant of penetrometer deployment is not rather well defined a priori for the given altitude and velocity components, then this information must also be obtained in order to aim the penetrometers, which would also require an aiming device.

f. Communications. The LEM operational communications system during the lunar landing phase provides two communications links--a direct two-way S-band link with the Earth-based Manned Space Flight Network (MSFN), and a VHF voice and telemetry link with the orbiting CSM. This latter link can be used as a relay between the LEM and the MSFN, using the CSM-MSFN S-band link.

The acceleration-time traces obtained by the penetrometers are required to be transmitted to the MSFN as well as diagnosed and displayed to the LEM crew. Either of the two LEM communications links could conceivably be used for transmitting the data. However, direct LEM-MSFN transmission of the data appears more feasible. A preliminary modulation method which appears promising is to first modulate the received data signals on a low-frequency constant-bandwidth subcarrier, then multiplex this subcarrier with the base-band crew voice for subsequent transmission of the composite waveform to the MSFN via the LEM's 1.25 MHz voice subcarrier. An electrical interface between the Data Processor and the LEM communications system will be required.

g. Electrical Power. The LEM has available for Sounding Probe use a 29 to 31.5 vdc power supply. Up to 50 watts are available for a period of up to 10 minutes. The Penetrometers may require a slight but continuous



FO4388 U

FIGURE 3-37. LEM APPROACH TRAJECTORY  
3-97

amount of additional power during the preceding Apollo mission phases in order to maintain a trickle charge on their batteries and to assist in thermal control.

In addition to power for the electronics, there is sufficient electro-explosive device power available from the EED batteries to ignite up to 8 squibs simultaneously. This is adequate for Sounding Probe purposes.

All Equipments are required to meet the LEM Electromagnetic Combatibility (EMC) standards relative to conducted and radiated electromagnetic interference.

h. Environments. Table 3.13, 3.14, 3.15, and 3.16 summarize the environmental criteria to which the Sounding Probe equipments must be designed. These criteria are excerpts from NASA General Working Paper No. 10,032, dated August 1964, and are intended only to serve as guidelines during conceptual design. The specific environmental constraints upon the equipment must be evaluated on an equipment-by-equipment basis after individual equipment location and configuration has been determined.

### 3.3.2 LEM SOUNDING PROBE

a. Purpose. The LEM Sounding Probe is to be used by the LEM crew to test the condition of the lunar surface prior to landing. Its sensors are Penetrometer spheres that are launched either singly or in salvo from the vicinity of low gate in the descent trajectory as shown in Figure 3-38. They are automatically aimed to land within the nominal LEM landing zone and during their moment of contact with the surface will most likely be seen by the crew. Each Penetrometer transmits an acceleration-time profile during impact. From the profile are deduced characteristics of surface hardness. On board the LEM is a separate receiver, data processor, and display console that digests the data and indicates the advisability of landing. Nevertheless, the final decision to land rests with the crew. Other than drawing power and monitoring LEM navigational data the Sounding Probe operates automously and is categorized as an add-on device.

b. Description. To allow the crew as much time as possible to make a decision after the data are displayed, Penetrometers should be launched just prior to low gate. The control electronics computes the proper launch pod orientation so that the Penetrometers can be launched at a fixed velocity and still impact in the nominal LEM trajectory area. Figure 3-39 shows the functions of the subsystems.

The Data Processor automatically analyzes the acceleration data from each Penetrometer. Parameters are selected for examination and a composite result is provided for each Penetrometer to the Display.

TABLE 3.13

CAPE KENNEDY ENVIRONMENT

CONDITION	SEQ.	PRE-LAUNCH(PKG 'D)	SEQ.	PRE-LAUNCH (UNPACKAGED)	PRE-LAUNCH (UNPKG-D) -EQUIP. OPER'G
Humidity	nc	LEM Standard	nc	15% to 100% relative humidity, including condensation	Same as pre-launch unpackaged.
Rain	nc	LEM Standard	nc	LEM Standard but no impingement	To be supplied
Salt Spray	nc	LEM Standard	nc	LEM Standard FOG	N/A
Sand and Dust	nc	LEM Standard	nc	LEM Standard	N/A
Fungus	--	LEM Standard	--	LEM Standard	N/A
Ozone	nc	LEM Standard	nc	LEM Standard	N/A
Hazardous Gases	--	LEM Standard	--	LEM Standard	To be supplied. Hazardous liquid also to be supplied.
Electromagnetic Interference	--	LEM Standard	--	LEM Standard	LEM Standard
Shock	ns	LEM Standard	ns	LEM Standard, except modify Procedure I: Shockpulse to sawtooth 15g peak 10-12 MS rise, 0-2 MS decay. (Except LEM Vehicle which is to be supplied.)	
Acceleration	ns	2.67g vertical with 1.0 lateral applied to the package.	v	1.0g vertical 2.67g vertical with 1.0g lateral	N/A

TABLE 3.13 (Concluded)

CONDITION	SEQ.	PRE-LAUNCH(PKG'D)	SEQ.	PRE-LAUNCH(UNPKG-D)	PRE-LAUNCH(UNPKG-D)-EQUIP. OPER 'G
Vibration	ns	LEM Standard		LEM Standard but applied to item	Random vibration shall be 75 sec for each of the 3 mutually perpendicular axes - x,y, &z. Input to equipment supports from primary structure. 10-28 cps .18g <sup>2</sup> /cps constant 28-37 cps 12db/octave dec. 37-1000 cps to .059g <sup>2</sup> /cps constant 1000-1200 cps to 12db/octave dec. 1200-2000 cps to .031g <sup>2</sup> /cps constant Sinusoidal Vibration - N/A
Radiation		N/A		N/A	
Meteoroids		N/A		N/A	
Temperature		-65°F to +160°F		-20°F to 110°F Ambient Air Temp plus 360 BTU/ft <sup>2</sup> Hr. up to 6 hr/day	Same as pre-launch unpackaged
Pressure		Sea Level to 50,000 ft		Ambient ground level pressure: (Hermetically sealed units installed in the crew compartment will be subjected to a limit pressure of 20 psi absolute during preflight checkout.)	5.8 psig O <sub>2</sub> in cabin, atmospheric pressure corresponding to sea level to 150,000 ft during engine firing. Thermal vacuum to be supplied.
Acoustics		N/A		N/A	To be supplied.

TABLE 3.14

EARTH LAUNCH ENVIRONMENT

CONDITION	LEM ASCENT & LEM DESCENT STAGES
Humidity	"none"
Rain	N/A
Salt Spray	N/A
Sand and Dust	N/A
Fungus	N/A
Ozone	To be determined
Hazardous Gases	LEM Standard
Electromagnetic Interference	LEM Standard
Shock	N/A
Acceleration	x axis, 5.0g for 17 min max y axis, $\pm$ 75g for 17 min max z axis, $\pm$ 75g for 17 min max
Vibration	Following random spectrum (a) or (b) applied for 17 min along each of the three mutually perpendicular axes, x, y, and z. (a) Input to equipment supports from exterior primary structure. 5-13 cps $.18g^2$ /cps constant 1.2g rms 13-15 cps 12db/octave rise to 15-32 cps $.30g^2$ /cps constant 2.2g rms 32-49 cps 12 db/octave decrease to 49-950 cps $.044g^2$ /cps constant 6.3g rms 950-1200 cps 12db/octave decrease to 1200-2000 cps $.01g^2$ /cps constant 3.5g rms

TABLE 3.14 (Concluded)

CONDITION		LEM ASCENT & LEM DESCENT STAGES
Vibration (continued)	(b) Input to equipment supports from interior primary structure.	
	5-27 cps	.18g <sup>2</sup> /cps constant 2g rms
	27-40 cps	12db/octave decrease to
	40-2000 cps	.036g <sup>2</sup> /cps constant 8.4g rms
Radiation	Procedure XXV	
Meteoroids	N/A	
Temperature	0 to 160°F uncontrolled cabin	
	0 to 160°F equipment bay	
	40°F to 100°F propulsion compartment	
	15°F to 100°F ambient sea level	
	-65°F to 165°F LEM external surface	
Pressure	Atmospheric pressure at sea level to $1 \times 10^{-8}$ mm Hg (N <sub>2</sub> ) except in cabin which is pure oxygen 20.5 psia to 5.8 psia.	
Acoustics	Sound pressure levels in db external to LEM (re .0002 dynes/cm <sup>2</sup> ):	
	<u>Octave Band (cps)</u>	<u>C-5 at max q level (db)</u>
	9 to 18.8	142
	18.8 to 37.5	141
	37.5 to 75	141
	75 to 150	138
	150 to 300	134
	300 to 600	130
	600 to 1200	123
	1200 to 2400	116
	2400 to 4800	110
	4800 to 9600	104
	Overall	147

TABLE 3.15

LEM TRANSLUNAR ENVIRONMENT

Humidity	40 to 70% in controlled cabin - 0 to 100% in uncontrolled cabin
Rain	N/A
Salt Spray	N/A
Sand and Dust	N/A
Fungus	N/A
Ozone	To be determined
Hazardous Gases	LEM Standard
Electromagnetic Interference	LEM Standard
Shock	Negligible
Acceleration	Negligible
Vibration	Following random spectrum applied for 6 min along each of the three mutually perpendicular axes, x, y, and z. Input to equipment supports from primary structure.
	5-47 cps      .089g <sup>2</sup> /cps constant
	47-65 cps      12db/octave decrease to
	65-1000 cps      .024g <sup>2</sup> /cps constant
	1000-2000 cps      12db/octave decrease
Radiation	Procedure XXV
Meteoroids	N/A

TABLE 3.15 (Concluded)

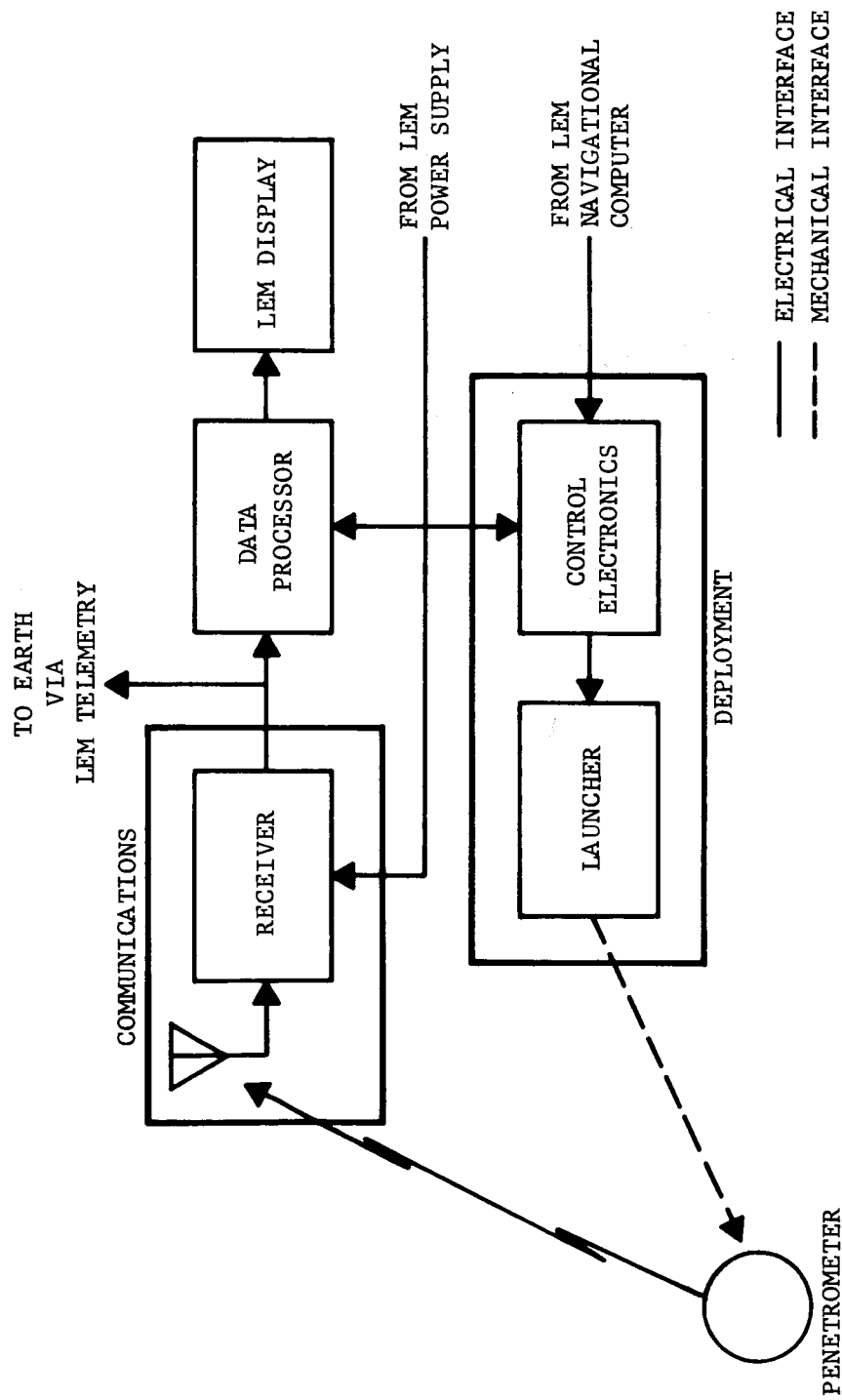
CONDITION	LEM ASCENT & DESCENT STAGES
Temperature	0 to +160°F uncontrolled cabin 0 to 160°F equipment bays 70°F to 80°F controlled cabin 40°F to 100°F propulsion bay -15° to -175° around fuel cell -260° to +260°F external surface
Pressure	For external items: Solar radiation = 440 BTU/ft <sup>2</sup> hr 5.8 psia controlled cabin (O <sub>2</sub> ) 5.8 to 0.1 psia uncontrolled cabin (O <sub>2</sub> ) 1.0 x 10 <sup>-10</sup> mm Hg uncontrolled vacuum
Acoustics	Negligible

TABLE 3.16 LUNAR DESCENT ENVIRONMENT

CONDITION	LEM ASCENT & DESCENT STAGES																																										
Humidity	Controlled cabin (O <sub>2</sub> ) 40 to 70% rh - Locally in cabin (O <sub>2</sub> ) to 100% rh																																										
Rain	N/A																																										
Salt Spray	LEM Standard Fog																																										
Sand and Dust	To be specified for external units																																										
Fungus	N/A																																										
Ozone	To be determined																																										
Hazardous Gases	LEM Standard																																										
Electromagnetic Interference	LEM Standard																																										
Shock	10-20 ms rise time-ramp; step shock (preliminary)																																										
Acceleration	<table border="1" data-bbox="844 1106 1218 1596"> <thead> <tr> <th data-bbox="852 1117 885 1181">Case</th> <th data-bbox="852 1181 885 1244">g</th> <th data-bbox="852 1244 885 1308">x rad/sec<sup>2</sup></th> <th data-bbox="852 1308 885 1372">g</th> <th data-bbox="852 1372 885 1436">y rad/sec<sup>2</sup></th> <th data-bbox="852 1436 885 1500">g</th> <th data-bbox="852 1500 885 1564">z rad/sec<sup>2</sup></th> </tr> </thead> <tbody> <tr> <td data-bbox="901 1117 933 1181">1</td> <td data-bbox="901 1181 933 1244">8.0</td> <td data-bbox="901 1244 933 1308"></td> <td data-bbox="901 1308 933 1372"></td> <td data-bbox="901 1372 933 1436">±14.0</td> <td data-bbox="901 1436 933 1500"></td> <td data-bbox="901 1500 933 1564"></td> </tr> <tr> <td data-bbox="950 1117 982 1181">2</td> <td data-bbox="950 1181 982 1244"></td> <td data-bbox="950 1244 982 1308"></td> <td data-bbox="950 1308 982 1372">+8.0</td> <td data-bbox="950 1372 982 1436"></td> <td data-bbox="950 1436 982 1500"></td> <td data-bbox="950 1500 982 1564">±14.0</td> </tr> <tr> <td data-bbox="998 1117 1031 1181">3</td> <td data-bbox="998 1181 1031 1244"></td> <td data-bbox="998 1244 1031 1308"></td> <td data-bbox="998 1308 1031 1372"></td> <td data-bbox="998 1372 1031 1436">±14.0</td> <td data-bbox="998 1436 1031 1500">±8.0</td> <td data-bbox="998 1500 1031 1564"></td> </tr> <tr> <td data-bbox="1047 1117 1079 1181">4</td> <td data-bbox="1047 1181 1079 1244">8.0</td> <td data-bbox="1047 1244 1079 1308"></td> <td data-bbox="1047 1308 1079 1372"></td> <td data-bbox="1047 1372 1079 1436"></td> <td data-bbox="1047 1436 1079 1500"></td> <td data-bbox="1047 1500 1079 1564">±14.0</td> </tr> <tr> <td data-bbox="1096 1117 1128 1181"></td> <td data-bbox="1096 1181 1128 1244">+1.1</td> <td data-bbox="1096 1244 1128 1308">±.31</td> <td data-bbox="1096 1308 1128 1372">±.11</td> <td data-bbox="1096 1372 1128 1436">±.47</td> <td data-bbox="1096 1436 1128 1500">±.11</td> <td data-bbox="1096 1500 1128 1564">±.47</td> </tr> </tbody> </table>	Case	g	x rad/sec <sup>2</sup>	g	y rad/sec <sup>2</sup>	g	z rad/sec <sup>2</sup>	1	8.0			±14.0			2			+8.0			±14.0	3				±14.0	±8.0		4	8.0					±14.0		+1.1	±.31	±.11	±.47	±.11	±.47
Case	g	x rad/sec <sup>2</sup>	g	y rad/sec <sup>2</sup>	g	z rad/sec <sup>2</sup>																																					
1	8.0			±14.0																																							
2			+8.0			±14.0																																					
3				±14.0	±8.0																																						
4	8.0					±14.0																																					
	+1.1	±.31	±.11	±.47	±.11	±.47																																					
Vibration	Random spectrums applied for 11-1/2 min along each of mutually perpendicular x, y, & z axes. Input to equipment supports from primary structure.																																										

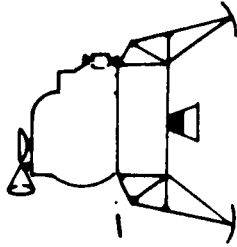
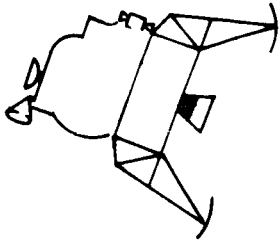
TABLE 3.16 (Concluded)

CONDITION	LEM ASCENT & DESCENT STAGES
Vibration	<p>10-28 cps      .18g<sup>2</sup>/cps constant            28-37 cps      12db/octave decrease to            37-1000 cps    .059g<sup>2</sup>/cps constant            1000-1200 cps   12db/octave decrease to            1200-2000 cps   .031g<sup>2</sup>/cps constant</p>
Radiation	<p>Procedure XXV</p>
Meteoroids	<p>N/A</p>
Temperature	<p>0 to +160°F equipment bays            +40 to -100°F propulsion bays            50°F to 90°F cabin - local spots            +70 to 80°F cabin - average            -15 to -175°F around fuel cell            +260° to - 260°F external surface</p>
Pressure	<p>External Items:            Solar Radiation = 440 BTU/FE<sup>2</sup>/hr            Lunar Surface +250 to -300°F depending upon sun's position            Space = -460°F            = 1 x 10<sup>-10</sup> mm Hg, uncontrolled vacuum            4.8 to 5.8 psia controlled cabin</p>
Acoustics	<p>N/A</p>



FO4348 U

FIGURE 3-39. SOUNDING PROBE FUNCTIONAL DIAGRAM



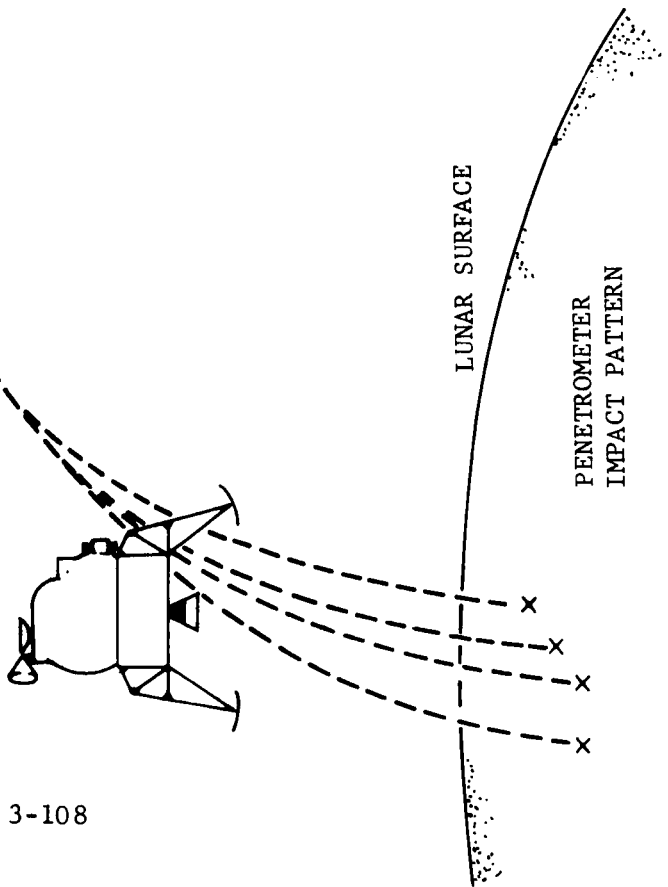
ORIENT AND FIRE PENETROMETERS

$\Delta V = 40/100$  FPS

ALTITUDE = 500/1000 FT

RANGE = 1200/3200 FT

3-108



F04346 U

FIGURE 3-3. SOUNDING PROBE OPERATIONAL PROFILE

c. Data Acquisition.

(1) Operational Profile. The Sounding Probe is energized for a five-minute warm-up time prior to use. In the vicinity of low gate one or more Penetrometers are launched. If the next launching does not occur until after receipt and display of data from the first launch then data from the second launch will be displayed just prior to the LEM reaching an altitude of 200 feet. There is time after low gate for no more than two complete Penetrometer flight trajectories. More than two overlapping trajectories may be accommodated but the number of channels in the receiver must correspond to the number of Penetrometers that are anticipated to be in flight simultaneously.

(2) Input

- (a) Contact of the Penetrometers with the lunar surface provides an acceleration-time history that is processed to determine specific characteristics of that data. Bearing strength, density, and depth of penetration as they are related to acceptable levels by the LEM, are measured.
- (b) The crew must arm and energize the launcher from a control panel in the LEM cabin.
- (c) LEM altitude, attitude, velocity components, and range to touchdown and time of flight to an altitude of 200 feet are continuously obtained from the LEM navigational computer after turn-on.

(3) Response. Time of flight of the Penetrometers varies from 6 to 20 seconds depending upon the launch velocity and altitude. After receipt of data each channel requires up to 2 seconds to process its data. With only one processing channel, the display is energized serially each 2 seconds.

(4) Output. A display for each Penetrometer provides both digital and analog data outputs that are related to the advisability of landing. The discrete output is a go/no-go indication and the continuous output gives a vernier indication for further interpretation by the crew. The raw acceleration data is not displayed but is relayed to Earth via LEM communications in real time.

d. Environmental Constraints

(1) Self-Induced. The impulse at Penetrometer launch must cause no objectionable tip-off to the LEM.

(2) Natural. The Sounding Probe must be compatible with the environment as specified in the LEM Interface Specification.

(3) Man-Induced. The last checkout will occur prior to Earth launch. There will not be tests conducted from this time, until the unit is used during descent. In the event of a landing abort where the descent stage is released from the ascent stage the Sounding Probe shall be deactivated so as not to cause any new concern or distraction.

e. Configuration

(1) Size. The weight of the Sounding Probe will not exceed 30 pounds.

(2) Deployment and Orientation. The Sounding Probe will be an add-on device. The launcher, exclusive of control electronics and the antenna will be mounted as one assembly on the exterior of the LEM, preferably to a nonactive strut. The launcher must be nominally pointed along the descent phase flight path. It shall not interfere with the LEM legs while they are in the stowed position. The Receiver, Data Processor and control electronics will be installed as one unit in the LEM descent stage. The control panel and display will be mounted in the ascent stage. An umbilical cable between the ascent and descent stages will separate upon crew command.

f. Support

(1) Activation and Control. Average power of 50 watts at 28 volts dc is required. Peak power to ignite up to 8 squibs simultaneously shall be available. If the LEM rolls around its thrust axis the magnitude of this movement must be compensated for in the launcher servo control. If the LEM pitches, the limits of these movements must be known and allowed for in the control servo.

(2) Calibration. All permanent initial conditions and adjustments are made prior to launch.

(3) Engineering Measurements. Launch temperature prior to activation.

g. Notes. This document is intended to specify functional requirements only. Reference to any particular method of mechanization is made for clarity only.

### 3.3.3 PENETROMETER

a. Purpose. The Penetrometers are designed to be deployed from the LEM descent stage during the trajectory to touchdown on the lunar surface upon astronaut command. They impact the surface at velocities from 140

to 200 feet per second for the purpose of sensing the resulting dynamic impact decelerations. These negative acceleration traces versus time constitute a "signature" of bearing strength and soil density for the material impacted. These data are converted into terrain identifiers which can be correlated with the probable soil characteristics to denote if the area is suitable for LEM touchdown.

b. Description. The penetrometer is designed as a 5.5 inch diameter ball, as shown in Figure 3-40. Weight of this unit is 3.5 pounds at time of deployment. Figure 3-41 is a functional diagram of the Penetrometer.

c. Data Acquisition. The analog output of the omnidirectional accelerometer in the Penetrometer is broadcast via the 0.5 watt FM transmitter in the 432 to 453 MHz VHF-band from the Penetrometer to the antenna on the LEM descent stage. Data processing occurs on-board the LEM descent stage.

d. Environmental Constraints. Shelf life for the Penetrometer sphere is six months minimum with provisions for calibration and battery re-charging.

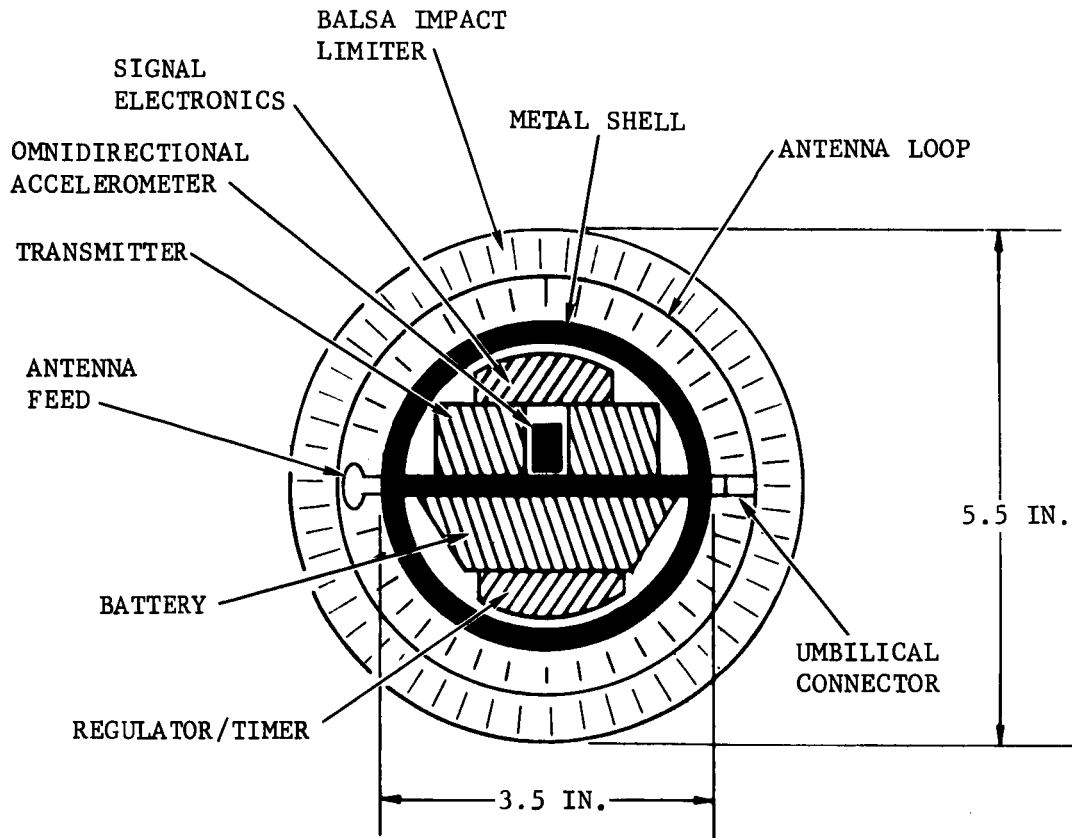
Operation time a few seconds after launch is limited to one minute. Level of detection in g's is from 50 to 7000 with flat response up to 2000 cps and 2 second time constant. Accuracy of measurement is 10 percent over the complete scale with higher accuracy attainable at the lower acceleration levels.

The Penetrometer survives after a 5 day deep space soak, operates through the temperature range of 40 to 100°F (0 to 100°F non-operating) and will withstand vibration levels of 10 g's (sine) with 5 minute sweep, 5 to 2000 cps, with a 0.1 inch limiting displacement; also, 10 g's random for 5 minutes band limited from 100 to 2000 cps.

3. Notes. This document is intended to specify functional requirements only. Reference to any particular method of mechanization is made for clarity only.

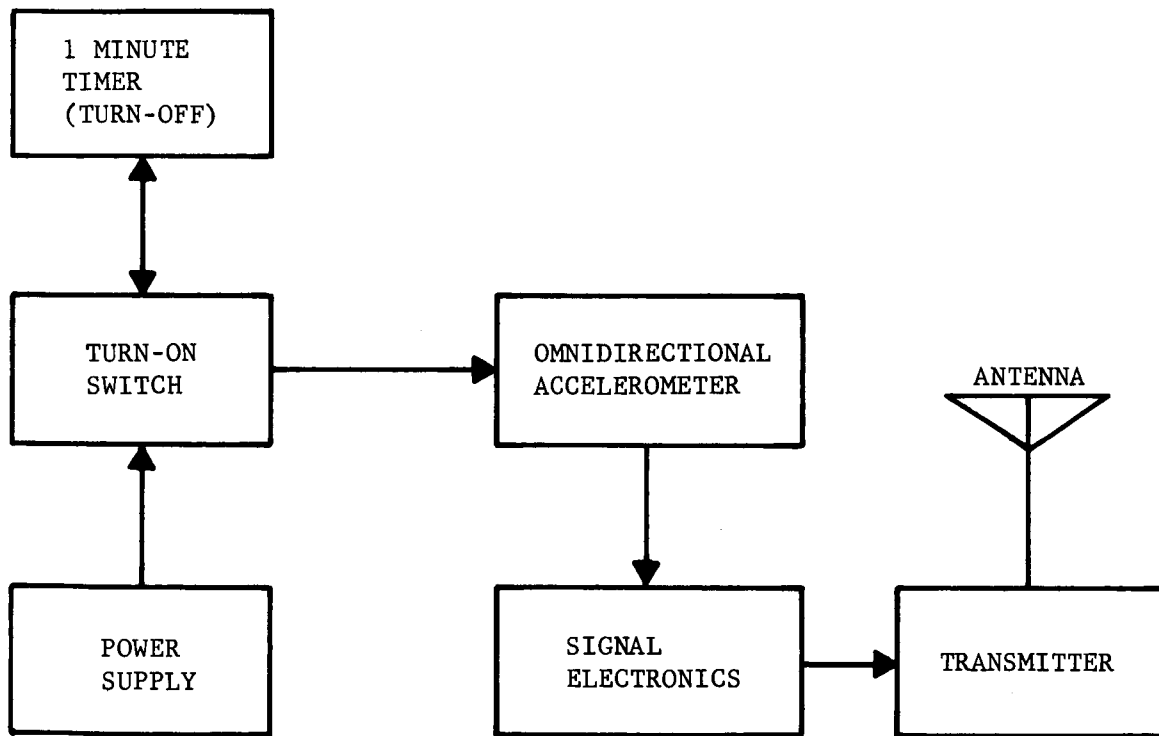
#### 3.3.4 DEPLOYMENT LAUNCHER

a. Purpose. The Launcher is required to inject the penetrometers into a trajectory that will place them at or near the LEM touchdown point. In addition, the launcher is required to house and provide environmental protection for the penetrometers during all mission phases beginning with launch of the Apollo from Earth surface. The launch control system is required to align the launcher at the correct angle prior to launch and to provide the signal for launch.



FO4389 U

FIGURE 3-40. PENETROMETER CONCEPT - CUT-AWAY



F04390 U

FIGURE 3-41. PENETROMETER FUNCTIONAL DIAGRAM

b. Description. The launcher consists of 4 nearly parallel tubes with closed breeches, each containing one Penetrometer. A pyrotechnic device in the closed breech of each tube generates the propulsion gas. Muzzle velocity is expected to be less than 100 ft/sec.

Mounting bracketry contains provision for remotely varying launcher vertical angle through approximately 45°. Launch angle is varied in only one direction, downward.

The launcher is entirely surrounded by a super insulation blanket approximately 0.4 inch thick. This, in addition to a small battery operated resistance heater (approximately 0.2 watt), provides a temperature environment of 50°F ± 5°F for the penetrometers. A bi-metal switch controls heater operation.

The launch control system consists of the launch angle positioning ratchet and solenoid, positioning and launch switches, and associated electronic circuitry.

c. Operation

(1) Event Sequencing

- . Resistance Heater operates intermittently beginning soon after injection into lunar transfer orbit, and continuing until approximately High Gate.
- . Penetrometer electronics turned on at High Gate.
- . Launcher is positioned between High Gate and Low Gate.
- . Penetrometers are launched at Low Gate + 14 sec. or -5 seconds.

(2) Input

- . Signal from LEM Navigational Computer to Launch Control System for positioning launcher.
- . 30V, 5 amp signal to launch angle position solenoid.
- . Signal from LEM Navigational Computer to Launch Control System for launch.
- . 30V, 5 amp signal to pyrotechnic devices in launcher.

(3) Output.

- . Four Penetrometers launched into a trajectory for impact at the nominal touchdown point.

d. Environmental Constraints

(1) Self-Induced. The resistance heater provides a nominal 50°F environment for the launcher, pyrotechnics, and penetrometers. Also at Penetrometer launch, the launcher is subjected to launch forces which are passed on to the LEM vehicle via mounting structure.

(2) Natural. The launcher system must withstand the cislunar space environment consisting of vacuum, solar heat flux, and the heat sink of outer space.

(3) Man Induced. The system must withstand vibration and "g" loads induced during spacecraft launch from Earth, during injection into landing trajectory, and during landing maneuver.

e. Configuration.

(1) Size. The launcher system is roughly a rectangular box 10" x 10" x 5" not including mounting and positioning provisions. Weight including insulation but not including heater, battery or Penetrometers is approximately 3.5 lbs. The battery will weigh less than 0.5 lb.

(2) Location and Orientation. The launcher is required to be on the outside of the LEM descent stage. Possible locations are the forward main struts or one of the two side main struts. An alternate approach that might be required to reduce launch perturbations, if the forward strut is not available, is to provide two launchers one on each side strut. The launcher is required to be positioned relative to local horizontal for range control. A single degree of freedom is provided.

Power is required prior to launch for establishing the correct launch angle. Power is required at launch to ignite the pyrotechnic devices.

f. Notes. This document is intended to specify functional requirements only. Reference to any particular method of mechanization is made for clarity only.

### 3.3.5 COMMUNICATIONS

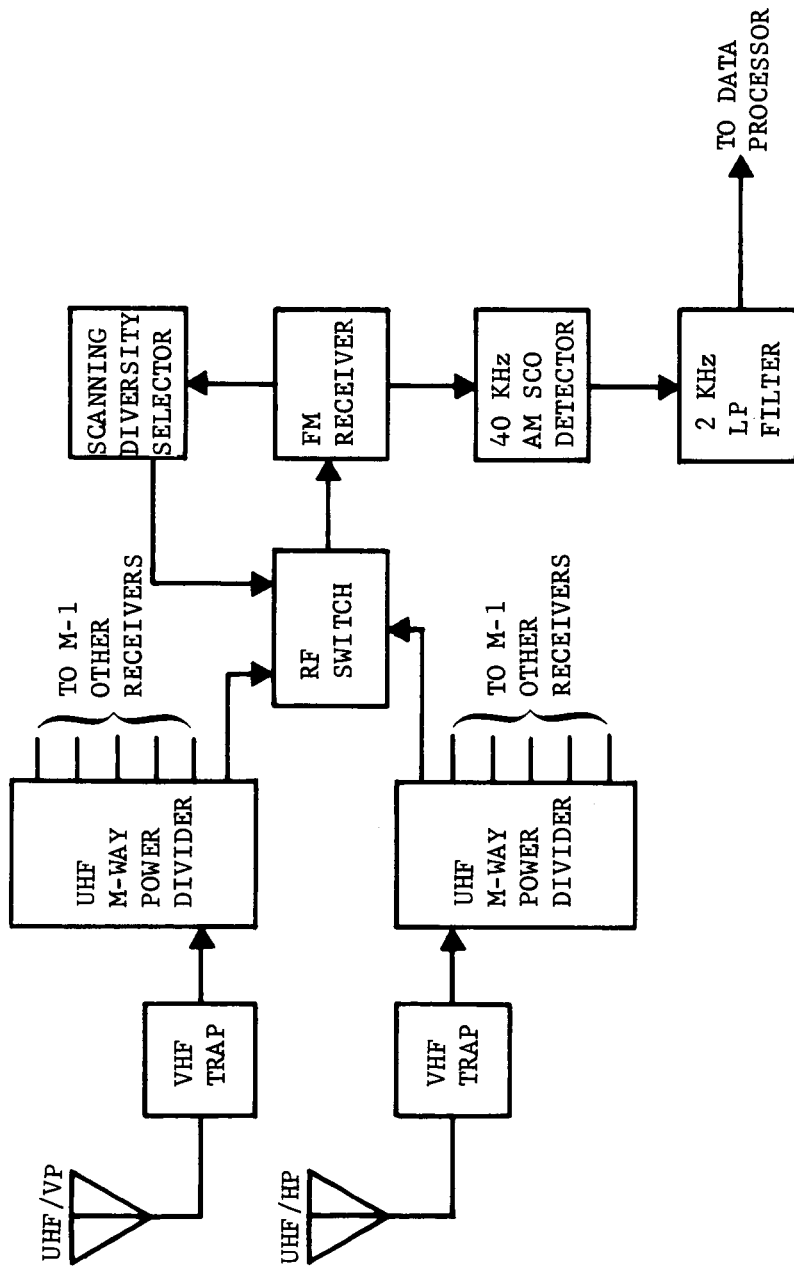
a. The communications subsystem receives and demodulates the acceleration versus time signature transmitted by the Penetrometers during impact into the lunar surface. The functional design is one with the capability of receiving transmissions from an m number of Penetrometers simultaneously.

b. Description. A functional diagram of this subsystem is illustrated in Figure 3-42. The communication subsystem requirements are very similar to the receiving portion of the Data Relay, which was functionally designed for the Lunar Penetrometer System for use with a Lunar Survey Probe delivery vehicle. Since the penetrometers are not attitude stabilized and can impact with any orientation and resulting polarization state of the transmitted signal, polarization diversity reception with two receiving antennas is necessitated for the communications subsystem. Each antenna is connected to a power divider which allows the  $m$  receivers (one for each penetrometer) to be used with either antenna. Due to the short transmission range between the Penetrometers, and the LEM at impact (approximately 1/4 mile maximum) the preamplifier proposed for the Data Relay is not required for the Sounding Probe.

An RF switch at the input to each FM receiver connects the receiver to either of the two antennas. If adverse polarization states between the antenna being used and the Penetrometer cause the received signal for a given receiver to drop below a preset threshold value, a diversity logic circuit automatically switches that receiver to the other antenna. Each of the  $m$  receivers is tuned to receive the transmission from one specific Penetrometer of the  $m$  Penetrometers launched simultaneously. It should be noted that Penetrometers launched sequentially rather than in salvo would enable the reduction in the number of receivers required by enabling a single receiver to time-share the reception of data from the sequentially launched penetrometers.

Referring again to Figure 3-42, the acceleration data obtained by each Penetrometer is transmitted by amplitude modulating a 40 KHz subcarrier, which in turn FM's the Penetrometer transmitter. Each of the communication subsystem receivers contains a wide-band FM discriminator, which produces at its output the 40 KHz AM subcarrier. This output is presented to a subcarrier demodulator, which yields at its output an analog signal proportional to the dynamic acceleration experienced by the particular Penetrometer being received. These analog signals from each Penetrometer transmission are routed to the signal data processor, where they are analyzed to determine the suitability of the area impacted by the Penetrometers for a LEM landing.

The analog acceleration-time signatures are also re-transmitted via the LEM S-band transmission system to the Manned Space Flight Network (MSFN). These signatures will be presented sequentially to the LEM S-band communications system for subsequent transmission. A preliminary investigation of the available modulation techniques for this transmission indicates that a promising method is to use the EVA (Extra-Vehicular Astronaut) telemetry channel, which is frequency multiplexed with EVA and LEM crew voice onto a 1.25 MHz subcarrier. The acceleration data can be first modulated onto a 12.5 kHz constant bandwidth subcarrier. This subcarrier can in turn be frequency multiplexed with the crew voice onto the 1.25 MHz subcarrier for S-band transmission to the MSFN.



FO4391 U

FIGURE 3-42. COMMUNICATIONS DIAGRAM FOR ONE OF M CHANNELS

c. Performance Requirements.

(1) Operational Profile. The communications subsystem is required to operate from Penetrometer deployment until reception of the acceleration data a few seconds later. Activation at Penetrometer deployment should be adequate to permit warm-up and damping of turn-on transients.

(2) Inputs. The communication subsystem inputs consist of RF carrier signals in the 432-450 MHz range from the m Penetrometers launched simultaneously. A minimum guard spacing between adjacent Penetrometer channels of 2 MHz is required. Each received RF carrier is frequency modulated by a 40 KHz subcarrier which in turn is amplitude modulated by the acceleration trace. Each receiver is required to operate for input signal levels over a dynamic range from -80 dbm and -20 dbm, and must not be damaged for input signal levels up to +20 dbm.

(3) Response. Each receiver is required to provide the following characteristics:

Input Bandwidth	(-3 db) 700 kHz minimum
Noise Figure	15 db
Subcarrier Output Response	0.5 volts per % AM
Subcarrier Output Bandwidth	0 to 2 kHz
Diversity Switching Level	-107 dbw nominal
Power Requirements	1.6 watts

(4) Outputs. The acceleration outputs from each receiver are presented to the data processor for reduction, display, and re-transmission to the MSFN via the LEM S-band transmission system. The data will be re-transmitted sequentially, using a data storage device in the data processor if required. The transmitted data will be first modulated onto a 12.5 kHz constant-bandwidth subcarrier, which in turn will be frequency multiplexed with the crew voice and the composite signal modulated onto the 1.25 MHz S-band subcarrier.

d. Environmental Constraints. The communications subsystem is required to operate satisfactorily after exposure to the ground, launch, and flight environments of the Apollo mission as summarized in Tables 3.13 to 3.16. No utilization of the LEM Environmental Control System for thermal control will be permitted.

The communications subsystem is required to be electromagnetically compatible with the LEM. Receiver Local Oscillator frequencies must be chosen to minimize generation of spurious frequency components within the operational LEM communication system RF and IF passbands.

e. Configuration. Minimization of weight and volume consistent with performance and reliability requirements is a primary objective for the

communication subsystem design. The electronics portion will be packaged in a unit mounted to the LEM descent stage. The antenna subassembly may be but is not necessarily required to be, mounted with the electronics portion. Location of the antenna subassembly is constrained by the requirement for an adequate coverage factor along a solid angle roughly described by a hemisphere centered upon the vector along the vehicle flight path during the LEM terminal landing maneuvers from Low Gate to the hover point.

f. Support

(1) Activation and Control. Subsystem operation will be initiated by an external circuit closure, probably during the terminal phase of the Final Approach. Sufficient self-check circuitry is required to reveal gross malfunctions in the system.

(2) Calibration. A design objective is that no in-flight calibration be required.

(3) Engineering Measurements. Adequate test points are required to permit detection by field personnel of equipment malfunction to the lowest replaceable subassembly level. Receiver Automatic Gain Control (AGC) will be conditioned for telemetering to the MSFN via the S-band PCM Telemetry system as a positive indication of both receiver and Penetrometer performance.

g. Notes. This document is intended to specify functional requirements only. Reference to any particular method of mechanization is made for clarity only.

3.3.6 DATA PROCESSOR

a. Purpose. A Penetrometer impacting on the lunar surface transmits a record of its acceleration-time history. From this signal, parameters may be measured that are related to depth of penetration and qualities of hardness and density. Comparing these values with those known to be acceptable for a safe LEM landing yields a decision.

The LEM crew will be too busy to interpret the raw data. The CSM may not be within line-of-sight of the LEM so that its crew cannot always do the interpreting. Sending the raw data to Earth and the decision back to the LEM would take an additional 3 seconds which is too valuable to use for communication at this phase of the LEM trajectory. Therefore, a Data Processor which is an electronic subsystem is on the LEM to extract the information from the Penetrometer signal.

b. Description. The input signal to the Data Processor is the Penetrometer acceleration-time history from the Receiver subsystem. This

profile as well as its successive integrals and differentials are detected for specific values of parameters. When more than one parameter is measured from a single Penetrometer then they are compared to yield a single decision. The operations occur rapidly to render an immediate decision. The result is transferred as an activating signal to the Display Subsystem. Since a decision about the lunar surface is made from each Penetrometer, no further interpretation nor data conversion is required of the Display subsystem. The subsystem can accept data from more than one Penetrometer simultaneously. However, there is but one processing assembly so that data is time buffered to allow for sequential operations. A functional diagram of the Data Processor is shown in Figure 3-43.

c. Data Handling.

(1) Operational Profile. The Data Processor is turned on five minutes prior to being used. It is notified which Penetrometers have been launched by the control electronics. An electronic commutator is sequentially switched among the activated channels searching for a signal. Dwell time is not more than 2 seconds per channel at the end of which all processing circuitry is reset. Total lifetime from turn-on is no more than ten minutes.

(2) Input.

- (a) Analog acceleration versus time profiles up to 400 msec duration each are presented to the Data Processor, each on a separate channel. The channels are activated by the receiver either separately or simultaneously.
- (b) Theoretical input velocity and impact angle are computed by and stored in the control electronics for each Penetrometer at time of launch. This information is delivered serially to the Data Processor when the commutator is connected to a receiver channel. When the commutator selects a new channel, all circuits are reset and new initial conditions computed. These operations take no more than 30 msec.
- (c) The control electronics switches the electronic commutator in the Data Processor.

(3) Response. The data is transformed from an analog input to a digital output. The bandwidth of analog processing circuits must be such that there is no more than 10 percent degradation in the parameter to be measured. Data should be rejuvenated if retained in holding circuits for long periods. Digital switching circuits have time constants that are

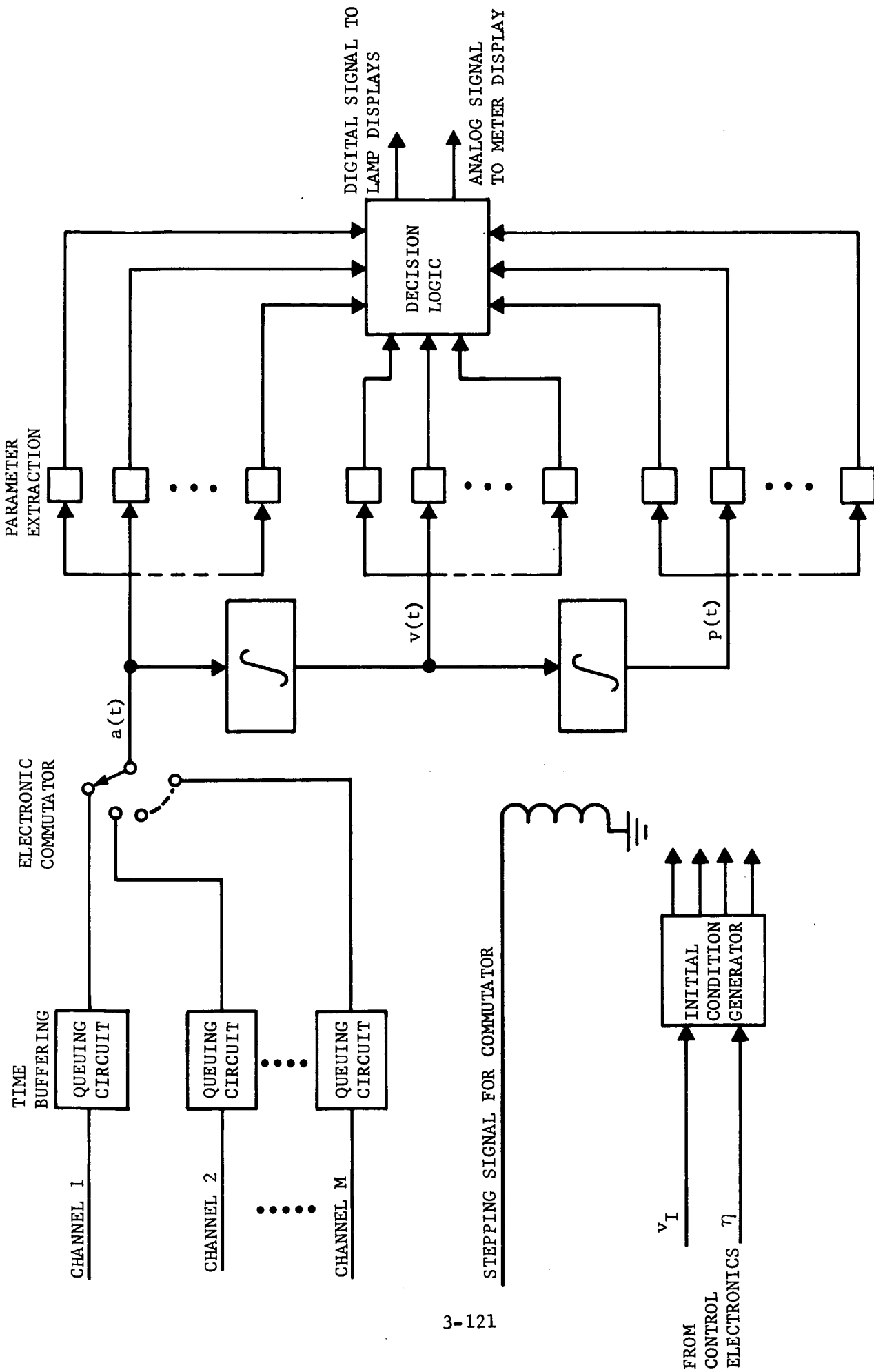


FIGURE 3-43. DATA PROCESSOR

within \_\_\_\_\_ percent of nominal. From the commutator to the display, an analog time signal is prepared so that it can be measured and parameters extracted and delivered digitally for logic comparison to yield a decision.

(4) Output

- (a) A digital signal is delivered to the Display subsystem for the purpose of registering a discrete decision concerning the surface, e.g., hard-medium-soft or good-marginal-bad. A signal output is given for each penetrometer launched.
- (b) From the decision circuit an activating signal is delivered to a continuous-reading meter in the Display. The signal represents a vernier on the coarse digital data that indicates the degree of hardness, etc.

d. Environmental Constraints.

(1) Self-Induced. During operation, the Data Processor may not overheat the compartment within which it is located. For a highly dissipative network a self-contained cooling unit must be provided as part of the Sounding Probe.

(2) Natural. During launch from Earth, Earth-Moon transit and lunar descent the Data Processor must survive the environment existing within the LEM descent stage. If heating is required for thermal control it must be provided by the Sounding Probe.

(3) Man-Induced. The last check-out will occur prior to Earth launch. There will be no tests conducted from this time until the unit is used during lunar descent. In the event of a landing abort where the descent stage is released from the ascent stage the Data Processor shall be deactivated so as not to cause any new concern or distraction.

e. Configuration.

(1) Size. The Data Processor is almost exclusively electronic. The major portions of its weight are independent of the number of Penetrometer channels. For \_\_\_\_\_ Penetrometers it weighs \_\_\_\_\_ pounds. The Data Processor is contained with an envelope whose volume is \_\_\_\_\_ in<sup>3</sup>.

(2) Deployment and Orientation. The subsystem is contained within the LEM descent stage but there is no preferred orientation. Prior to lift-off from the Moon, an umbilical cable is disconnected between the ascent and descent stages.

f. Support

(1) Activation and Control. The control electronics provide signals for stepping the commutator switch and it provides input data to the initial condition generator. Voltage at 28 volts DC is obtained from the LEM power supply. Average power requirements are \_\_\_\_\_ watts. Peak surges of \_\_\_\_\_ watts for \_\_\_\_\_ seconds will occur when up to eight squibs are ignited simultaneously. In the event of a landing abort where the descent stage is disconnected from the ascent stage, voltage shall be removed from the Data Processor in order not to draw power from the LEM power supply.

(2) Calibration. All permanent initial conditions and adjustments are made prior to Earth launch.

(3) Engineering Measurements. None required during operation.

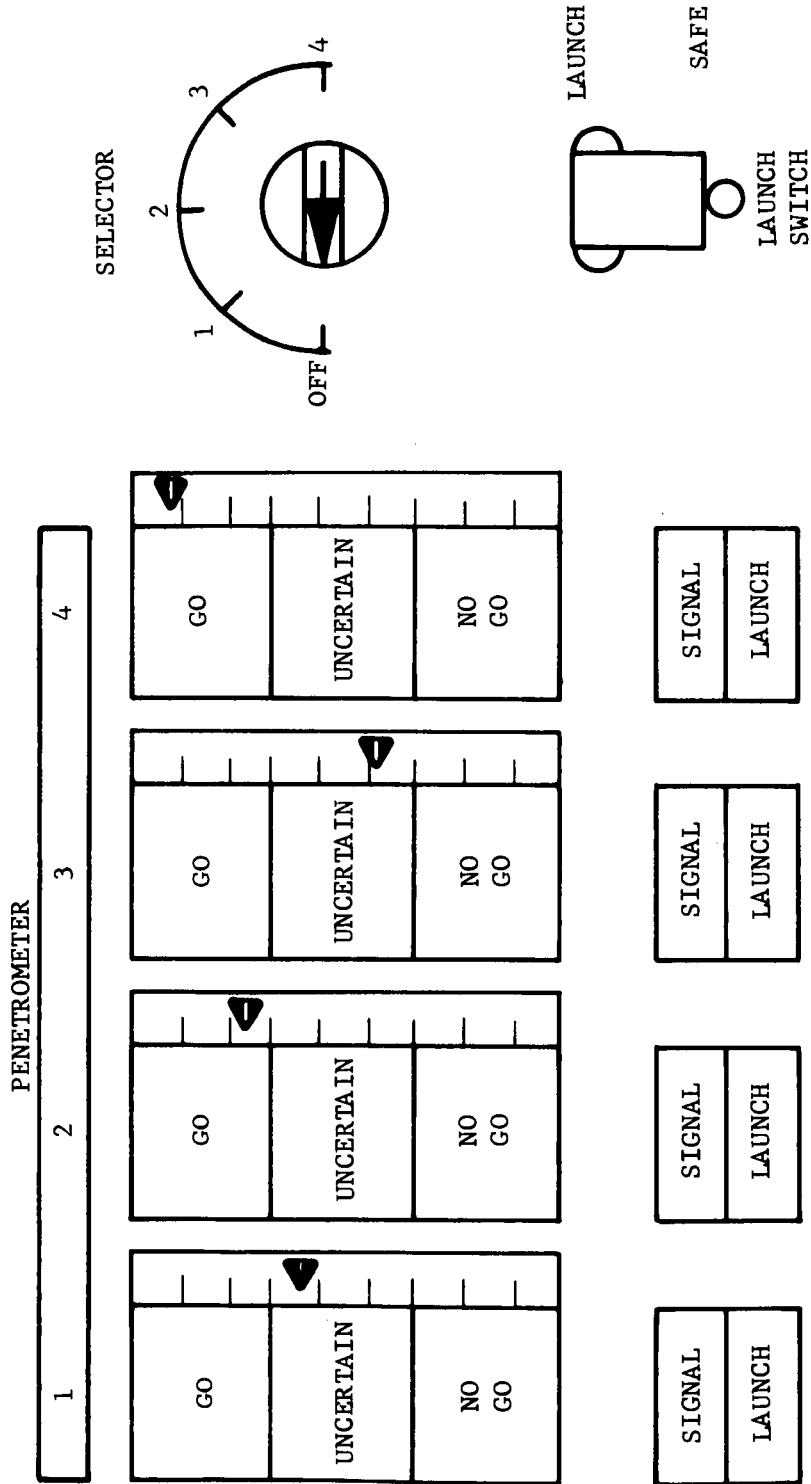
g. Notes. This document is intended to specify functional requirements only. Reference to any particular method of mechanization is made for clarity only.

3.3.7 DISPLAY

a. Purpose. The Display System is intended to provide the LEM astronauts with a visual indication of the local safe landing probability based upon a Penetrometer impact.

b. Description. The Display is composed of two miniature consoles, each measuring 2" x 3" x 4". These consoles are preferably attached to the wrists of each LEM astronaut during the time of use. They are connected to their respective LEM console panels by means of a \_\_\_\_\_ wire harness and a mating connector at the panel. One of the two display consoles is shown in Figure 3-44. This system is shown prior to deployment. The readout is provided by two separate means. Analog readout is derived by a linear pointer. This pointer moves upward proportional to the bearing strength of the soil as detected by the Penetrometer. Additionally, a three-stage set of digital steps is provided between. Each of these readings is a light panel and will successively indicate the terrain condition. The "launch" light is activated at Penetrometer launch. The Consoles are disconnected after landing and left on the lunar surface.

c. Data Acquisition. Inputs to the Display Consoles are provided by means of the \_\_\_\_\_ wire harness. Signals originate in the signal processing electronics located in the Descent Stage and are relayed to the console as discrete signals for the digital data and an analog output for the linear pointer. The display system contains no signal electronics or other processing circuits.



FO4386 U

FIGURE 3-44. DISPLAY PANEL

d. Environmental Constraints. The display consoles are designed to be compatible with the LEM Environmental Specification requirements.

e. Interface Definition. This system is integral to the LEM Descent package portion of the Sounding Probe. Electrical service is via a 40 pin umbilical at the ascent/descent interface.

f. Notes. This document is intended to specify functional requirements only. Reference to any particular method of mechanization is made for clarity only.

## SECTION 4

### LEM PAD IMPACT TESTING AND DATA ANALYSIS

LEM Pad Impact Testing was extended to obtain a wider range of parametric data, notably the variation of impact velocity to 3 and 7 ft/sec from the previously tested 10 ft/sec. The results are reported below. There was analysis of this test data and further work accomplished in correlating penetrometer test results with LEM Pad test results. Also, there was further investigation of the analytical model for a body impacting into particulate soil examples. No final conclusions were reached for understanding the complex dynamic penetration phenomena, but suggestions are made for continued effort involving more basic soil mechanics studies. At the moment it is necessary to rely upon empirical correlations without the satisfaction of analytical understanding.

#### 4.1 LEM PAD IMPACT TESTING

##### 4.1.1 TEST OBJECTIVES AND DESCRIPTION

The test objectives were to obtain LEM pad impact data for velocities of less than 10 ft/sec in order to establish trends of pad penetration with respect to impact speeds. The nominal free-fall velocities used in these tests were 3 ft/sec and 7 ft/sec. The target materials were:

- (1) Loose Nevada 120 mesh sand (Nev 120-2L).
- (2) Compacted Nevada 120 mesh sand (Nev 120-1).
- (3) Loose Nevada 60 mesh sand (Nev 60-2).

These materials were conditioned to duplicate those used in the LEM 10 ft/sec tests. Static bearing strength measurements were made prior to each test using a 2-1/2 inch spherical probe to verify proper target material conditioning. The LEM test matrix shown in Table 4.1 defines the test program conducted

The test facility, which was described in detail in Reference 1, required slight changes to accomplish these tests. Spacers were made to allow changes of free fall distance which governed the impact velocity. A velocity transducer was added to the existing load, acceleration, and displacement sensing systems to provide a direct measurement of mass velocity at the instant the pad contacted the target material. Because this transducer was limited to velocity measurements over a 7-inch travel, it was positioned to provide data starting three inches before contact of the pad on the target surface. The following dynamic time histories were recorded.

- (1) Mass Velocity
- (2) Mass Displacement
- (3) Gravity Simulator Load
- (4) Mass Acceleration
- (5) LEM Pad Acceleration
- (6) Strut Compression Load
- (7) Strut Compression

#### 4.1.2 DYNAMIC TEST RESULTS

a. Composite Data Table. The composite data table shown in Table 4.2 tabulates the data taken from oscillograph records of each test. For each recorded parameter, the percent deviation of the recorded value from the specified or nominal value is indicated. As expected, control over the 3 ft/sec parameter was difficult to hold. Statistically, the standard deviation of velocity from the average value was 15.5 percent in the set of 3 ft/sec tests. Closer control over the other parameters will be noted.

---

Reference 1. "Research, Development and Preliminary Design for the Lunar Penetrometer System Applicable to the Apollo Program," Final Report (Publication No. U-3556).

TABLE 4.1

LEM IMPACT TEST MATRIX

Equivalent LEM Mass	Free Fall Velocity (ft/sec)	Target Material		
		Nevada 60 Sand	Nevada 120-2L Sand	Nevada 120-1 Sand
4000 LBS	3	X	X	X
	7	X	X	X
8000 LBS	3	X	X	X
	7	X	X	X

	UNITS	NEVADA 12					
		LEM-20 4000 LB 3 FT/SEC			LEM-26 8000 LB 3 FT/SEC		
		NOM OR MEAS	DYNAM DATA	% DIFF	NOM OR MEAS	DYNAM DATA	% DIFF
A VELOCITY	FT/SEC	3.0	3.28	9.3	3.0	3.11	3.5
B DEPTH OF PENETRATION	INCHES	7.0	7.23	3.3	8.80	8.37	5.0
C STRUT CHARACTERISTICS							
1. COMPRESSION LOAD - (6000 LBS)	LBS	—	—	—	6000	6490	8
2. COMPRESSION LOAD (12,000 LBS)	LBS	—	—	—	—	—	—
3. CRUSHED LENGTH (6000 LBS)	INCHES	0.125	0.152	21	0.375	0.500	33
4. CRUSHED LENGTH (12,000 LBS)	INCHES	—	—	—	—	—	—
D GRAVITY SIMULATOR							
1. GRAVITY SIMULATOR LOAD	LBS	—	3274	—	—	6200	—
2. WEIGHT	LBS	3776	—	—	7680	—	—
3. GRAVITY FACTOR		0.833	0.866	4.1	0.833	0.807	3.2

44-1

TABLE 4.2  
COMPOSITE DATA

0-2L SAND						NEVADA 60-2 SAND								
LEM-24 4000 LB 7 FT/SEC			LEM-29 8000 LB. 7FT/SEC			LEM-22 4000 LB 3 FT/SEC			LEM-28 8000 LB 3 FT/SEC			LEM-32 4000 LB 7 FT/SEC		
NOM OR MEAS	DYNAM DATA	% DIFF	NOM OR MEAS	DYNAM DATA	% DIFF	NOM OR MEAS	DYNAM DATA	% DIFF	NOM OR MEAS	DYNAM DATA	% DIFF	NOM OR MEAS	DYNAM DATA	% DIFF
7.0	7.10	1.4	7.0	7.66	9.2	3	3.53	17.5	3.0	3.57	19	7.0	7.3	4.3
9.94	10.70	8	12.4	12.25	1.0	4.4	4.37	0.6	5.5	5.41	1.6	6.7	7.1	6
—	—	—	6000	5664	5.6	—	4526	—	6000	5800	3.5	—	3640	—
—	—	—	—	—	—	—	—	—	—	—	—	—	—	—
0.125	0.061	49	6.875	7.23	5.1	1/16	0	—	1.31	1.37	4.5	0.25	0.24	4
—	—	—	—	—	—	NONE	NONE	—	—	—	—	—	—	—
—	3530	—	—	6586	—	—	3000	—	—	6215	—	—	3240	—
3720	—	—	7670	—	—	3776	—	—	7680	—	—	3740	—	—
0.833	0.948	14	0.833	0.858	3	0.833	0.795	4.6	0.833	0.809	2.5	0.833	0.866	4

4-4-2

NEVADA 120-1 SAND														
LEM-30 8000 LB 7 FT/SEC			LEM-21 4000 LB 3 FT/SEC			LEM-27 8000 LB 3 FT/SEC			LEM-25 4000 LB 7 FT/SEC			LEM-31 8000 LB 7 FT/SEC		
NOM OR MEAS	DYNAM DATA	% DIFF	NOM OR MEAS	DYNAM DATA	% DIFF	NOM OR MEAS	DYNAM DATA	% DIFF	NOM OR MEAS	DYNAM DATA	% DIFF	NOM OR MEAS	DYNAM DATA	% DIFF
7.0	7.56	8.0	3.0	3.71	23.5	3.0	3.7	23	7.0	7.37	5.3	7.0	7.9	12.7
7.75	7.81	0.8	2.0	2.96	48	2.4	2.13	11.3	2.6	3.12	12	2.6	1.80	31
6000	5755	4	6000	6500	8.3	6000	5870	2.2	6000	5740	4.4	6000	6200	3.3
—	—	—	—	—	—	—	—	—	—	—	—	—	—	—
8.88	8.91	0.3	0.25	0.252	0.8	2.5	2.58	3.2	5.375	5.48	2.2	14.94	14.97	0.2
—	—	—	NONE	NONE	—	—	—	—	—	—	—	—	—	—
—	6513	—	—	2980	—	—	6376	—	—	3260	—	—	6500	—
7670	—	—	3776	—	—	7680	—	—	3720	—	—	7670	—	—
0.833	0.850	2	0.833	0.789	5.3	0.833	0.830	0.4	0.833	0.876	5.2	0.833	0.847	1.6

F04393 U

b. LEM Pad Penetration Versus Velocity Data. LEM pad penetration and total strut displacement data are summarized graphically in Figure 4-1 for the 4000 lb mass and in Figure 4-2 for the 8000 lb mass. The solid curves represent pad penetration while the dashed lines represent total LEM mass displacements. Some indicated trends are:

- (1) At 3 ft/sec, total mass displacement consisted primarily of pad penetration.
- (2) As velocity was increased from 3 ft/sec to 7 ft/sec, only slight increases in penetration occurred, but sharp increases in honeycomb crush were noted.

c. LEM Landing Pad Penetration Versus Bearing Strength. A summary of the LEM Pad measured depth of penetrations as a function of material relative bearing strength is shown graphically in Figure 4-3. Some trends indicated from this curve are:

- (1) A rapid increase in penetration occurred in materials of lower bearing strength than the Nevada 60-2 Sand.
- (2) The Nevada 120-1 (compacted) material exhibited high resistance to penetration, and the landing mass and velocity only slightly affected the penetration.

d. LEM Landing Pad Penetration Versus Time. Figure 4-4 shows LEM Pad penetration versus time for three materials with a nominal 4000 pound mass and a nominal velocity of 3 ft/sec. Figure 4-5 shows LEM Pad penetration versus time for the three materials and 4000 pound mass at a velocity of 7 ft/sec. Some trends indicated are:

- (1) Almost no penetration overshoot occurred like that observed during the 10 ft/sec landing tests.
- (2) Penetration rise time showed little dependence on velocity.

Individual pad penetration-time curves for each test are included in the LEM test data book along with copies of oscillograph records, static test measurements and bearing strength records. The data book is being submitted under separate cover to the Langley Research Center.

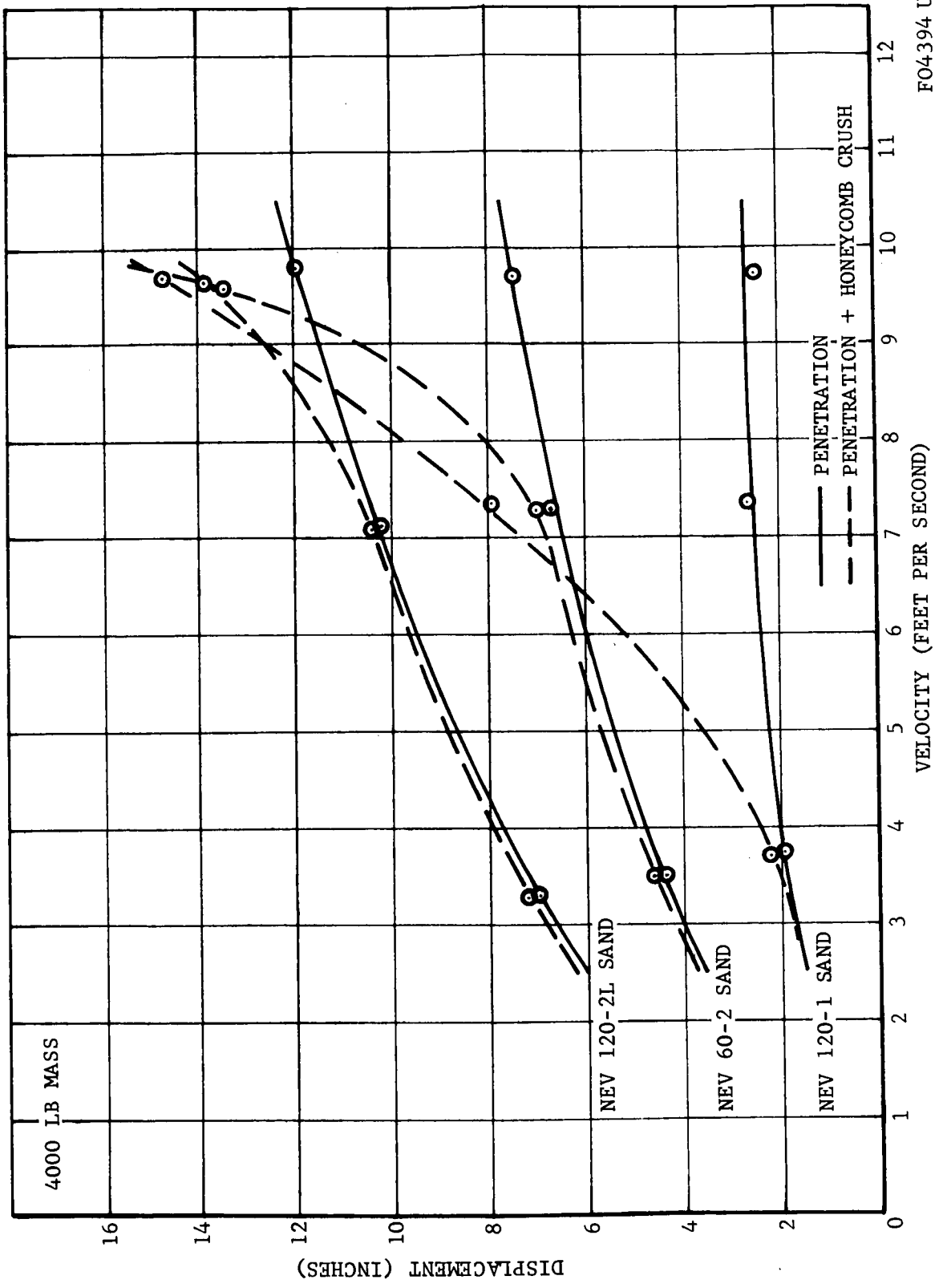
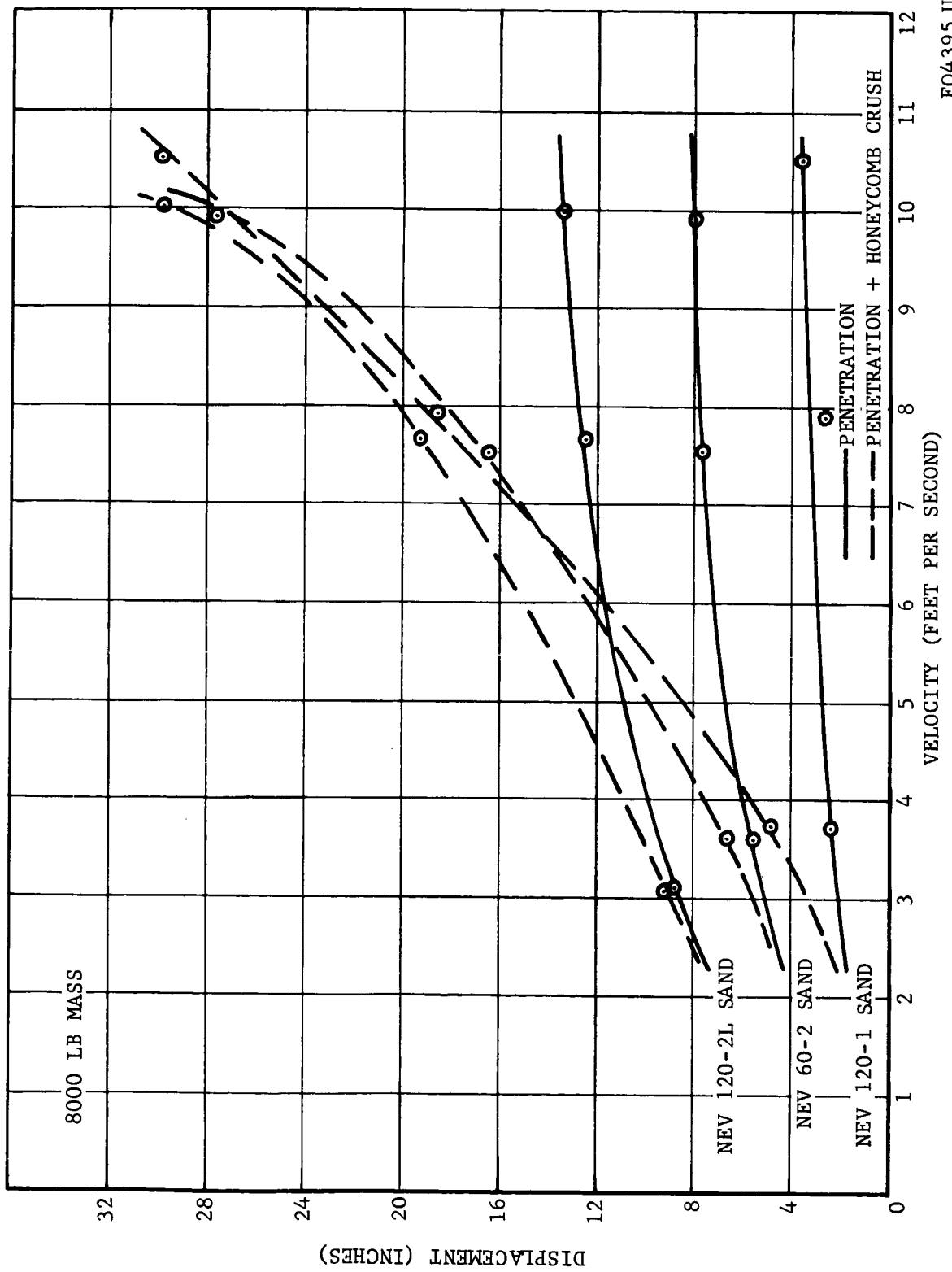
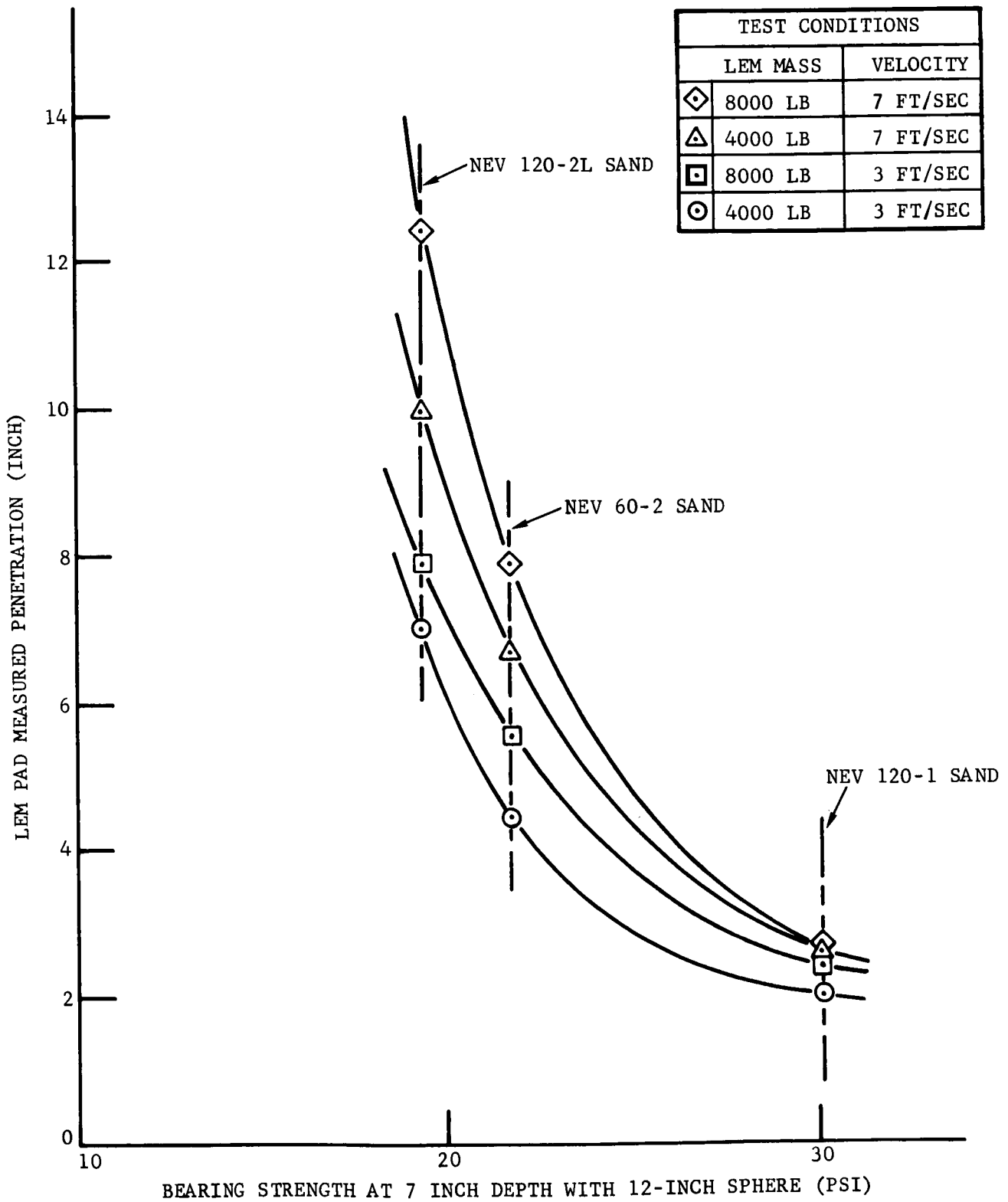


FIGURE 4-1. LEM PAD PENETRATION VERSUS VELOCITY



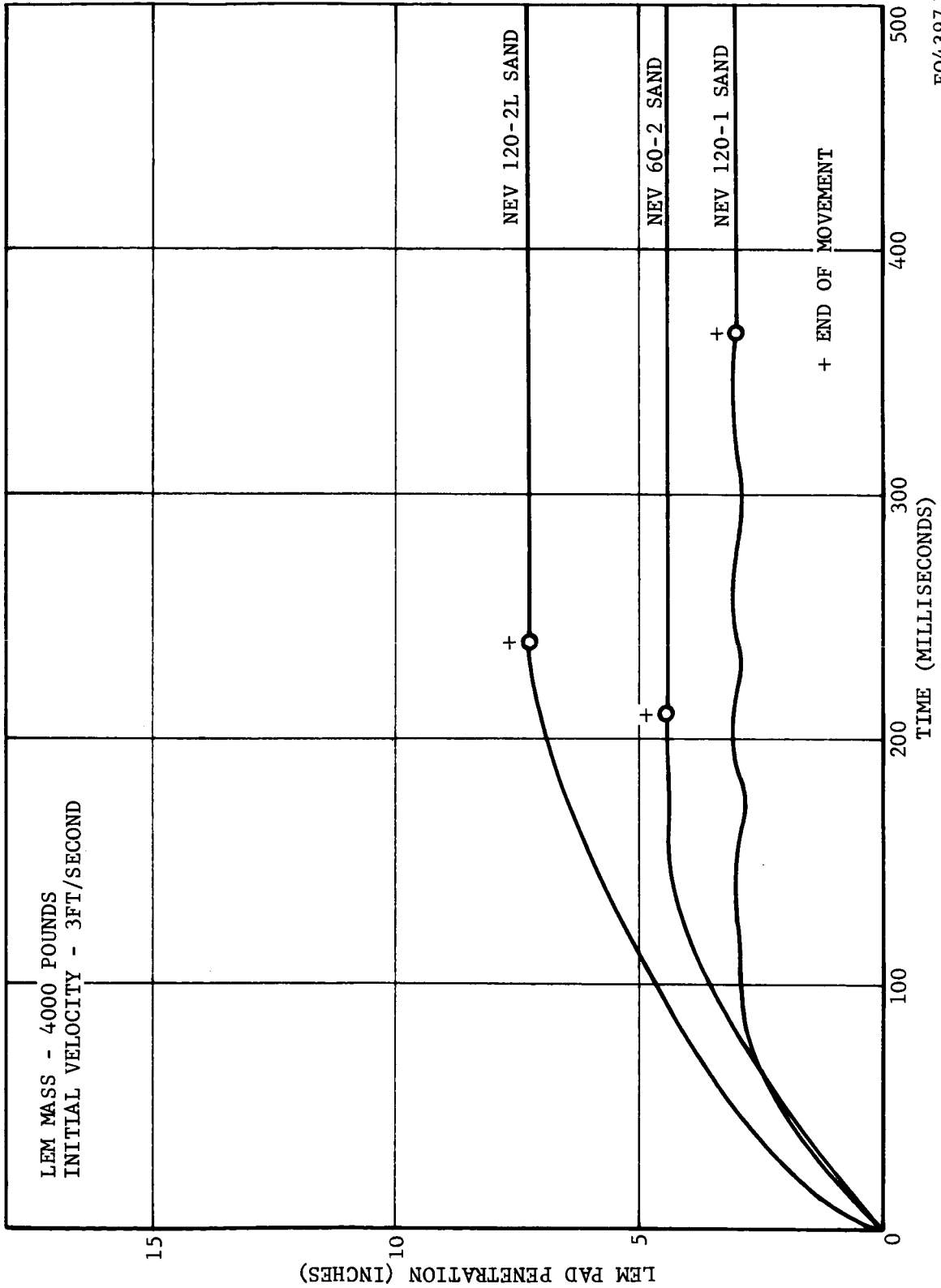
FO4395 U

FIGURE 4-2. LEM PAD PENETRATION VERSUS VELOCITY



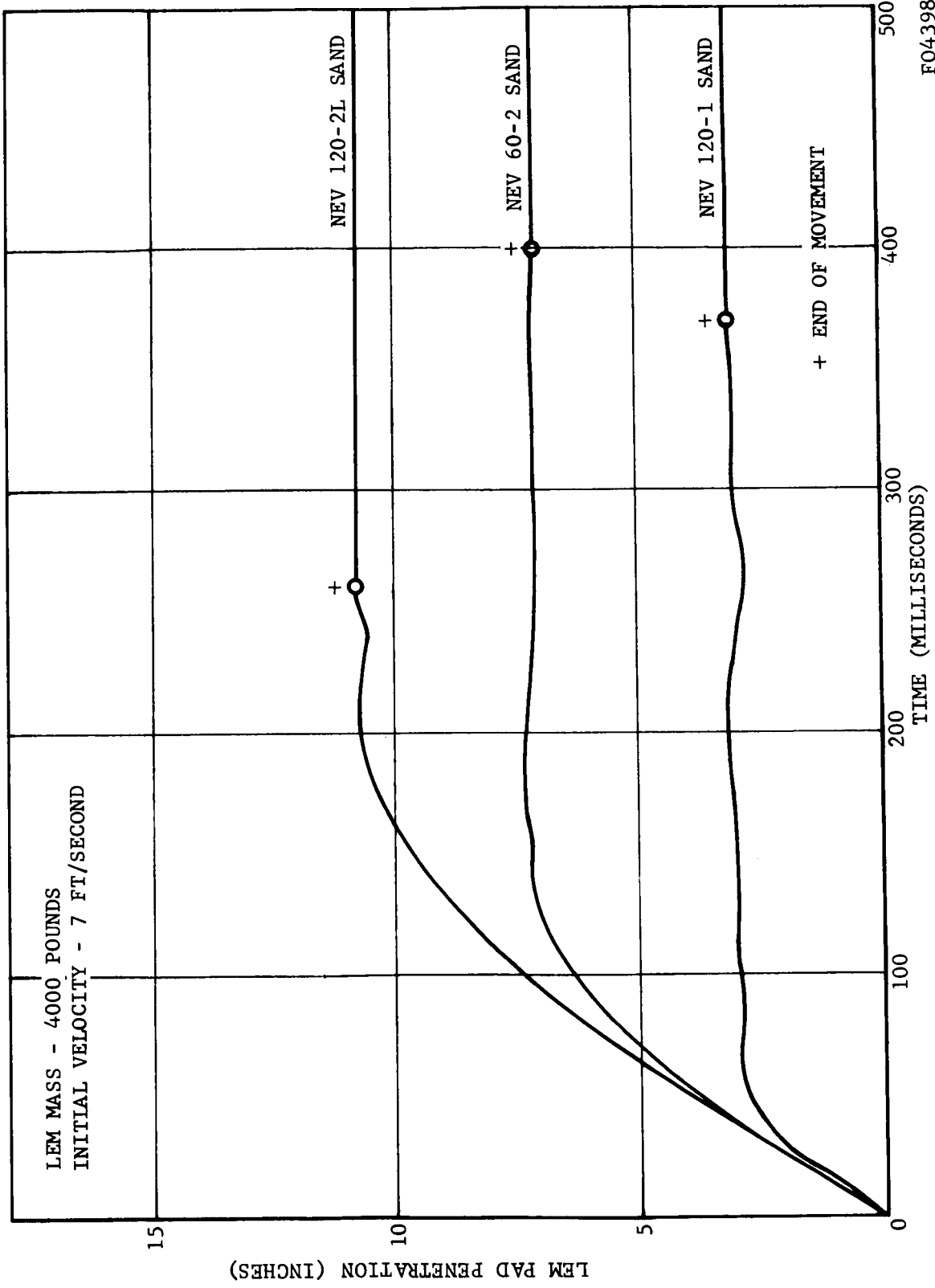
FO4396 U

FIGURE 4-3. LEM LANDING PAD PENETRATION VERSUS BEARING STRENGTH



F04397 U

FIGURE 4-4. LEM PAD PENETRATION VERSUS TIME



FO4398 U

FIGURE 4-5. LEM PAD PENETRATION VERSUS TIME

## 4.2 DATA CORRELATION AND ANALYTICAL MODELS

### 4.2.1 LEM PAD TEST DATA

Prior tests conducted at 10 ft/sec had indicated that LEM pad penetration into loosely packed materials, such as Nevada 120-2L sand, was considerably greater than predicted. This phenomenon had been attributed to a "jackhammer effect" related to the crushing of individual cells in the crushable honeycomb strut. The current series of tests at velocities of 3 ft/sec, where honeycomb crushing is negligible, demonstrated that penetration depths in the loose materials are still significantly in excess (50 - 100 percent) of analytic predictions based on measured LEM pad static resistance characteristics for loose granular target materials. Therefore, the "jackhammer action" arising from non-uniform honeycomb crushing characteristics cannot explain the deep penetration phenomena in the new data. Table 4.3 illustrates these excessive penetration values.

Continued study of this problem indicates that there may be a general impact-induced void ratio reduction in the more loosely packed granular targets. The resulting general "slump" or compaction condition is offered as a new tentative hypothesis to explain these anomalies.

### 4.2.2 CONTINUED DETAILED STUDY OF PENETROMETER DATA

The ultimate aim of this study is to determine the relationship between velocity and dynamic force and to examine the nature of the so-called "stagnation mass" (or "apparent mass") effects. In order to accomplish this aim, the precise integration of acceleration-time traces is required to obtain detailed velocity and depth relations. The study is fundamentally handicapped by an absence of projectile-size static penetration data measured in the target bin at the time of dynamic testing. Of necessity, LEM pad test pit data must be utilized to determine these static penetration values.

Penetrometer test data indicate that the static penetration resistance of granular target materials are considerably in excess of the dynamic force levels given by the "tail-off plateau" or "pedestal" of the individual acceleration trace, especially at low velocities. When dynamic force is plotted against depth of penetration at increasing velocities and the static bearing strength curve superimposed, the static force excess can be illustrated and relationships relative to velocity obtained. The concept of the static-dynamic cross-point is illustrated in Figure 4-6. Figure 4-7 consists of three curves for penetration of  $D_2M_2$  five-pound projectiles in Nevada 120-2 sand:

- (1) 'd' curve - depth of penetration (in inches)  
at cross-point of static and dynamic force  
curves versus velocity (in ft/sec).

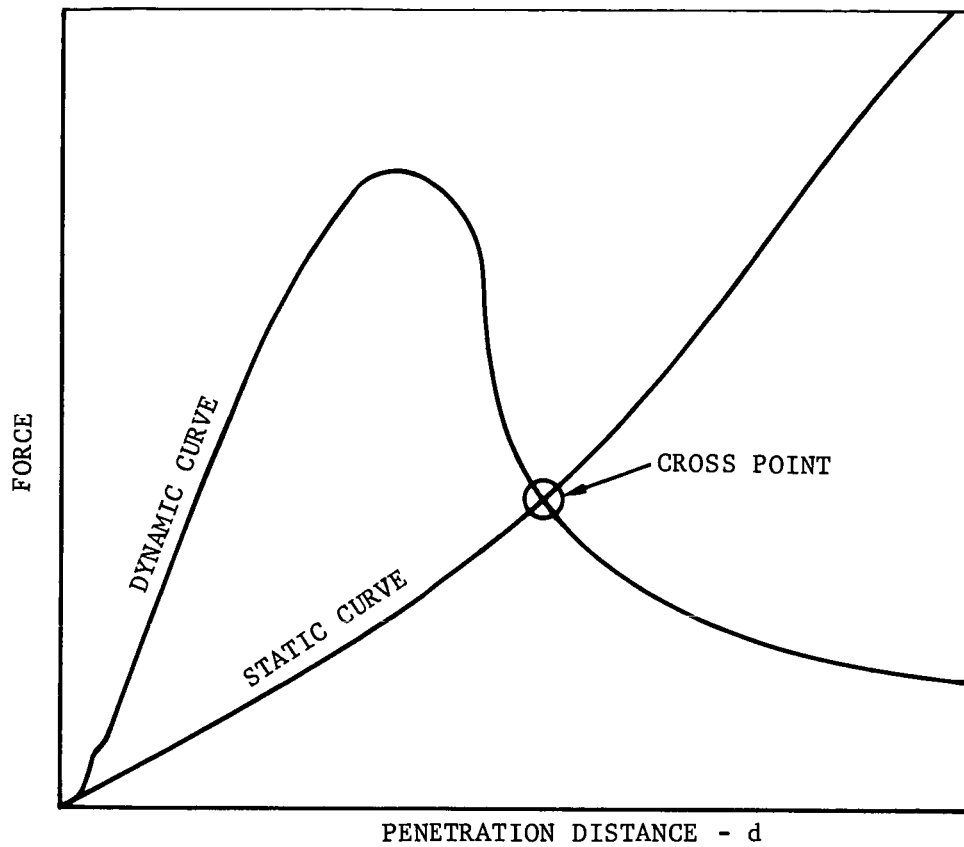
TABLE 4.3

CALCULATED VERSUS EXPERIMENTAL PENETRATION DEPTH  
4000 lb LEM Pad Load Case

Material	3 ft/sec		7 ft/sec	
	Calculated Penetration*	Measured Penetration**	Calculated Penetration	Measured Penetration **
Nevada 120-1 Sand	2.6 in.	2.0 (3.0) in.	2.7 in.	2.6 (3.1) in.
Nevada 120-2 Sand	3.3 in.	7.0 in.	6.4 in.	10 in.
Nevada 60-2 Sand	2.6 in.	4.4 in.	4.8 in.	6.7 (7.0) in.

\*Based on experimental honeycomb crush values and previously measured static force versus penetration data.

\*\*Values in parenthesis are points of deepest penetration from the dynamic measurement data, as opposed to the post-test measurements.



F04399 U

FIGURE 4-6. STATIC-DYNAMIC CROSS POINT FOR SOIL PENETRATION

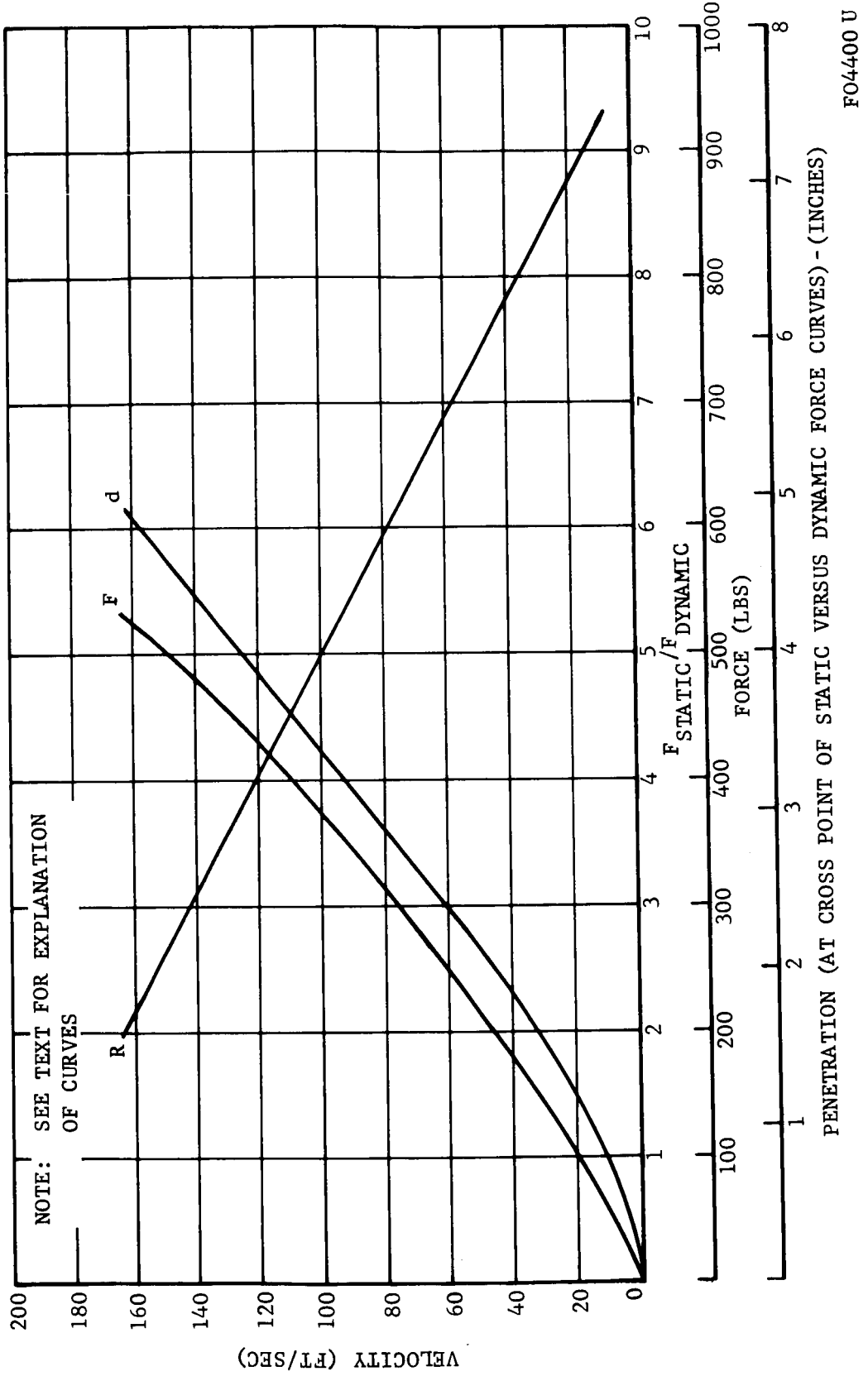


FIGURE 4-7. ANALYTICAL PENETRATION DATA

- (2) "F" curve - force (in lbs) at cross-point versus velocity.
- (3) "R" curve - ratio  $F_{\text{stat}}/F_{\text{dyn}}$  versus velocity.

It was originally hoped that the "stagnation mass effect" would account for these differences, but "reasonable" estimates of this effect based on parametric investigations of the so-called "conical wedge" concept do not appear to account for this entire anomaly as shown in Table 4.4. Therefore, it appears that the "slump" or compaction reduction in void ratios may also be an influential factor in relation to this effect.

#### 4.2.3 SOIL MECHANICS STUDIES

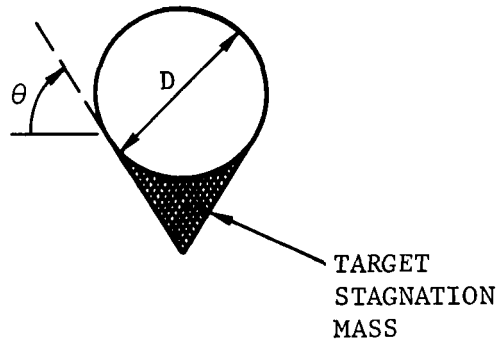
During the course of the Impact Research Program conducted under Phase I of the Lunar Penetrometer System Contract, several semi-empirical models and mathematical expressions were developed by Aeronutronic to depict penetrometer and LEM pad impact and penetration phenomena into particulate target materials. These analytical models and expressions were based upon target-bearing strength and gross density parameters. They were adequate to demonstrate that an overall correlation between impact and penetration parameters for the penetrometer and LEM pad cases will rest upon defining more specific static and dynamic soil properties that enter into expressing the dynamic reaction for the two cases. In order to expedite the isolation of these specific properties and mathematically relate them to an analytical model, it has been deemed desirable to obtain the assistance of an expert in the field of soil mechanics who has had both static and dynamic experience, and is well versed in the physics and mathematics of soil reactions to dynamic loads. Accordingly, the consulting services of Dr. Ronald F. Scott, Associate Professor, Division of Engineering and Applied Science, California Institute of Technology, have been obtained.

TABLE 4.4

STAGNATION MASS (LB) VERSUS  
STAGNATION CONE ANGLE AND SPHERICAL PROJECTILE DIAMETER

$\theta$	D	4 in.	8.5 in.	12 in.
30°		0.01	0.1	0.3
40°		0.03	0.3	1.0
60°		0.24	2.3	6.6

Stagnation Mass (LB)  
(for target density = 100 lb/ft<sup>3</sup>)



## SECTION 5

### EVALUATION AND IMPROVEMENT OF PROTOTYPE PENETROMETERS

This task included the testing of existing prototype penetrometers and the evaluation of potential improvements in the detail design features of various penetrometer modules.

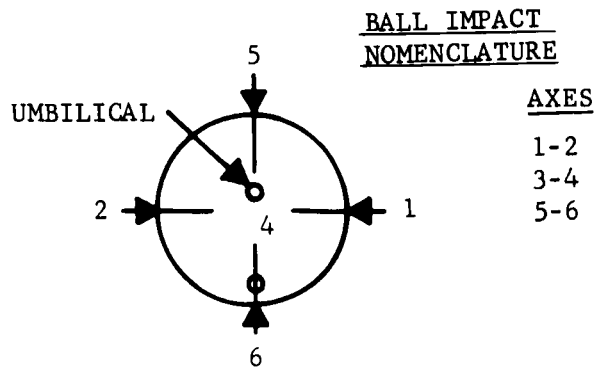
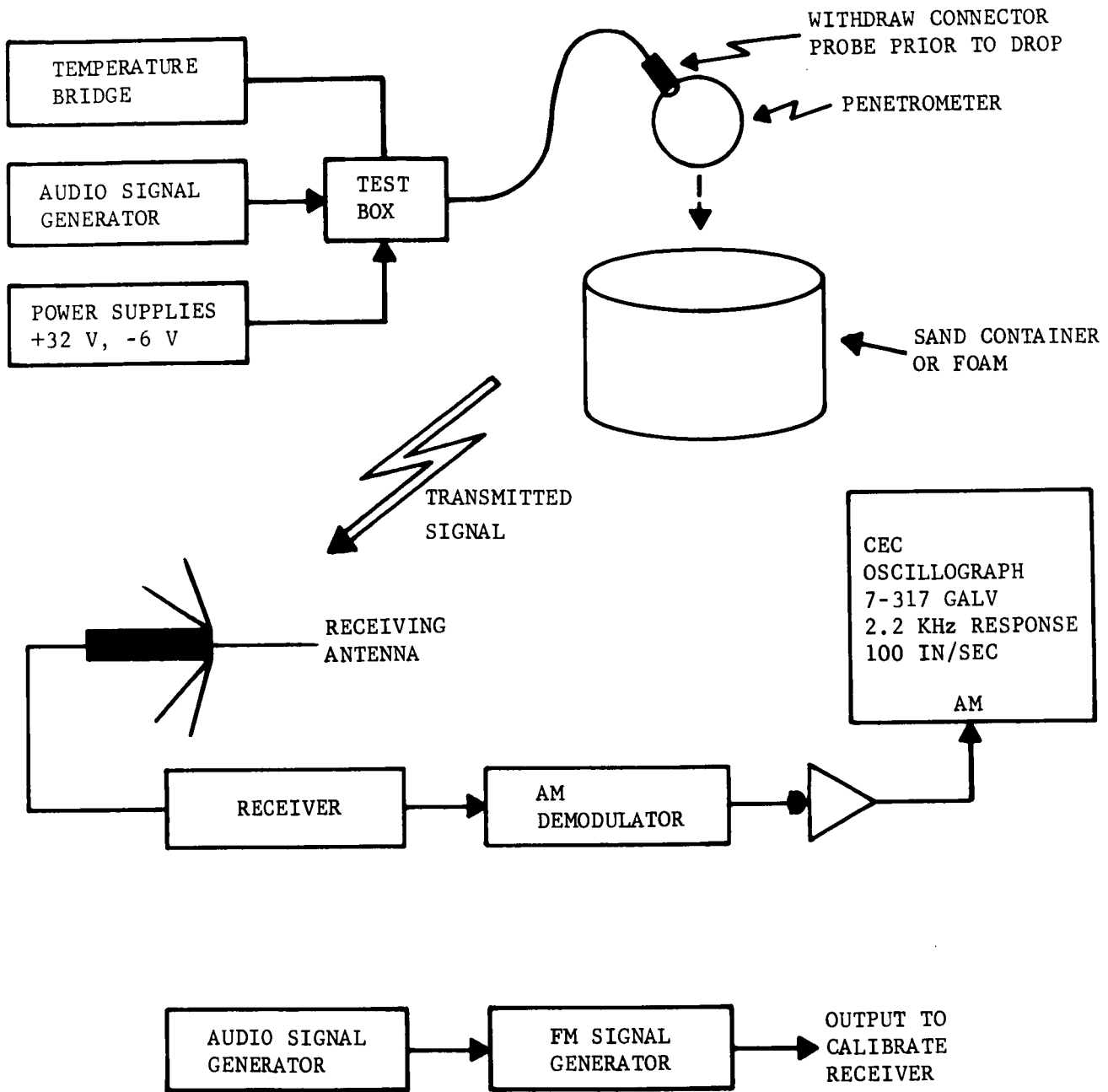
#### 5.1 TESTING OF PROTOTYPE PENETROMETERS

A series of field test impacts, a single rigid impact test, and a captive Hyge calibration check were completed during this report period to facilitate the evaluation of Prototype Penetrometer No. 3. By generating added subsystem performance data, a better measure of penetrometer performance was established. From this basis, design modifications may be derived to include in the specification of a flight model penetrometer. Analysis and data reduction efforts were completed, and an account of the test results obtained is presented in the following paragraphs.

##### 5.1.1 IMPACT TESTS

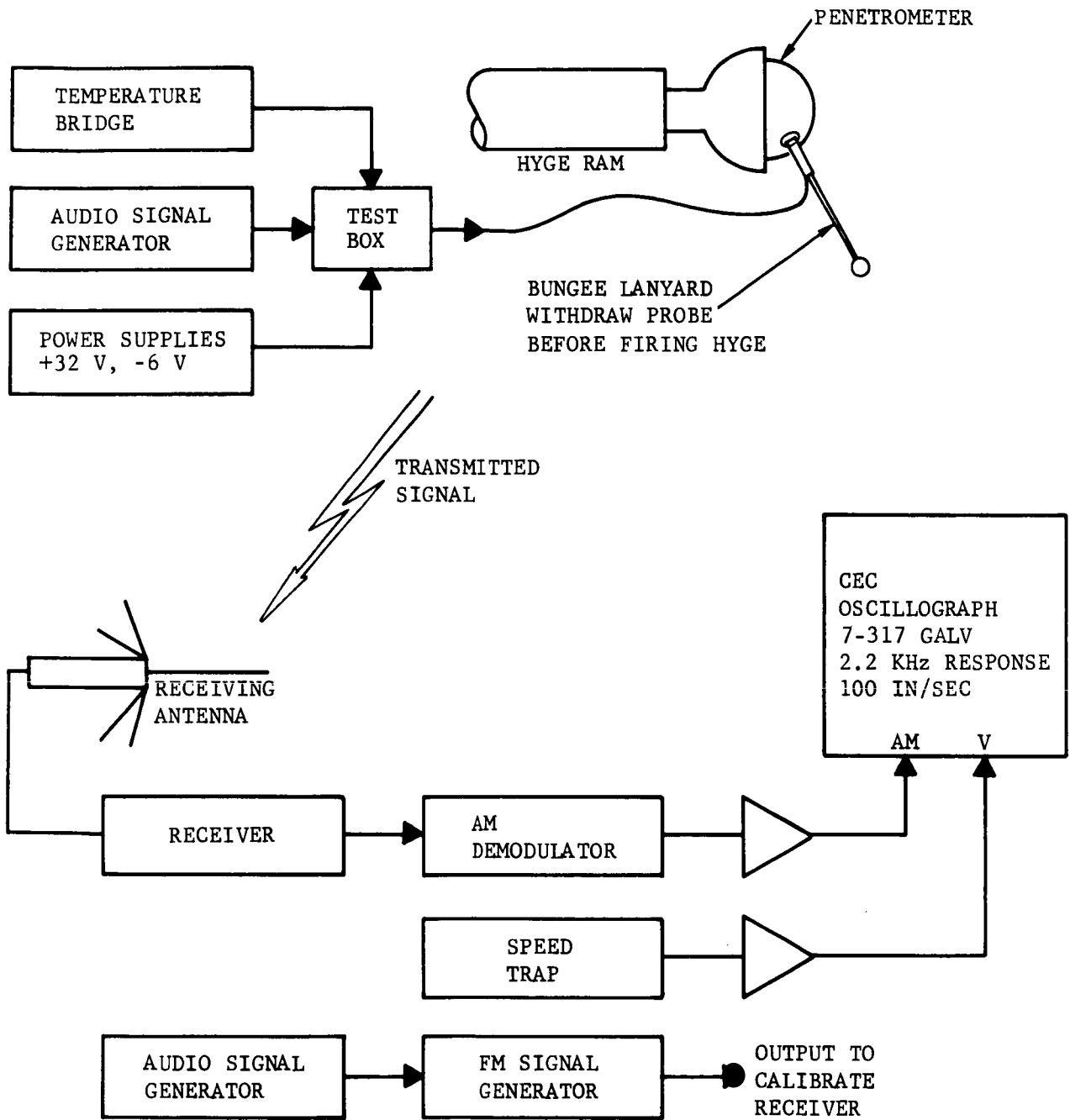
The block diagrams of Figures 5-1 and 5-2 depict the test setup employed for the field test and Hyge impacts, respectively. Multiple tests were conducted under the following test conditions:

- (1) Impact test at 27.7 ft/sec into urethane foam.
- (2) Impact tests at 20 ft/sec into Nevada 120-2L Sand.
- (3) Impact test at 45 ft/sec into Nevada 120-2L Sand.
- (4) Rigid Impact test at 200 ft/sec onto rigid steel plate using Hyge.



F03963 U

FIGURE 5-1. FIELD IMPACT TEST SETUP FOR PROTOTYPE PENETROMETER NO. 3



F03964 U

FIGURE 5-2. HYGE IMPACT TEST SETUP FOR PROTOTYPE PENETROMETER NO. 3

Figure 5-3 denotes the results observed in the low velocity drop tests into foam. Figure 5-4 shows the results obtained with 20 ft/sec drops into aerated test samples of Nevada 120-2L. Figure 5-5 depicts the data obtained in the 45 ft/sec impacts into aerated test samples of Nevada 120-2L.

Table 5.1 presents a summary of the low-velocity drop test data. Because of the multiplicity of drop tests, the penetrometer was kept in a trickle charge mode between tests. The interval between tests coincided with the delay time of 20 minutes assigned to the Nevada 120-2L sand-settling function. The impact axes for the test results shown in Table 5.1 and Figures 5-4 and 5-5 are defined in Figure 5-1.

In general, good repeatability and excellent omnidirectional sensitivity were observed in the Prototype No. 3 low velocity tests. The six drops of Figure 5-4 show a peak acceleration mean value of 67.2 g with a mean deviation of 1.6 g. In Figure 5-5 the peak acceleration mean value of 323 g was noted with a mean deviation of 6.6. The three drops of Figure 5-3 show a peak acceleration mean value of 46.8 g with mean deviation of 3.1 g. The acceleration time histories recorded were observed to be superimposed on a residual 40 KHz output or bias. The bias plus acceleration magnitude were below the signal electronics compression point and were easily interpreted with application of the initial high-sensitivity scale factor.

Figure 5-6 shows the test record for the Hyge impact of Penetrometer Prototype No. 3 against a rigid surface. Pre- and post-test results indicated satisfactory penetrometer performance with the exception of a significant 40 KHz residual output or bias. Because the acceleration-time pulse developed about the biased operating level, there was an effective variation in the original channel data compression characteristic. Subsequent data reduction efforts required application of both the high and low sensitivity scale factors determined in the original Prototype No. 3 captive calibrations. The scale factor for the region below compression is 0.174 KHz/g and for that region above compression is 0.008 KHz/g. The compression point was observed to have a mean value of 85 KHz based upon the individual axis calibrations of Prototype No. 3. Consequently the impact peak deflection of 107.3 KHz is interpreted by applying the high-sensitivity scaling for the initial 85 KHz, i.e. 492 g and adding to it the g value corresponding to 22.3 KHz at the low sensitivity scaling, i.e., 2790 g, resulting in a peak value of 3282 g. It should be noted that some limiter rupture occurred on impact and some reduction in the "g" level registered may have occurred. The Hyge ram acceleration pulse, also shown in Figure 5-6, was observed to exhibit 289 peak g value.

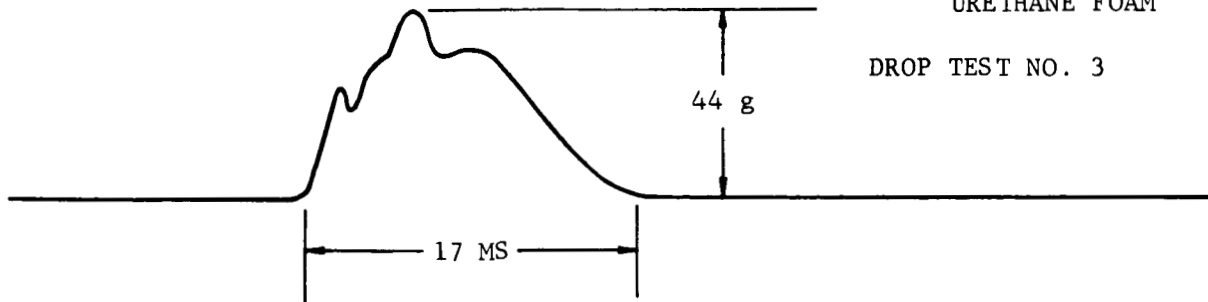
The Hyge impact data of Prototype No. 2 reported in Appendix C of the LPS Final Report (U-3556) is updated here by compensating for the residual

CONDITIONS

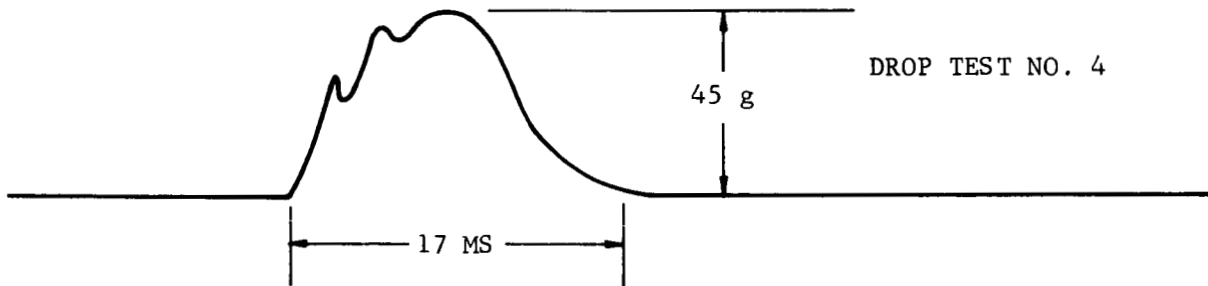
IMPACT VELOCITY =  
27.7 FT/SEC

SOIL MATERIAL =  
URETHANE FOAM

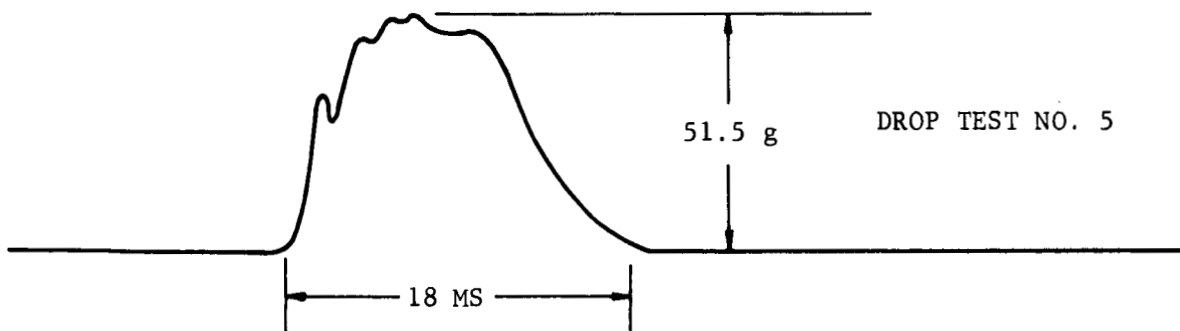
DROP TEST NO. 3



DROP TEST NO. 4



DROP TEST NO. 5



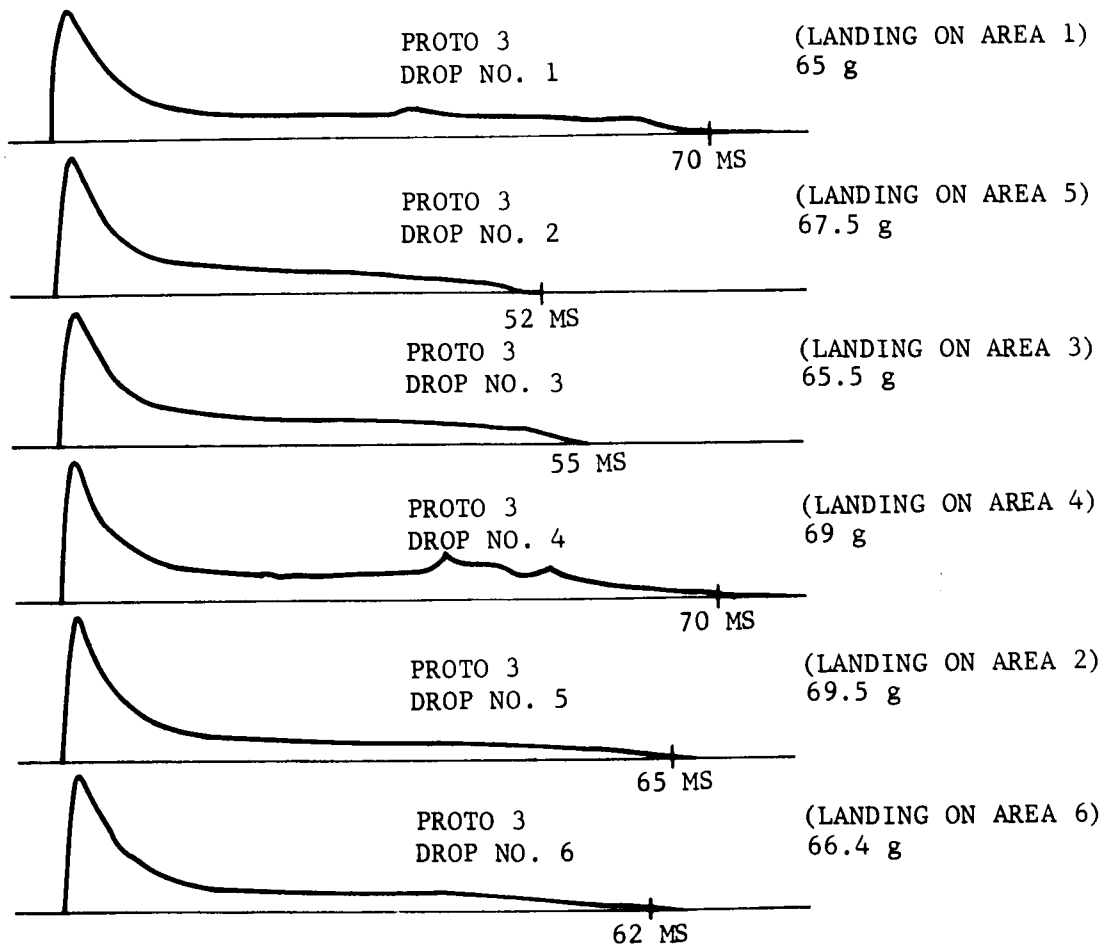
F03965 U

FIGURE 5-3. ACCELERATION OUTPUT RESULTS FOR DROPS OF PROTOTYPE PENETROMETER NO. 3

CONDITIONS

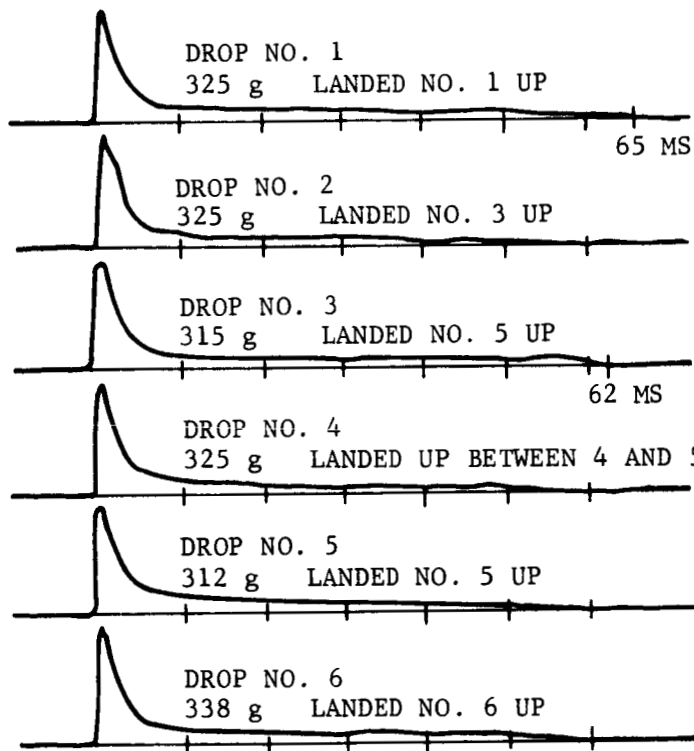
IMPACT VELOCITY =  
20 FT/SEC

SOIL MATERIAL =  
NEVADA 120-2L SAND



FO3966 U

FIGURE 5-4. ACCELERATION OUTPUT RESULTS FOR DROPS OF PENETROMETER PROTOTYPE NO. 3



CONDITIONS

IMPACT VELOCITY =  
45 FT/SEC

SOIL MATERIAL =  
NEVADA 120-2L SAND

F03967 U

FIGURE 5-5. ACCELERATION OUTPUT RESULTS FOR DROPS OF PENETROMETER  
PROTOTYPE NO. 3

TABLE 5.1

PENETROMETER PROTOTYPE NO. 3 DROP TEST DATA

A. Nevada 120-2L Sand  
20 ft/sec (6.2 ft drop distance)

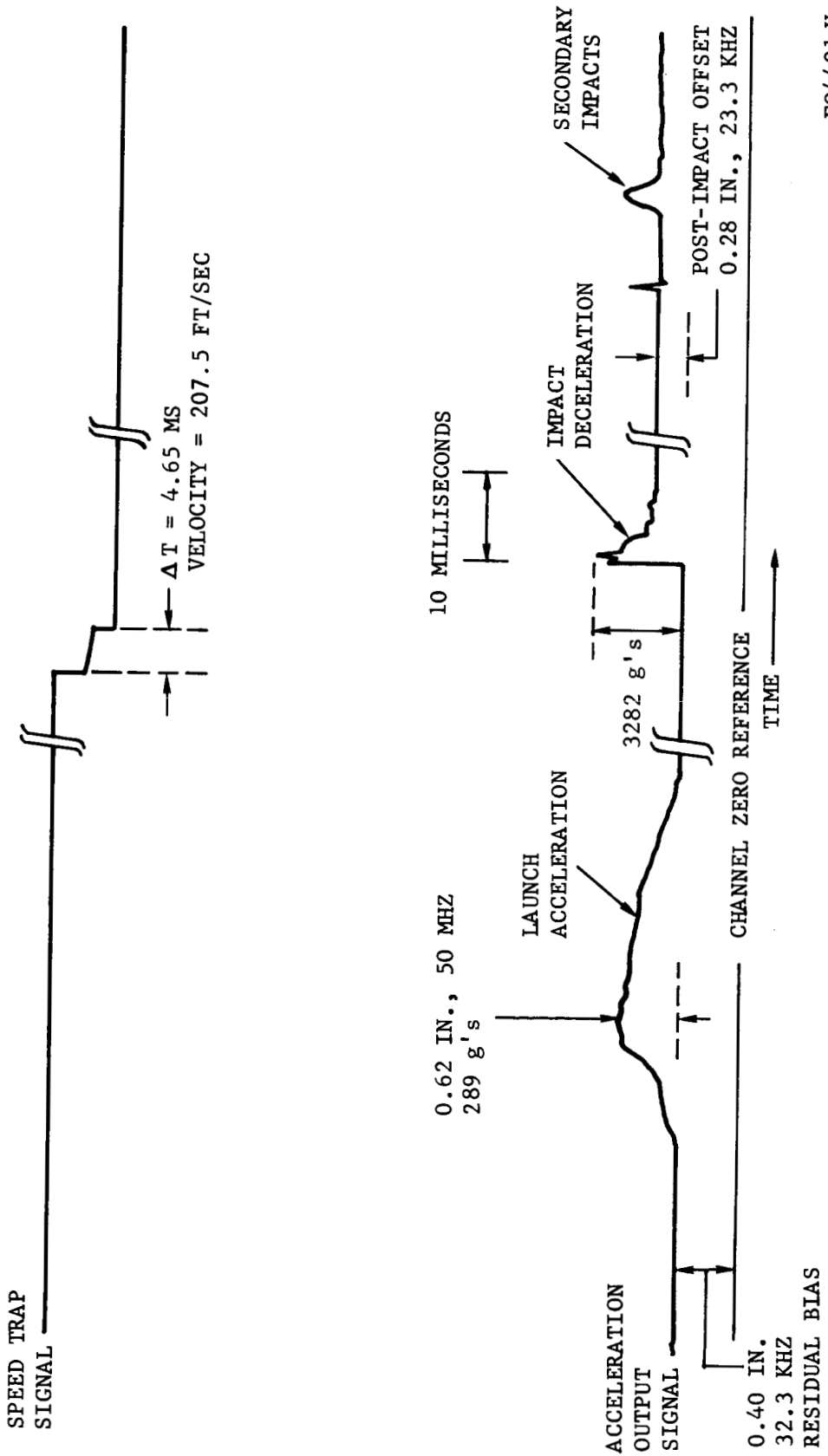
Drop No.	G-Level	Impact Axis
1	65	Axis No. 1
2	67.5	Between 3 & 5
3	65.5	Axis No. 3
4	69	Axis No. 4
5	69.5	Axis No. 2
6	66.4	Between 4 & 6

B. Nevada 120-2L Sand  
45 ft/sec (32 ft drop distance)

Drop No.	G-Level	Impact Axis
1	325	Axis No. 1 Up
2	325	Axis No. 3 Up
3	315	Between 3 & 5 Up
4	325	Between 4 & 5 Up
5	312	Axis No. 5 Up
6	338	Axis No. 6 Up

C. Urethane Foam  
20 ft/sec

Drop No.	G-Level		Duration		Bounce Delay
	1st Impact	Bounce	1st Impact	Bounce	
3	0.98" = 44 g	0.3" = 13.4 g	17 ms	12 ms	To + 383 ms
4	1.0 " = 45 g	0.2" = 12.8 g	17 ms	20 ms	
5	1.15" = 51.5 g	0.4" = 17.9 g	18 ms	14 ms	To + 461 ms



FO4401 U

FIGURE 5-6. HYGIE IMPACT TEST RECORD FOR PENETRATOR PROTOTYPE NO. 3

offset observed during the impact test. A lesser value was exhibited in Prototype No. 2 which represented about 7 percent of full scale. Data was determined by using the high and low sensitivity scale factors (i.e., 0.131 KHz/g and 0.0106 KHz/g, respectively) obtained from the A calibration curve of Figure C-8 of the above-cited Appendix. The Hyge ram acceleration pulse peak value was 275 g and the impact shock peak acceleration was 3215 g, when including compensation for a zero bias error. The values noted for both Prototypes, Nos. 2 and 3, compare favorably, although greater uncertainty is assumed prevalent in the low sensitivity region, above the compression "knee".

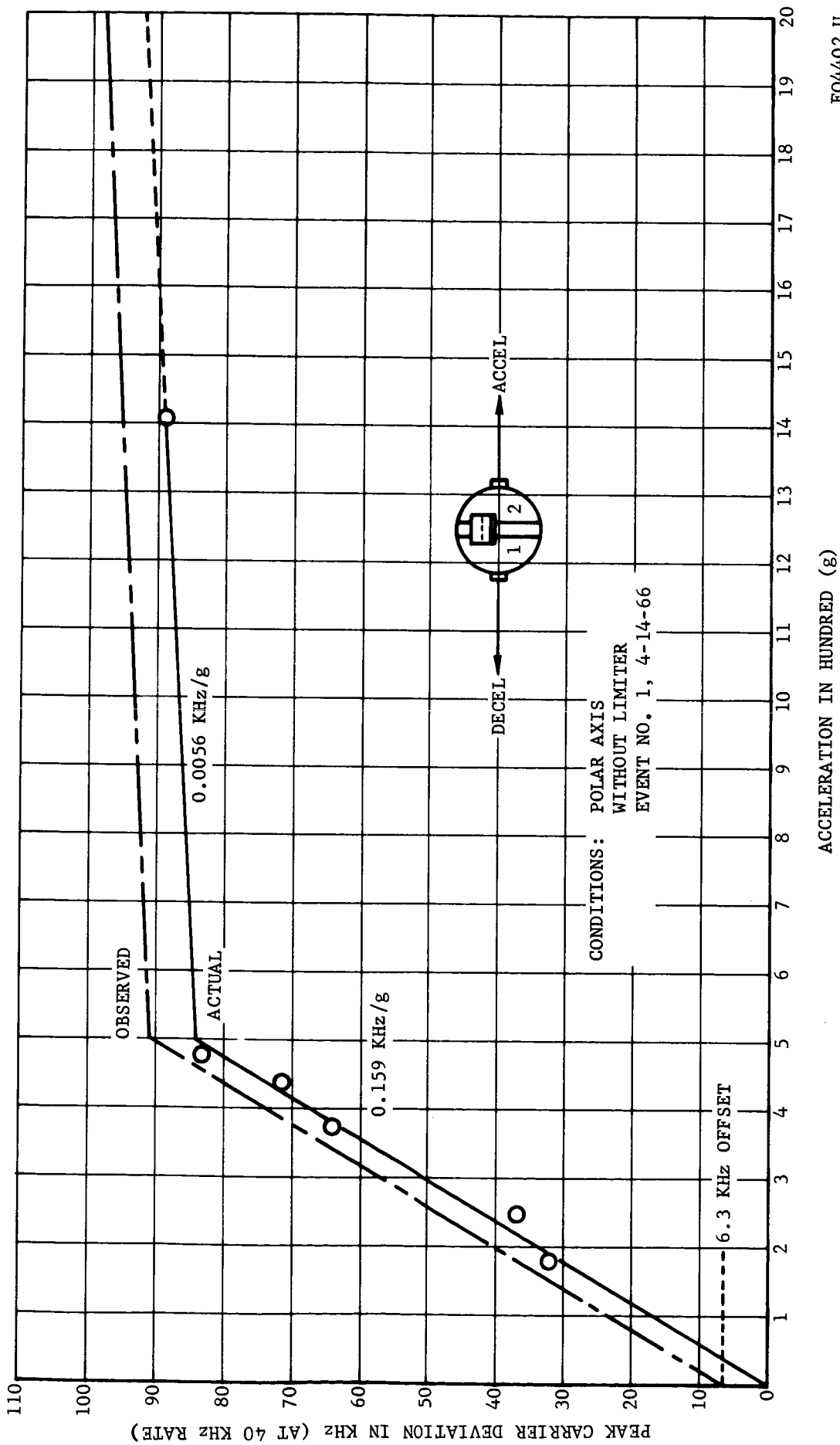
The acceleration trace of Prototype No. 3 following impact was observed to "hang up". This performance anomaly was also observed in the Prototype No. 2 impact data. Gradual decay to the bias level occurred prior to oscillograph shutdown, which was on the order of impact plus two seconds for Prototype No. 3. Similar effects were noted on Prototype No. 2 data. The "nominal time constant" denoted in the level decay was 1.2 sec and 0.5 sec for Prototype Nos. 2 and 3, respectively.

#### 5.1.2 CAPTIVE HYGE SHOCK TEST

A captive calibration check was made on Prototype No. 3 to verify overall performance characteristics following the extensive low-velocity tests and single rigid impact test. Because of the limiter rupture at impact, the entire limiter was removed for the calibration check.

The penetrometer prototype No. 3 (without limiter) was subjected to two captive Hyge shocks of 1400g peak acceleration along its polar axis. Hyge ram acceleration, demodulated specimen signal, and specimen carrier frequency were recorded on oscillograph paper at 100 ips using the standard set of instrumentation apparatus which has been documented in earlier reports. Minimum flat frequency response in the recording system was 2200 cps with linear phase delay up to 3700 cps. An attempt to execute a third shock test was unsuccessful due to insufficient energy in the penetrometer power supply.

The data from the first test is shown in Figure 5-7. The bias level or offset was observed to be much less than that observed in the previous impact tests. The high sensitivity scale factor (below the compression knee) was determined to be 0.169 KHz/g. This was within 3 percent of the value obtained in the initial Hyge captive test. The low sensitivity scaling check involved only a one-point check and, because of a much greater uncertainty associated with this region, was not evaluated. The second test, data shown in Figure 5-8, denoted a marked reduction in performance, implying some form of intermittent behavior. As mentioned, a third test was aborted because of insufficient battery power supply energy. Power supply problems may have occurred during Test 2 when a shorted umbilical connector was noted.



FO4402 U

FIGURE 5-7. PENITROMETER PROTOTYPE NO. 3 TRANSFER FUNCTION

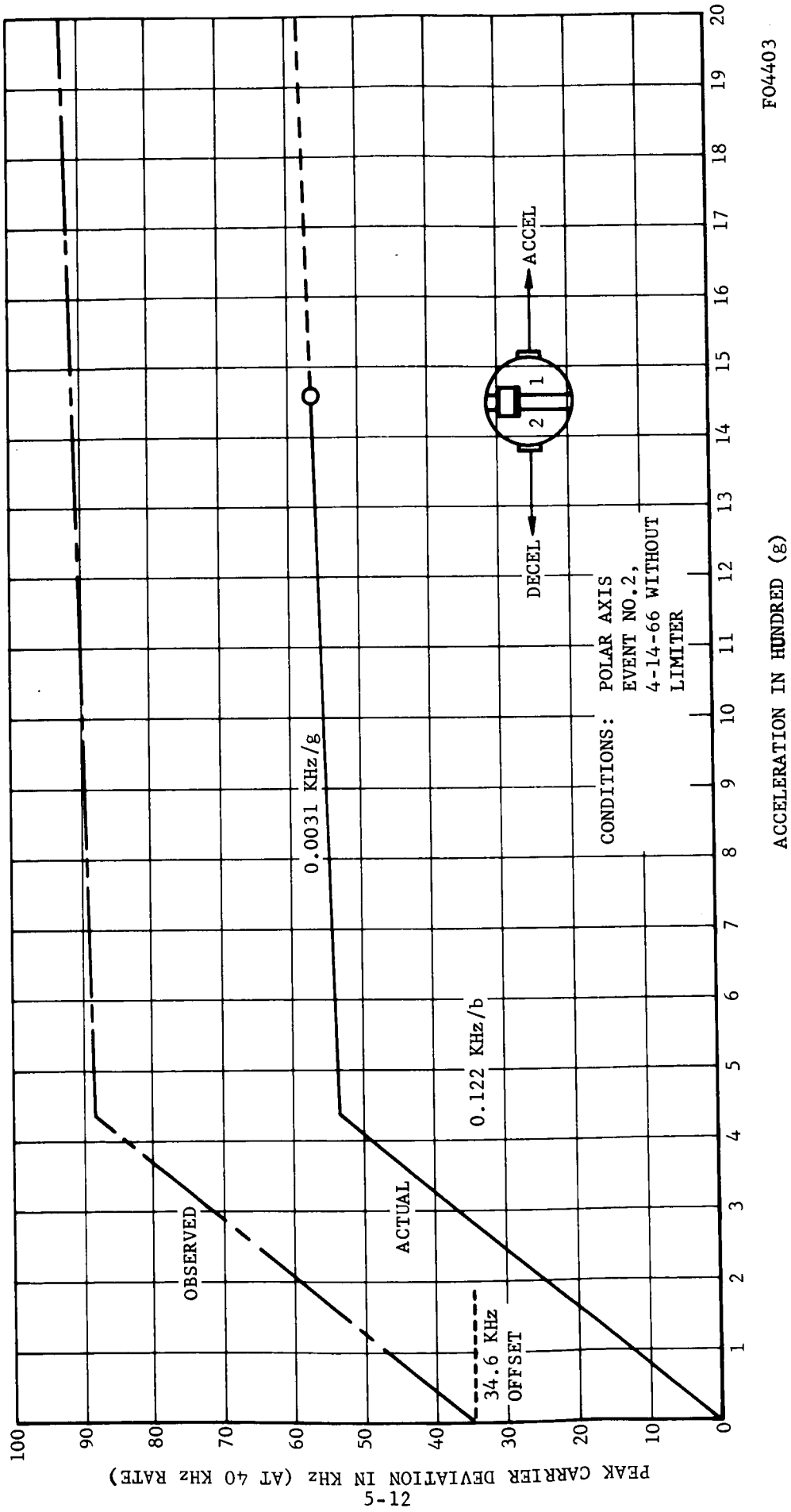


FIGURE 5-8. PENITROMETER PROTOTYPE NO. 3 TRANSFER FUNCTION

### 5.1.3 DISASSEMBLY AND DIAGNOSTIC TESTING

It was evident from the second Hyge captive shot that Prototype No. 3 penetrometer had developed some internal problems. One problem noted was failure of the +17 volt regulator. Another problem was associated with an abnormally high offset as evidenced by a residual 40 KHz output equal to approximately 20 percent of full scale. This output would imply a constant 180 g acceleration. It was therefore decided that Penetrometer No. 3 would be disassembled to determine the nature of its problems.

The problem in the regulator was found to be a defective 2N222A transistor which functions as the series regulator for the +17 volt supply. An autopsy performed upon this unit disclosed a collector-to-emitter short and an open base lead, all internal to the transistor case. It is difficult to determine the cause of this malfunction because the regulator performed normally upon replacing the faulty transistor. The transistor normally is required to dissipate approximately 320 milliwatts. It has a total dissipation rating at room ambient temperature of 500 milliwatts, derating with elevated temperature at 3.33 milliwatt per °C. This implies that the transistor can handle safely the load at temperatures up to 79°C (174°F). It can be assumed from earlier thermal testing that the penetrometer internal temperature never approaches this figure. It is therefore felt that the transistor failed due to some other cause.

As described earlier, the captive Hyge tests were performed without the balsa impact limiter. A fixture was fabricated to hold the penetrometer inner sphere on the ram. There is evidence to indicate that in the process of fastening the fixture on the ram, the fixture was tightened excessively, thereby mechanically stressing the penetrometer. This could have resulted in a momentary short inside the ball, causing regulator failure. Further disassembly and testing were performed to determine the residual 40 KHz offset problem. The signal electronics compartment was disassembled to investigate the offset problem. These and other diagnostic investigations are reported in further detail in the following paragraphs.

### 5.1.4 SUMMARY OF CALIBRATION AND PERFORMANCE ANOMALIES

During the course of testing initial prototype penetrometers in the original LPS program, both calibration and performance anomalies were observed to exist. Additional observations were gained from the evaluation testing described above. The principal problem areas noted are summarized briefly in the following paragraphs and an account of the subsequent investigations and findings are described under separate headings following the summary.

(a) Electrical vs. Dynamic Calibration. Both Prototype 2 and 3 penetrometers exhibited problems associated with correlation of captive Hyge dynamic calibration and electrical calibration utilizing the signal

calibration input to the signal electronics. The variation was greatest in Prototype No. 2 (2:1) and somewhat less in No. 3. To visualize the elements of the problem under investigation, a simplified block diagram of the functional elements involved is shown in Figure 5-9. As may be noted, the physical and electrical input stimuli for calibration were applied at two different points in the system. The FM receiver (discriminator) and AM demodulator have served as output monitoring points at various stages of testing. Differences in output characteristics could occur, therefore, if anomalies occurred in the accelerometer, in the signal electronics input stage, in the different readout monitor points, or within any element in the penetrometer subsystem while subject to the physical dynamic shock input.

(b) Internal vs. External Power. All test records of Prototype No. 3 indicate an apparent increase of signal electronics gain while operating on internal power. There are many possible causes for this, including:

- (1) Shift of 40 KHz multivibrator frequency beyond filter response.
- (2) Possibility of transmitter RF output being detected and supplied as input signal in high impedance circuits.
- (3) Power supply impedance variation when operating from high-voltage external source.
- (4) Low voltage effects and/or poor regulation on internal supply due to partially discharged battery.

(c) Residual 40 KHz Offset. Appreciable and differing magnitudes of a residual 40 KHz AM subcarrier output existed during the evaluation testing of prototype penetrometers. This was more pronounced and variable in Prototype No. 3. The principal effect is a reduction in signal dynamic range in the high sensitivity region below the compression point. Consequently, the offset contributed greatly to the apparently poor acceleration time signature recorded in the 200 ft/sec rigid impact test of Prototype No. 3. Balance of the signal electronics amplifier is initially set for a maximum 5 millivolt offset. This was noted to increase to 50 millivolts during impact qualification of the Prototype No. 3 signal electronics module (12 to 15,000 g impacts). This increased to 150 millivolts during the high-energy impact. This problem may be related to deterioration in balance due to impact sensitive components. Various tests were conducted on the disassembled signal electronics module.

(d) Accelerometer Trace "Hang-Up". The high-energy (200 fps) impact test data of Prototypes Nos. 2 and 3 showed a significant apparent "hang-up" of the acceleration data following the impact. The trace slowly falls

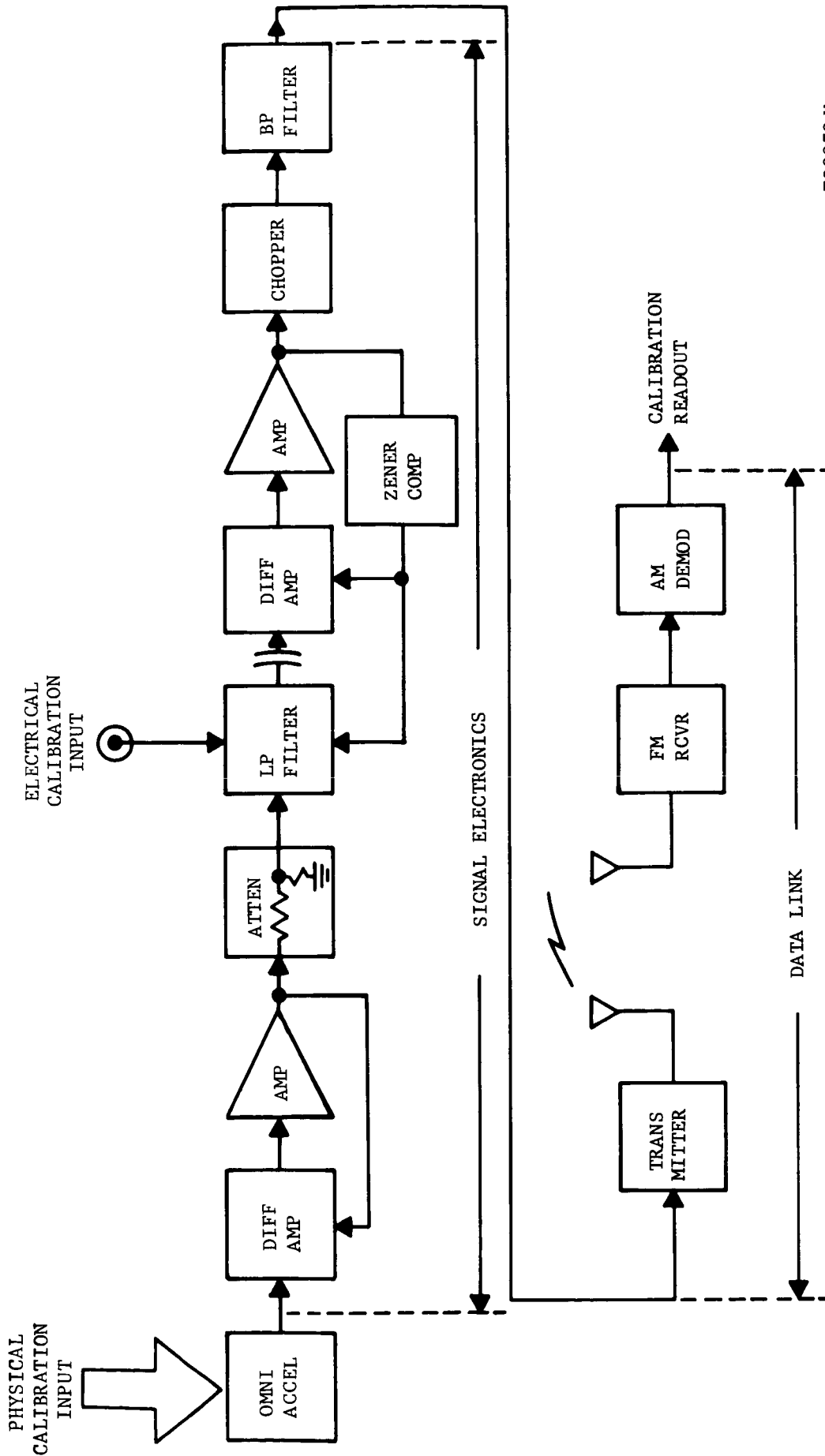


FIGURE 5-9. SIMPLIFIED DIAGRAM OF THE LUNAR PENETROMETER SYSTEM

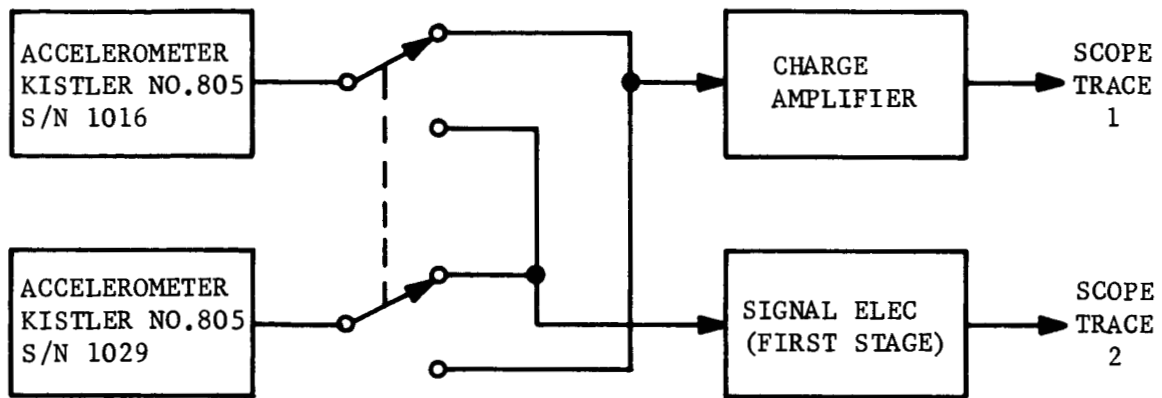
off at an unrealistic rate, obscuring tail-off plateau data presently considered useful in the LEM sounding device application for indicating bearing strength. A likely cause is that of latch-up in the integrated operational amplifiers and this investigation is briefly discussed later.

#### 5.1.5 SIGNAL ELECTRONICS - ACCELEROMETER COMPATIBILITY TESTS

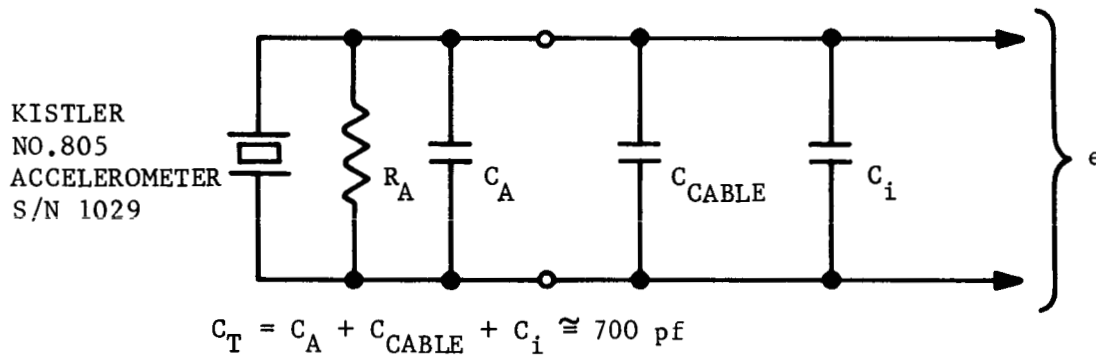
During the high-energy impact test of Prototype No. 3, it appeared that the acceleration amplitude read-out of the penetrometer system was much lower than anticipated. One of the possible causes for this phenomenon was thought to be a reduction in transducer sensitivity due to depolarization caused by the signal voltage developed during impact. Conventional accelerometer instrumentation techniques and equipment utilize charge amplifiers, a characteristic of which prevents signal voltage build-up across the transducer. Since all the Endevco omnidirectional accelerometers had been tested and calibrated with charge amplifier instrumentation, a test was conducted to verify proper transducer action with LPS signal electronics which allows transducer voltage build-up.

Two similar single-axis accelerometers were mounted on the hand-swung hammer. The test setup is shown in Figure 5-10. A conventional charge amplifier was used as the reference for comparison measurements with the signal electronics first stage output (voltage gain of unity). The necessary corrections were made for the different charge sensitivities of the accelerometers. A number of hammer tests established that there was no measurable loss in accelerometer sensitivity when used with the signal electronics amplifier.

Additional tests were made to verify that the accelerometer output voltage equals the charge sensitivity divided by the capacity, as shown in Figure 5-10. The test results using the hammer did confirm that the sensitivity with a total capacity of 700 pf was 0.343 millivolts/g (see Figure 5-11) while this sensitivity was halved by doubling the total capacity (see Figure 5-12). These breadboard tests served to verify satisfactory operation of the signal electronics input stage while accommodating uni-axial crystal accelerometer input signals during subjection to a shock environment.



(a) COMPATIBILITY TEST SETUP



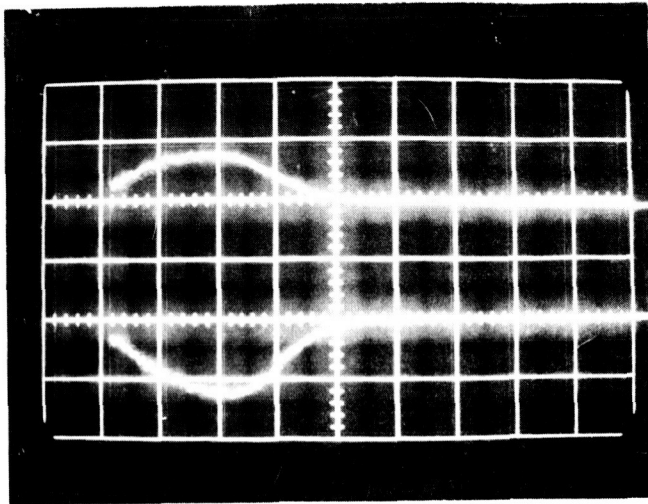
$q = \text{ACCELEROMETER CHARGE SENSITIVITY} = 0.24 \text{ p cb/g}$

$$e = \frac{q}{C_T} = \frac{0.24 \text{ p cb/g}}{700 \text{ pf}} = 0.343 \text{ MILLIVOLT/g}$$

(b) ACCELEROMETER CALCULATIONS

F04404 U

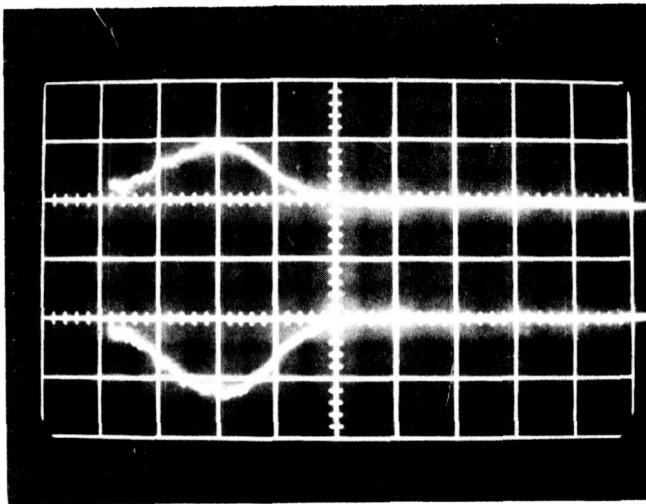
FIGURE 5-10. SIGNAL ELECTRONICS-ACCELEROMETER COMPATIBILITY TEST SET-UP AND CALCULATIONS



IMPACT TEST NO. 1

UPPER TRACE: CHARGE AMPLIFIER  
OUTPUT, 5000 g/DIV

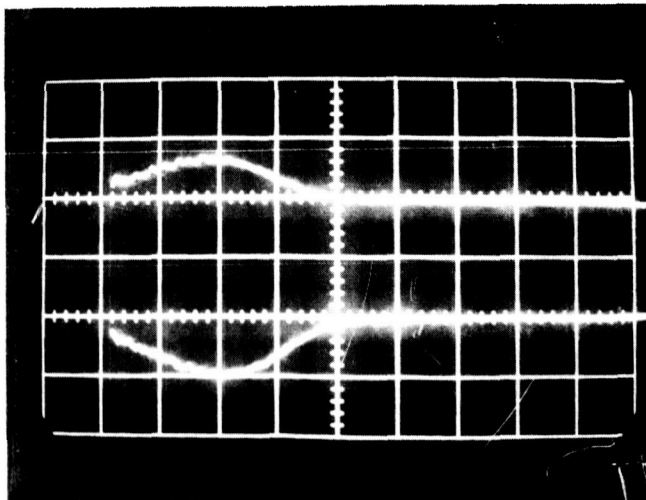
LOWER TRACE: PENETROMETER SIGNAL  
ELECTRONICS OUTPUT,  
2900 g/DIV



IMPACT TEST NO. 2

UPPER TRACE: CHARGE AMPLIFIER  
OUTPUT, 5000 g/DIV

LOWER TRACE: PENETROMETER SIGNAL  
ELECTRONICS OUTPUT,  
2900 g/DIV



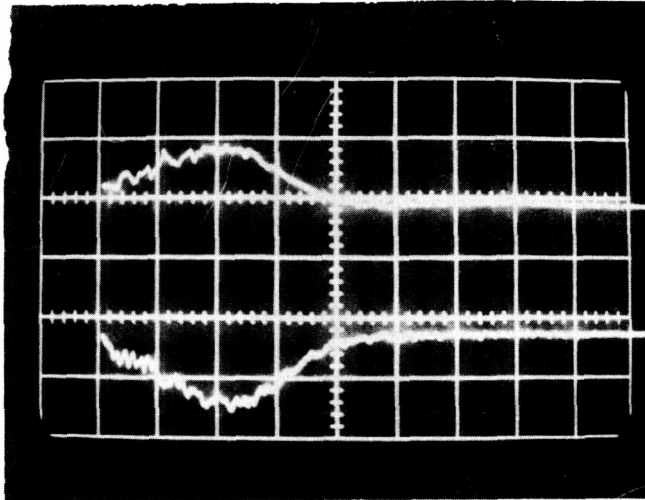
IMPACT TEST NO. 3

UPPER TRACE: CHARGE AMPLIFIER  
OUTPUT, 5000 g/DIV

LOWER TRACE: PENETROMETER SIGNAL  
ELECTRONICS OUTPUT,  
2900 g/DIV

FO4405 U

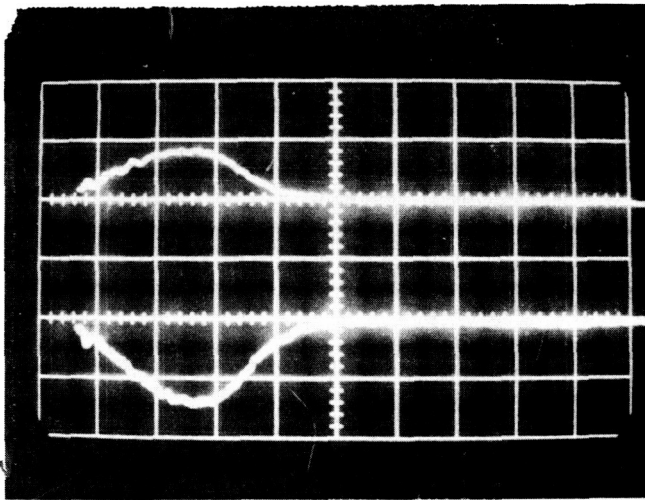
FIGURE 5-11. SIGNAL ELECTRONICS, ACCELEROMETER COMPATIBILITY TEST RESULTS FOR  $C_{TOTAL} = 700$  pf



IMPACT TEST NO. 4

UPPER TRACE: CHARGE AMPLIFIER  
OUTPUT, 5000 g/DIV

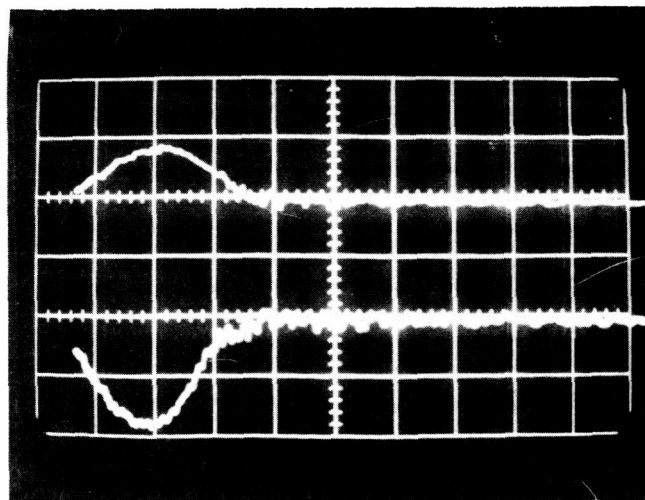
LOWER TRACE: PENETROMETER SIGNAL  
ELECTRONICS OUTPUT,  
2900 g/DIV



IMPACT TEST NO. 5

UPPER TRACE: CHARGE AMPLIFIER  
OUTPUT, 5000 g/DIV

LOWER TRACE: PENETROMETER SIGNAL  
ELECTRONICS OUTPUT,  
2900 g/DIV



IMPACT TEST NO. 6

UPPER TRACE: CHARGE AMPLIFIER  
OUTPUT, 5000 g/DIV

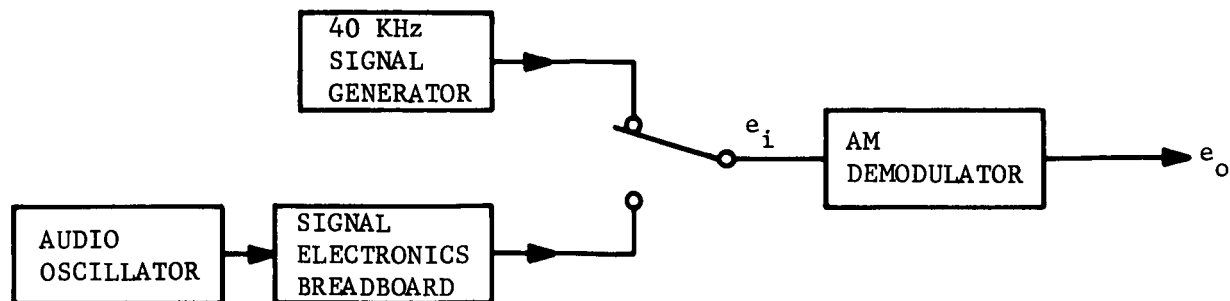
LOWER TRACE: PENETROMETER SIGNAL  
ELECTRONICS OUTPUT,  
2900 g/DIV

FO4406 U

FIGURE 5-12. SIGNAL ELECTRONICS, ACCELEROMETER COMPATIBILITY TESTS FOR  $C_{TOTAL} = 1400$  pf

### 5.1.6 AM DEMODULATOR WAVEFORM SENSITIVITY TESTS

A bench test setup which employed the following elements



was used to conduct waveform sensitivity tests. Two types of signals were employed, an unmodulated 40 KHz CW signal and an amplitude modulated (AM) 40 KHz which is identical to penetrometer waveforms used in testing. By means of Lissajou pattern checks, frequencies of the two separate sources were verified to be equal (i.e., each frequency was adjustable). The AM demodulator was in its normal configuration as employed in previous prototype tests, i.e., BPF centered at 40 KHz with the 3 db bandpass limits at  $\pm 2.5$  KHz and output LPF cutoff at 2 KHz.

The data in Table 5.2 shows the results obtained for three basic input AM subcarrier frequencies with and without modulation. Figure 5-13 denotes waveforms observed in the 40 KHz operating frequency case. With the CW unmodulated signal as a reference, outputs are observed to be reduced with modulation. Modulated outputs were read as peak values from the residual zero of the trace and not the absolute zero reference shown as a straight line on the bottom trace (2 divisions up from bottom reference line). This corresponds to previous data readouts and facilitates data correlation. As was noted in previous discussions, the existence of a residual zero encroaches upon the signal dynamic range and further enhances the reduced output characteristic. The bottom row of Table 5.2 denotes typical LPS system performance under two versions of AM demodulator input signal sources. It would appear that unlike calibration signals are likely to contribute errors ranging from 12 to 22.5 percent in output variation. With other anomalies present, this may become worse.

These observations indicate differences in electrical and dynamic (physical) calibrations previously noted and are partly due to waveform

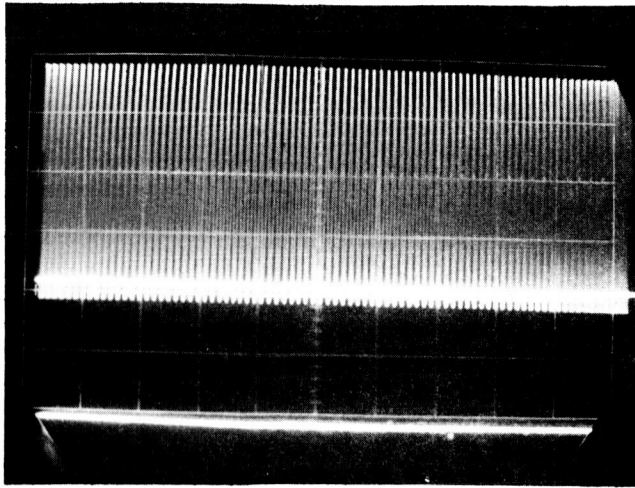
TABLE 5.2

## AM DEMODULATOR WAVEFORM SENSITIVITY TESTS

Signal Input			Signal Output $e_o$ (V <sub>p</sub> )	T (s) $e_o/e_i$	Relative Change %
$f_o$ (KHz)	Type	$e_i$ (V <sub>p-p</sub> )			
41	CW	1.97	4.48	2.27	Ref.
41	100 Hz AM	2.00	3.66	1.83	- 19.3
41	500 Hz AM	1.99	3.61	1.81	- 18.9
40	CW	2.01	4.65	2.32	Ref.
40	100 Hz AM	2.02	4.08	2.02	- 12.2
40	500 Hz AM	2.02	3.96	1.97	- 14.5
39	CW	2.04	4.41	2.16	Ref.
39	100 Hz AM	1.79	3.38	1.89	- 12.5
39	500 Hz AM	1.96	3.60	1.83	- 15.3
40	CW	--	--	2.40 *	Ref.
40.2	Proto 3	--	--	1.86**	- 22.5

\* RCVR Cal determined from 10 incremental T(s)'s.

\*\* Ball Cal determined from 16 incremental T(s)'s.

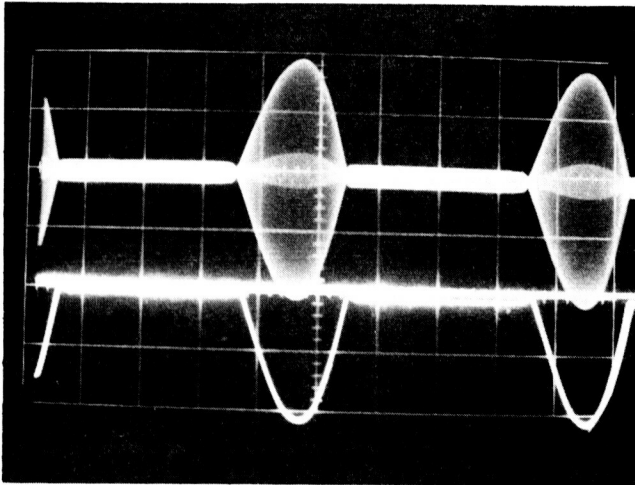


a. UNMODULATED 40 KHZ TEST

UPPER TRACE: INPUT, 40 KHZ,  
0.5 V/DIV

CENTER TRACE: OUTPUT ZERO REFERENCE

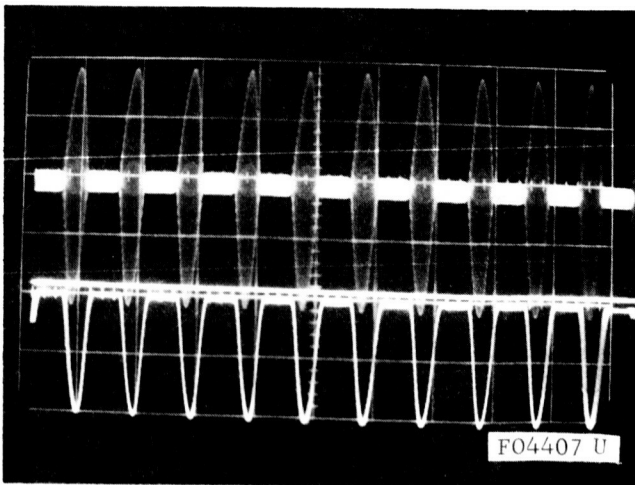
LOWER TRACE: DEMODULATOR OUTPUT,  
DC, 2 V/DIV



b. 100 HZ HALF-SINE AM TEST

UPPER TRACE: INPUT, 100 HZ MODULATED  
40 KHZ, 0.5 V/DIV

LOWER TRACE: DEMODULATOR OUTPUT,  
100 HZ HALF-SINE,  
2 V/DIV



c. 500 HZ HALF-SINE AM TEST

UPPER TRACE: INPUT, 500 HZ  
MODULATED 40 KHZ,  
0.5 V/DIV

LOWER TRACE: DEMODULATOR OUTPUT,  
500 HZ HALF-SINE,  
2 V/DIV

FIGURE 5-13. TYPICAL TEST RESULTS FOR AM DEMODULATOR WAVEFORM SENSITIVITY

sensitivity exhibited by the demodulator. The nominal 2:1 and 1.5:1 differences noted in previous penetrometer tests are not accounted for wholly but a significant contribution may be attributed (e.g., 1.3:1) to waveform characteristics.

#### 5.1.7 40 KHz MULTIVIBRATOR FREQUENCY STABILITY TESTS

During the extensive testing of Prototype No. 3, it was noted that the apparent gain of the signal electronics module for a given calibration signal was greater when operating on internal power rather than on external power. One possible cause for this effect would be an appreciable shift in the frequency of the 40 KHz multivibrator (chopper driver) as the supply voltages varied. This would cause a reduction in the 40 KHz amplitude output of the data relay AM detector related to the bandwidth and skirt attenuation of the various 40 KHz filters in the overall penetrometer system.

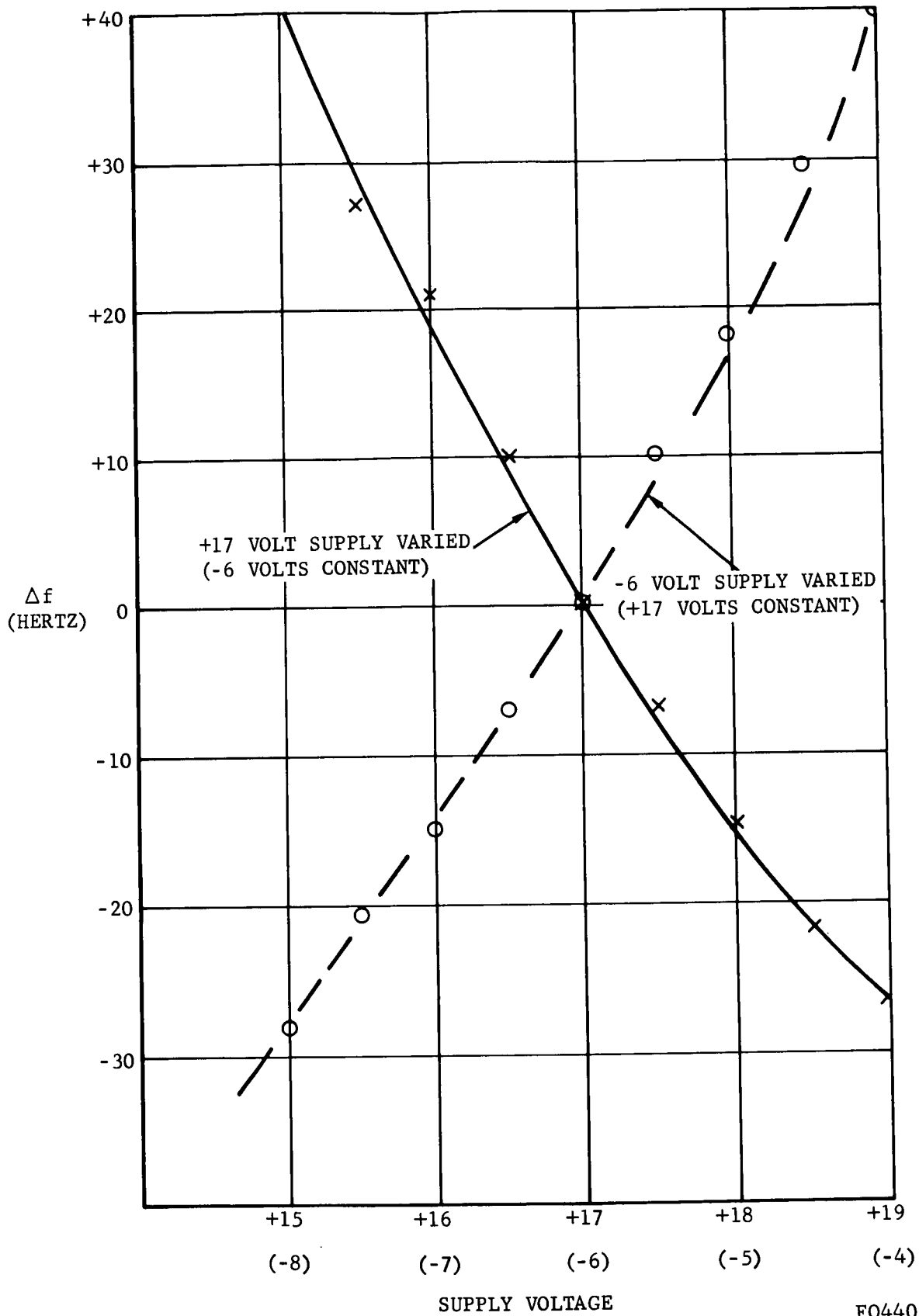
Tests were conducted to determine the frequency stability of the 40 KHz multivibrator (chopper) in the signal electronic module as a function of power supply voltage. The frequency of the 40 KHz multivibrator in the breadboard signal electronics was measured over a wide range of +17 volt and -6 volt supply variations. The test results are shown in Figure 5-14. Maximum frequency shift does not exceed 70 Hz for a 4-volt excursion in either the 17-volt supply or the -6 volt supply. Since the overall system bandwidth for the 40 KHz subcarrier exceeds 1 KHz, the 70 Hz shift attributable to supply voltage variations is negligible and does not result in amplitude reduction due to exceeding filter bandwidth.

These test results, when applied to the electrical vs. dynamic (physical) calibration anomaly, essentially remove the consideration of a varying AM subcarrier frequency as a possible contributor.

#### 5.1.8 INTERNAL VS. EXTERNAL POWER PERFORMANCE TESTS

Prototype No. 3 bench tests on the partially disassembled model were conducted to explore the subject performance characteristics. The penetrometer was operated on both external and internal power and signals were received, discriminated, and demodulated in an AM/FM equivalent LPS receiving channel.

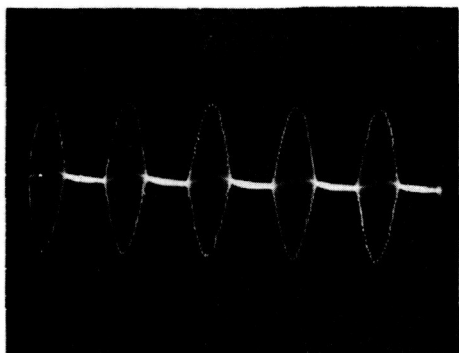
Figure 5-15 also denotes the receiver discriminator (AM demodulator input) and AM demodulator outputs for these same conditions of applied signal and power. The demodulator output was observed to be larger on internal power. Investigation into this showed that the +17 volt line was normal on external power but was low (15 - 16 volts) on internal. The high voltage (+31.5 volts) also was low ( $\approx$  20 volts) on internal power. It appeared as though regulation of the +17 supply was lost on internal power.



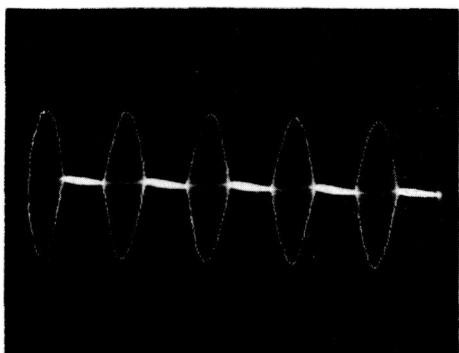
FO4408 U

FIGURE 5-14. 40 KHz MULTIVIBRATOR FREQUENCY STABILITY

A. SIGNAL ELECTRONICS OUTPUT WITH 100 MV CALIBRATION SIGNAL INPUT

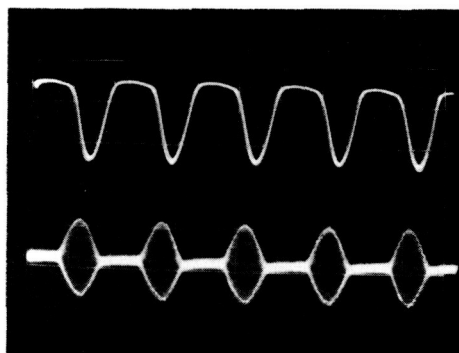


(1) WITH EXTERNAL POWER SUPPLIED TO PENETROMETER.

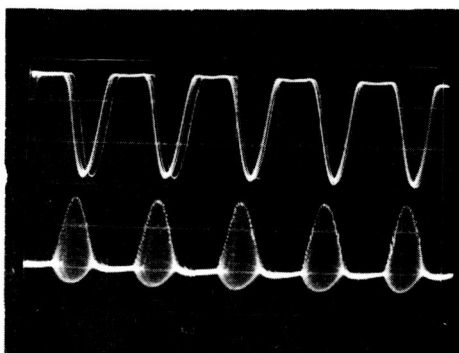


(2) WITH PENETROMETER OPERATING ON INTERNAL POWER.

B. AM DEMODULATOR WAVEFORMS WITH 220 MV CALIBRATION SIGNAL APPLIED TO PENETROMETER SIGNAL ELECTRONICS



UPPER TRACE: AM DEMODULATOR OUTPUT } WITH EXTERNAL  
 LOWER TRACE: AM DEMODULATOR INPUT } PENETROMETER POWER



UPPER TRACE: AM DEMODULATOR OUTPUT } WITH INTERNAL  
 LOWER TRACE: AM DEMODULATOR INPUT } PENETROMETER POWER

FIGURE 5-15. PERFORMANCE CHECKS OF PENETROMETER PROTOTYPE NO. 3 OPERATING ON INTERNAL VS. EXTERNAL POWER

This increases the supply impedance and reduces the supply decoupling. Upon bypassing the +17 volt line with a 100 $\mu$ f capacitor, the problem disappeared, even when +17 volt went as low as 12 to 13 volts. The problem apparently is associated with the transmitter section and can be eliminated with better supply decoupling. Under conditions of low battery power supply voltage, which occurred several times during prototype testing, variations in internal vs. external performance characteristics evidenced are traceable. However, previous system checks with a completely assembled penetrometer did not exhibit any appreciable waveform distortion as evidenced in the bench tests. Differences in receiver/discriminator outputs for the same applied input were, of course, noted and showed internally powered data was 20 percent larger in magnitude than externally powered results.

#### 5.1.9 RESIDUAL 40 KHz OFFSET IN PROTOTYPE NO. 3

Prototype Penetrometer No. 3 was further disassembled to determine the offset problem. It was also noted that there was low gain through the signal electronics after the +17 volt regulator had been repaired. The low gain was in the second stage of the signal electronics. Over 300 millivolts (rms) at the calibrate test point were required to reach compression where normally compression should occur at an input of 175 millivolts (rms). In final prototype assembly some epoxy had leaked through to the case of the  $\mu$ A702 flat-pak amplifier of the signal electronics second stage. This bonded the unit to the first stage which is located directly above. During disassembly, the top of 702A flat-pak was lifted off, but the unit functioned as before with high offset and low gain. This flat-pak was replaced but low gain still existed. However, the offset was considerably less than before. An autopsy performed upon the removed flat-pak did not disclose the failure mechanism.

After noticing erratic and unusual drifts, a defective ground wire connected to the signal electronics was found. Upon repairing this connection, all problems were corrected and the penetrometer appeared to be functioning normally in all respects. It is impossible to determine how or when this broken or intermittent ground lead affected previous data. However, the turn-on transient test was repeated and compared to an earlier test. Figure 5-16 gives the results which show that the offset problem has disappeared and operation appears to be normal.

#### 5.1.10 ACCELERATION TRACE HANG-UP

The high-energy (200 fps) impact tests on both penetrometer Prototype Nos. 2 and 3 exhibited a significant "hang-up" or offset following the principal impact pulse. A probable cause for the observed effect is that of latch-up in the integrated operational amplifier employed in the signal electronics. Limited bench tests were made on a bread-board version

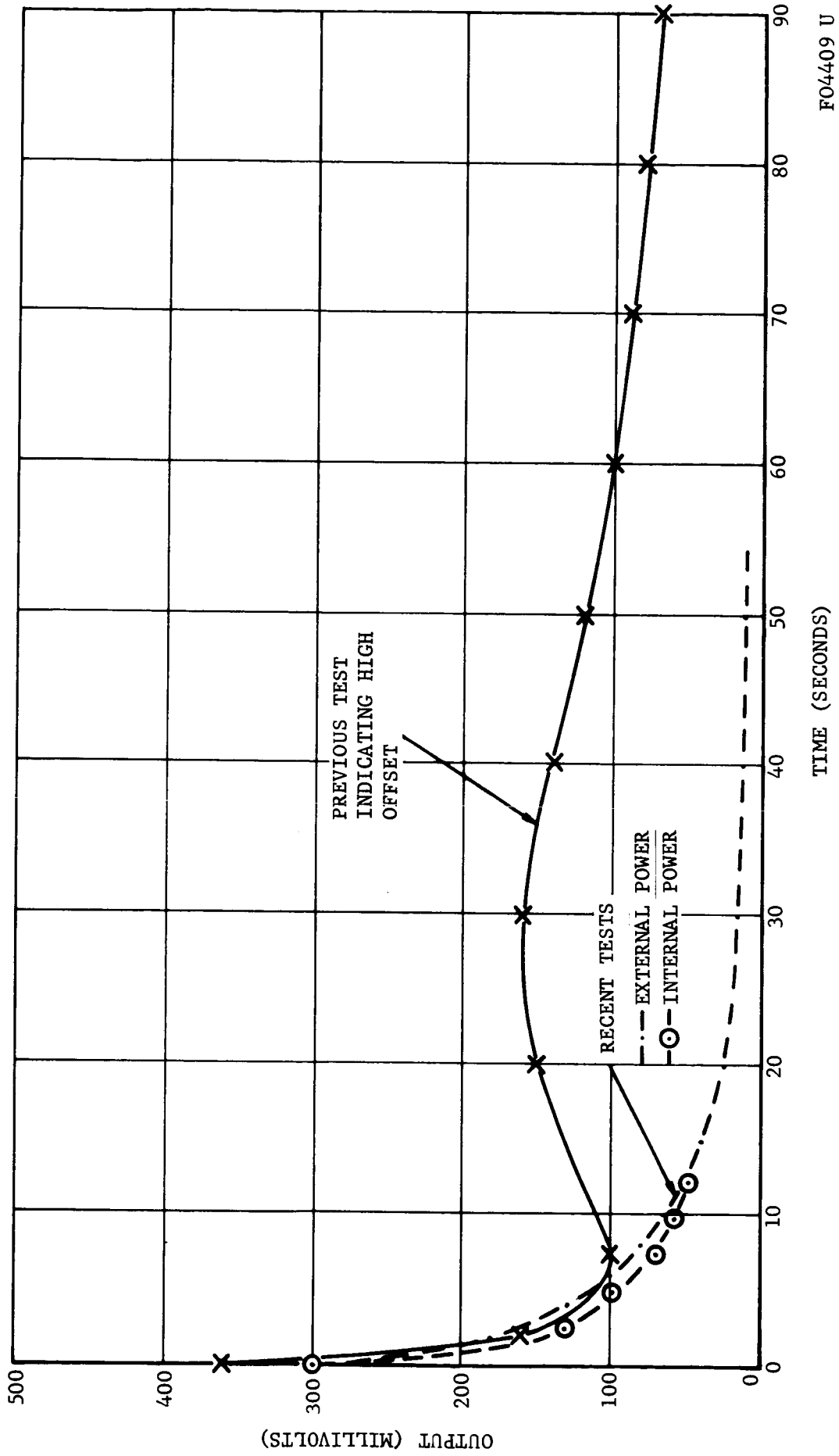
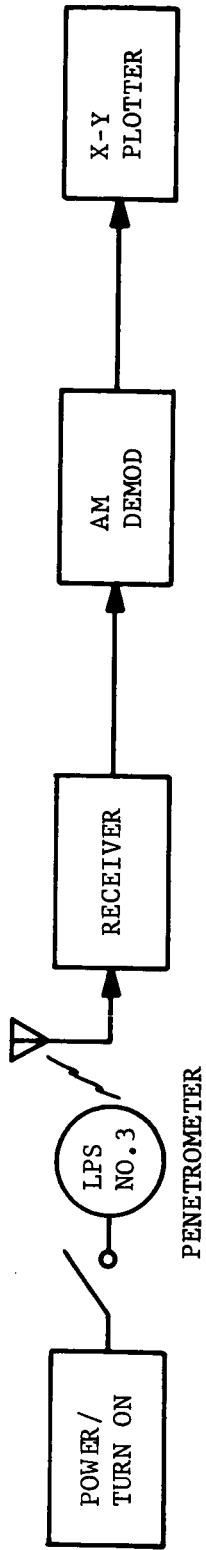


FIGURE 5-16 TURN-ON TRANSIENT FOR PROTOTYPE #3

FO4409 U

of a  $\mu$  702 amplifier stage and latch-up was caused with power supply interruptions on the order of a 0.5 second. Perturbations of this duration or other anomalies were not evidenced, however, in any module testing, etc. to date. On the other hand, actual penetrometer signal electronics assembly layout configuration may be a contributing factor. This was unable to be checked because of Prototype No. 3 disassembly. Improvements can be executed (and are discussed in the following paragraphs) which will involve use of an improved version of the operational amplifier ( $\mu$  709) and revised layout techniques. Completed assemblies in penetrometer configuration will then be examined and tested for latch-up vulnerability. A satisfactory explanation of the apparent latch-up effect, consequently, demands additional module and system test and evaluation.

## 5.2 PENETROMETER MODULE EVALUATION

### 5.2.1 CRYSTAL-CONTROLLED OSCILLATOR MODULE

Further impact tests were conducted on the oscillator described in the LPS Tenth Monthly Progress Report. This oscillator employs a JPL furnished high-impact crystal. Prior tests indicated excellent frequency stability during impact. During this reporting period, emphasis was placed on the design and test of an FM modulation circuit to be incorporated into this oscillator. The oscillator was modified by placing a varicap (voltage variable capacitor) across the collector tank circuit. (See Figure 5-17a). This resulted in low deviation frequency modulation, on the order of  $\pm 2$  KHz maximum, and a high percentage of amplitude modulation.

During hammer impact the apparent frequency deviation shifted to less than  $\pm 1$  KHz while the amplitude modulation remained constant. It is felt that the method of modulation was contributing to this undesirable apparent frequency deviation shift during impact. The oscillator was further modified with a varicap placed in series with the crystal. (See Figure 5-17b). This system allowed a greater frequency deviation ( $\pm 4$  KHz); however, a large percentage of amplitude modulation still existed. Up to this point the output signal had been taken off the power supply lead which was common to both the basic oscillator and the bias network for the varicap. This supply was lightly bypassed for the modulation frequency at 40 KHz. Further modifications were made with the collector tuning capacitor split to allow a 50 ohm output tap to be brought out. This point was heavily padded resistively to minimize the effect of load change due to the long instrumentation cables. Amplitude modulation was negligible at the 50 ohm output point. Further hammer tests were conducted on this oscillator with essentially the same results; namely, the reduction of deviation from  $\pm 4$  KHz to 2 KHz during impact. In all cases this oscillator gave indication of good frequency stability



during impact with the exception of short-duration, high-amplitude spikes. This is considered normal for any crystal when operated in a high-impact environment.

After more than fifty hammer impact tests conducted using this crystal in different oscillators, the crystal became noisy. During impact, many abnormal short-duration, high-amplitude spikes were observed. This indicated that something within the crystal housing had either shifted, loosened, or become broken. The crystal was removed from the oscillator and was shock-tested independent of any other circuit elements. This was done by injecting a signal into the crystal from a signal generator at the series resonant frequency and observing the crystal output on an oscilloscope. When the crystal was lightly tapped, a variation in amplitude of more than two to one was observed on the scope. This confirmed that the noisy element was definitely the crystal. Further work in this area must await receipt of four more impact-resistant crystals now on order.

Significant results to date indicate that a crystal-controlled transmitter with small deviation capability should be modulated or deviated in a stage following the crystal. High-impact crystals have been developed by Valpey-Fisher in the ranges from 19 MHz to 33 MHz and are designed to operate on the third or fifth overtone. Overtone crystals, being high "Q" devices, are more difficult to "pull" in frequency than fundamental types. A 40 MHz, fifth overtone crystal (as used in these tests) can only be pulled practically about  $\pm 2$  KHz. Multiplying the 40 MHz oscillator frequency to the penetrometer output frequency results in a deviation of  $\pm 22$  KHz which does not produce desired S/N performance in the penetrometer-relay communications link. Phase modulation in a stage following the crystal oscillator can more readily produce a higher deviation and will be investigated following receipt of the new crystals.

#### 5.2.2 CALIBRATION SIGNAL INJECTION

The calibration signal is injected into the signal electronics between the first and second stages in the present prototype design. This point of calibration injection, therefore, does not give a performance check of the first stage amplifier. It is desirable to inject a simulated accelerometer signal for calibration purposes at the input to the signal electronics so that both qualitative and quantitative measurements can be made. The input stage of the signal electronics must present a very high resistance and low capacitance to the accelerometer so that the accelerometer's full sensitivity and low frequency characteristics may be utilized. Input resistances of several thousand megohms are required. The problems of injecting a calibration signal at the input are associated with high-impedance, low-leakage circuits.

Figure 5-18a shows a schematic of a portion of the signal electronics input stage. Any attempt at applying a signal directly at the accelerometer input would introduce another permanent noise source at the amplifier input due to the required cable to the umbilical plug and the high impedance at this point. (See Figure 5-18b.) A more indirect approach is therefore in order.

Figure 5-18c shows one approach where the simulated signal is placed in series with the high-megohm resistor, R37. Assuming low calibration generator impedance, the effective time constant at the input is composed of R37 and the effective capacitance of the accelerometer. This RC product is typically  $(2000 \times 10^6) (400 \times 10^{-12}) = 0.8$  second. Thus any reasonable calibration signal frequency would be greatly attenuated by this effective low-pass filter. AC calibration signals are required because of the AC coupling between signal electronics stages.

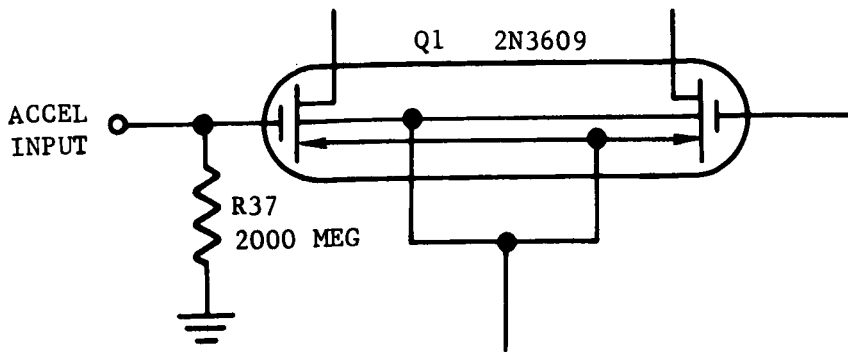
Figure 5-18d shows another possible approach whereby the signal generator calibration is injected in series with the accelerometer. This approach appears feasible; however, changes would be required in the accelerometer and its mounting provisions. The accelerometer normally has one side of the crystal transducer electrically connected to the case. The case is directly bolted to the structure.

The first method appears least desirable; therefore, the second method was pursued. This method may be used if two ungrounded connections are brought out of the accelerometer case instead of the present single connection. Delivery was arranged for one accelerometer from Endevco minus the usual case to facilitate further investigation of these potential modifications.

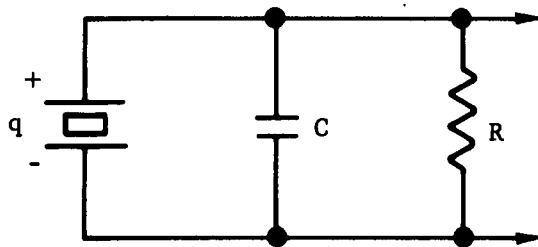
### 5.2.3 SHOCK QUALIFICATION OF EPOXY-ENCAPSULATED DIODES.

The silicon diodes presently used in both the signal electronics and the timer/regulator modules are of the conventional glass DO-7 configuration. Past impact tests with these units have resulted in glass cracks and breakage due to stresses built up in the unit during assembly, soldering, or potting operations. A fix for this difficulty has been the use of shrink-fit tubing over the diode package. This is a time-consuming operation with questionable merit. Recently, epoxy-encapsulated diodes have become available which meet or exceed the electrical specifications of the presently used diodes but are physically smaller, more rugged, and considerably less expensive. The epoxy-pac diode, Type FDM 6000, has been tested and is recommended for replacement of all conventional diodes now in use in the penetrometer.

Eight FDM 6000 diodes were subjected to hammer tests to determine their qualifications for high-shock penetrometer usage. The reference accelerometer



(a) PORTION OF PRESENT INPUT STAGE

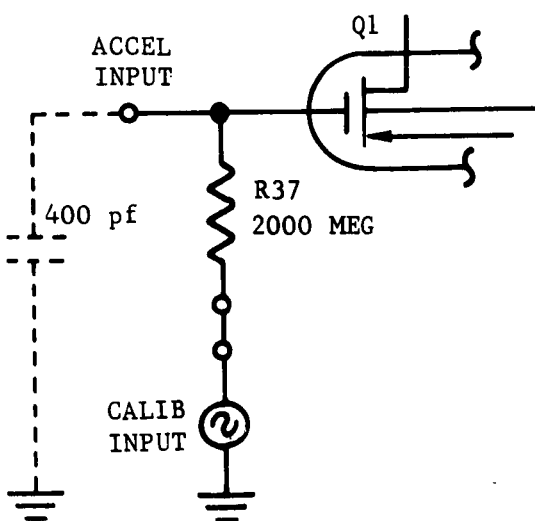


$$q = +0.3 \frac{\text{pC}}{\text{g}}$$

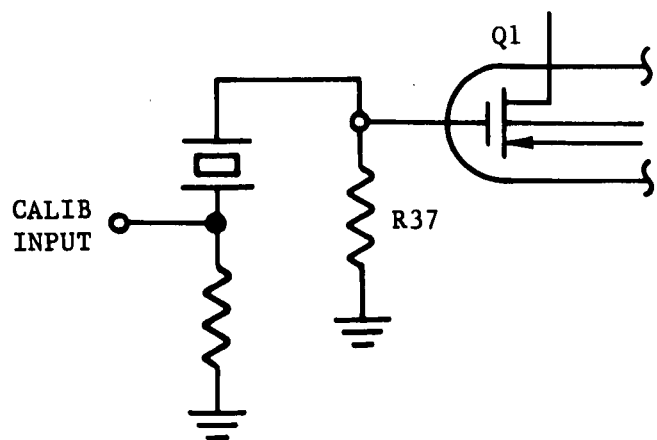
$$c = 400 \text{ pf}$$

$$R = 2 \times 10^{10} \Omega, \text{ MIN}$$

(b) ACCELEROMETER EQUIVALENT CIRCUIT



(c) CALIBRATION APPROACH NO. 1



(d) CALIBRATION APPROACH NO. 2

FIGURE 5-18. SIGNAL ELECTRONICS INPUT CALIBRATION CIRCUITS

FO3969 U

indicated peak acceleration levels from 5,000 to 10,000 g during twelve hammer tests. A number of the diodes were forward biased and the forward voltage drop was monitored during the shock. The forward and reverse characteristics of all the diodes were checked and recorded before and after the hammer tests. The results showed no change in any of the diodes tested in either their forward conduction or their reverse breakdown characteristics. All diodes functioned normally both during and following the hammer tests.

#### 5.2.4 SHOCK INVESTIGATION OF METAL-FILM RESISTORS

The present prototype penetrometer modules design uses both conventional carbon composition resistors and low-noise metal-film microresistors manufactured by Bourns. The Bourns units, although acceptable once they are assembled and potted, are quite fragile due to their tiny size and fine leads. They are also comparatively expensive. These shortcomings of the Bourns unit prompted the investigation of the more conventional metal-film resistors.

Metal-film resistors have been shock-qualified by other companies in the past. Therefore, the objective of this investigation was directed primarily at selecting a suitable type to be stocked for use in the penetrometer program. The miniature units similar to the IRC Type MMC are somewhat less expensive than the Bourns units when a large number of different values are needed.

A number of miniature metal-film resistors, IRC Type MMC, were received and shock-investigated along with conventional carbon composition 1/4-watt units. It was verified that the carbon units were noisy during high shock (10,000 g) while the metal-film units were relatively noise-free. It was also noted that some of the carbon composition resistors, after a number of hammer tests, exhibited a permanent change in resistance. In one instance the permanent resistance change was greater than 1/2 percent. No changes were noted in the metal-film units.

#### 5.2.5 SUBSTITUTION OF MOS FET'S WITH JUNCTION FET'S

The present signal electronics design uses dual P-channel MOS FET's (metal oxide silicon field-effect transistors) in both the first and second stages. Since the MOS FET is susceptible to damage by static charges and therefore easily damaged or destroyed in assembly, it is advisable to replace it with junction FET's whenever possible. The MOS-FET was used in the first stage for its low gate-drain capacitance and low leakage. However, these characteristics are not so important in the second stage, and it was examined first for possible change.

Until recently, dual P-channel junction FET's were expensive and difficult to make. This dictated, to a certain extent, the use of the circuit shown in Figure 5-19a. A dual N-channel type could have been used except for the fact that the only available integrated differential amplifier available was the Fairchild  $\mu$ A702. This unit has an input level restriction of +1.5 volts maximum. Recently Fairchild released the  $\mu$ A709 amplifier which is an improved, ungrounded version of the  $\mu$ A702 and can handle  $\pm 10$  volt inputs. This makes it useful in the signal electronics in that dual junction N-channel units (easily obtainable and relatively inexpensive) as source followers may now be utilized. The schematic of a proposed new second stage is shown in Figure 5-19b. This unit functions in much the same way as its predecessor in providing the necessary gain and frequency characteristics. The performance of this new stage with regard to these two parameters is shown in Figure 5-20.

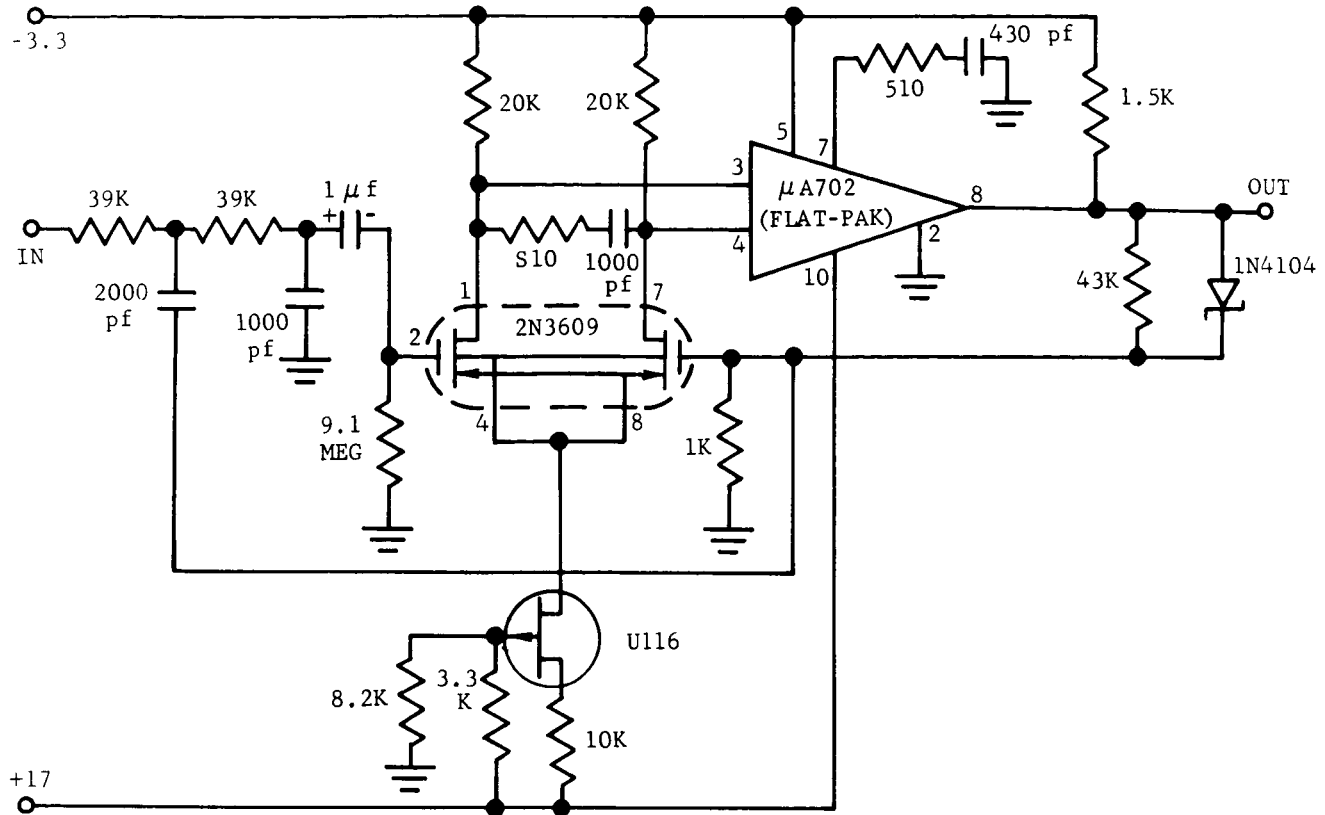
Additional tests were conducted on this new second stage. The unit was placed into an oven and the residual output caused by unbalance (offset) was measured for various temperatures. The source-follower source resistors were changed to obtain optimum dual field-effect matching conditions. The resulting offset magnitude and thermal stability is equivalent to that obtained with the dual MOS-FET and  $\mu$ A702 amplifier in the present signal electronics second stage. (See Figure 5-21.) This concludes the electrical tests on this second stage with recommendation that it be incorporated into future penetrometers, provided the unit qualifies successfully under high shock conditions.

#### 5.2.6 HIGH-MEGOHM METAL FILM RESISTOR SEARCH

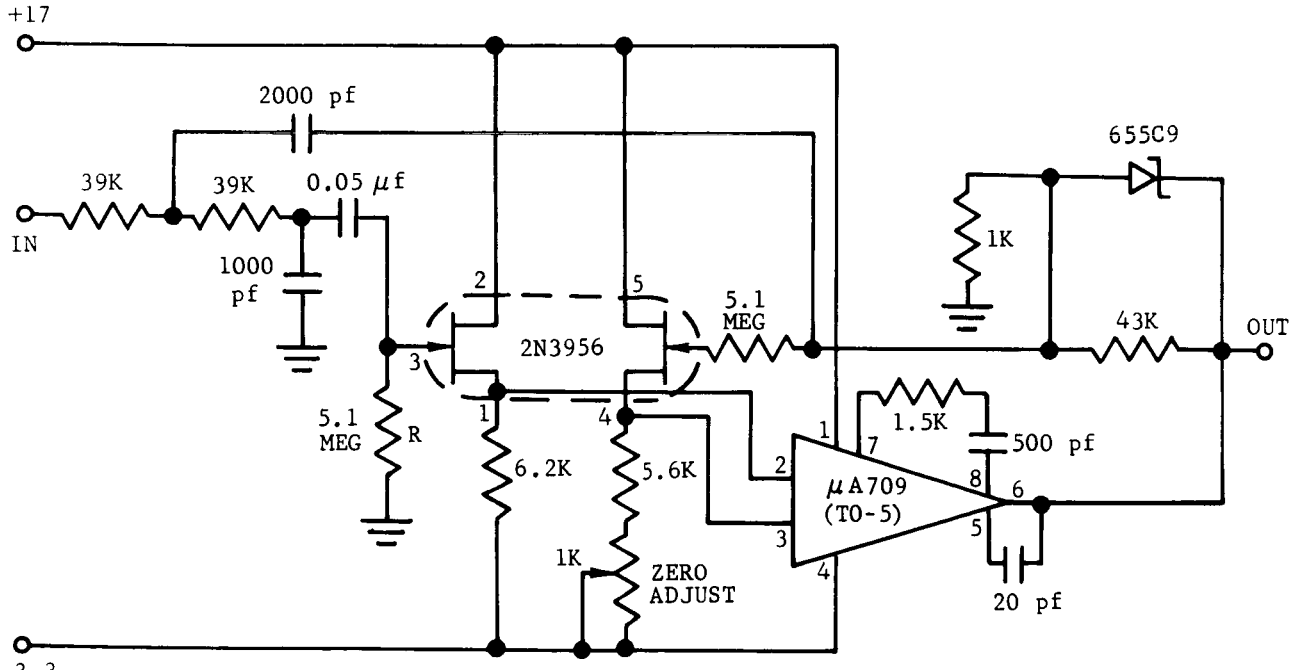
The present signal electronics uses a 2000-megohm resistor to set the input time constant. This resistor is a composition type which could be a source of noise and has questionable long-term stability. A search was made for a suitable metal film replacement. A potential replacement was found to be available from Pyrofilm Resistor Company, Inc. A number of these units in 1000, 2000, 3000, and 5000 megohm values have been ordered. These units have not yet been received. They are 0.11 inch in diameter by 9/16 inch long.

#### 5.2.7 ESTABLISHMENT OF AMERICAN BATTERY SOURCE

An effort is in progress to establish an American source for the penetrometer battery. This battery is presently fabricated using Epic B-80 button cells. This is a high-performance, rechargeable, silver-zinc button cell. No available replacement has been found. Therefore, proposals are being solicited from established American battery vendors to quote on the development of a suitable battery and/or cell tailored to the penetrometer requirements.



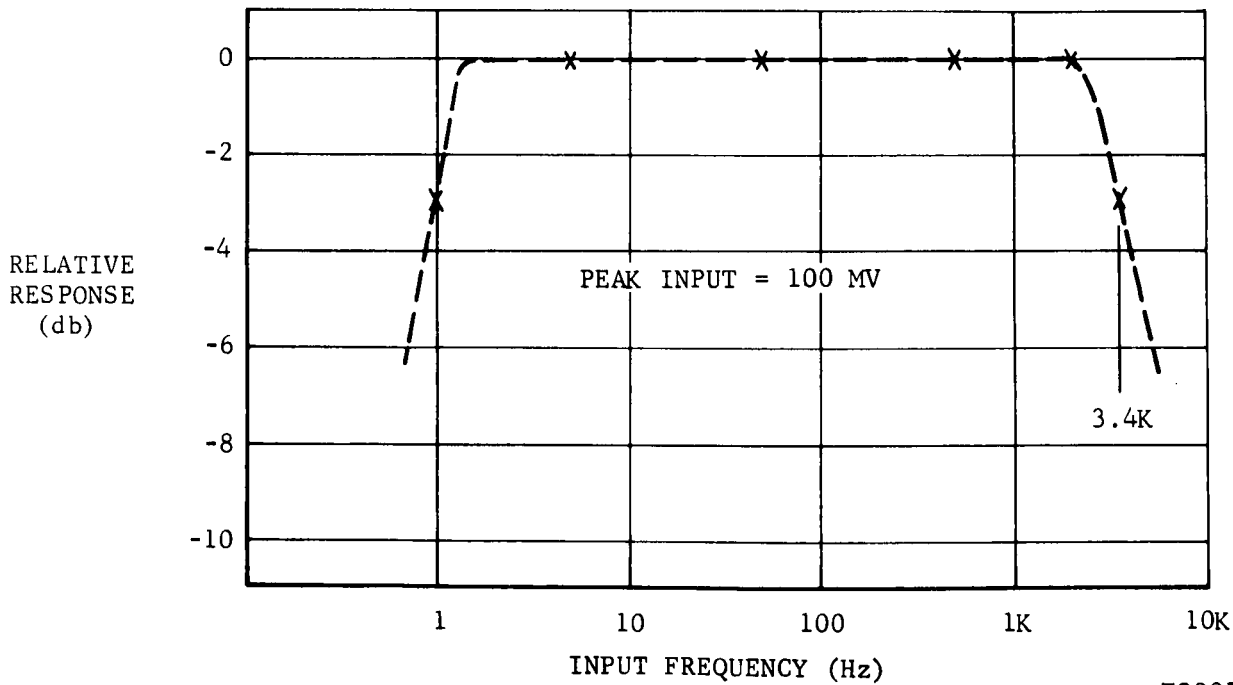
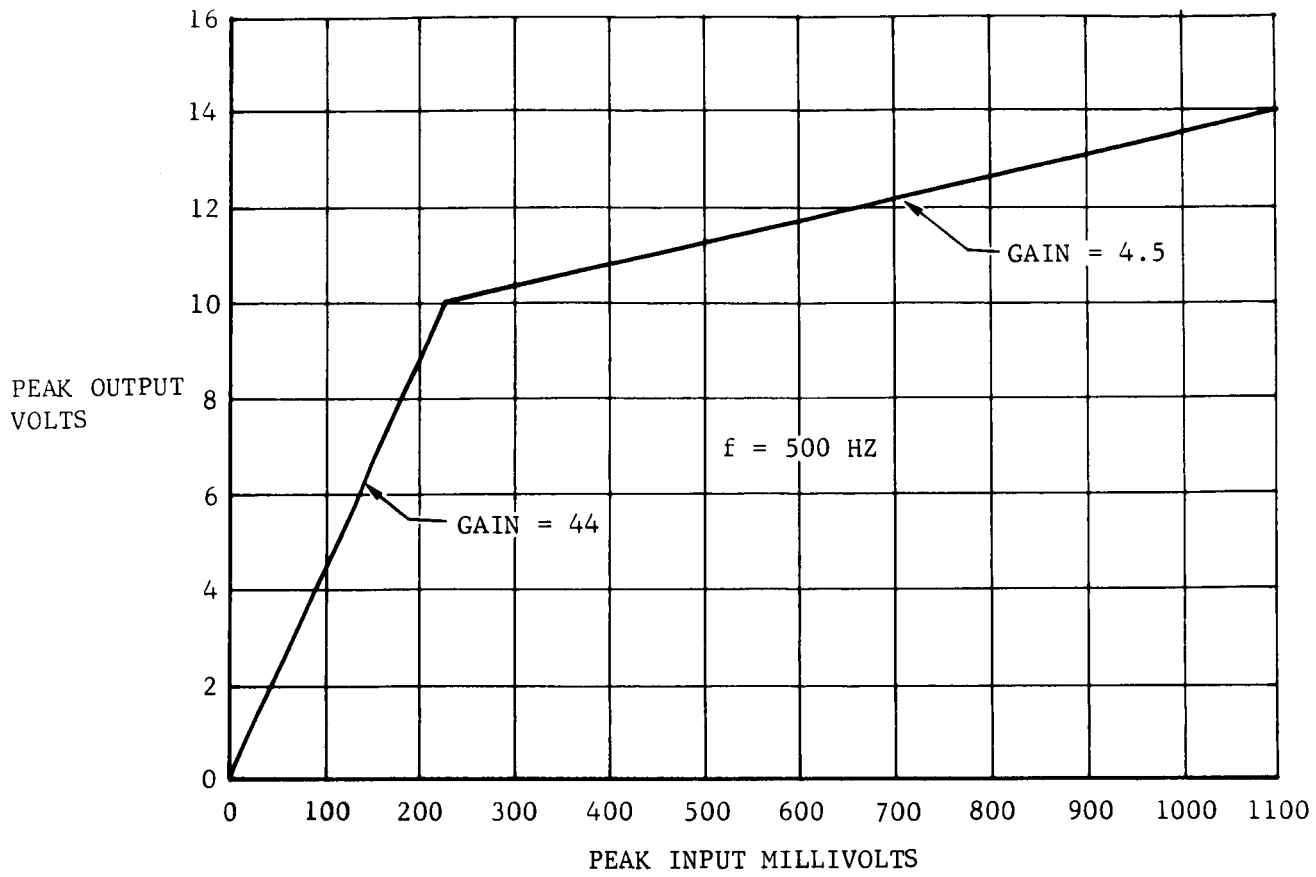
(a) PRESENT SECOND STAGE



(b) PROPOSED NEW SECOND STAGE

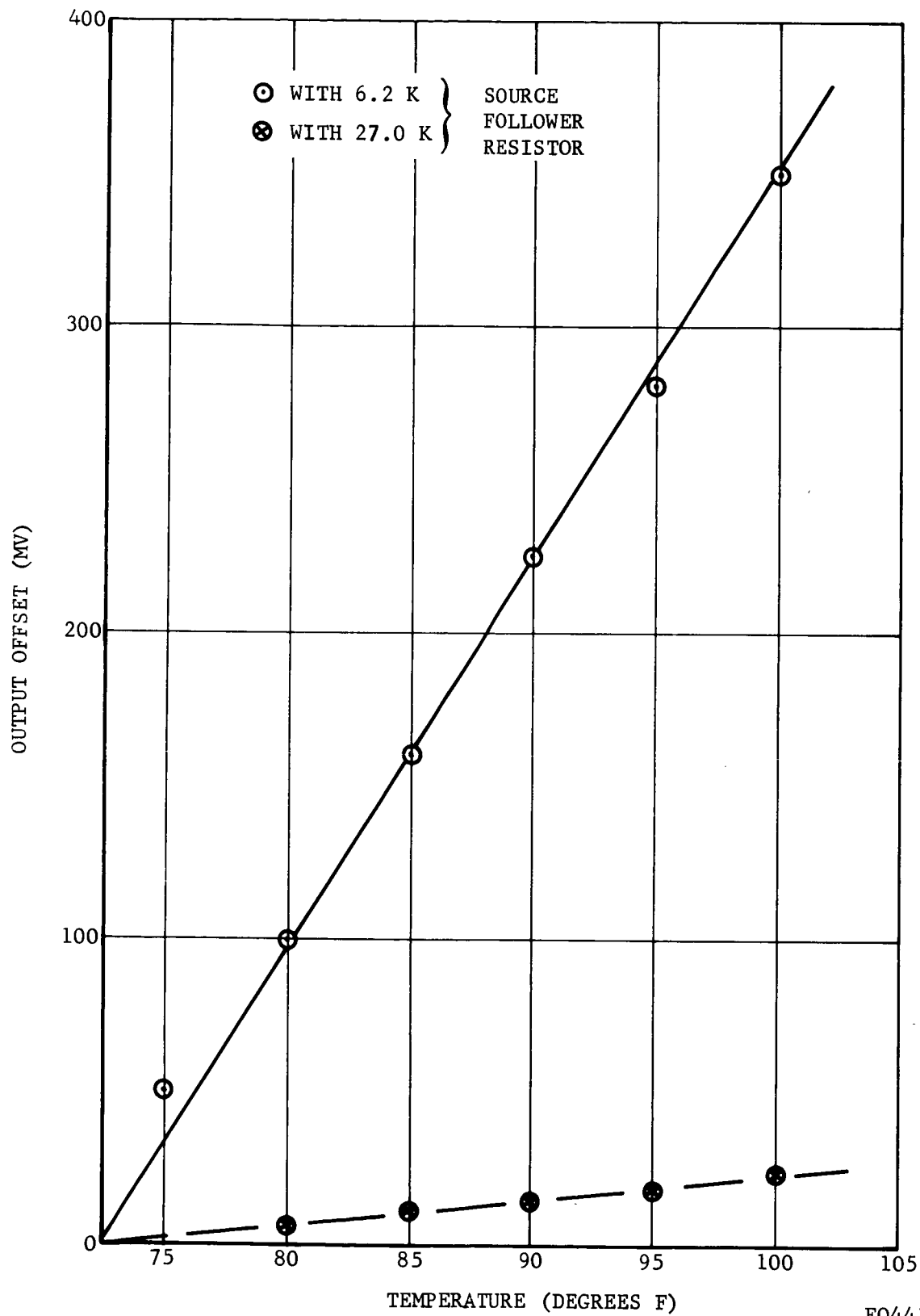
F03971 U

FIGURE 5-19. SECOND-STAGE SIGNAL ELECTRONICS SCHEMATIC



F03972 U

FIGURE 5-20. PERFORMANCE OF SECOND STAGE SIGNAL ELECTRONICS UTILIZING JUNCTION FETS AND  $\mu\text{A}709$  AMPLIFIER



FO4410 U

FIGURE 5-21. VOLTAGE OFFSET VERSUS TEMPERATURE FOR THE PROPOSED NEW SIGNAL ELECTRONICS SECOND STAGE

Two PIR's were issued (No. 194764 and No. 194765) to twelve battery vendors requesting price quotes for either a complete penetrometer battery or individual button cells from which a battery could be assembled. The responses from each company to date are listed in the following summary:

<u>Company Solicited</u>	<u>Comments</u>
1. Mallory Battery Co.	Apparently misdirected PIR. Second copy of RFQ mailed 5/12/66 to Mr. F. Cruze. Answer pending. Recent phone conversation indicates willingness to develop single silver-zinc button cells.
2. Gulton Industries Metuchen, N. J.	No reply.
3. Union Carbide Palmer, Ohio	RFQ referred to N. Y. office and Mr. Klopfenstein. Previous willingness to develop rechargeable button cell apparently overruled by company policy. Seem willing to supply battery developed for Picatinny Arsenal (30,000g) nonrechargeable. Also require larger volume than available. Requires repackaging in penetrometer. Quote forthcoming.
4. Union Carbide Bennington, Va.	No bid. N. Y. office directing PIR response.
5. Sonotone Elmsford, N. Y.	No bid. Unable to meet requirements.
6. Yardney Electric Corp.	No bid. Do not manufacture silver-zinc button cells and are unwilling to do so. Retain on bidder's list for silver-cad., silver-chloride-magnesium.
7. Electric Storage Battery Co., Raleigh, N. C.	No bid. Do not manufacture this type of cell. Apparently unwilling to undertake button cell development and believe flat-plate cell cannot fit in volume allocated.
8. Ray-O-Vac Madison, Wisconsin	No bid.

- |     |                                       |  |
|-----|---------------------------------------|--|
| 9.  | Burgess Battery Co.<br>Freeport, Ill. | No bid.  |
| 10. | ESB Research Center<br>Yardley, Pa.   | No bid because of current work load.   |
| 11. | Eagle Picher<br>Joplin, Mo.           | Mr. Lucas called. Requested extension.<br>Extension granted 5/13.  |
| 12. | G. E. Co.<br>Gainesville, Fla.        | Mr. W. H. Roberts contacted. No bid on<br>silver-zinc. Initial willingness by<br>Dr. Carson in New York to develop silver-<br>zinc apparently overruled by G. E. manage-<br>ment. Story now is absolutely no silver-<br>zinc development. Mr. Roberts will propose<br>ni-cad within 6 weeks. |

It is very evident from these responses that none of the companies contacted are willing to undergo a battery development program specifically directed towards penetrometer needs. Due to present penetrometer design based upon the high-energy density of silver-zinc cells, use of any lower density cell such as ni-cad would result in increased battery volume requirements. The only cell remotely capable of being used is the Union Carbide primary cell. Even accepting this cell with somewhat limited operational life restrictions placed upon penetrometers, the use of such cells would require relocation of the timer-regulator board and terminal block due to increased volume requirements.

Because of the rather negative response to a specific penetrometer battery development, coupled with the undesirability of using the Hungarian Epic B-80 cell, other power supply configurations should be investigated. One configuration in particular has been used with success by Sandia Corporation in their penetrometer development. This device utilizes a few large-capacity, ni-cad cells and a dc-dc converter. The large cells are capable of more efficient energy transfer at high discharge current rates than small MAH capacity cells. The main problems associated with such a supply involve voltage stability of the larger cells at impact and stress effects on the saturable core used in the transformer.

This approach should be investigated because it may allow use of "off-the-shelf" ni-cad or silver-cad button cells.

### 5.3 CRITICAL LONG-LEAD-TIME PARTS PROCUREMENT

A determination was made of which parts now used in the penetrometers require a long procurement lead time. Parts falling into this category were then ordered, assuming an impending build-up of five prototype

penetrometer assemblies. Other items were ordered in support of the investigation into the improvements to the penetrometer system. The following components from the above categories were ordered.

<u>Item and Quantity</u>	<u>Delivery</u>
1. High-impact crystals from Valpey-Fisher (4)	Scheduled 6/27/66
2. B-80 battery cells from Epic, Inc. (300)	Partial shipment 4/27/66 Complete 5/28/66
3. Glass coils from LRC (25)	Scheduled 5/27/66
4. High-resistance metal-film resistors from Pyrofilm (6 each of 4 values)	Scheduled 5/4/66
5. Transistor 2N3866 (50)	Received complete 4/14/66
6. Dual FET 2N3956 (4)	Received complete 4/21/66
7. Capacitors, VY Series (350 various values)	Scheduled 6/7/66
8. Tantalum capacitors (75, 2 values)	Received complete 4/25/66
9. RF connectors (25 pairs)	Scheduled 5/27/66
10. Trimmer capacitors from Johanson (175 various values)	Partial 5/6/65 Complete 5/27/66
11. Temp-compensating capacitors (25)	Scheduled 5/17/66
12. Epoxy diodes type FDM 6000 (100)	Received complete 4/18/66
13. Integrated differential amplifiers from Fairchild type $\mu$ A709 (6)	Received complete 5/2/66